



Terms and Conditions of Use of Digitised Theses from Trinity College Library Dublin

Copyright statement

All material supplied by Trinity College Library is protected by copyright (under the Copyright and Related Rights Act, 2000 as amended) and other relevant Intellectual Property Rights. By accessing and using a Digitised Thesis from Trinity College Library you acknowledge that all Intellectual Property Rights in any Works supplied are the sole and exclusive property of the copyright and/or other IPR holder. Specific copyright holders may not be explicitly identified. Use of materials from other sources within a thesis should not be construed as a claim over them.

A non-exclusive, non-transferable licence is hereby granted to those using or reproducing, in whole or in part, the material for valid purposes, providing the copyright owners are acknowledged using the normal conventions. Where specific permission to use material is required, this is identified and such permission must be sought from the copyright holder or agency cited.

Liability statement

By using a Digitised Thesis, I accept that Trinity College Dublin bears no legal responsibility for the accuracy, legality or comprehensiveness of materials contained within the thesis, and that Trinity College Dublin accepts no liability for indirect, consequential, or incidental, damages or losses arising from use of the thesis for whatever reason. Information located in a thesis may be subject to specific use constraints, details of which may not be explicitly described. It is the responsibility of potential and actual users to be aware of such constraints and to abide by them. By making use of material from a digitised thesis, you accept these copyright and disclaimer provisions. Where it is brought to the attention of Trinity College Library that there may be a breach of copyright or other restraint, it is the policy to withdraw or take down access to a thesis while the issue is being resolved.

Access Agreement

By using a Digitised Thesis from Trinity College Library you are bound by the following Terms & Conditions. Please read them carefully.

I have read and I understand the following statement: All material supplied via a Digitised Thesis from Trinity College Library is protected by copyright and other intellectual property rights, and duplication or sale of all or part of any of a thesis is not permitted, except that material may be duplicated by you for your research use or for educational purposes in electronic or print form providing the copyright owners are acknowledged using the normal conventions. You must obtain permission for any other use. Electronic or print copies may not be offered, whether for sale or otherwise to anyone. This copy has been supplied on the understanding that it is copyright material and that no quotation from the thesis may be published without proper acknowledgement.

Magnetic Nanoparticle-Supported Catalysts and Novel Organocatalysts for Enantioselective Synthesis



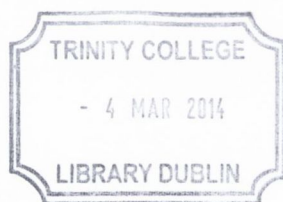
A thesis submitted to the University of Dublin for the degree of Doctor of
Philosophy

by
Oliver Gleeson M.Sc.

Under the supervision of
Prof. Stephen Connon

May 2013

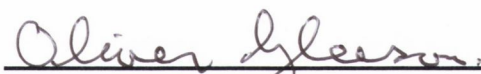
Trinity College Dublin



Thesis 10142

I declare that this thesis has not been submitted as an exercise for a degree at this or any other university and it is entirely my own work. Due acknowledgements and references are given to the work of others.

I agree to deposit this thesis in the University's open access institutional repository or allow the library to do so on my behalf, subject to Irish Copyright Legislation and Trinity College Library conditions of use and acknowledgement.



Oliver Gleeson

O. Gleeson, R. Tekoriute, Y. K. Gun'ko and S. J. Connon, "The first magnetic nanoparticle-supported chiral DMAP analogue: highly enantioselective acylation and excellent recyclability" *Chem. Eur. J.*, 2009, **15**, 5669.

O. Gleeson, G.-L. Davies, A. Peschiulli, R. Tekoriute, Y. K. Gun'ko and S. J. Connon, "The immobilisation of chiral organocatalysts on magnetic nanoparticles: the support particle cannot always be considered inert" *Org. Biomol. Chem.*, 2011, **9**, 7929.

O. Gleeson, Y. K. Gun'ko, S. J. Connon, '(S)-Proline-derived catalysts for the kinetic resolution of alcohols: a remote structural change from hydrogen-bond donor to acceptor allows a complete selectivity switch' *Synlett*, 2013, **24**, 1728.

Table of Contents

	Page
Acknowledgements.....	v
Abstract	vi
Abbreviations	viii
1.1 General	1
1.1.1 Asymmetric organocatalysis	2
1.2 Kinetic resolution (KR)	3
1.2.1 Theory of kinetic resolution	4
1.2.2 Acylative KR of alcohols	7
1.2.2.1 Enzymatic KR of alcohols.....	8
1.2.2.2 Asymmetric KR of alcohols catalysed by artificial organocatalysts..	12
1.2.3 4- <i>N,N</i> -dialkylaminopyridine catalysis	13
1.2.3.1 The first chiral 4- <i>N,N</i> -dialkylaminopyridine catalyst.....	14
1.2.3.2 Planar-chiral 4- <i>N,N</i> -dialkylaminopyridine catalysts	15
1.2.3.3 Atropisomer 4- <i>N,N</i> -dialkylaminopyridine catalysts.....	20
1.2.3.4 Important developments in 4- <i>N,N</i> -dialkylaminopyridine catalysts....	21
1.2.3.5 Overview of alternative 4- <i>N,N</i> -dialkylaminopyridine catalysts	26
1.2.3.6 Substituted 4- <i>N,N</i> -dialkylaminopyridine catalysts operating <i>via</i> an 'induced-fit' mechanism.....	27
1.2.4 Non-pyridine nucleophilic chiral organocatalysts.....	30
1.2.4.1 <i>N</i> -Alkylimidazole based catalysis	30
1.2.4.2 <i>N</i> -Heterocyclic carbene based catalysis	32
1.2.4.3 Vicinal diamine based catalysis.....	33
1.2.4.4 Amidine based catalysis	34
1.2.4.5 Phosphine based catalysis.....	38
1.3 Heterogeneous catalysis	40
1.3.1 Background and history.....	41
1.3.1.1 Solid supports commonly used in heterogeneous catalysis.....	41
1.3.2 Polymeric supported catalysts	42
1.3.2.1 Poly(ethylenimine)-supported catalysts	42
1.3.2.2 Polystyrene-supported catalysts	43
1.3.2.3 Polyethylene glycol-supported catalysts	47

1.3.3	Inorganic material-supported catalysts.....	51
1.3.3.1	Zeolites and clay-supported catalysts.....	51
1.3.3.2	Silica-supported catalysts.....	55
1.3.4	Magnetic nanoparticle supported catalysis.....	60
1.3.5	Conclusion.....	65
2.1	Synthetic strategy for the development of a magnetic-nanoparticle supported chiral 4- <i>N,N</i> -dialkylaminopyridine organocatalyst	67
2.1.1	First generation system: design and synthesis of a 4- <i>N,N</i> -dialkylaminopyridine siloxane bound catalyst	69
2.1.2	Second generation system: attempted immobilisation of a catalyst precursor to a thiol-functionalised nanoparticle <i>via</i> a thiol-ene reaction	71
2.1.3	Third Generation system: catalyst immobilisation <i>via</i> a S_NAr reaction with an <i>N</i> -methyldopamine functionalised nanoparticle.....	73
2.1.3.1	Catalyst loading and preliminary evaluation.....	74
2.1.3.2	Optimisation of reaction parameters	79
2.1.3.3	Kinetic resolution of <i>sec</i> -alcohols: substrate scope under optimised conditions	83
2.1.3.4	Recycling of the magnetic nanoparticle supported 4- <i>N,N</i> -dialkylaminopyridine catalyst	85
2.2	Conclusions	91
3.1	Magnetic nanoparticle supported 9- <i>epi</i> -quinine urea based catalyst..	93
3.1.1	Synthesis of catalyst precursor	95
3.1.2	Catalyst loading.....	96
3.1.3	Catalyst evaluation: preliminary studies	97
3.1.4	Asymmetric Michael additions to nitroolefins catalysed by magnetic nanoparticle supported catalyst 266	100
3.2	Conclusion.....	104
4.1	Proline-derived catalysts for the kinetic resolution of alcohols	106
4.1.1	Synthesis of the hydroxy chiral pendent moiety 275	108
4.1.2	Synthesis of a chiral azide analogue of 276	109
4.1.2.1	Synthesis of chiral moiety of basic characteristic from azide 276 ...	110
4.1.2.2	Synthesis of chiral substrate of basic characteristic	111
4.1.2.3	Synthesis of chiral substituent with acidic characteristic	112
4.1.2.4	Attempted synthesis of a urea substituted chiral pendant	113

4.1.3	Synthesis of chiral substituted 4-chloro pyridine derivatives.....	114
4.1.3.1	Synthesis of final catalysts bearing alternative functional groups ...	115
4.1.3.2	Synthesis of triazole and urea functionalised DMAP-based catalyst	116
4.2	Investigations into the acylative KR of <i>sec</i> -alcohols using novel chiral catalysts	117
4.2.1	Investigation of the influence of reaction temperature on selectivity	120
4.2.2	KR of mono-protected diols under optimised conditions.....	121
4.2.3	¹ H-NMR spectroscopic analysis of catalysts mode of action.....	123
4.3	Conclusion.....	125
5.1	Experimental.....	126
5.2	Appendix	182
5.2.1	Analysis and characterisation of catalyst 246	182
5.2.2	Analysis and characterisation of catalyst 266	185

Acknowledgements

First of all, I would like to thank my friends and family especially my late mother Delia for the enormous encouragement and support I received during the course of my PhD.

I am extremely grateful to my supervisor Prof. Stephen Connon for his constant help, advice and active encouragement throughout the project and for introducing me to the fascinating field of asymmetric catalysis.

Special thanks to Claudio, Sean, Luran, Simon, Sivaji, Francesco, Emiliano, Clare-Louise, Michelle, Eoin and Aldo for their critical reading of my manuscript and the many valuable suggestions. I am especially grateful to Alessandro for his valuable assistant and insight throughout my PhD and during the writing phase of this thesis.

I would also like to thank all the past and present members of the Connon group and the Southern group for provided an enjoyable and entertaining working atmosphere.

Finally, I would like to express my gratitude to all the staff in the School of Chemistry, especially the technical staff for their help and support with all the practical aspects of the laboratory environment. I am particularly grateful to Dr. John O' Brien, Dr. Manuel Ruether, Dr Martin Feeney, Fred Cowzer, Teresa McDonnell, Brendan Barry and a very special thanks to Brendan Mulvaney.

Abstract

A study concerning the immobilisation onto magnetic nanoparticles of two useful classes of chiral organocatalyst which rely on a confluence of weak, easily perturbed van der Waals and hydrogen bonding interactions to promote enantioselective reactions has been undertaken for the first time. The catalysts were evaluated in two synthetically useful reaction classes: the kinetic resolution of *sec*-alcohols and the conjugate addition of dimethyl malonate to a nitroolefin.

This study has demonstrated that a chiral 4-*N,N*-dialkylaminopyridine derived catalyst can be readily immobilised on magnetite nanoparticles. The resulting heterogeneous catalyst was demonstrated to be highly active and capable of promoting the kinetic resolution of *sec*-alcohols with synthetically useful selectivity values under process-scale friendly conditions (ambient temperature, low catalyst loading and acetic anhydride as the acylating agent) - which allowed for the isolation of resolved alcohols with good-excellent enantiomeric excess. The magnetic nanoparticle-supported catalyst was readily prepared, insensitive to air/moisture and easily recoverable by exposure of the reaction vessel to an external magnetic field and were demonstrated to be reusable in a minimum of 32 consecutive cycles while retaining high activity and selectivity profiles.

The successful immobilisation of a quinine derived urea organocatalyst onto magnetic nanoparticles *via* a thiol-ene radical reaction has also been accomplished. Evaluation of the magnetic nanoparticle-supported 9-*epi*-quinine urea catalyst showed it to be capable of promoting enantioselective asymmetric Michael-type additions of dimethyl malonate to nitroolefins. However, activity and selectivity was less effective than in the homogeneous system even at higher catalytic loadings. Investigation into the role the magnetite nanoparticles exerted on the homogeneous system lent insight into the lower levels of enantioselectivity observed, although it did not account for poor catalyst activity. Moreover, it revealed that the utilisation of magnetite nanoparticles as a solid support must be assessed on a case-by-case basis: where the unfunctionalised magnetite nanoparticles were capable of promoting the Michael addition of dimethyl malonate to nitroolefins whereas they were found to be inert in the acylative kinetic resolution of *sec*-alcohols.

The design and synthesis of novel L-proline derived substituted 4-*N,N*-dialkylaminopyridine organocatalysts which differ only by the characteristics of a remote substituent has also been accomplished. When this substituent is capable of donating hydrogen bonds the catalyst preferentially promotes the acylation of the opposite enantiomer of a racemic *sec*-alcohol to that acylated when the substituent is a basic amine capable of accepting hydrogen bonds, despite the catalysts possessing the same configuration at their only stereogenic centre. ¹H-NMR spectroscopic analysis did indicate that both systems underwent similar, yet not exactly analogous conformational change which controls the remote stereochemical information to bear on the acylation event *via* an ‘induced-fit’ type mechanism.

Abbreviations

ABH	aza-Baylis Hillman
Ac	Acetyl
AIBN	Azobisisobutyronitrile
AKR	Acylative Kinetic Resolution
Ar	Aryl
atm	atmosphere
BH	Baylis Hillman
Bn	Benzyl
BOC	<i>tert</i> -Butoxycarbonyl
Bu	Butyl
Bz	Benzoyl
cat.	Catalyst
Conv.	Conversion
Cp	Cyclopentadiene
CSP	Chiral stationary phase
DABCO	1,4-diazabicyclo[2.2.2]octane
DCC	<i>N,N'</i> -Dicyclohexylcarbodiimide
DCM	Dichloromethane
<i>de</i>	Diastereomeric excess
DIAD	Diisopropyl azodicarboxylate
DIPE	Diisopropyl ether
DIPEA	<i>N,N'</i> -Diisopropylethylamine
DKR	Dynamic Kinetic Resolution
DMAP	4-(Dimethylamino)pyridine
DMF	Dimethylformamide
DMSO	Dimethyl sulphoxide
DPPA	Diphenylphosphoryl azide
EDG	Electron donating group
<i>ee</i>	Enantiomeric excess
eq.	Equivalent
equiv.	Equivalent
Et	Ethyl
EWG	Electron withdrawing group
FDA	Food and Drug Administration
HPLC	High Performance Liquid Chromatography
IPA	<i>Iso</i> -propyl alcohol
IR	Infra red
KR	Kinetic Resolution
k	Rate constant
<i>m</i>	<i>meta</i>
MCPBA	<i>m</i> -Chloroperoxybenzoic acid
Me	Methyl
MeCN	Acetonitrile
mEq	Mass equivalence
MNP	Magnetic nanoparticles
Ms	Mesyl
MS	Molecular sieves

MTBE	Methyl <i>tert</i> -butyl ether
NMR	Nuclear magnetic resonance
Np	Naphthyl
Nu	Nucleophile
<i>o</i>	<i>ortho</i>
<i>p</i>	<i>para</i>
PEG	Polyethylene glycol
Ph	Phenyl
PPY	4-Pyrrolidinopyridine
<i>rac</i>	Racemic
rt	Room temperature
S	Selectivity factor
<i>sec</i>	Secondary
TBDMS	<i>tert</i> -Butyldimethylsilyl
TBS	<i>tert</i> -Butylsilyl
TEA	Triethylamine
TFA	Trifluoroacetic acid
TFAA	Trifluoroacetic anhydride
THF	Tetrahydrofuran
TMS	Trimethylsilyl
TS	Transition state
Ts	Tosyl

1.1 General

Chirality is defined as “the geometric property of a rigid object (or spatial arrangement of points or atoms) of being non-superimposable on its mirror image”.¹ The word chiral, first coined by Lord Kelvin in 1873,² is derived from the Greek word for handedness as the hand is one of the best examples of a non-superimposable mirror image of itself. Chirality is ubiquitous in nature. RNA and DNA are chiral, all but one of the naturally occurring amino acids are chiral and almost all naturally occurring carbohydrates are chiral. Many living organisms physically display chirality; the honeysuckle (*Lonicera sempervirens*) winds in a left-handed helix, whereas bindweed (*Convolvulus arvensis*) winds in the opposite helical form.³

A molecule that contains a single chiral centre that is a non-superimposable mirror image of itself is defined as an enantiomer. The synthesis and isolation of individual enantiomers has always proven challenging, as enantiomers display equivalent chemical properties in an achiral environment and only differ physically in their ability to rotate a plane of polarised light in opposite orientations. The demand for enantiopure compounds is driven by the fact that individual antipodes can display different biological activities and effects. There are many example of this, one of which is the drug penicillamine.⁴ The (*S*) enantiomer is an effective anti-arthritis agent whereas the (*R*) enantiomer is a potent liver toxin. Another example is the drug ethambutol. One enantiomer is used in the treatment of tuberculosis whereas the other enantiomer causes blindness. One of the most famous examples is the infamous drug thalidomide,⁵ where the (*R*) enantiomer is an active anti-nausea agent whereas the (*S*) enantiomer caused foetal mutations and death. The drug was marketed in the 1950s as the racemic mixture and caused the malformation of limbs in many children whose mothers were prescribed the drug during pregnancy to preventing ‘morning sickness’.

Catalysis has proven to be an important strategy in the synthesis of enantiopure compounds.⁶ This was recognised in 2001 with the Nobel Prize in chemistry being awarded for the development of catalytic asymmetric synthesis, with one half jointly shared by Knowles⁷ and Noyori⁸ for their work on chiral catalytic hydrogenation, while Sharpless,⁹ received the other half for his work on chiral catalytic oxidation. By definition a catalyst should remain unchanged after the reaction, therefore its recovery

and recyclability is not only highly plausible but of great environmental and economic importance. The use of insoluble polymer^{10,11} and inorganic¹² supports are a well-known and documented means of catalyst recovery, but these strategies do have associated drawbacks:

- (i) Heterogeneous catalysis tends to be less active than its homogeneous counterpart due to the limited mass transfer of the reactants from solution to the surface of the solid support.
- (ii) The recyclability of air and moisture sensitive metal-based catalysts for organic reactions is often limited due to the leaching of the metal ions into solution.
- (iii) Polymer supports, particularly polystyrenes, are often not robust enough: they must be agitated without stirring and nonetheless exhibit limited life expectancy.

1.1.1 Asymmetric organocatalysis

Asymmetric organocatalysis is an important synthetic strategy for the synthesis of chiral compounds, that otherwise would be attained *via* alternative strategies, such as the use of naturally occurring optically pure precursors (chiral pool), asymmetric metal-based catalysis, enzymatic catalysis or with the use of chiral auxiliaries and chiral reagents. The problems associated with chiral pool precursors is their finite number and availability; the amount of the naturally occurring compounds may be inadequate for a synthetic process due to its limited natural production or the rarity of the organism producing it. There may also be monetary costs or environmental repercussions associated with obtaining the chemicals in question. Or simply the required isomer may not exist; for example, the vast majority of naturally occurring amino acids only exist as the (*S*)-enantiomer.

Metal catalysis has consistently dominated the field of enantioselective synthesis and is still preeminent in industrial catalytic asymmetric processes.¹³ The advantages associated with organocatalysts over their metal-based counterparts include their general lack of sensitivity towards oxygen and moisture, ready availability, low cost and

toxicity, all of which are seen as of great direct benefit, especially in the pharmaceutical industry.¹⁴⁻¹⁶

Enzymes have shown to be a very successful group of catalysts for a variety of asymmetric transformations, only second to metal-based catalysts.¹⁷ Organocatalysts are often viewed as simplified versions of enzymes, from which they are conceptually derived and very often compared.¹⁸ However, enzymes tend to suffer from long reaction times (low activity), are sensitive to reaction parameters (organic solvent degradation, *etc.*), lack of batch reproducibility (potentially due to small genome mutation) and substrate specificity (lock-and-key enzymatic specificity).¹⁹

The problem associated with the use of chiral auxiliaries is the addition of extra synthetic steps due to the attachment and removal of the chiral auxiliary. Although an equimolar quantity of the auxiliary is required, it theoretically can be recycled after recovery, which normally incurs in small losses. It is also important that the attachment and detachment of the auxiliary takes place under mild conditions to ensure maximum product yield and auxiliary recoverability, therefore limiting reaction scope.

Asymmetric organocatalysis relies on the ability of the catalyst to pass on chiral information to the substrate being catalysed in order to achieve selectivity. It is accepted that small organocatalyst molecules do not benefit from the strong enthalpic substrate binding associated with metal-based catalysts. Therefore it is plausible to hypothesise that the weaker binding interactions of organocatalysis leads to improved chemoselectivity in many cases and tolerance of reaction conditions.

1.2 Kinetic resolution (KR)

By definition, kinetic resolution is “The achievement of partial or complete resolution by virtue of unequal rates of reaction of the enantiomers in a racemate with a chiral agent (reagent, catalyst, solvent, *etc.*)”.²⁰

The maximum discrimination in the catalytic kinetic resolution of a racemic substrate under ideal conditions is 100% *ee* of each antipode at 50% conversion; this will afford 50% of the enantiopure starting material and 50% of the enantiopure product. In this

idyllic process only one enantiomer undergoes the catalytic process while the other remains unchanged. However, what determines the catalytic discrimination is the rate at which each enantiomer reacts with the catalytic species relative to the other. This relative reaction rate is determined by the rate constant, k_{rel} , where k_{rel} is the rate of the reaction involving the fast reacting antipode divided by the slow reacting antipode ($k_{rel} = k_{fast}/k_{slow}$).

1.2.1 Theory of kinetic resolution

In catalytic kinetic resolution, each antipode of a substrate interacts with the chiral catalytic species to form two diastereomeric transition states, which gives rise to an energy difference (ΔE_a) between the transition states. The greater the energy difference between the transition states of the fast reacting enantiomer and the slow reacting enantiomer offers a greater potential for enantiodiscrimination. A generic example of this energy difference is represented in Figure 1.1, where S^S and S^R represents the substrates of the fast and slow reacting antipodes respectively, and P^S and P^R are the products.

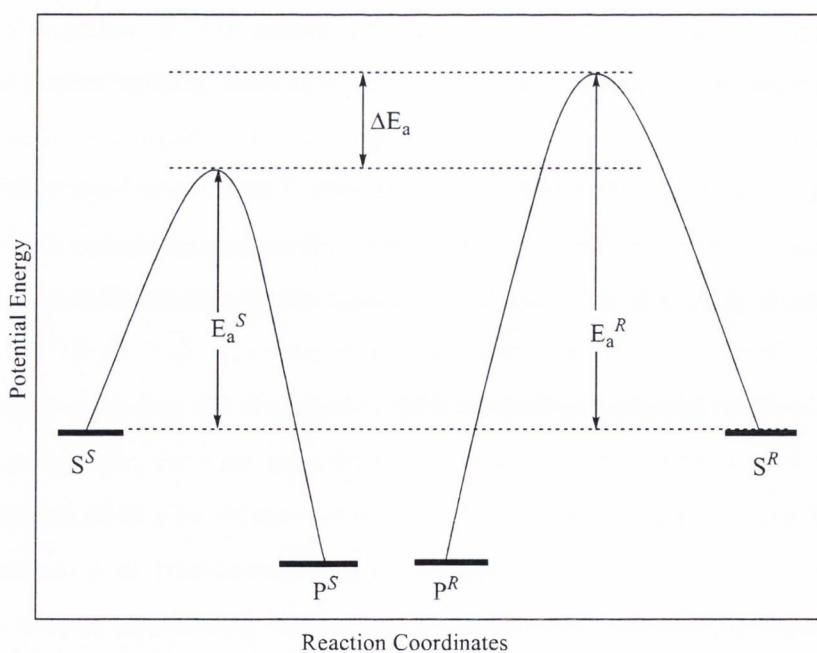


Figure 1.1 Potential energy diagram for a generic kinetic resolution process

Eq. 1.1 gives the magnitude of the energy barrier between the transition states associated with the reaction of the fast and slow reacting enantiomers.

$$\Delta E_a = E_a^R - E_a^S \quad \text{Eq. 1.1}$$

Where E_a^R and E_a^S are the activation energies of the transition states for the slow and the fast reacting enantiomer, respectively, and ΔE_a is the energy difference between the transition states.

The magnitude of ΔE_a can be represented as the ratio of the rate constants for the reaction of each enantiomer; k_{rel} , and is also known as the selectivity factor S ,²¹ in Eq. 1.2.

$$S = k_{rel} = \frac{k_{fast}}{k_{slow}} = \Delta E_a \quad \text{Eq. 1.2}$$

The selectivity factor can also be represented as a function of the enantiomeric excess (ee). For the reaction sequence shown in Figure 1.1 the reaction of the (*S*)-enantiomer represents the fast reacting antipode, *i.e.*, the reaction which passes through the lowest energy transition state. The (*R*)-enantiomer is the slow reacting antipode. ee is given by Eq. 1.3.

$$ee = \frac{[S] - [R]}{[S] + [R]} \quad \text{Eq. 1.3}$$

The selectivity factor can be determined using either the substrate or the product. Eq. 1.4 determines selectivity using the values obtained for the substrate.

$$S = \frac{\ln[(1 - C)(1 - ee)]}{\ln[(1 - C)(1 + ee)]} \quad \text{Eq. 1.4}$$

Where C represents the conversion for the substrate (Eq. 1.5) and ee' is the enantiomeric excess of the product.

$$C = \frac{ee}{ee + ee'} \quad \text{Eq. 1.5}$$

Alternatively the selectivity factor can be determined from the ee and conversion values of the product using Eq. 1.6.

$$S = \frac{\ln[1 - C'(1 - ee')]}{\ln[1 - C'(1 + ee')]} \quad \text{Eq. 1.6}$$

Conversion of the product can be determined by employing eq. 1.7.

$$C' = \frac{ee'}{ee' + ee} \quad \text{Eq. 1.7}$$

One of the great advantages of kinetic resolution over other asymmetric synthetic techniques is the ability to achieve high enantiopurity of the substrate with even moderate selectivity values. A selectivity value of 10 is usually considered synthetically useful, as it will allow the isolation of the substrate in > 95% ee at 70% conversion, which is equivalent to 30% yield of the desired enantiomer. Whereas a selectivity value of 5 will only afford approximately 10% of the enantioenriched product in > 95% ee . Of course even higher values are more desirable, however because the selectivity factor is an exponential function, there is no great advantage associated with achieving selectivity values beyond 100, as can be seen in Figure 1.2. However, one major drawback associated with kinetic resolution is the loss of at least 50% of component regardless of the selectivity inherent in the resolution process.

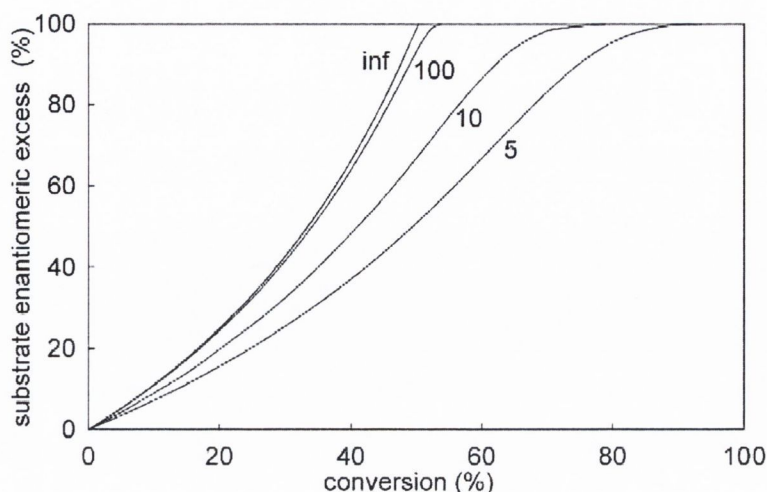
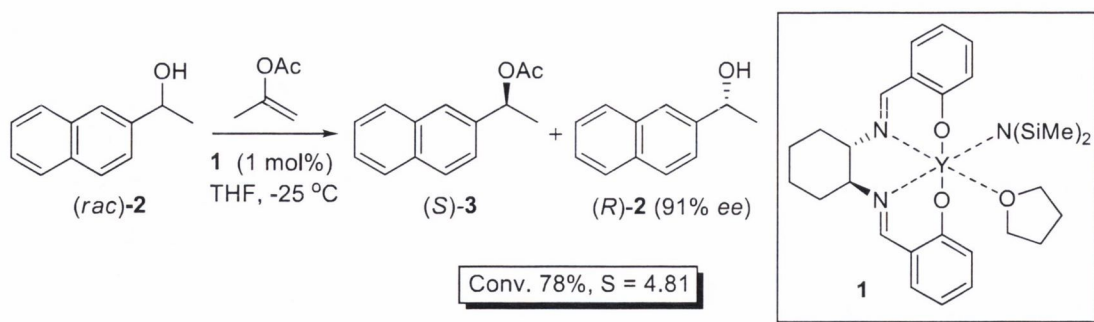


Figure 1.2 Plot of substrate *ee* versus conversion for different *S* values.²²

1.2.2 Acylative KR of alcohols

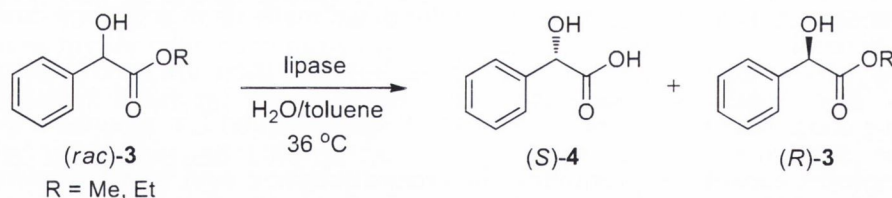
Acylative kinetic resolution is a highly desirable approach to obtaining enantioenriched *sec*-alcohols, which are of great importance as chiral building blocks.²³ The use of acylating agents such as anhydrides and acyl chlorides are also very appealing due to their diversity, commercial availability and low cost. Enzymatic catalysis and organocatalysis are by far the most predominant methods in achieving enantioselectivity in acylative kinetic resolution of alcohols, however there are several examples reported using metal based catalysts.^{24,25} In 2002 RajanBabu and Lin reported a class of yttrium complexes capable of promoting the enantioselective acyl transfer between enolesters and secondary alcohols.²⁶ The most successful result was achieved using 1 mol% of yttrium complex **1** in the acylative kinetic resolution of 1-(naphthalen-2-yl)ethanol (*rac*)-**2** with isopropenyl acetate at -25 °C: a modest selectivity value of 4.81 at 76% conversion. This afforded the alcohol (*R*)-**2** in 24% yield and 91% *ee* (Scheme 1.1).



Scheme 1.1 Yttrium catalyzed acylative KR of 1-(naphthalen-2-yl)ethane.

1.2.2.1 Enzymatic KR of alcohols

Enzymes are catalytic proteins, with the exception of ribozymes which are catalytic RNA.²⁷ Among the great number of known chemically useful enzymes, lipases are one of the most successful enzymes employed in kinetic resolution, demonstrating great stability and activity in organic solvents plus an ability to deliver high degrees of chemo-, regio- and stereoselectivity.²⁸ The first documented lipase catalyzed kinetic resolution was reported by Dakin in 1903 with the use of crude pig liver lipase in the hydrolysis of mandelic esters (Scheme 1.2).²⁹



Scheme 1.2 Enantioselective hydrolysis of mandelic ester using crude pig liver lipase.²⁹

Dakin's experiments showed that enzymes are not perfectly enantioselective; he demonstrated that the enantiopurity obtained products was related to the enzyme's substrate affinity, reaction rate and conversion. In the hydrolysis of ethyl mandalate ((*rac*)-3) to mandelic acid (4, Scheme 1.2), Dakin found the *dextro*-mandelic acid ((*S*)-4) to be present in 25.5% relative to the enantiopure *dextro*-mandelic acid at 5.8% conversion (Table 1.1, Entry 1). At 36.5% conversion the purity of the mandelic acid

had diminished 20.2% and at 99.8 % conversion the mandelic acid was found to be racemic (Table 1.1, Entries 2 and 3). Under the same conditions using ethyl mandalate Dakin found the *dextro*-mandelic acid to be present in 38.3% at 5.2% conversion (Table 1.1, Entry 4), 24.6% purity at 32.4% conversion (Table 1.1, Entry 5) and 5.3% purity at 93.6% conversion (Table 1.1, Entry 6).

Table 1.1 Kinetic resolution of mandelic ester analogues using pig liver lipase

Entry	R	Conversion (%)	$[\alpha]_{\text{D}}^{20}$	(<i>S</i>)-mandelic acid ^a (%)
1	Me	5.8	+39.9	25.5
2	Me	36.5	+31.5	20.2
3	Me	99.8	0	0.0
4	Et	5.2	+59.7	38.3
5	Et	32.4	+50.5	32.4
6	Et	93.6	+8.3	5.3

^aDetermined as a percentage of enantiopure *dextro*-mandelic acid
 $[\alpha]_{\text{D}}^{20}$: +156.0

Unfortunately Dakin was only interested in analysing the acid product. If he simultaneously monitored the enantioenrichment of both starting material and product a greater understanding of kinetic resolution could have been accomplished much earlier than proved later to be the case.

The lipase CAL-B, extracted from the yeast *Candida antarctica*, has been widely used in the transesterification of *sec*-alcohols.³⁰ CAL-B is a serine hydrolase and the reaction mechanism involves a two-step process (Figure 1.3). In the first step, the serine amino acid attacks the ester substrate *via* the first transitional state to give the first alcohol product and the acyl enzyme intermediate. In the second step the acyl enzyme is attacked by the second alcohol substrate *via* the second transition state to form the acylated alcohol product and the free enzyme. The reaction is base-catalysed by serine (Ser105) acting as the nucleophile. It has been proposed that the nucleophilicity of the serine moiety is enhanced by the charge relay that forms with histidine (His224) and aspartic acid (Asp187) through a general acid base type mechanism (Figure 1.3).^{31,32} In kinetic resolution only the second transition state is significant, this is when the chiral

information embedded in the enzyme will induce discrimination against the less favoured alcohol antipode.

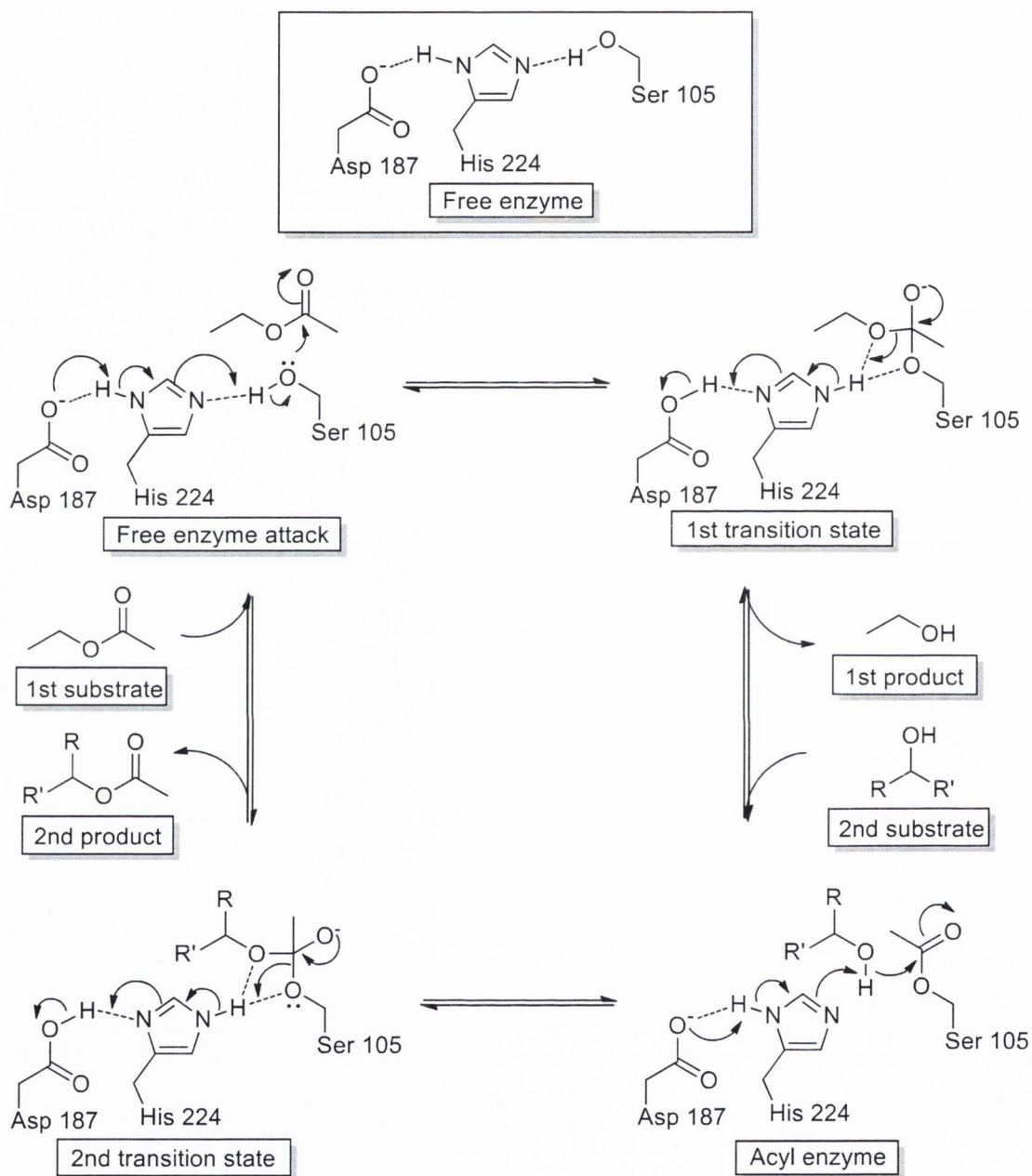
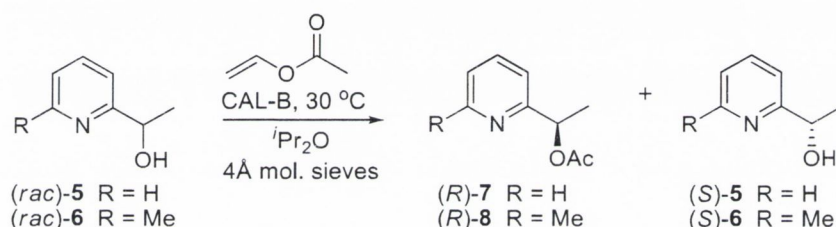


Figure 1.3 Reaction mechanism for the transesterification of *sec*-alcohols with CAL-B.³¹

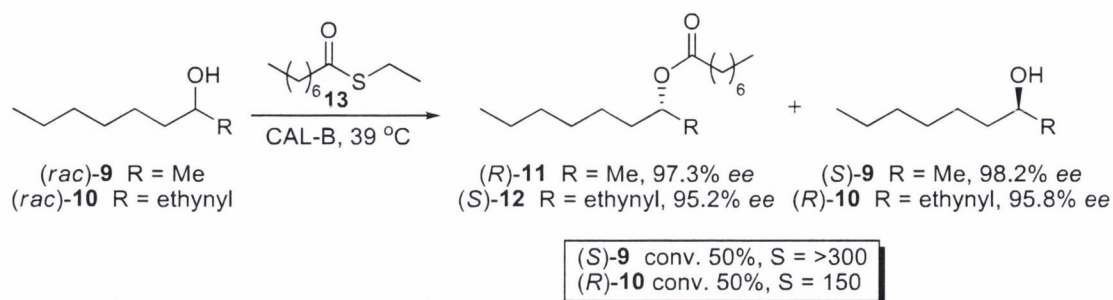
Uenishi *et al.* used CAL-B in the kinetic resolution of 1-(2-pyridyl)- and 1-[6-(2,2'-bipyridyl)]ethanols.³³ Pyridylethanols and bipyridylethanols are of significant interest to chemists because they form the basic structure of many biologically active

compounds,³⁴ and optically active forms have widespread application as ligands in metal catalysis.³⁵ Uenishi screened several lipase enzymes; (*Mucor miehei*), AK (*Pseudomonas sp.*), PS (*Pseudomonas cepacia*), and CAL-B (*Candida antarctica* lipase), all of which gave the same stereo configuration but CAL-B gave the best enantioselectivities and chemical yields for both the acetate and alcohol. The reactions were carried out at 30 °C in *iso*-propyl ether using vinyl acetate as the acylating agent (Scheme 1.3). The 1-(pyridin-2-yl)ethanol ((*rac*)-**5**) was recovered in 47% yield and 99% *ee* after four hours reaction time, equating to a selectivity factor of greater than 500. The methyl substituted equivalent 1-(6-methylpyridin-2-yl)ethanol ((*rac*)-**6**) was also recovered in 47% yield and 97% *ee*, giving it a selectivity factor of 278, but the reactivity of (*rac*)-**6** was considerably slower with a reaction time of 46 hours.



Scheme 1.3 KR of pyridylethanols with *Candida antarctica* lipase (CAL-B).³³

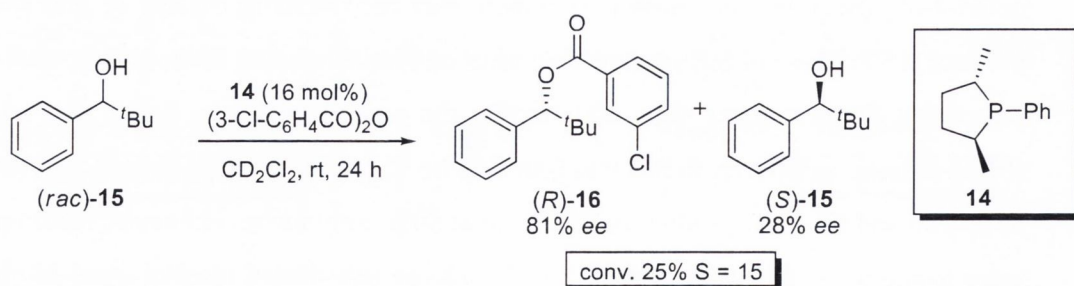
Lipase-catalysed kinetic resolution can also be very effective in the acylation of aliphatic *sec*-alcohols. Orrenius *et al.* used CAL-B in the acylative kinetic resolution of *sec*-alcohols with *S*-ethyl thiooctanoate (**13**, Scheme 1.4).³⁶ In the kinetic resolution of octan-2-ol ((*rac*)-**9**), the unreacted alcohol was recovered in 98.2% *ee* and the ester product at 97.3% *ee* at 50% conversion after one hour reaction time, corresponding to a selectivity factor greater than 300. Under the same conditions using non-1-yn-3-ol ((*rac*)-**10**), the selectivity factor was found to be 150, affording the remaining alcohol in 95.8% *ee* and the ester product in 95.2% *ee* at 50% conversion. However, reaction times were found to be four times longer for the alkyne substituted alcohol (*rac*)-**10** than the alkane alcohol (*rac*)-**9**. Orrenius also found other bulkier *sec*-alcohols containing *i*-propyl and *t*-butyl groups to be completely inactive in the acylative process after 170 hours reaction time.



Scheme 1.4 Acylative kinetic resolution of aliphatic *sec*-alcohols with CAL-B.³⁶

1.2.2.2 Asymmetric KR of alcohols catalysed by artificial organocatalysts

Artificial organocatalysis has gained huge popularity as an alternative to enzymatic catalysis in the kinetic resolution of alcohols over the past two decades.³⁷ There has been a large variety of chiral catalysts developed capable of enantioselective kinetic resolution of alcohols, such as; 4-*N,N*-dialkylaminopyridines, *N*-alkylimidazoles, *N*-heterocyclic carbenes, vicinal diamines, amidines and phosphines. One of the first practical methods was developed by Vedejs, achieving synthetically useful selectivity values of greater than 10 using a C_2 -symmetric chiral phosphine catalyst **14**.³⁸ In the kinetic resolution of 2,2-dimethyl-1-phenylpropan-1-ol ($(rac)\text{-15}$) with catalyst **14**, employment of 2.5 equivalents of 3-chlorobenzoic anhydride as the acylating agent led to a selectivity value of 15. This gave the ester product $(R)\text{-16}$ in 81% *ee* at 25% conversion (Scheme 1.5).



Scheme 1.5 KR of 2,2-dimethyl-1-phenylpropan-1-ol using a chiral phosphine catalyst.³⁸

1.2.3 4-*N,N*-dialkylaminopyridine catalysis

4-*N,N*-dialkylaminopyridine is an important nucleophilic catalyst capable of the promotion of a variety of synthetically important transformations such as acylation of alcohols and amines,^{39,40} silylation of alcohols,^{41,42} Dakin–West reaction^{43–45} and Baylis–Hillman reaction.^{46,47} Nucleophilic catalysis is the process by which a nucleophile can enhance the reaction rate relative to the non-catalysed reaction pathway by lowering the energy barrier in going from reactants to products. For this to happen the nucleophile must react faster with the electrophilic reagent than the substrate, and the subsequent ammonium intermediate must also be more reactive than the original electrophile. To fulfil these criteria the catalyst must be an effective nucleophile and also a good leaving group when reacted with the electrophile.

4-*N,N*-dialkylaminopyridine can catalyse the conversion of alcohols to the corresponding esters using acyl chlorides or anhydrides. In 1967 Litvinenko and Kirichenko,⁴⁸ found 4-(dimethylamino)pyridine (DMAP, **17**) to be ten thousand times more reactive than pyridine in the benzylation of 3-chloroaniline. Since its discovery DMAP has been exploited in a wide range of process susceptible to the influence of nucleophilic catalysis.⁴⁹ The advantage DMAP possesses over pyridine is its ability to stabilise the acylated pyridinium ion **18** through resonance donation of the 4-substituted nitrogen lone pair (Figure 1.4).

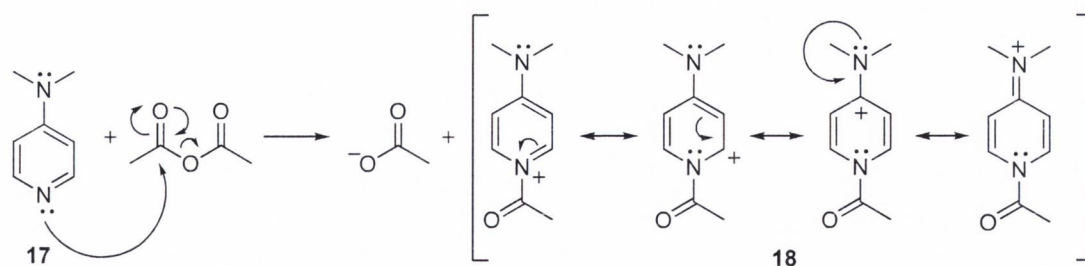


Figure 1.4 Reaction of DMAP with acetic anhydride and resonance stabilisation of acylated pyridinium ion.

In the acyl transfer of *sec*-alcohols, the acylated pyridinium ion **18** undergoes attack by the alcohol substrate with the loss of a proton, usually facilitated with the addition of base, to form the ester product (Figure 1.5).

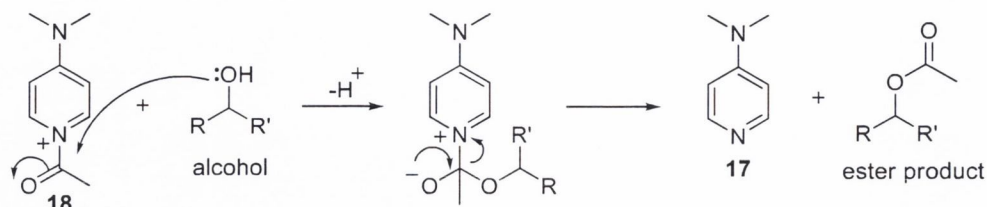


Figure 1.5 Reaction mechanism of *sec*-alcohol with acylated pyridinium ion **18**

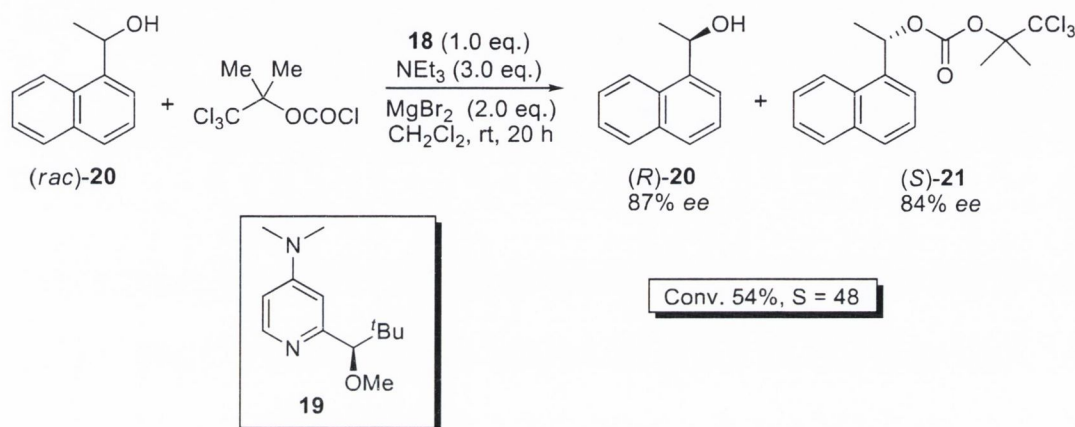
In developing a substituted DMAP catalyst capable of carrying out asymmetric transformations, the balance between reactivity and selectivity must be considered. Substitution of a chiral centre at the 2-position would appear to be the best approach to have maximum influence on the enantiodiscriminating event because of its close proximity to the catalytic site. However, studies by Litvinenko and Kirichenko found 2-methyl pyridine to be twenty fold less active than pyridine in the benzylation of benzyl alcohol.⁵⁰

The challenges associated with the design of chiral DMAP analogues for acylative kinetic resolution are thus clear: the catalyst must incorporate chiral information able to influence the outcome of the acylation, however the chiral substituent cannot be installed in close proximity to where the acylation takes place. Work done by Held and Zipse³⁹ on pyridine-based acyl-transfer catalysts found that varying the substituents at the 3 and 4-position of the pyridine ring with electron donating or electron withdrawing groups could impact the reactivity in a positive or negative manner, respectively, relative to DMAP.

1.2.3.1 The first chiral 4-*N,N*-dialkylaminopyridine catalyst

In 1996 Vedejs and Chen⁵¹ reported the kinetic resolution (KR) of racemic *sec*-alcohols using the first asymmetric DMAP analogue **19** (Scheme 1.6). The results were very promising with yields from 20 – 44% with the ester product being recovered in 76 to

94% *ee*, corresponding to selectivity values ranging from 11 to 53. The major drawback with this experiment was the requirement for stoichiometric amounts of catalyst **19** as well as 2 equivalents of Lewis acid and 3 equivalents of amine to activate the acylated intermediate. Although this experiment paved the way for chiral substituted DMAP analogues, the positioning of the chiral moiety at the 2-position severely reduced catalyst reactivity.



Scheme 1.6 KR of *sec*-alcohol (*rac*)-**20** using 2-substituted chiral DMAP catalyst **19**.⁵¹

1.2.3.2 Planar-chiral 4-*N,N*-dialkylaminopyridine catalysts

In developing a chiral DMAP catalyst, the planes of symmetry within the molecule must be considered. DMAP has two planes of symmetry, one in the *xy*-plane and one in the *zx*-plane, **17** (Figure 1.6). Therefore in the acylated pyridinium ion **18** (Figure 1.6) there is one plane of symmetry in the *xy*-plane. The pyridinium ion can be approached by a reactant from the front face or the back face at the Bürgi-Dunitz angle without any restriction or differentiation. In order for DMAP to function as an asymmetric catalyst the planes of symmetry must be eliminated. Using a planar chiral catalyst developed by Fu and co-workers,⁵² as an example, a fused cyclopentadiene (Cp) ring at the 2 and 3 position of the pyridine ring to form a bicyclic ring system which eliminated the *zx*-plane of symmetry, leaving just the *xy*-plane, **22** (Figure 1.6). Further addition of an FeCp moiety in the *xy*-plane generates a molecule with no planes of symmetry, affording the DMAP (π -heterocycle) FeCp complex **23**.

Elimination of the symmetry within the nucleophilic species does not necessarily guarantee that the molecule will be capable of asymmetric catalysis, but it is a criterion which limits possible modes of approach of the oncoming substrate. The acylated pyridinium ion **24** (Figure 1.6), is a representation of the crystal structure determined by Fu and co-workers.⁵³ This model shows the acyl group in the *s-cis* conformation, (i.e. the larger methyl substituent of the acyl group avoids steric clash with the ferrocenyl moiety) indicating that the approach of the substrate would be less hindered on the side opposite the Cp moiety. The substrate must also approach at an angle of attack of 107° (Bürgi-Dunitz angle), which potentially can be restricted on the lower face depending on the size of the substituents on the bottom Cp ring. Therefore the substrate's least hindered path of approach will be from the upper face opposite the Cp substituted ring, represented by arrow **a** (**24** Figure 1.6).

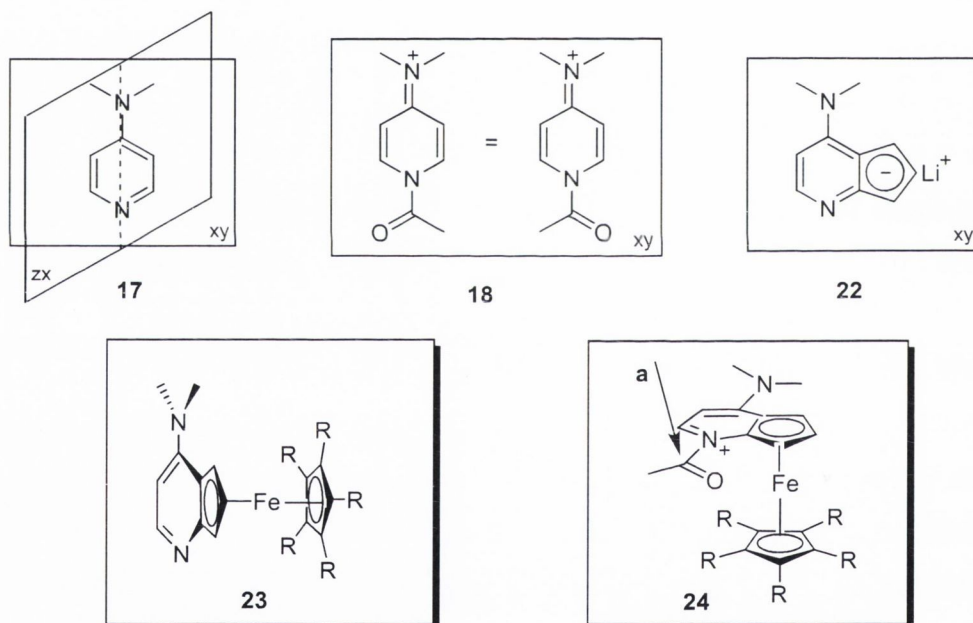


Figure 1.6 Representation of the symmetry planes of DMAP and substituted DMAPs

Based on the principles outlined *vide supra*, Fu and co-workers developed a range of planar-chiral nucleophilic catalyst analogues (Figure 1.7).^{54,55}

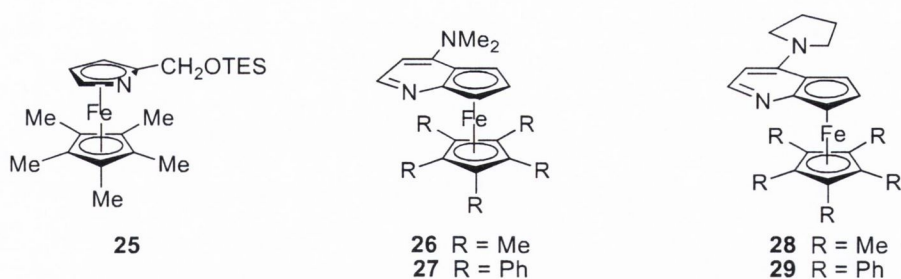
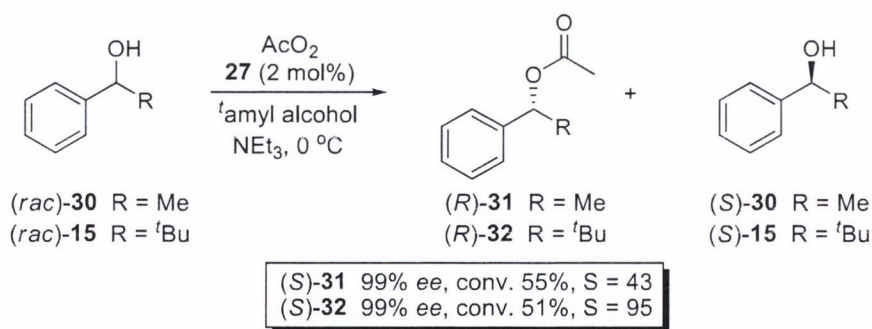


Figure 1.7 Planar-chiral catalyst analogues developed by Fu and co-workers.^{54,55}

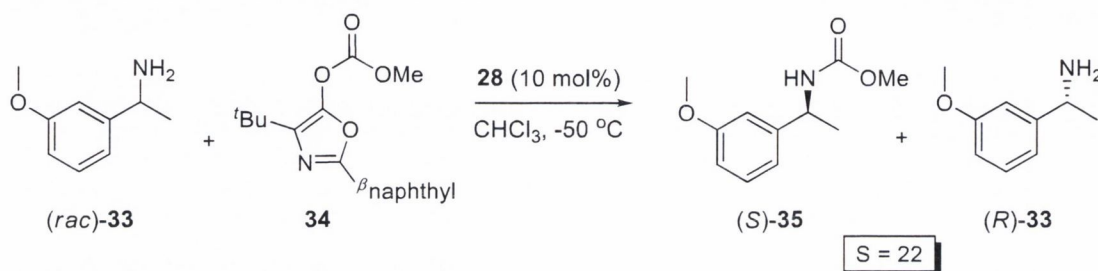
Catalyst **25** was found to be inactive in the acylation of secondary alcohols with acetic anhydride. This was presumably due to the presence of the bulky triethylsilane substituent in the 2-position of the pyrrole moiety. Catalyst **26** exhibited poor selectivity in the kinetic resolution of 1-phenylethanol (*(rac)*-**30**) using acetic anhydride, resulting in a meagre selectivity factor of 1.7. Catalyst **27** proved a lot more successful under optimised conditions with selected *sec*-alcohols substrates, where a selectivity value of 95 was observed in acylative kinetic resolution of α -*t*-butylbenzyl alcohol (*(rac)*-**15**) with acetic anhydride (Scheme 1.7). These results were in line with expectations, as the phenyl substituted Cp ring on the lower face of the DMAP moiety provides better steric hindrance than the methyl substituted Cp ring.



Scheme 1.7 KR of *sec*-alcohols *(rac)*-**15** and *(rac)*-**30** using planar-chiral catalyst **27**.⁵⁵

The kinetic resolution of amines has conventionally proved challenging due to their high reactivity towards acyl chlorides and anhydrides. Fu and co-workers overcame this problem with the use of a less electrophilic *tert*-leucine derived *O*-carbonyloxyazlactone **34** (Scheme 1.8).⁵⁶ In the carbamation of primary amines, synthetically useful

selectivity values between 11 and 27 were accomplished.⁵⁶ Using 10 mol% of catalyst **28** (Figure 1.7), the kinetic resolution of 1-(3-methoxyphenyl)ethanamine (*rac*-**33**) via carbamation with *O*-carbonlyoxyazlactone **34** in chloroform at -50 °C, afforded the methyl 1-(3-methoxyphenyl)ethylcarbamate (*S*-**35**) product with a selectivity factor of 22 (Scheme 1.8), which is a highly desirable selectivity factor in the non-enzymatic kinetic resolution of amines.



Scheme 1.8 KR of amine (*rac*-**33**) using planar-chiral catalyst **28**.⁵⁶

Fu proposed a mechanism that involves the initial fast formation of the ion-pair with the rapid reaction of the 4-pyrrolidino catalyst (PPY*) **28** with the *O*-carbonlyoxyazlactone. This is followed by the slower enantioselective-determining step of methylcarbonate transfer to the amine to afford the carbamate product (Figure 1.8).

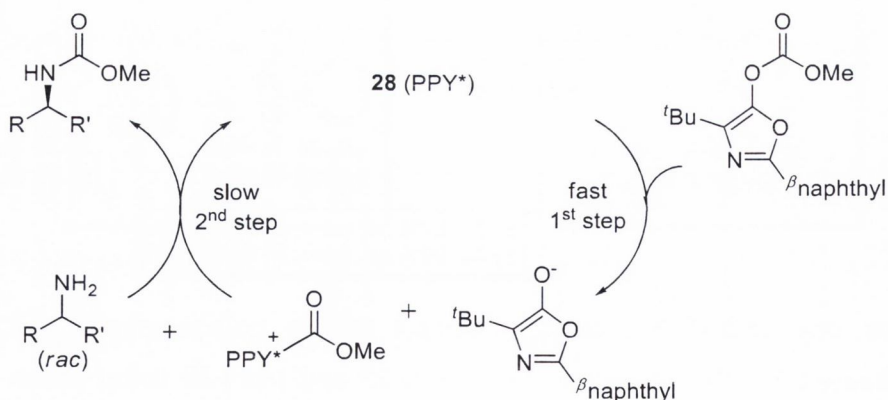
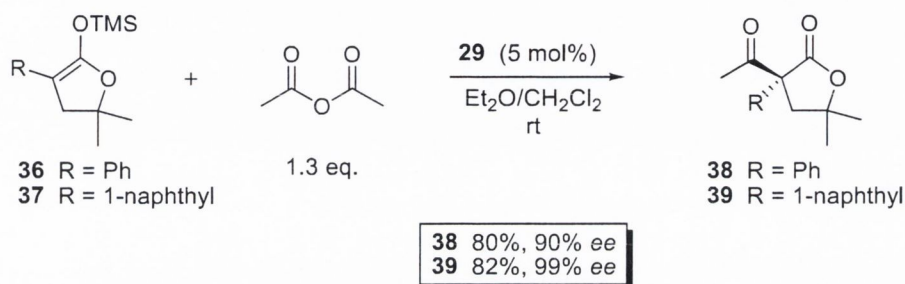


Figure 1.8 Proposed mechanism for the KR of amines using catalyst **28**.⁵⁶

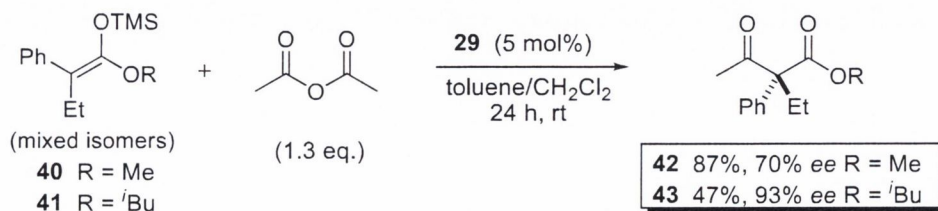
Fu and co-workers also reported the *C*-acylation of silyl ketene acetals with acetic anhydride using the DMAP (π -heterocycle) FeCp complexes **26** – **29** (Figure 1.7). This

reaction is a variation on the Steglich rearrangement where *O*-acylated azlactones are rearranged to their *C*-acylated isomers with the formation of a new chiral quaternary carbon centre.^{57,58} Catalyst **29** proved the most enantioselective on a range of substrates with *ee* values from 76 to 99% and excellent overall yields.⁵⁹ Of particular interest is the 1-naphthyl silyl acetal which was recovered in 82% yield and 99% *ee*, demonstrating a very high degree of enantioselectivity and yield (Scheme 1.9).



Scheme 1.9 *C*-acylation of cyclic silyl ketene acetals with planar-chiral catalyst **29**.⁵⁹

Fu and co-workers also found that they could further extend the reaction scope to include acyclic silyl ketene acetals.⁶⁰ In the *C*-acylation of **40** (as mixed isomers) with acetic anhydride using 5 mol% catalyst loading, yields of 87% and moderate enantioselectivity of 70% *ee* were achieved. Whereas the slightly bulkier *iso*-butyl analogue **41** substituent gave 93% *ee*, however conversion was greatly diminished to 47% (Scheme 1.10). One of the most significant factors in this reaction is the fact that mixed isomers undergo *C*-acylation to afford the 1,3-dicarbonyl product as opposed to the *O*-acylated product, which is much more common, with good enantioselectivity. The ratio of the *cis/trans* isomers does not appear to affect enantioselectivity, whereas cyclic silyl ketene acetals are largely dependent on the α -ester substituent to achieve enhanced enantioselectivity (Scheme 1.10).

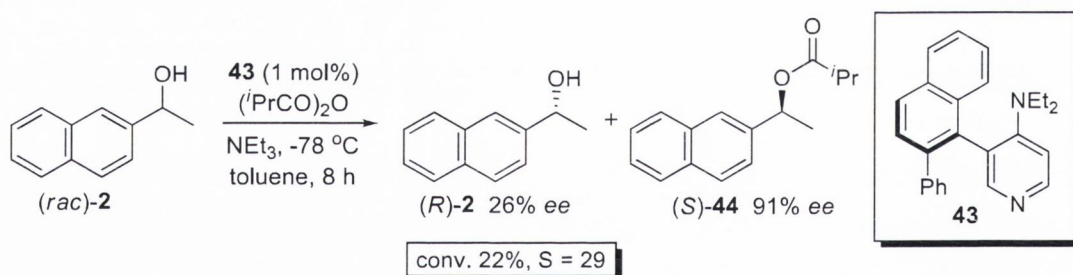


Scheme 1.10 *C*-acylation of acyclic silyl ketene acetal with chiral-planar catalyst **29**.⁶⁰

Catalysts **26** – **29** have also demonstrated excellent versatility in a number of other asymmetric transformations: the kinetic resolution of allylic and propargylic *sec*-alcohols,^{54,61} desymmetrisation of *meso*-diols,^{62,63} enantioselective synthesis of *N*-protected amino acids from racemic azlactones⁶⁴ and asymmetric ester synthesis from ketenes.^{65,66}

1.2.3.3 Atropisomer 4-*N,N*-dialkylaminopyridine catalysts

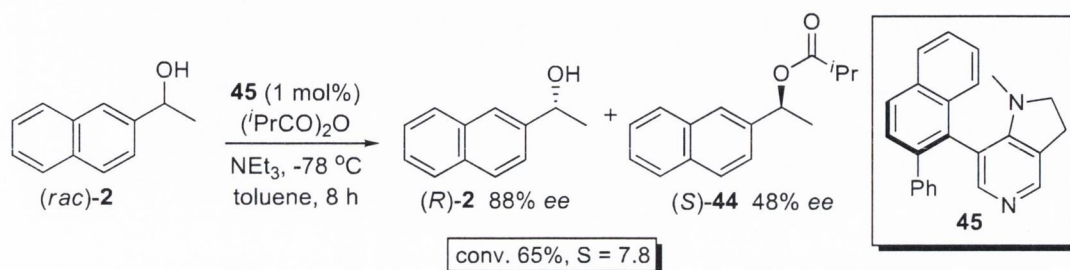
In 1989 Spivey *et al.* reported the synthesis of a class of atropisomeric DMAP analogues⁶⁷ and later demonstrated the conformational stability of the biaryl analogues as a class of novel nucleophilic catalysts.⁶⁸ The utilisation of these chiral *C*-3 substituted DMAP catalysts proved very effective in the kinetic resolution of *sec*-alcohols. Of the various atropisomeric catalyst analogues, the biaryl substituent 2-phenylnaphthalene proved the most effective in kinetic resolution using isobutyric anhydride.⁶⁹ Catalyst **43** was capable of promoting the acylative kinetic resolution of (*rac*)-**2** with selectivity values of up to 29 being achieved. This afforded the ester product in 91% *ee* at 22% conversion (Scheme 1.11).



Scheme 1.11 Acylative KR of *sec*-alcohols using the DMAP analogue **43**.⁶⁸

Of particular interest to this class of DMAP analogues is the reactivity versus selectivity conundrum which is evident from small structural modifications to the catalyst. The DMAP (catalyst analogue **45** Scheme 1.12) exhibited greater reactivity than its structural counterpart **43** (Scheme 1.11), 65% and 22% conversion respectively under the same reaction conditions, which only differ in the steric bulk at the 4-amino substituent. The relative difference in reactivity is to be expected based on the findings of Zipse *et al.*,³⁹ who found a tricyclic DMAP analogue substituted at the 3 and 5-

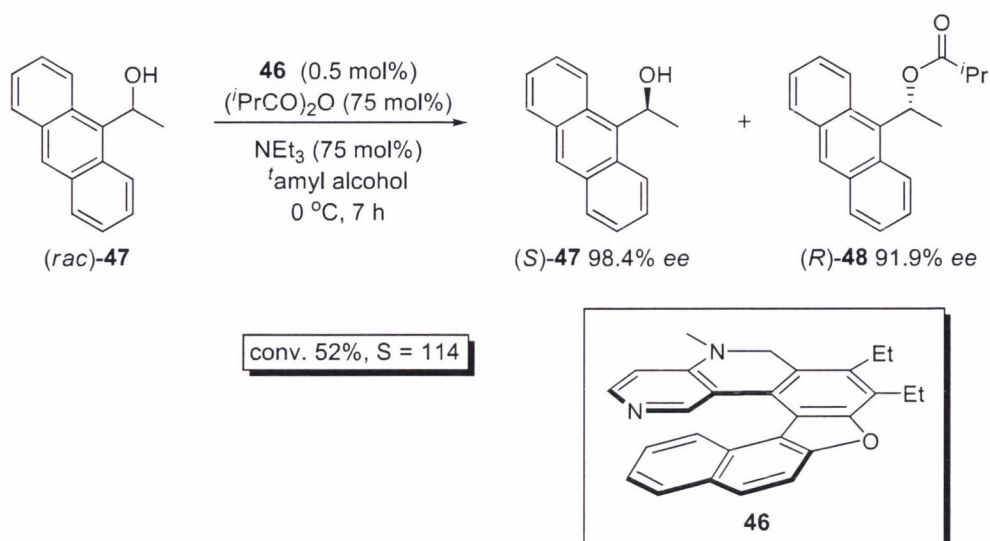
position to be more reactive than unsubstituted DMAP or 4-pyrrolidinopyridine (PPY). However, this reactivity increment is far outweighed by the loss in selectivity, where a modest selectivity value of 7.8 was achieved in the kinetic resolution of (*rac*)-**2** (Scheme 1.12) catalysed by **45**, whereas a selectivity value of 29 was achieved under the same reaction conditions using catalyst **43** (Scheme 1.11).



Scheme 1.12 Acylative KR of *sec*-alcohols using DMAP analogue **45**.⁶⁹

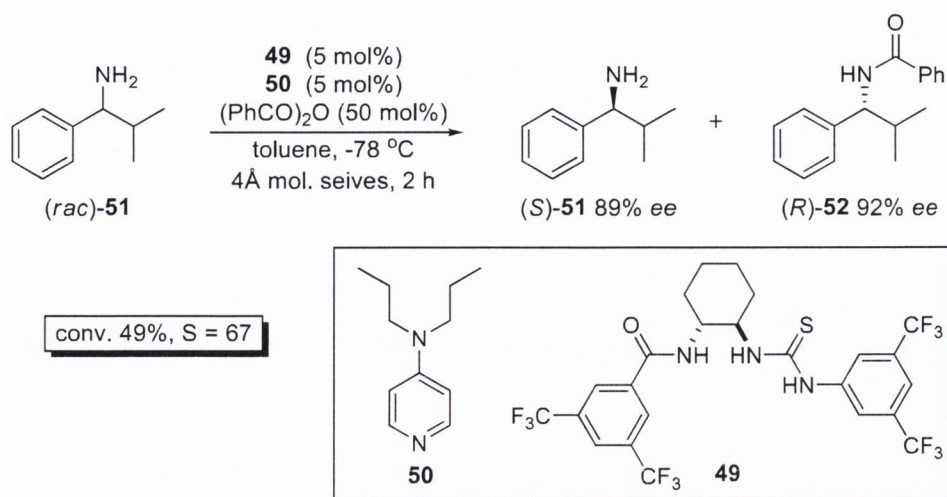
1.2.3.4 Important developments in 4-*N,N*-dialkylaminopyridine catalysts

Helicenes have been known to chemists for over one hundred years⁷⁰ although little was understood about their chemistry until Newman and co-workers reported the synthesis and resolution of hexahelicene in the 1950s.⁷¹⁻⁷³ Since then helicenes have been developed for a number of practical application such as optical and electronic materials^{74,75} and telomerase inhibitors.⁷⁶ The first reported catalyst based on a helical chiral ligand was in 1997 by Reetz and co-workers.⁷⁷ In 2011 Carbery *et al.* reported the development of a heliceneoidal DMAP-based catalyst capable of achieving good to excellent selectivity values for a number of aryl alkyl *sec*-alcohols.⁷⁸ Of particular interest was 1-(anthracen-9-yl)ethanol ((*rac*)-**47**), where the heliceneoidal DMAP-based catalyst **46** was found to promote the acylative kinetic resolution of *sec*-alcohol (*rac*)-**47** using isobutyric anhydride at 0 °C in a 7 hour reaction time to give the alcohol and ester products in 98.4% *ee* and 91.9% *ee*, respectively, equating to a selectivity value of 116 at 51% conversion (Scheme 1.13).



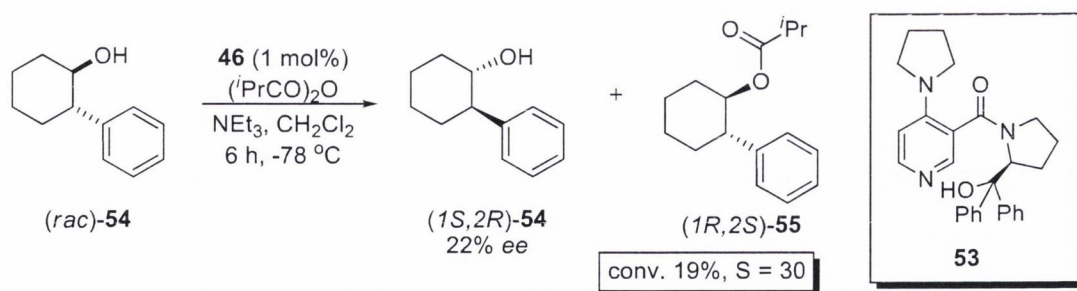
Scheme 1.13 KR of *sec*-alcohols promoted by a helicoidal DMAP-based catalyst.⁷⁸

In 2012 Seidel *et al.* reported a dual catalyst system capable of the kinetic resolution of a variety of primary amines using an achiral DMAP-based catalyst and a hydrogen bonding thiourea-amide catalyst.⁷⁹ Previous studies conducted by Seidel and co-workers demonstrated that a chiral vicinal dithiourea hydrogen bonding catalyst developed by Nagasawa⁸⁰ along with DMAP were capable of resolving racemic amines with good selectivity values.⁸¹ Further development of the reaction lead Seidel and co-workers to investigate the thiourea-amide hydrogen bonding catalyst **49** (Scheme 1.14), which enabled Seidel and co-workers to improve selectivity values at lower catalyst loading.⁸² This dual catalyst reaction sequence proved very successful in the kinetic resolution of amines, which lead Seidel to investigate alternative nucleophilic catalysts to DMAP. The optimal nucleophilic catalyst proved to be the DMAP-based catalyst **50** (Scheme 1.14), with selectivity values ranging from 21 for 2,2-dimethyl-1-phenylpropan-1-amine to 67 for the less sterically hindered analogue 2-methyl-1-phenylpropan-1-amine. The acylative kinetic resolution of 2-methyl-1-phenylpropan-1-amine (*(rac)*-**51**) using benzoic anhydride at -78 °C in toluene, with 5 mol% of each catalysts **49** and **50** gave the amine (*(S)*-**51**) in 89% *ee* and the amide (*(R)*-**52**) in 92% *ee* after two hours reaction time, corresponding to a selectivity value of 67 (Scheme 1.14).



Scheme 1.14 KR of racemic primary amines promoted by dual catalysts **49** and **50**.⁷⁹

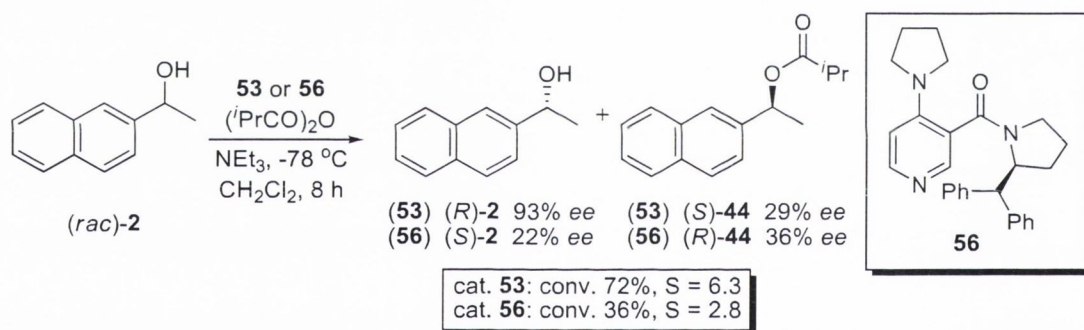
In 2005 Connon *et al.* reported a class of chiral DMAP-based catalysts capable of moderate to good selectivity values in the acylative kinetic resolution of *sec*-alcohols across a range of substrates and in the kinetic resolution of Baylis–Hillman adducts.⁸³⁻⁸⁵ The straightforward catalyst synthesis, from available precursors and the ability to tune the catalyst pendant aromatic substituents make it both practical and versatile. The kinetic resolution of *trans*-2-phenylcyclohexanol (*(rac)*-**54**) with isobutyric anhydride at $-78\text{ }^\circ\text{C}$ employing 1 mol% of catalyst **53** resulted in a selectivity value of 30 (Scheme 1.15).



Scheme 1.15 KR of 2-phenylcyclohexanol with chiral DMAP derived catalyst **53**.⁸⁵

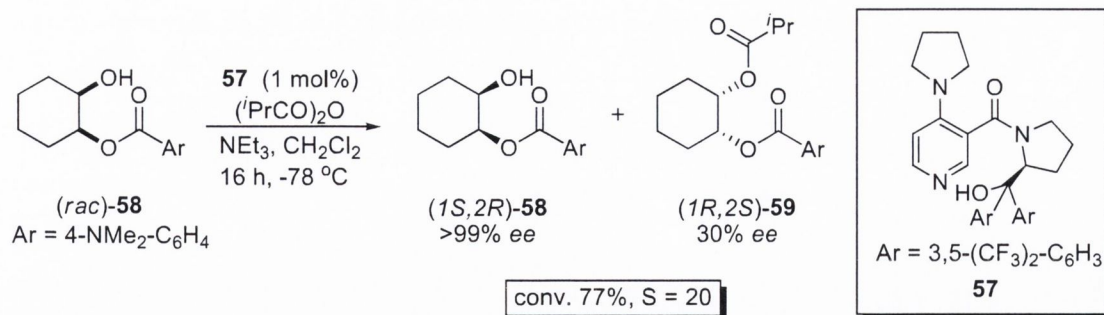
The presence of the hydroxy group on the chiral pendant unit was found to be of fundamental importance in determining the stereochemical outcome, enantioselectivity and reaction rate. In the kinetic resolution of 1-(naphthalen-2-yl)ethanol (*(rac)*-**2**) with

catalyst **53** at $-78\text{ }^{\circ}\text{C}$ using isobutyric anhydride, a selectivity value of 6.3 was achieved, affording the alcohol in 93% *ee* at 72% conversion. Under identical reaction conditions employing the reduced catalyst analogue **56**, a meagre selectivity value of 2.8 with a significantly lower conversion of 36% was achieved (Scheme 1.16). Moreover, the removal of the hydroxy group resulted in a reversal of the stereochemical outcome; catalyst **53** favoured the acylation of (*S*)-**2** whereas catalyst **56** marginally favoured the acylation of (*R*)-**2** (Scheme 1.16). The reversal of the sense of stereoinduction by the removal of the hydroxy functional group would indicate that it plays an important role in the enantiodiscriminating event, either through hydrogen bond stabilisation or general acid-base catalysis. Bentley *et al.* have demonstrated that alcohols can participate as both nucleophiles and general base catalysts in the acylation of primary alcohols by aroyl and α -chloro acid chlorides.^{86,87} This would suggest that substituting the hydroxy group with alternative functional groups could have the potential for further enhancement of catalytic performance.



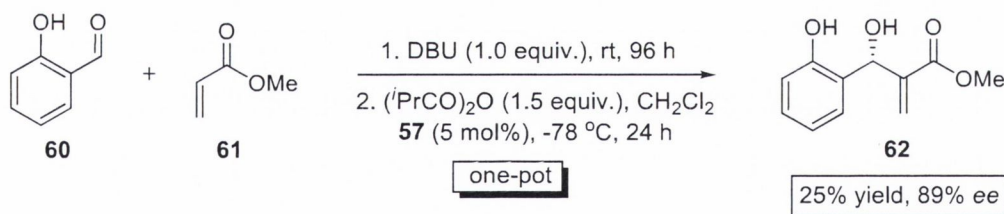
Scheme 1.16 KR of (*rac*)-**2** using chiral DMAP catalyst analogues **53** and **56**.⁸⁵

Consequently, Cannon *et al.* also found that alternative aryl functionalities on the chiral pendent moiety could greatly enhance catalyst selectivity. Exchanging the phenyl moieties for 3,5-*bis*(trifluoromethyl)benzene substituents resulted in a dramatic increase in enantioselectivity for choice substrates. In the kinetic resolution of the mono-protected diol (*rac*)-**58** with catalyst **56** using isobutyric anhydride a modest selectivity value of 9.4 was achieved,⁸⁵ whereas under the same reaction conditions employing 1 mol% catalyst loading of **57** a selectivity value of 20 was achieved, affording the alcohol in 99% *ee* at 77% conversion (Scheme 1.17).⁸³



Scheme 1.17 KR of mono-protected diol (*rac*)-**58** with catalyst **57**.⁸³

Catalyst **57** was also found to be proficient in the kinetic resolution of Baylis–Hillman (BH) adducts.⁸³ The DBU promoted Baylis–Hillman one-pot reaction afforded the racemic BH alcohol adduct **62** after 96 hours at room temperature (Scheme 1.18). The kinetic resolution of *sec*-alcohol BH adducts flanked by two sp² hybridised carbon substituents have conventionally proved difficult due to the similarities of the chemical environment. Catalyst **57** was capable of promoting the kinetic resolution of adduct **62** using isobutyric anhydride at -78 °C in 24 hours, affording the product in 25% yield and 89% ee (Scheme 1.18). Interestingly, DBU showed little competitive acylation at reduced temperatures.



Scheme 1.18 One-pot KR of Baylis–Hillman adduct using catalyst **57**.⁸³

One of the great advantages associated with catalysts **53**, **56** and **57** is their straightforward synthesis from readily available precursors such as 4-chloro pyridine and proline derivatives. Another advantage is the C-3-substituted pyridine moiety, which can potentially be converted to other functional groups that could further augment catalyst enantioselectivity.

1.2.3.5 Overview of alternative 4-*N,N*-dialkylaminopyridine catalysts

There are a number of other important chiral 4-*N,N*-dialkylaminopyridine catalysts; analogues that have been developed over the past two decades that have achieved moderate to excellent selectivity values in the kinetic resolution of *sec*-alcohols.^{16,19,88,89} The mechanism by which enantioselectivity is achieved differs depending on substituents and their positioning relative to the catalytically active site. Significant contributions to this field of research include those from Levacher,⁹⁰ Vedejs,⁹¹ Yamada,⁹² Inanaga,⁹³ Diez,⁹⁴ Johannsen,⁹⁵ Fuji and Kawabata,⁹⁶ and Campbell⁹⁷ (Figure 1.9).

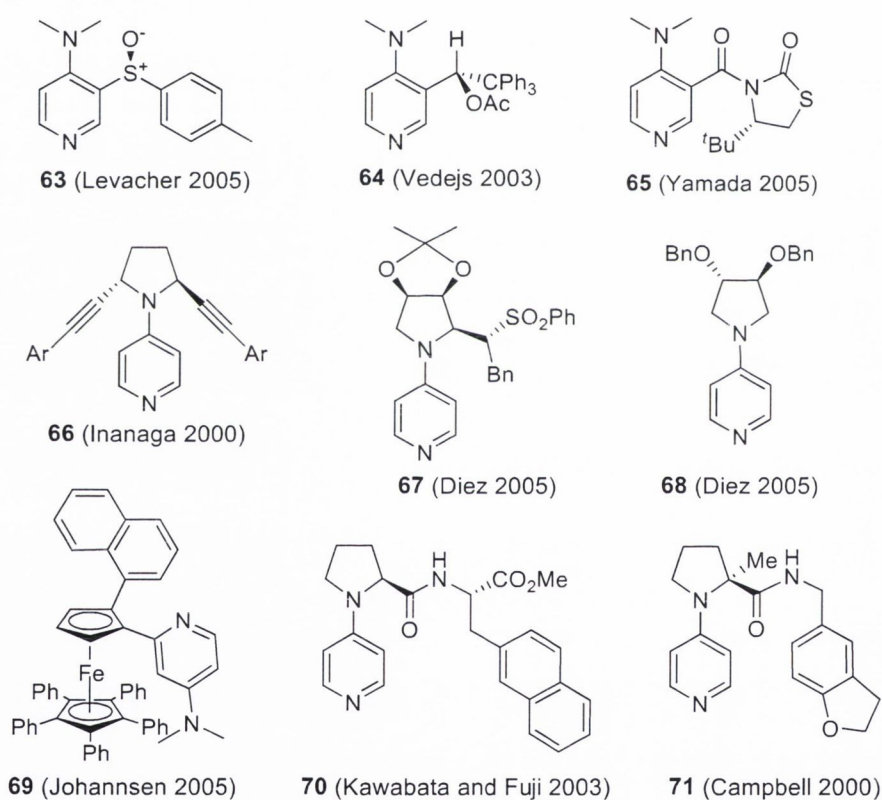
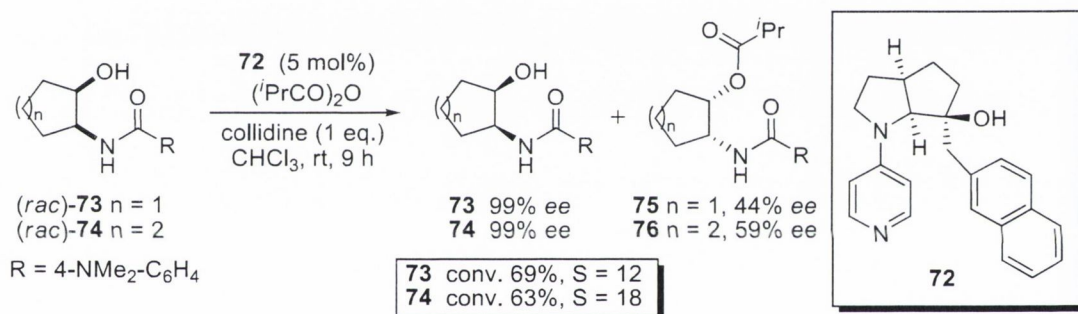


Figure 1.9 Alternative chiral DMAP derived catalysts of significant importance

1.2.3.6 Substituted 4-*N,N*-dialkylaminopyridine catalysts operating via an ‘induced-fit’ mechanism

In 1997 Fuji *et al.* reported a class of chiral PPY catalyst capable of promoting the kinetic resolution of mono-protected *cis*-diols.⁹⁸ Selectivity values varied from 2.4 for a *para*-nitrobenzoate protected *cis*-1,2-cyclohexane diol substrate to 12.3 for a dimethyl aminobenzoate protected *cis*-1,2-cyclohexane diol substrate. In 2001 Fuji reported the kinetic resolution of *N*-protected *cis*-amino alcohols utilising the same catalyst species with greater success.⁹⁹ Using 5 mol% of catalyst **72** a selectivity value of 18 was observed in the acylation of *N*-protected *cis*-2-aminocyclohexanol (*rac*)-**74** and a selectivity value of 12 for the corresponding reaction involving the *N*-protected *cis*-2-aminocyclopentanol (*rac*)-**73** (Scheme 1.19).



Scheme 1.19 KR of *N*-protected cyclic amino alcohols promoted by catalyst **72**.⁹⁹

Interestingly, despite the remote chiral substituent of catalyst **72** being situated at the 4-position of the pyridine ring, the catalyst still displayed a high degree of enantioselectivity. Fuji rationalised this observation in terms of the catalyst's alternating conformation. ¹H-NMR spectroscopic studies showed that the unbound catalyst **A** adopted an open conformation where the naphthalene ring and the pyridine ring lie apart from each other. When the catalyst undergoes acylation, the acyl pyridinium ion **B** adopts a closed conformation where the naphthalene ring lies in close proximity to the pyridine ring due to the attractive π - π interactions between the two aromatic species (Figure 1.10). This conformational change is described as ‘induced fit’ mechanism where the catalyst can readily undergo acylation in the open conformation, where upon

acylation adopts the closed conformation intermediate that controls the enantioselectivity of the subsequent acylation of alcohols.

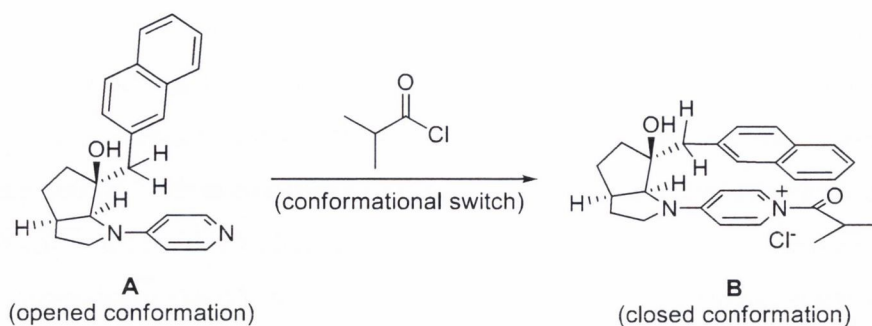
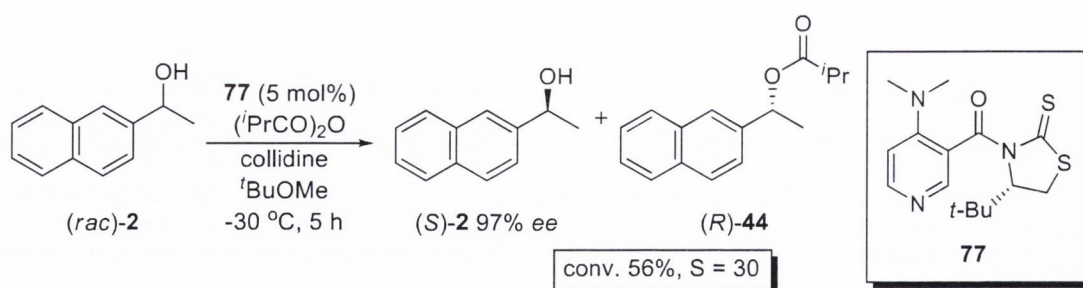


Figure 1.10 Catalyst **72**: ‘induced fit’ mechanism conformational switch.⁹⁹

In 2005 Yamada *et al.* reported a class of chiral DMAP catalysts that could deliver moderate to good enantioselectivity in the acylative kinetic resolution of *sec*-alcohols.⁹² The 3-substituted *tert*-butylthiazolidin-2-one and *tert*-butylthiazolidine-2-thione chiral DMAP analogues demonstrated equal enantioselectivity, but the *tert*-butylthiazolidine-2-thione substituted catalyst **77** exhibited higher catalyst turnover. In the kinetic resolution of 1-(naphthalen-2-yl)ethanol (*rac*-**2**) with catalyst **77** using isobutyric anhydride at -30 °C and employing 5 mol% catalyst loading gave the alcohol product in 97% *ee* at 56% conversion, corresponding to a selectivity value of 30 (Scheme 1.20).



Scheme 1.20 KR of *(rac)*-**2** with 3-*tert*-butylthiazolidine-2-thione substituted DMAP catalyst **77**.⁹²

Based on previous observations by Yamada and co-workers concerning the stabilisation of 3-substituted dihydropyridines with thiocarbonyl derivatives,^{100,101} Yamada proposed

a mechanism that paralleled Fuji's induced fit conformational switch. Yamada demonstrated that catalyst **77** also underwent a conformational change upon acylation. The interaction observed by Yamada differed from the π - π interaction observed by Fuji in that it was an interaction between the acylated pyridinium ring and a thiocarbonyl substituent (Figure 1.11). Yamada proposed that the attractive cation- π stabilisation effect positioned the *tert*-butyl chiral pendant in relatively close proximity to the pyridinium ring nitrogen atom, whereby it could influence the path of the approaching alcohol and bring about enantio-discrimination to achieve kinetic resolution.

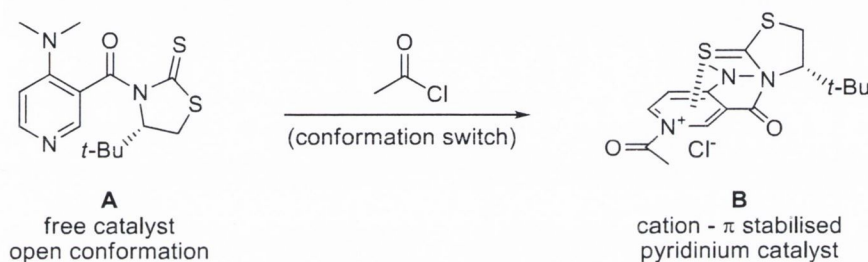


Figure 1.11 Catalyst **77**: conformation stabilised by cation- π attractive interaction.¹⁰¹

Investigations by Cannon *et al.* to explain the mechanistic behaviour of catalyst **53** and **56** led to the discovery of some interesting conformational changes, similar to those observed by Fuji⁹⁶ and Yamada.⁹² Although an X-ray crystal structure of the acylated pyridinium ion was not possible, the X-ray crystal structure of the corresponding benzylated catalyst **53** was obtained.⁸⁵ This revealed that the amide pendant moiety adopted a (counter-intuitive) *s-cis* rotameric conformation where the diaryl tertiary alcohol substituent is orientated towards the H-2 of the pyridine ring. ¹H-NMR spectroscopy studies revealed that the acylated pyridinium catalyst also orientated in a similar conformation, indicated by a strong *upfield* shift observed for the H-2 proton. This is associated with one of the aryl rings being in close proximity to the H-2 proton of the pyridine ring (Figure 1.12).⁸⁵ Similar ¹H-NMR chemical shifts were also observed for the reduced diaryl substituent **56**. The resulting π - π or π -H interactions are responsible for the conformational behaviour which allows catalysts **53** and **56** to induce enantio-discrimination in the kinetic resolution of alcohols, where catalyst **53** has the added advantage of a hydroxy moiety in the vicinity of the nucleophilic ring nitrogen to potentially participate in hydrogen bonding.

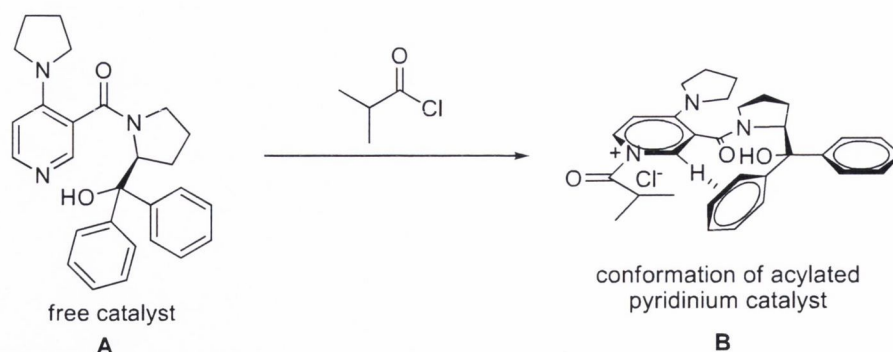


Figure 1.12 The *s-cis* rotameric conformation of the acylated pyridinium catalyst **56**.⁸⁵

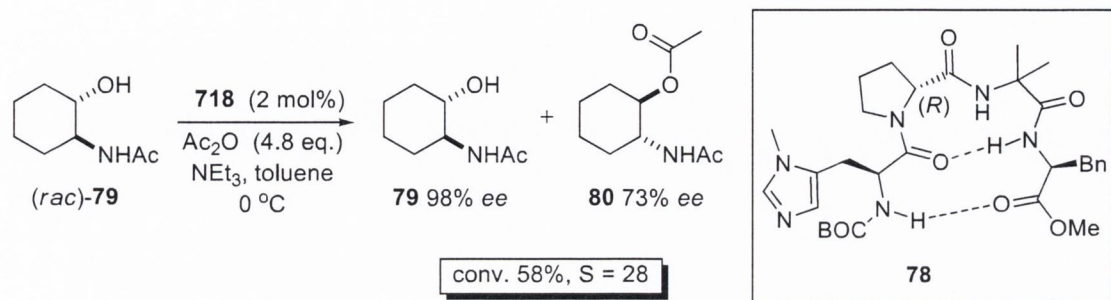
1.2.4 Non-pyridine nucleophilic chiral organocatalysts

Chiral 4-*N,N*-dialkylaminopyridine based catalysts have been demonstrated to be highly versatile promoters of acylative kinetic resolution, exhibiting a broad reaction/substrate scope and substrate versatility.^{19,23,88,102} There are also a number of other examples of non-pyridine based nucleophilic chiral organocatalysts such as; *N*-alkylimidazoles, *N*-heterocyclic carbenes, vicinal diamines, amidines and phosphines, which are comparable and in some instances surpass those of their pyridine counterparts.

1.2.4.1 *N*-Alkylimidazole based catalysis

N-alkylimidazoles have been found to be capable of catalysing the acylation of alcohols with acetic anhydride through a nucleophilic mechanism,¹⁰³ thereby qualifying them as a potential class chiral kinetic resolution catalyst. Miller *et al.* utilised this property in the synthesis of a class of catalysts based on polypeptides, where the catalytic site was an *N*-alkylimidazole of a histidine moiety.¹⁰⁴ The tetrapeptide **78**, containing the unnatural amino acid D-proline was employed in the kinetic resolution of *N*-acyl *trans*-2-aminocyclohexanol (*rac*-**79**) with acetic anhydride. The enantioenriched alcohol and ester product were recovered in 98% *ee* and 73% *ee*, respectively, at 58% conversion, corresponding to a selectivity value of 28 (Scheme 1.21). Miller demonstrated that changing the central D-proline moiety to the naturally occurring amino acid L-proline caused a dramatic shift in selectivity with the opposite sense of stereoinduction, where the L-proline tetrapeptide catalysed kinetic resolution of *N*-acyl *trans*-2-

aminocyclohexanol with acetic anhydride only gave a selectivity value of 3. Miller accounted for both for these changes as being associated with hydrogen bonding interactions both within the peptide chain and between the peptide and the substrate.



Scheme 1.21 Acylation of *N*-acyl aminoalcohol with *N*-alkylimidazole catalyst **78**.¹⁰⁴

Miller also demonstrated that the use of catalysts with longer peptide chains could lead to higher levels of enantioselectivity.¹⁰⁵ The octapeptide catalyst **81** (Figure 1.13) was employed in the kinetic resolution of the *N*-acyl *trans*-2-aminocyclohexanol (*(rac)*-**79**) using acetic anhydride at 0 °C, resulting in a selectivity value of 51. Whereas employing tetrapeptide **78** under the same reaction conditions the selectivity factor was only 28. The octapeptide catalyst **82** (Figure 1.13) only differs from **81** in the absolute configuration of the proline moiety, although under identical reaction conditions in the kinetic resolution of (*rac*)-**79** with acetic anhydride, catalyst **82** only achieved a selectivity value of 7.

Miller accounted for the large differences in selectivity been associated with hydrogen bonding within the peptide molecule. He suggested that the most important feature of the polypeptide catalysts was the β -hairpin structure, where the conformational rigidity afforded by the β -hairpin was the key to determining the enantio-differentiation. NMR spectroscopic studies by Miller and co-workers demonstrated that the D-proline based octapeptide catalyst **81** and the tetrapeptide catalyst **78** adopted the β -hairpin conformation, whereas their L-proline derived isomers did not.

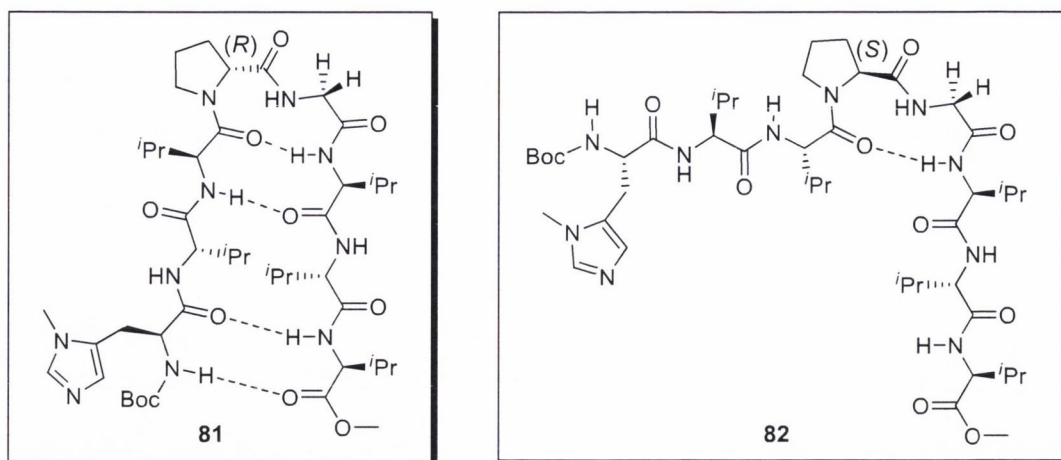
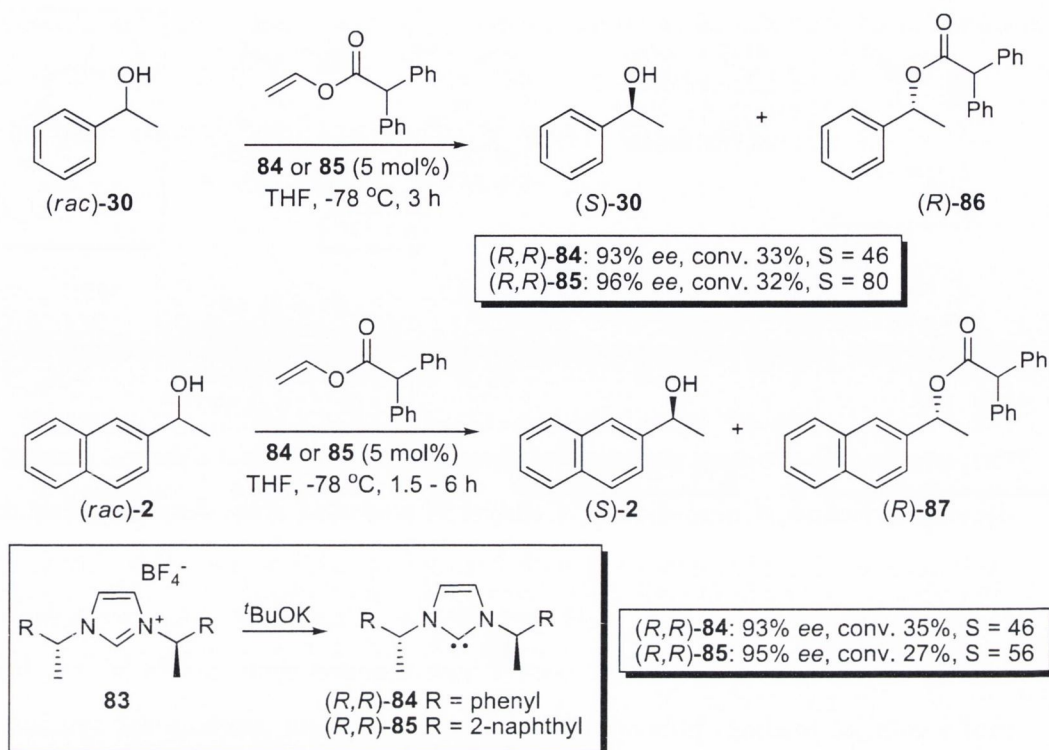


Figure 1.13 The β -hairpin structured octapeptide catalyst **81** and catalyst **82**.¹⁰⁵

1.2.4.2 *N*-Heterocyclic carbene based catalysis

Carbenes have been known to promote transesterification reactions (when used in stoichiometric quantities) since 1994.¹⁰⁶ In 2005 Maruoka *et al.* reported the kinetic resolution of *sec*-alcohols using a class of *C*-2 symmetrical *N*-heterocyclic carbenes.¹⁰⁷ In the kinetic resolution of 1-phenylethanol (*rac*-**30**) with vinyl diphenylacetate as acylating agent, catalyst **84** gave the acylated product (*R*)-**86** in 93% *ee* after 33% conversion, corresponding to a selectivity value of 46. Under identical reaction conditions employing the more sterically hindered catalyst **85** gave the corresponding ester product in 96% *ee* after 32% conversion, corresponding to a selectivity value of 80 (Scheme 1.22).

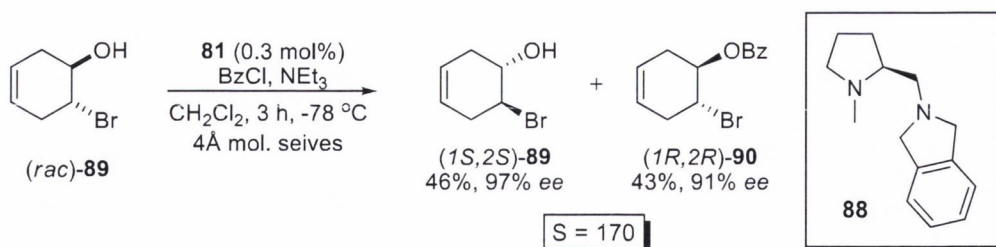
In the kinetic resolution of the bulkier *sec*-alcohol naphthalene derivative (*rac*-**2**) with vinyl diphenylacetate using catalyst **84**, the ester product (*R*)-**87** was determined to be 93% *ee* after 35% conversion, corresponding to a selectivity value of 46. Curiously this is the same selectivity value as that observed for the 1-phenylethanol substrate using the same catalytic species, although reaction times were halved to 1.5 hours. Catalyst **85** was also employed in the kinetic resolution of the naphthalene derived alcohol (*rac*-**2**) with vinyl diphenylacetate, where the ester product (*R*)-**87** was determined to be 95% *ee* after 27% conversion, corresponding to a selectivity value of 56 (Scheme 1.22).



Scheme 1.22 KR of *sec*-alcohols using *C*-2 symmetrical *N*-heterocyclic carbenes.¹⁰⁷

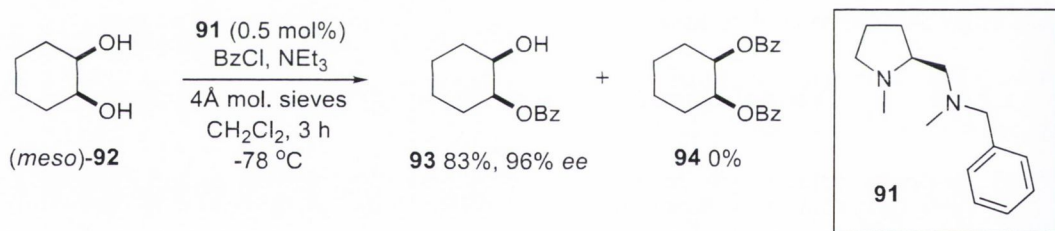
1.2.4.3 Vicinal diamine based catalysis

In 1999 Oriyama *et al.* reported the use of the L-proline derived diamine catalyst **88** in the kinetic resolution of *sec*-alcohols, achieving selectivity values from 4 to 170.^{108,109} The acylative kinetic resolution of 6-bromocyclohex-3-enol (*(rac)*-**89**) with benzoyl chloride employing catalyst **88** at 0.3 mol% catalyst loading, led to a highly desirable selectivity value of 170, affording the alcohol in 97% *ee* and the ester product in 91% *ee* at close to 50% conversion (Scheme 1.23). Catalyst **88** also exhibited a high degree of activity, with reaction times of three hours at $-78\text{ }^\circ\text{C}$. In general catalyst **88** proved very successful in the kinetic resolution of cyclic *cis*- β -substituted *sec*-alcohols, with selectivity values ranging from 27 in the case of ethyl ester substituted cyclohexanol and 160 in the case of *cis*-2-phenylcyclohexanol.



Scheme 1.23 KR of 6-bromocyclohex-3-enol with vicinal diamine catalyst **88**.^{108,109}

Oriyama and co-workers also demonstrated the use of vicinal diamine catalysts in the desymmetrisation of *meso*-diols.¹¹⁰ Catalyst **91** was used in the desymmetrisation of *cis*-cyclohexane-1,2-diol (*meso*)-**92** with benzoyl chloride to give 2-hydroxycyclohexyl benzoate product **93** in 83% yield and 96% *ee*. Catalyst **91** also demonstrated high activity at sub-zero temperatures, with 3 hour reaction times at -78 °C employing 0.5 mol% catalyst loading. Interestingly, catalyst **91** did not promote the synthesis of the undesirable *meso*-di-acylated *vic*-diol **94** (Scheme 1.24).

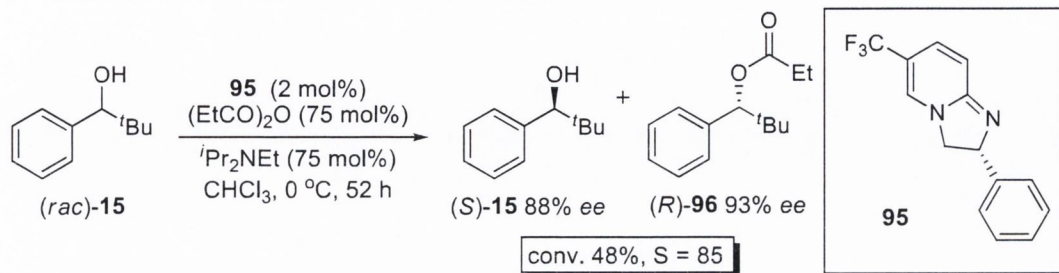


Scheme 1.24 Desymmetrisation of *meso*-diol **92** with the vicinal diamine catalyst **91**.¹¹⁰

1.2.4.4 Amidine based catalysis

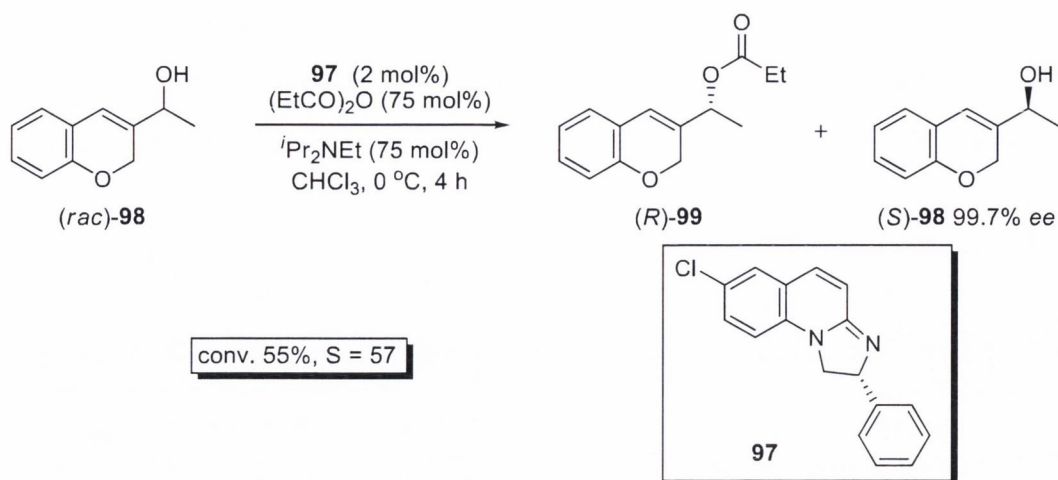
In 2004 Birman *et al.* reported a new class of chiral organocatalyst based on a (*R*)-2-phenyl-2,3-dihydroimidazo[1,2-*a*]pyridine (PIP) core which proved very effective in the kinetic resolution of *sec*-alcohols.¹¹¹ Initial structure-activity relationship studies involving the 6-substituted bromo, nitro and trifluoromethyl analogues revealed the trifluoromethyl derivative to be the most reactive and enantioselective, demonstrating good yields and selectivity values across a range of aryl alkyl substrates. Employing catalyst **95** at 2 mol% loading in the kinetic resolution of (*rac*)-**15** at 0 °C with

propionic anhydride and *N,N*-diisopropylethylamine as an auxiliary base, afforded the initial alcohol (*S*)-**15** in 88% *ee* and the ester product (*R*)-**96** in 93% *ee* at 48% conversion, corresponding to a selectivity value of 85 (Scheme 1.25).



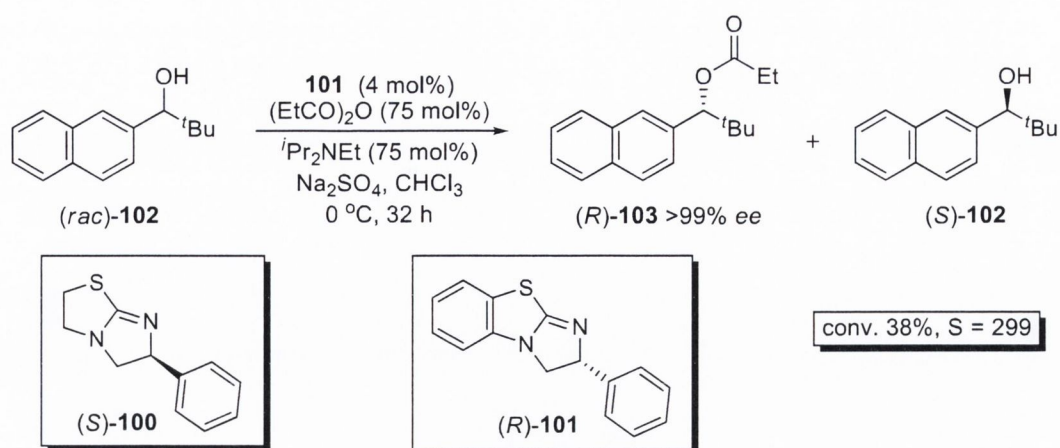
Scheme 1.25 KR of (*rac*)-**15** using the first generation chiral amidine catalyst **95**.¹¹¹

In 2005 Birman *et al.* extended the scope of the CF₃-substituted PIP catalyst **95** to include the kinetic resolution of cinnamyl alcohols, with moderate to good selectivity values ranging from 6 to 26 achieved for selected substrates.¹¹² Birman proposed a π - π stacking interaction between the catalyst and substrate as being fundamentally important in promoting enantio-discrimination. This led Birman and co-workers to further develop the PIP catalyst core with the use of a quinoline derived precursor that could maximise the π - π stacking interaction between substrate and catalyst. This modification proved very successful: the employment of (*R*)-7-chloro-2-phenyl-1,2-dihydroimidazo[1,2-*a*]quinoline (Cl-PIQ) catalyst **97** lead to greatly enhanced enantioselectivities compared to its CF₃-substituted PIP counterpart in the kinetic resolution of both cinnamyl and aryl alkyl *sec*-alcohols. In the kinetic resolution of 1-(2*H*-chromen-3-yl)ethanol ((*rac*)-**98**) with propionic anhydride at 0 °C, the use of catalyst **97** resulted in 55% conversion after 4 hours (2 mol% catalyst loading). This delivered a highly desirable selectivity value of 57, affording the alcohol (*S*)-**98** in 99.7% *ee* (Scheme 1.26).



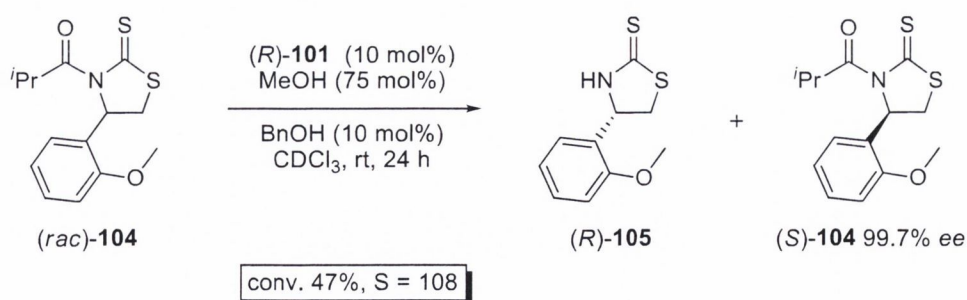
Scheme 1.26 KR of cinnamyl alcohol $(rac)\text{-98}$ using chiral amidine catalyst **97**.¹¹²

In 2006 Birman *et al.* demonstrated the use of the commercially available tetramisole $(S)\text{-100}$ as a proficient enantioselective acylation catalyst, leading to selectivity values ranging from 25 to 31 in the kinetic resolution of aryl alkyl *sec*-alcohols.¹¹³ This revelation motivated Birman and co-workers to develop a chiral organocatalyst that incorporated both the catalytic properties of the imidothioate tetramisole core with the established reactivity of the 6-substituted PIP catalyst structure. The additional aromatic moiety resulted in the benzotetramisole (BMT) catalyst $(R)\text{-101}$, which proposed stronger $\pi\text{-}\pi$ and $\pi\text{-cation}$ interactions than its tetramisole counterpart and consequently resulted in a superior enantioselective catalyst. Catalyst $(R)\text{-101}$ has proven to be one of the most broad spectrum enantioselective amidine catalyst to date in the kinetic resolution of aryl alkyl and propargylic *sec*-alcohols.^{113,114} In the kinetic resolution of 2,2-dimethyl-1-(naphthalen-2-yl)propan-1-ol ($(rac)\text{-102}$) with propionic anhydride at 0 °C, catalyst $(R)\text{-101}$ was capable of promoting the reaction to afford the ester product $(R)\text{-103}$ in >99% *ee* at 38% conversion after a 32 hour reaction time, corresponding to a selectivity value of 299 (Scheme 1.27).



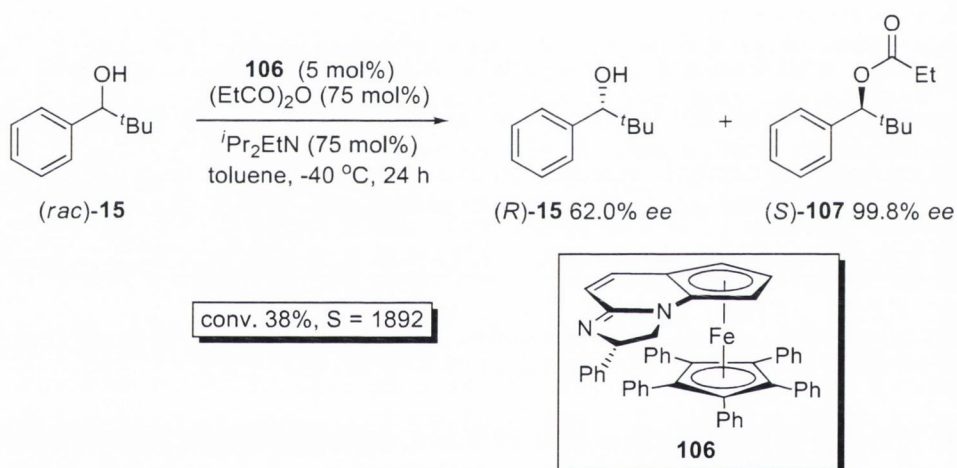
Scheme 1.27 KR of $(rac)\text{-102}$ using benzotetramisole (BMT) catalyst $(R)\text{-101}$.¹¹⁴

Nonenzymatic kinetic resolution of racemic alcohols, thiols and amines has been largely dominated by the enantioselective acylation process *via* acyl transfer catalysts,^{19,40,115,116} whereas, enantioselective deacylation has generally been dominated by enzyme catalysis.^{117,118} In 2013 Birman *et al.* reported the kinetic resolution of *N*-acyl-thiolactams *via* catalytic enantioselective deacylation using the amidine-based catalyst $(R)\text{-101}$ (Scheme 1.27) with synthetically useful selectivity values.¹¹⁹ The deacylation of the *N*-acyl-thiolactam $(rac)\text{-104}$ was accomplished using methanol (75 mol%) and benzyl alcohol (10 mol%) in deuterated chloroform at room temperature with 10 mol% catalyst loading (Scheme 1.28). This gave the unreacted *N*-acyl-thiolactam $(S)\text{-104}$ in 99.7% *ee* at 47% conversion after 24 hours, corresponding to a selectivity value of 108 (Scheme 1.28).



Scheme 1.28 KR of *N*-acyl-thiolactams *via* catalytic enantioselective deacylation.¹¹⁹

In 2010 Fossey *et al.* reported a class of catalyst that combined both the properties of Fu's ferrocene-based planar-chiral catalyst^{120,121} and Birman's amidine-based catalyst^{122,123} that was capable of promoting the kinetic resolution of *sec*-alcohols with selectivity values comparable to those of enzymatic catalysts.¹²⁴ The ferrocene-based planar-chiral amidine catalyst **106** was investigated in the acylative kinetic resolution of a number of selected aryl alkyl carbinols, but the most significant result was achieved using 2,2-dimethyl-1-phenylpropan-1-ol ((*rac*)-**15**). The acylative kinetic resolution of (*rac*)-**15** using propionic anhydride in toluene at -40 °C with 5 mol% catalyst loading gave the alcohol and corresponding ester product in 62.0% and 99.8% *ee*, respectively, at 38% conversion after 40 hours reaction time. This equated to a very impressive selectivity value of 1892, which set the new standard in nonenzymatic acylative kinetic resolution (Scheme 1.29).



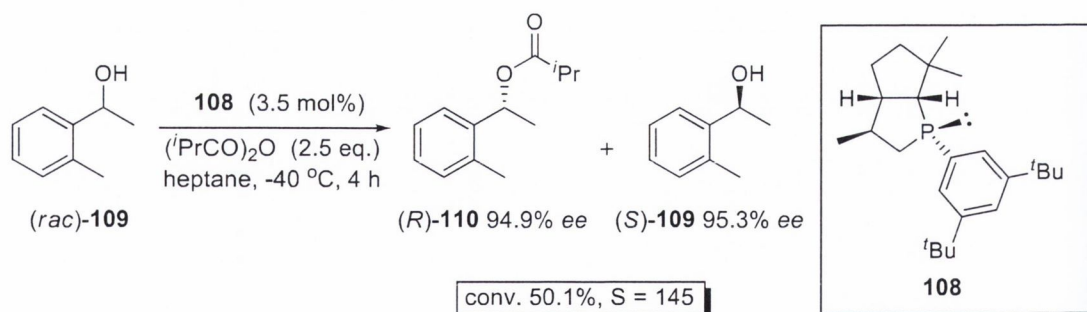
Scheme 1.29 KR of (*rac*)-**15** using ferrocene-based planar-chiral amidine catalyst **106**.¹²⁴

1.2.4.5 Phosphine based catalysis

In 1993 Vedejs *et al.* reported the use of tributylphosphine in the catalytic acylation of cyclohexanol using three equivalents of acetic anhydride in dichloromethane, resulting in a vigorous exothermic reaction.¹²⁵ This led Vedejs and co-workers to comparatively investigate the activity of tributylphosphine with that of DMAP in the acylation of methanol with benzoic anhydride at 23 °C under identical reaction conditions. Initial

results revealed tributylphosphine to be over three times more reactive than DMAP, however in the presence of excess triethylamine base, catalytic reactivity was almost identical. This paved the way for the use of tributylphosphine as a nonbasic alternative to DMAP in the acylation of alcohols.

In 1996 Vedejs *et al.* reported a *C*-2 symmetrical chiral phosphine catalyst that could promote the acylative kinetic resolution of 2,2-dimethyl-1-phenylpropan-1-ol, achieving a selectivity value of 15 (Section 1.2.2.2).³⁸ Subsequently in 1999 Vedejs and co-workers reported a series of chiral phosphine catalysts comprising of a *P*-aryl-2-phospha-bicyclo[3.3.0]octanes (PBO) skeletal structure that proved far superior in the acylative kinetic resolution of *sec*-alcohols than their *C*-2 symmetric counterparts.¹²⁶ The *bis*(3,5-*tert*-butyl)-PBO catalyst **108** proved to be the optimal structure, capable of promoting the kinetic resolution of *sec*-alcohols resulting in selectivity values from 31 to 369 across a range of aryl alkyl substrates at -40 °C. Employing catalyst **108** in the kinetic resolution of (*rac*)-**109** using isobutyric anhydride at -40 °C, afforded the alcohol (*S*)-**109** in 95.3% *ee* and the ester product (*R*)-**110** in 94.9% *ee* after a 4 hour reaction, corresponding to a selectivity value of 145 at 50.1% conversion (Scheme 1.30).

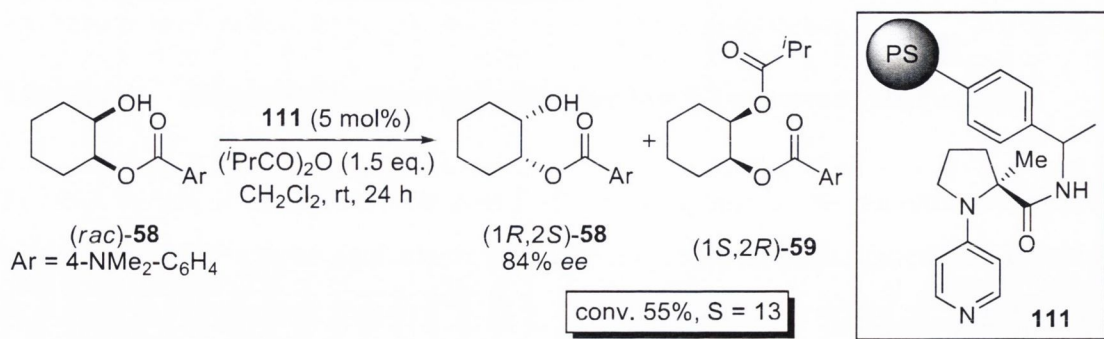


Scheme 1.30 Acylative KR of (*rac*)-**109** using the chiral phosphine catalyst **108**.³⁸

1.3 Heterogeneous catalysis

Heterogeneous catalysis is of huge importance to the chemical industry and has gained increasing popularity in the past few decades.¹²⁷ The driving force behind this has been both commercial and environmental; it is desirable to recover and recycle any catalyst of high monetary value and/or high toxicity.¹²⁸ One of the drawbacks associated with heterogeneous catalysis is the tendency for the catalysts to be less active than their homogeneous counterparts due to the limited mass transfer of the reactants from solution to the surface of the solid support. Recycling can also be restricted due to the catalyst leaching or support degradation.

The use of polymer-based and inorganic solid supports in the immobilisation of catalysts to enable recycling is a technique that has received much attention.^{12,129} The successful immobilisation of DMAP with enhanced reactivity relative to the homogeneous phase has also been accomplished,¹³⁰ however, this is an exception to the rule. The immobilisation of asymmetric DMAP derivatives has also been accomplished. In 2003, Campbell *et al.* reported the first heterogeneous chiral DMAP analogue for use in the kinetic resolution of *sec*-alcohols with good selectivity values of up to 13.0.¹³¹ These values are only slightly lower than that observed in the homogeneous phase, where selectivity values of up to 13.2 were achieved.⁹⁷ In the kinetic resolution of the mono-protected diol (*rac*)-**58** using isobutyric anhydride at room temperature with 5 mol% of the Merrifield Resin¹³² supported catalyst **111**, a selectivity value of 13 was achieved in a 24 hour reaction time. This afforded the initial alcohol in 84% *ee* at 55% conversion (Scheme 1.31).



Scheme 1.31 KR of (*rac*)-**51** with the polymer supported DMAP-based catalyst **111**.¹³¹

1.3.1 Background and history

Heterogeneous catalysis was known as early as the 1770s, when Joseph Priestley documented the dehydration of ethanol using metals.¹³³ Although, at the time, the actual concept of catalysis was not yet conceived, as a result the phenomenon was thought to be more of a curiosity rather than an actual scientific process. It was not until 1817 that the first conceptual evidence of heterogeneous catalysis was recognised when Sir Humphrey Davy discovered that coal gas (hydrogen and carbon monoxide gas) could be oxidised on the surface of a hot platinum wire in aerobic conditions without producing a flame, causing the metal wire to glow long after the initial flame had extinguished.¹³⁴ Davy deduced that the coal gas combined with oxygen on the surface of the hot platinum wire where it produces enough heat to keep the wire incandescent. Davy also found that this process worked equally well with palladium wire, but not with iron, copper, silver or gold wires. This can be regarded as one of the first records of catalytic activity of metals.

In 1820, Edmund Davy, at the Royal Cork Institute¹³⁵ prepared a finely divided platinum gauze that was so reactive it was capable of oxidising alcohol under aerobic conditions at room temperature causing the metal gauze to glow with heat.¹³⁶ This discovery was further developed by the German chemist Johann Wolfgang Döbereiner in 1823 with the introduction of a spongy platinum metal that was capable of oxidising hydrogen gas at room temperature.¹³⁷ Döbereiner can also be credited with the first supported metal catalyst by moulding a mixture of platinum sponge and potter's clay into spherical balls.¹³⁸ This supported platinum catalyst proved to be an improvement on the platinum sponge used in the 'Döbereiner lamp'.

1.3.1.1 Solid supports commonly used in heterogeneous catalysis

The most prominent feature of solid supported-catalysts is their easy recovery; this can be achieved by filtration from the reaction mixture and ideally they can be reused until the catalyst is no longer active, therefore, the choice of support to fulfil this requirement is of great importance. There are numerous examples of solid supports over a wide range of materials such as organic polymer supports (polystyrenes, poly(ethylene-glycol), polyethylene and polyacrylamide) and inorganic solid-supports (silicas,

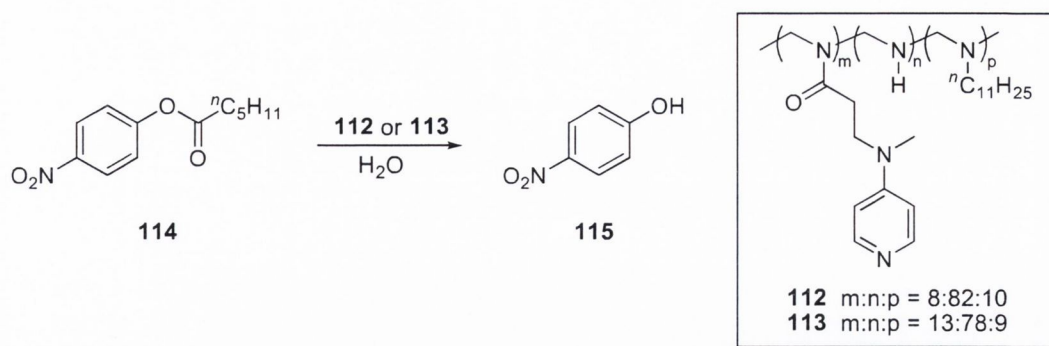
mesoporous solids, zeolites, and clays).¹³⁹ However, despite the diversity, there is no protocol to commend one as a general optimal support.¹²⁸

1.3.2 Polymeric supported catalysts

Polymeric supported catalysts have been of great research interest over the past few decades. This has been largely associated with the growing interest in asymmetric catalyst recovery.^{140,141} There are two basic strategies employed in the immobilisation of catalysts on polymeric supports; one involves solid-phase synthesis, where the catalyst or ligand is anchored to the functionalised insoluble support. There is a wide range of functionalised polymers commercially available for this purpose; chloromethyl, hydroxyl, amino, thiol and pyridine rings which can be utilised in the immobilisation of both metal and organocatalysts.¹⁴² Alternatively, the catalyst or ligand can be anchored through a copolymerisation with styrene and divinylbenzene.

1.3.2.1 Poly(ethylenimine)-supported catalysts

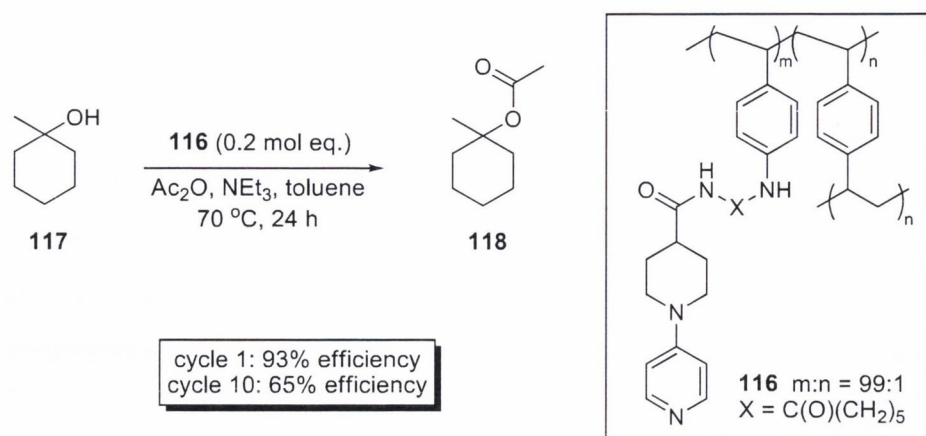
The first polymer supported DMAP analogues was reported Koltz *et al.* in 1979.¹⁴³ The supported catalysts were prepared using poly(ethylenimine) containing C₁₂H₂₅ adducts, coupled to 3-(methyl(pyridin-4-yl)amino)propanoic acid *via* the coupling reagent 1-ethyl-3-(3-dimethylaminopropyl)carbodiimide. The catalytic active sites were demonstrated to be 8% and 13% for polymer **112** and **113**, respectively (Scheme 1.32). Immobilised catalysts **112** and **113** performed better than DMAP under optimised condition in the hydrolysis of *p*-nitrophenyl caproate in water, with catalyst **113** demonstrating a higher reactivity rate. Koltz and co-workers did not report on the ability of the immobilised catalysts to be recycled.



Scheme 1.32 Hydrolysis of *p*-nitrophenyl caproate using polymer-supported catalysts **112** and **113**.¹⁴³

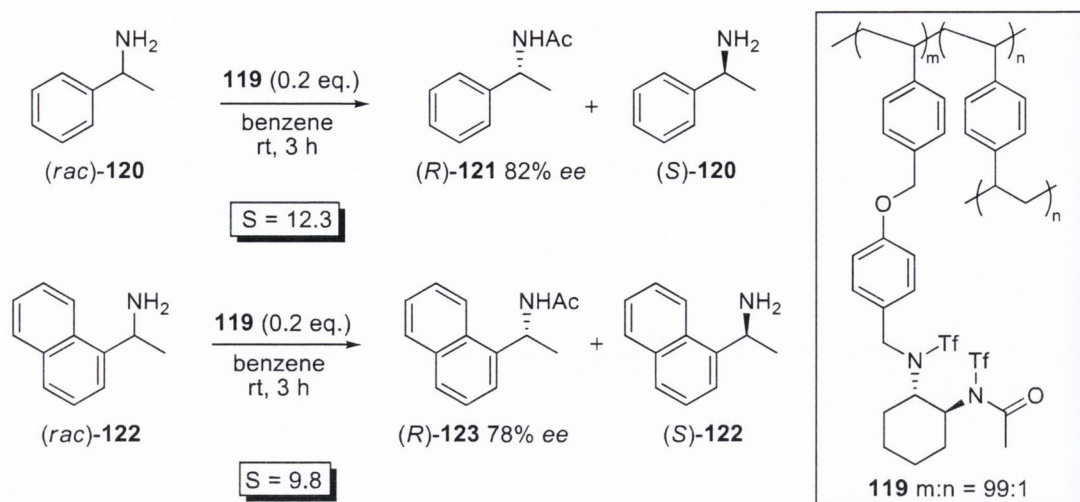
1.3.2.2 Polystyrene-supported catalysts

In 1988 Verducci *et al.* reported a class of polystyrene-supported DMAP derived catalysts anchored *via* a 4-substituted piperidine-4-carboxamide linker.¹⁴⁴ The 1% divinylbenzene (DVB) cross-linked heterogeneous catalyst **116** proved the most effective species studied, demonstrating to have 93% of the efficiency of DMAP in the acylation of 1-methylcyclohexanol (**117**) with acetic anhydride at 70 °C in a 24 h reaction time (Scheme 1.33). Catalyst loading also influenced efficiency where the optimum catalyst loading of 0.67 mass equivalents (mEq) was observed. A higher catalytic loading of 3.30 mEq was demonstrated to only have 61% of the efficiency of DMAP. This was rationalised in terms of catalytic self-inhibition, where the catalyst's nucleophilic pyridine interacts with the amide linker of an adjacent catalyst moiety. Catalyst **116** also proved to be recoverable and recyclable, although a 30% loss in efficiency was observed after 10 consecutive cycles.



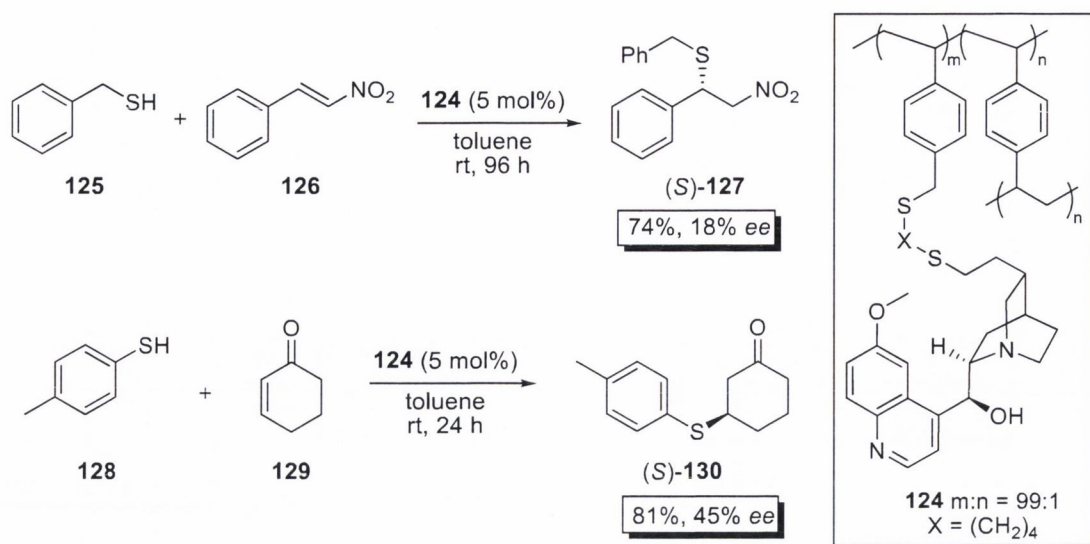
Scheme 1.33 Acylation of 1-methylcyclohexanol with supported catalyst **116**.¹⁴⁴

In 2005 Mioskowski *et al.* reported the synthesis of a polystyrene-supported vicinal disulfonamide reagent proficient in the acylative kinetic resolution of primary amines with synthetically useful selectivity values.¹⁴⁵ The *bis*-1,2-disulfonamide **119** was prepared from a 1% DVB cross-linked polystyrene support at a loading of 0.58 mmol/g. In the kinetic resolution of 1-phenylethanamine (*rac*)-**120** promoted by **119** at room temperature, a selectivity value of 12.3 was achieved, resulting in 82% *ee* for the recovered amide (*R*)-**121** (Scheme 1.34). The immobilised disulfonamide **119** also proved to be equally as good in the kinetic resolution of 1-(naphthalen-2-yl)ethanamine (*rac*)-**122** at room temperature, achieving a selectivity value of 9.8, corresponding to 78% *ee* for the amide product (*R*)-**123** (Scheme 1.34). Interestingly better selectivity values were observed for the supported disulfonamide **119** than its homogeneous counterpart at room temperature, and it also represented the first polymer-supported non-enzymatic acylative kinetic resolution of racemic amines. The disulfonamide **119** was also recycled four times through a process of recovery and regeneration using acyl chloride with no reported loss in selectivity.



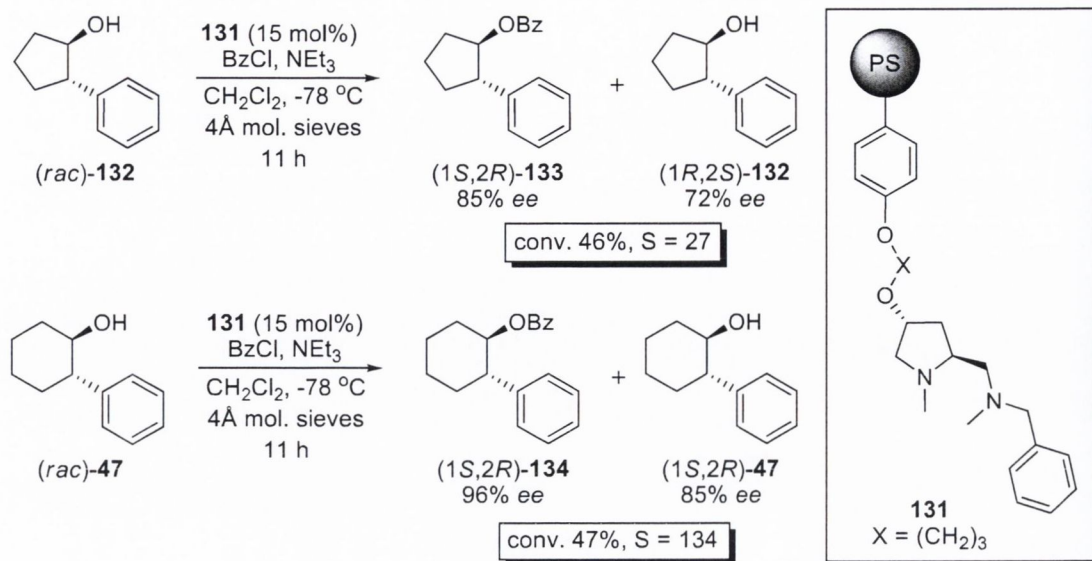
Scheme 1.34 KR of racemic amines with polymer-supported disulfonamide **119**.¹⁴⁵

In 1985 Hodge *et al.* reported the preparation of polymer-supported cinchona alkaloids on 1% DVB cross-linked polystyrene, utilising the terminal alkene of the quinuclidine moiety to form a thioether linker with the catalyst, at a loading of 0.65 mmol/g.¹⁴⁶ The polystyrene-supported catalyst **124** was screened in the Michael addition of thiols and thioesters to Michael acceptors. In the conjugate addition of phenylmethanethiol (**125**) to β -nitrostyrene (**126**) using 5 mol% equivalents of catalyst **124** at room temperature, the α -phenyl thioether product (*S*)-**127** was recovered in 74% yield and 18% *ee* after a 96 hour reaction time (Scheme 1.35). The employment of catalyst **124** at 5 mol% catalyst loading in the conjugate addition of 4-methylbenzenethiol (**128**) to cyclohex-2-enone (**129**) at room temperature proved more successful. The phenyl thioether product (*S*)-**130** was recovered in 81% yield and 45% *ee* in 24 hours (Scheme 1.35). The recovery and recyclability of catalyst **124** was also demonstrated for three additional cycles with no apparent loss in either enantioselectivity or yield.



Scheme 1.35 Michael addition using polystyrene-supported cinchonine catalyst **124**.¹⁴⁶

In 2001 Janda *et al.* reported the immobilisation of a vicinal diamine catalyst on a 1% 1,4-diphenoxybutane cross-linked polystyrene-support that proved successful in the kinetic resolution of selected *sec*-alcohols.¹⁴⁷ Janda and co-workers used the commercially available 4-hydroxyproline to synthesise a vicinal diamine catalyst that contained the same catalyst core as a proline derived diamine catalyst previously reported by Oriyama *et al.* in the desymmetrisation of *meso*-vicinal diols (Section 1.2.4.3).¹⁴⁸ The catalyst was immobilised *via* the hydroxy group of the pyrrolidin-4-ol with an ether linker to the polymer support to form supported catalyst **131**. Employing catalyst **131** in the acylative kinetic resolution of 2-phenylcyclopentanol (*(rac)*-**132**) using benzoyl chloride at -78 °C, a selectivity value of 27 was achieved in an 11 hour reaction time using 15 mol% catalyst loading. This afforded the ester (*1S,2R*)-**133** in 85% *ee* and the alcohol (*1R,2S*)-**132** in 72% *ee* at 46% conversion (Scheme 1.36). Higher selectivity values were observed in the kinetic resolution of 2-phenylcyclohexanol (*(rac)*-**47**) under identical reaction conditions, where a selectivity value of 134 was achieved. This afforded the ester (*1S,2R*)-**134** in 96% *ee* and the alcohol (*1R,2S*)-**47** in 85% *ee* at 47% conversion (Scheme 1.36). Catalyst **131** proved less successful in the kinetic resolution of acyclic aryl alkyl *sec*-alcohols with selectivity values ranging from 0 for 2-phenylethanol to 2 for 1-(2-naphthyl)ethanol. Catalyst **131** was also recovered and recycled 5 times without any apparent loss in reactivity or selectivity.



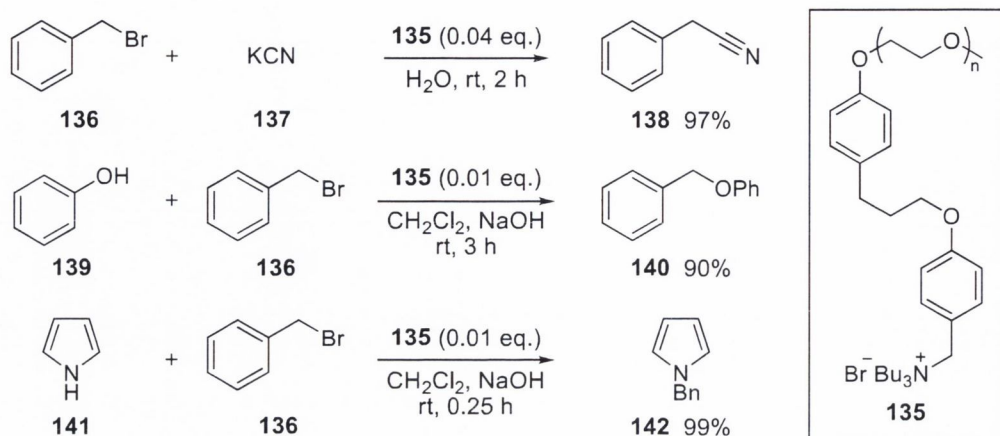
Scheme 1.36 KR of *sec*-alcohols using polystyrene-supported catalyst **131**.¹⁴⁷

1.3.2.3 Polyethylene glycol-supported catalysts

Polyethylene glycol has been extensively used as a solid support in heterogeneous catalysis.¹⁴⁹ The advantage associated with polyethylene glycol over polystyrene is its solubility in polar solvents such as water, acetonitrile, dimethylformamide and dimethyl sulfoxide; which enables the supported catalyst to behave as a homogeneous catalyst in polar solvents. Catalyst recovery can be achieved *via* trituration with the addition of a less polar solvent such as hexane, diethyl ether and *tert*-butylmethyl ether. The disadvantage associated with this methodology is the loss of small quantities of catalyst that remain solubilised after the addition of the apolar solvent.

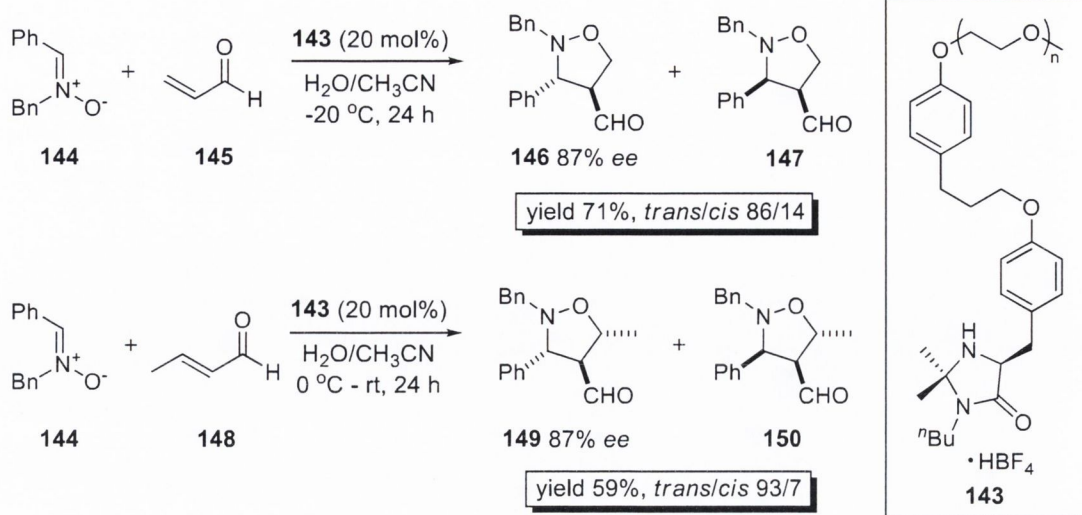
In 2000 Benaglia *et al.* reported the immobilisation of a quaternary ammonium salt phase-transfer catalyst on a soluble polyethylene glycol (PEG) support *via* a phenol ether linker.¹⁵⁰ Catalyst **135** was screened under previously tested conditions in a series of standard catalytic transformations and demonstrated to be equally as good, and better in some examples, than its non-supported counterpart. In the cyanation of benzyl bromide, the catalyst proved equally as good as its non-supported counterpart with yields of up to 97% (scheme 1.37). The benzylation of phenol and pyrrole in the presence of catalyst **135** gave yields of 90% and 99%, respectively with reduced reaction times in otherwise identical reaction conditions to its non-supported catalyst (Scheme 1.37).

Catalyst recoverability and recyclability was also demonstrated for three consecutive cycles with no appreciable loss in activity.



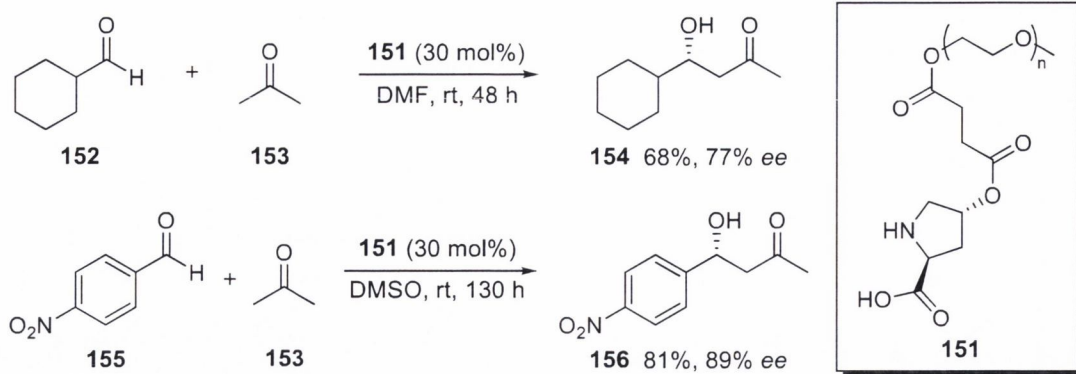
Scheme 1.37 Phase-transfer reactions catalysed by ammonium salt **135**.¹⁵⁰

In 2004 Benaglia *et al.* reported the synthesis of a PEG-supported chiral imidazolidinone organocatalyst.¹⁵¹ The immobilised imidazolidin-4-one catalyst core was based on a catalyst previously reported by MacMillan and co-workers capable of enantioselective Diels-Alder,¹⁵² Friedel-Crafts alkylation¹⁵³ and nitrene cycloaddition reactions.¹⁵⁴ Catalyst **143** was demonstrated to be very effective in the enantioselective 1,3-dipolar cycloaddition of unsaturated aldehydes to *N*-benzylated nitrones. In the cycloaddition of acrolein (**145**) to the nitron **144** at -20 °C using catalyst **143** gave a *trans/cis* isomers ratio of 86:16 respectively in 71% yield, with the *trans* isomer product **146** obtained in 87% *ee* (Scheme 1.38). These values were only slightly lower than those obtained using the non-supported imidazolidinone catalyst, where the *trans/cis* ratio was also 86:16 and product yield of 80% with 90% *ee* for the *trans* isomer.¹⁵⁴ The cycloaddition of but-2-enal (**148**) to the nitron **144** at 0 °C using catalyst **143** gave the *trans/cis* isomers in a ratio of 93:7 in 59% yield, with 87% *ee* for the *trans* isomer **149** (Scheme 1.38). The non-supported catalyst gave the *trans/cis* isomers in a 94:6 ratio respectively and in 86% yield and 90% *ee* for the *trans* isomer.¹⁵⁴ Catalyst **143** also exhibited good recoverability and recyclability over six consecutive cycles with no appreciable loss in activity reported.



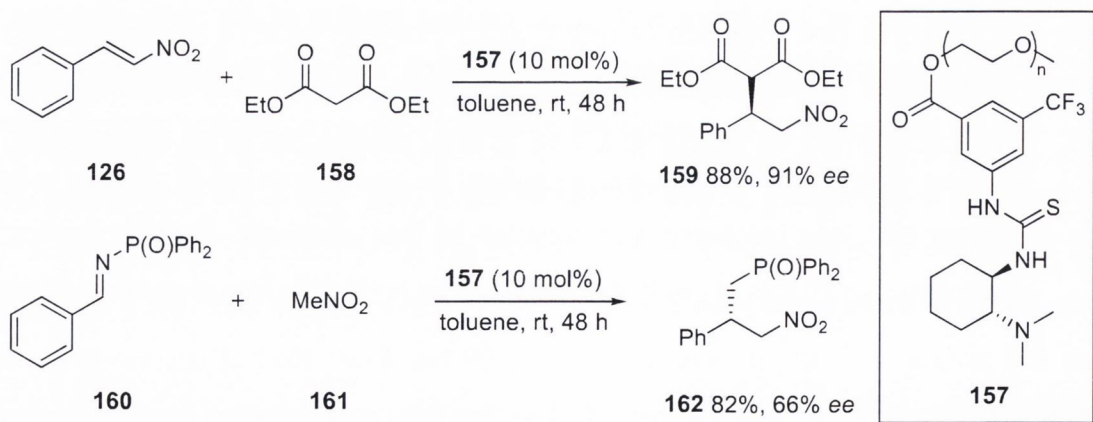
Scheme 1.38 1,3-dipolar cycloadditions of aldehydes promoted by catalyst **143**.¹⁵⁴

In 2000 Cozzi *et al.* reported the immobilisation of 4-hydroxyproline on a PEG-support via a succinic ester linker.¹⁵⁵ Catalyst **151** was screened in the enantioselective aldol reaction of cyclic alkyl and aryl aldehydes with acetone at room temperature. Supported catalyst **151** demonstrated good reactivity and selectivity in the reaction of cyclohexanecarbaldehyde (**152**) with acetone (**153**) in DMF at room temperature using 30 mol% catalyst loading, delivering the β -hydroxy carbonyl product **154** in 68% yield and 77% *ee* (Scheme 1.39). The employment of catalyst **151** in the aldol addition of acetone (**153**) to 4-nitrobenzaldehyde (**145**) at room temperature gave the β -hydroxy carbonyl product **146** in 98% *ee*, although reactivity was much lower with an increased reaction time of 130 hours with equal catalyst loading of 30 mol% (Scheme 1.39). Enantioselectivity values achieved by the PEG-supported proline catalyst **151** were similar to those of its non-supported counterpart, however, catalyst reactivity proved to be lower with longer reaction times required for the conversion of selected substrates. Catalyst **151** was recovered and recycled in two additional catalytic cycles which resulted in a small loss in catalyst activity and no noticeable loss in enantioselectivity.



Scheme 1.39 Aldol reaction promoted by PEG-supported proline derived catalyst **151**.¹⁵⁵

Takemoto *et al.* reported the preparation of a PEG-supported chiral thiourea catalyst which was demonstrated to be efficient in the promotion of enantioselective Michael addition reactions and aza-Henry reactions.¹⁵⁶ In the asymmetric Michael addition of diethyl malonate (**158**) to β -nitrostyrene (**126**) using a 10 mol% loading of immobilised catalyst **157** at room temperature, the Michael adduct **159** was obtained in 88% yield and 91% *ee* after 48 hours (Scheme 1.40). The aza-Henry addition of nitromethane (**161**) to the *N*-phosphinoylimine substrate **160** in the presence of 10 mol% of catalyst **157** was less efficient, as the adduct **162** was recovered in 82% yield and 66% *ee* after 48 hours (Scheme 1.40). Catalyst **157** was recovered and recycled for three consecutive cycles with no loss in yield or product *ee* being observed.



Scheme 1.40 Asymmetric Michael and aza-Henry reactions promoted by PEG-supported thiourea catalyst **157**.¹⁵⁶

1.3.3 Inorganic material-supported catalysts

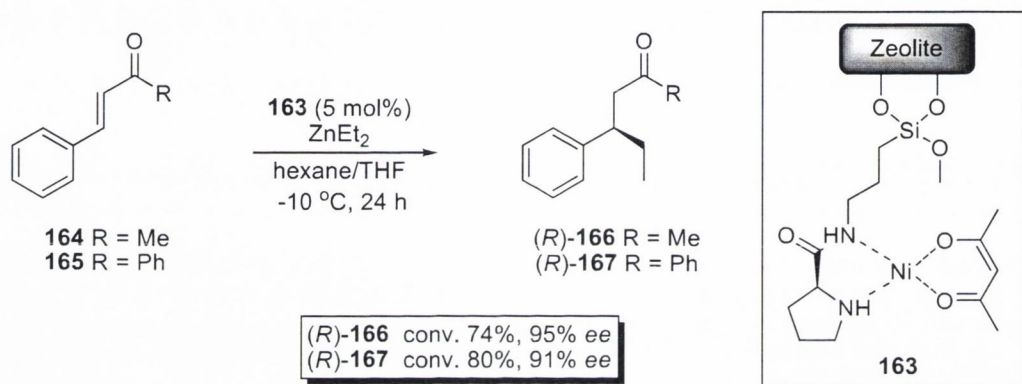
Inorganic material-supports are an attractive immobilisation strategy due to their increased durability relative to polymer organic-supports and the large diversity of inorganic materials currently utilised in this field.^{157,158} Durability is largely associated with the superior chemical and thermal stability properties of inorganic supports, rendering them a more versatile solid-support alternative throughout a range of solvents and relatively harsh reaction conditions such as high temperatures that would normally degrade polymer-supports. The mechanical properties of the rigid inorganic framework are also generally superior than their organic counterparts, making them less prone to attrition due to mechanical stirring and solvent degradation.

1.3.3.1 Zeolites and clay-supported catalysts

Zeolites are naturally occurring crystalline aluminosilicates that contain frameworks of cavities and channels.¹⁵⁹ However, most zeolites have been made synthetically because of their widespread commercial application in the petrochemical and detergent industries.¹⁶⁰ Clays are also naturally occurring porous sheet minerals comprising a large family of fine-grained crystalline hydrous aluminium phyllosilicates.¹⁶¹ Both zeolites and clays have been extensively used as catalysts and insoluble catalytic-supports in a range of reaction processes.¹⁶²⁻¹⁶⁴ The disadvantages associated with zeolite and clay supports is their ability to act as catalysts themselves. This can cause competitive catalysis with the immobilised catalytic species resulting in reduced enantioselectivity or stereoselectivity in the desired product.¹⁶⁴

In 1992 Sánchez *et al.* reported a zeolite-supported chiral nickel catalyst immobilised *via* a covalently attached alkoxy silane linker used in the conjugated addition of ethyl zinc to enones.¹⁶⁵ The employment of catalyst **163** in the addition of ethyl zinc to α,β -unsaturated ketones demonstrated better enantioselectivity than its homogeneous counterpart in a hexane/THF solvent mixture at -10 °C, however reaction times were considerably longer. In the addition of ethyl zinc to (*E*)-4-phenylbut-3-en-2-one (**164**) using catalyst **163** resulted in the saturated ketone product (*R*)-**166** been obtained in 74% yield and 95% *ee* after 24 hours (Scheme 1.41). The equivalent non-supported catalyst gave 75% yield and 77% *ee* after 2 hours. Under the same reaction conditions,

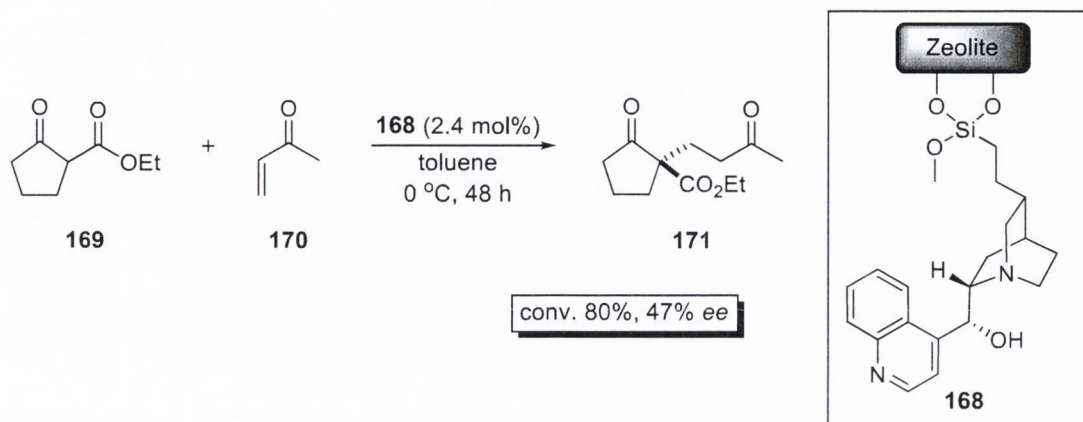
the conjugate addition of diethyl zinc to (*E*)-chalcone (**165**) using catalyst **163** gave the ketone product (*R*)-**167** in 80% yield and 91% *ee* (Scheme 1.41), whereas the non-supported catalyst gave an 85% yield and 75% *ee* after 18 hours. When the chiral nickel complex was also immobilised on a silica support, catalytic reactivity showed improvement with shorter reaction times observed, although enantioselectivity was lower. Sánchez accounted for the subsequent improvement in enantioselectivity associated with the zeolite-supported catalyst as a result of the increased steric constraints imposed by the porous zeolite structure.



Scheme 1.41 Conjugated addition of diethyl zinc to enones with zeolite-supported catalyst **163**.¹⁶⁵

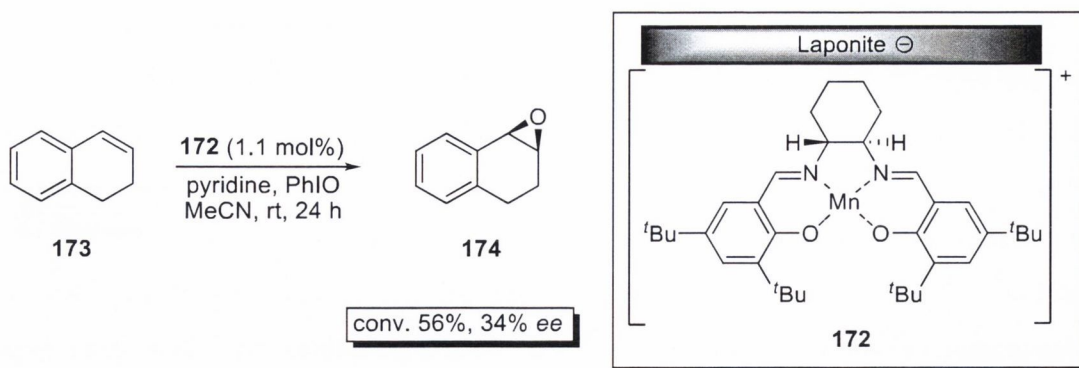
In 2002 Sánchez *et al.* reported the immobilisation of cinchonine and cinchonidine alkaloids on zeolites *via* a covalently attached alkoxy-silane linker.¹⁶⁶ The cinchonidine derived supported-catalyst **168** was demonstrated to be better in the enantioselective Michael addition of ethyl 2-oxocyclopentanecarboxylate (**169**) to methyl vinyl ketone (**170**) than the immobilised cinchonine catalyst. Using 2.4 mol% loading of catalyst **168**, the 1,5-diketo product **171** was recovered in 80% yield and 47% *ee* after a 48 hour reaction time at 0 °C (Scheme 1.42). The zeolite immobilised catalyst **168** proved to be less effective in the enantioselective Michael addition than the homogeneous catalyst, where under otherwise identical conditions the homogeneous catalyst giving 98% yield and 65% *ee*. The reduced yield and *ee* of the heterogeneous catalyst was associated with the interaction of the free hydroxy sites of the zeolite interacting with the substrate intermediate as opposed to the chiral hydroxy group of the cinchonidine catalyst.

Sánchez did not report on the ability of the cinchonidine supported-catalyst to be recycled.



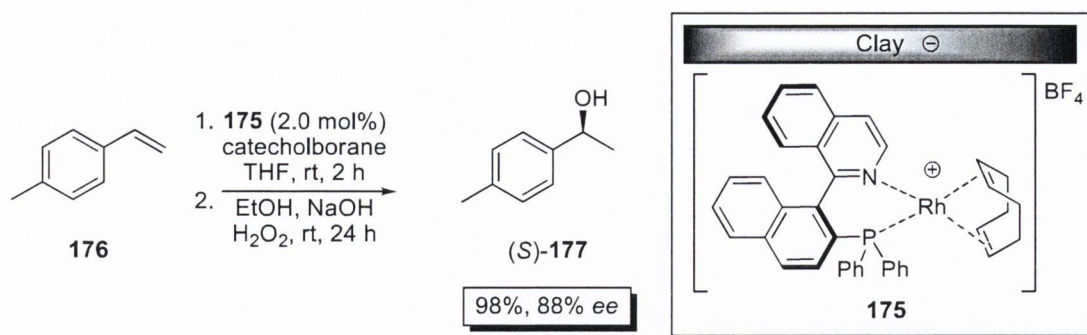
Scheme 1.42 Enantioselective Michael reaction promoted by catalyst **168**.¹⁶⁶

In 1995 Jacobsen *et al.* reported the synthesis of a homogeneous chiral Mn(salen) complex for use in the catalysis of asymmetric olefin epoxidation.¹⁶⁷ Mayoral *et al.* further developed Jacobsen catalyst by immobilising the Mn(salen) complex on various types of clay solid supports.¹⁶⁸ Initial results found the use of laponite clay-supported catalysts to deliver the highest ratio of the desired epoxide product relative to the allylic oxidation by-product. In the epoxidation of 1,2-dihydronaphthalene (**173**) using 1.1 mol% catalyst loading at room temperature using supported catalyst **172**, the epoxide product **174** was recovered in 34% *ee* at 56% yield after 24 hours (Scheme 1.43). The homogenous catalyst proved more reactive, with similar enantioselectivity achieved under the same reaction conditions; 74% yield and 36% *ee*. Catalyst **172** was recovered and recycled for one addition cycle with very poor results; 18% yield and 1% *ee*. In 1999 Jacobsen and co-workers demonstrated that a covalently attached polymer supported version of the Mn(salen) catalyst to be more versatile, delivering better enantioselectivity and demonstrating greater recyclability.¹⁶⁹



Scheme 1.43 Epoxidation of olefins using clay-supported Mn(salen) catalyst **172**.¹⁶⁷

In 2003 Fernández *et al.* reported the immobilisation of a class of rhodium complexes on clay solid-supports capable of the enantioselective hydroboration of vinylarenes.¹⁷⁰ The resulting hydroboranes were easily converted to the subsequent *sec*-alcohols in good enantioselectivity and yields. In the oxidation of 1-methyl-4-vinylbenzene (**176**) using supported catalyst **175** at room temperature with 2 mol% catalyst loading, the corresponding *sec*-alcohol (*S*)-**177** was recovered in 98% yield at 88% *ee* after a 2 hour reaction time (Scheme 1.44). The immobilised catalyst **175** demonstrated to be as efficient as its homogenous counterpart, which gave 96% yield and 91% *ee* under identical reaction conditions. Curiously the first epoxidation reaction cycle employing catalyst **175** afforded poor yields and enantioselectivity (31% yield and 74% *ee* for substrate **176**) which greatly improved on the second cycle (98% yield and 97% *ee*). Overall the recycling of supported catalyst **175** exhibited good reproducibility over four cycles, with the second, third and fourth cycles achieving equal yield and enantioselectivity to that obtained using the analogous homogeneous catalyst.



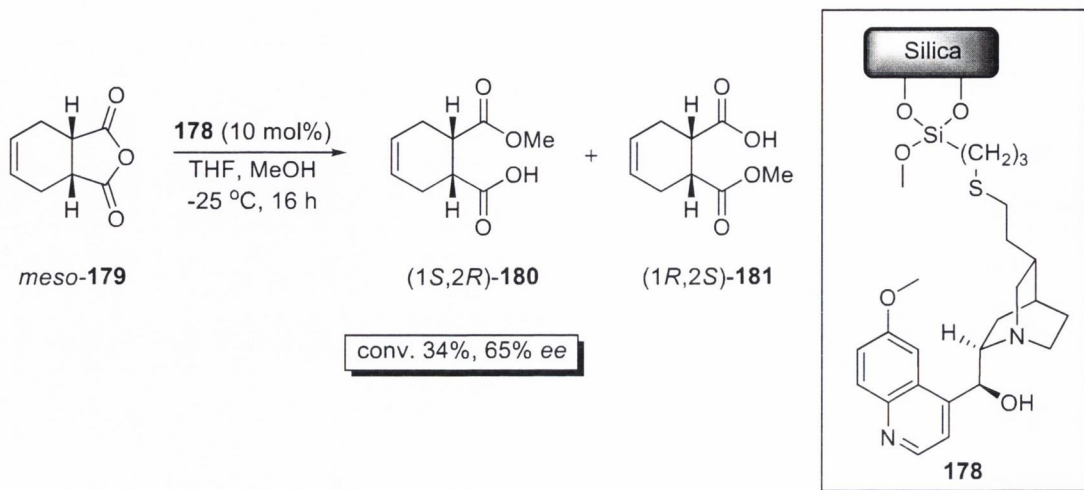
Scheme 1.44 Oxidation of vinylaryl **176** using clay-supported rhodium catalysts **175**.¹⁷⁰

1.3.3.2 Silica-supported catalysts

Silica is a highly abundant naturally occurring silicon based compound, more commonly known as sand or quartz, and is renowned for its toughness and durability which makes it a desirable candidate for solid-supported catalysis. Silica is one of the most commonly utilised inorganic-supports in the heterogenisation of homogeneous catalysts.¹⁵⁸ This is generally associated with its capability to form covalent bonds between the solid-support and the chiral ligand or catalyst, which is the most common immobilisation strategy.^{11,171}

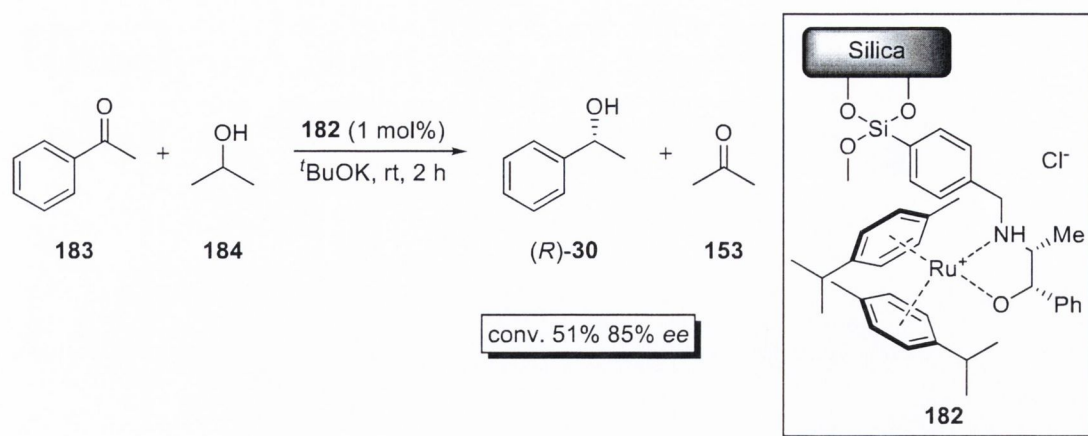
In 2002 Carloni *et al.* reported the immobilisation of the naturally occurring cinchona alkaloids quinidine and quinine on amorphous silica *via* a covalently tethered alkoxy silane linker.¹⁷² Initial results revealed the use of quinidine in the desymmetrisation of *meso*-anhydride **179** to be more effective in promoting enantiodiscrimination than its quinine counterpart, qualifying it as the optimal support candidate of the two catalysts. The silica-supported quinidine catalyst **178** was employed in the desymmetrisation of the *meso*-anhydride **179** with methanol in THF at -25 °C using 10% catalyst loading. The resulting (1*S*,2*R*)-**180** product was recovered in 34% yield and 65% *ee* after a 16 hour reaction time (Scheme 1.45). These values were lower than those obtained for the homogeneous catalyst equivalent under the same reaction conditions, where 45% yield and 85% *ee* was observed. Catalyst **178** was recovered and recycled for a further three cycles with small losses in reactivity and

enantioselectivity being observed. Carloni and co-workers reported the average yield to be 31% and the average *ee* to be 60% over the final three cycles.



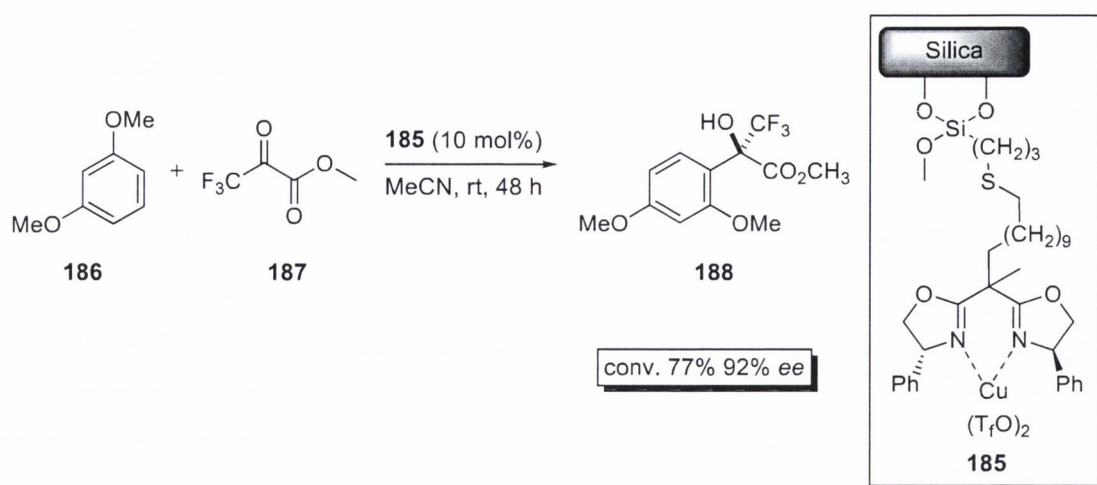
Scheme 1.45 Desymmetrisation of *meso*-anhydride **179** using supported catalyst **178**.¹⁷²

The use of chiral (1*R*,2*S*)-norephedrine ligands in ruthenium complexes for the asymmetric transfer hydrogenation of ketones in the synthesis of *sec*-alcohols was first reported by Leeuwen *et al.* in 1999.¹⁷³ This process was further developed by Leeuwen and co-workers in 2001 with the immobilisation of a chiral ruthenium complex on a silica solid-support *via* an alkoxy silane linker.¹⁷⁴ The silica-supported ruthenium catalyst **182** was tested in the asymmetric transfer hydrogenation of acetophenone (**183**) using isopropanol and potassium *tert*-butoxide at room temperature employing 1 mol% catalyst loading. The resulting 1-phenylethanol ((*R*)-**30**) product was recovered in 85% *ee* at 51% conversion after a 2 hour reaction time (Scheme 1.46). The use of supported catalyst **182** in asymmetric transfer hydrogenation proved equally enantioselective as the analogous homogeneous chiral ruthenium complex which gave 93% *ee* for the alcohol product (*R*)-**30**. However, the non-supported catalyst possessed better reactivity with 81% conversion under identical reaction conditions. Catalyst **182** was recovered and recycled three times without showing any loss in enantioselectivity, although conversion did diminish greatly from 51% on the first cycle to 34% on the third cycle.



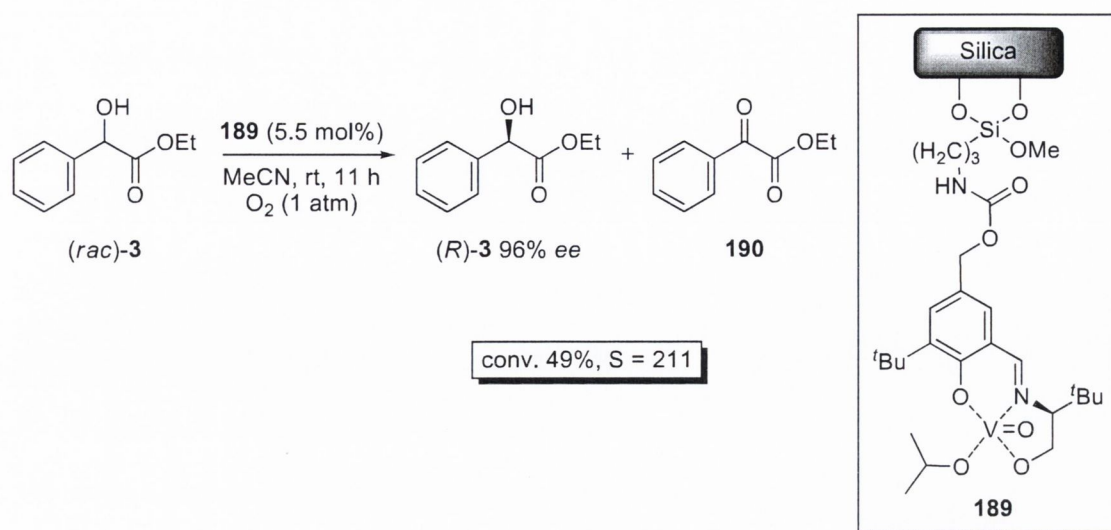
Scheme 1.46 Asymmetric transfer hydrogenation using silica-supported catalyst **182**.¹⁷⁴

The use of chiral copper bisoxazoline complexes in the enantioselective Friedel-Crafts reaction of aromatic compounds to trifluoropyruvate was first reported by Jørgensen *et al.* in 2001.¹⁷⁵ In 2002 Corma *et al.* reported the immobilisation of the chiral copper bisoxazoline complex on a mesoporous zeolite and silica solid-supports *via* a covalently attached alkoxy silane linker.¹⁷⁶ The silica-supported catalyst proved to be capable of promoting more enantioselective reactions than its zeolite-supported counterpart in the Friedel-Crafts hydroxylation, although reactivity was slightly lower. Silica-supported catalyst **185** was utilised in the asymmetric Friedel-Crafts hydroxylation of 1,3-dimethoxybenzene (**186**) with to trifluoropyruvate (**187**) using 10 mol% catalyst loading at room temperature. The subsequent benzyl alcohol product (**188**) was recovered in 92% *ee* at 72% conversion after a 48 hour reaction time (Scheme 1.47). These values surpass those associated with the use of the homogeneous catalyst counterpart, where 72% *ee* and 44% conversion was observed under identical reaction conditions. Catalyst **185** was recovered and recycled for only one additional cycle with no noticeable loss in enantioselectivity, although conversion was reported to be slightly lower. Corma and co-workers attributed the marginal loss in reactivity to potential leaching of the copper metal ion into solution.



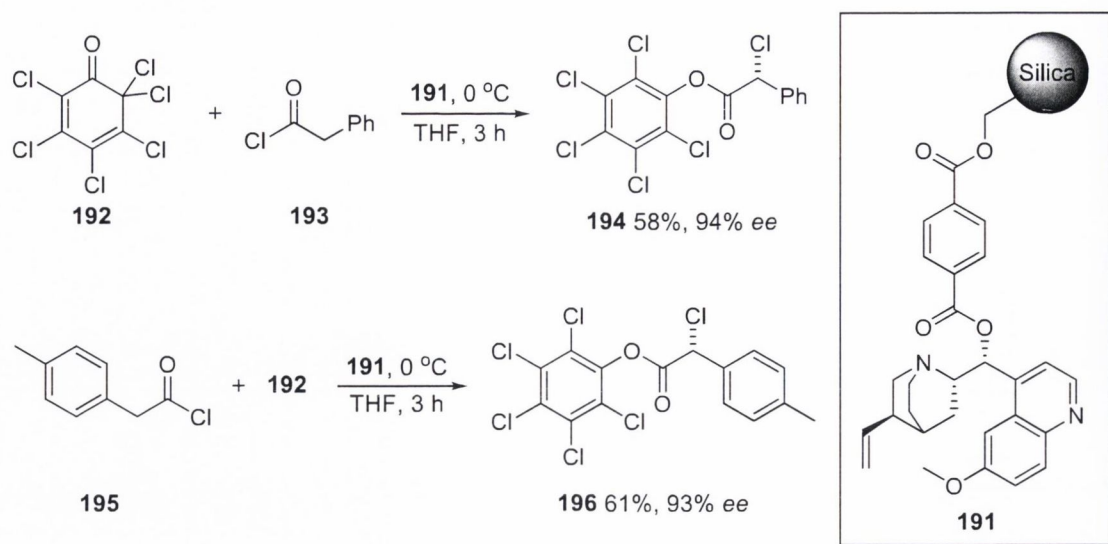
Scheme 1.47 Enantioselective Friedel-Crafts hydroxylation catalysed by silica-supported catalyst **185**.¹⁷⁶

In 2008 Jones *et al.* reported the immobilisation of a tridentate Schiff base vanadium catalyst on both silica and polymer-supports *via* a covalently attached alkoxy silane anchor.¹⁷⁷ The supported catalysts were tested in the asymmetric oxidative kinetic resolution of α -hydroxy esters, where in the presence of the silica-supported catalyst superior selectivity values were observed. Catalyst **189** proved capable of excellent activity and enantioselectivity in the oxidative KR of ethyl mandelate (*rac*-**3**) using 5.5 mol% catalyst loading in acetonitrile at room temperature, with selectivity values of 211 being observed. This delivered the ethyl mandelate product (*R*)-**3** in 96% *ee* at 49% conversion after an 11 hour reaction time (Scheme 1.48). The reaction proved effective in the presence of the equivalent polymer-supported catalyst, where a selectivity value of 12 was obtained under identical reaction conditions. This result was rather poor relative to the heterogeneous catalyst equivalent where a selectivity value of 458 was observed under the same reaction conditions. Supported-catalyst **189** was recovered and recycled for two additional cycles with small losses in reactivity and selectivity observed. Elemental analysis showed decreases in the nitrogen and carbon percentages suggested ligand decomposition and/or cleavage from the solid-support.



Scheme 1.48 Oxidative KR of ethyl mandelate promoted by supported catalyst **189**.¹⁷⁷

In 2005 Lectka *et al.* reported a column-based silica-supported cinchona alkaloid for use in the asymmetric α -chlorination of acyl halides.¹⁷⁸ The derivatisation of a quinine-based alkaloid catalyst on silica beads and the subsequent integration of these into a ‘flow’ column, allowed the generation of a flow process in which the reactants are dissolved in the mobile phase and the stationary phase contains the catalyst. In the asymmetric α -chlorination of 2-phenylacetyl chloride (**193**) with the chlorinating agent **192** at 0 °C through the silica resin immobilised catalyst **191**, the α -chloro adduct **194** was recovered in 58% yield and 94% *ee* after 3 hours (Scheme 1.49). The α -chlorination of 2-4-tolylacetyl chloride (**195**) proved almost equally as effective under the same reaction conditions, as the α -chloro adduct **196** was recovered in 61% yield and 93% *ee* after 3 hours (Scheme 1.49). Due to the generation of hydrochloric acid as a by-product in the reaction, which would render the quinuclidine moiety of the quinine catalyst inactive due to protonation, an excess of catalyst must be present in order to insure maximum conversion. The presence of the resulting quinuclidinium salt also inhibits the prospect of recycling. Lectka and co-workers overcame this problem by regenerating the quinuclidine free base by flushing of the flow column with an appropriate quantity of a 10% solution of Hünig’s base in THF, followed by an adequate THF washing to insure the removal of any remaining Hünig’s base or its salts that could potentially compete with the quinine catalyst. This enabled the recycling of catalyst **191** in over 100 cycles without any loss in activity reported.



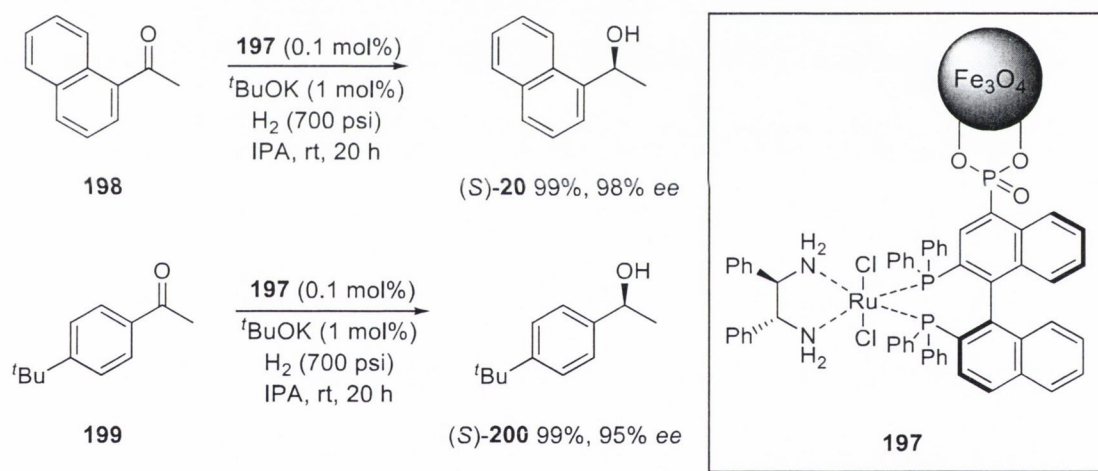
Scheme 1.49 Column-based silica-supported cinchona alkaloid catalyst **191**.¹⁷⁸

1.3.4 Magnetic nanoparticle supported catalysis

Magnetic nanoparticles (MNPs) have received much attention over the past number years due to their potential application in a number of fields such as biomedicine,¹⁷⁹ magnetic resonance imaging,¹⁸⁰ magnetic fluids,¹⁸¹ data storage,¹⁸² environmental remediation,¹⁸³ catalysis and catalytic supports.¹⁸⁴ One of the great advantages associated with nanoparticles as catalytic supports is the large surface-to-volume ratio, therefore enabling a higher degree of catalytic loading per unit volume than conventional solid-support materials.¹⁸⁵ Enhanced catalytic loading per unit volume leads to greater probability of component collision, therefore increased reaction rates. Magnetic nanoparticles also have the added benefit of been easily separated from a reaction mixture without the need for either centrifugation or filtration. The use of an external magnet can easily isolate the magnetic nanoparticles from the reaction mixture by attracting them to one side of the reaction vessel; easily facilitating the removal of the solution *via* suction or decanting.

In 2005 Lin *et al.* reported the immobilisation of a chiral ruthenium complex on magnetite nanoparticles *via* an aryl phosphonate anchor.¹⁸⁶ The ruthenium complex was evaluated in the asymmetric hydrogenation of a variety of aryl alkyl ketones to the corresponding *sec*-alcohols. Catalyst **197** was used in the asymmetric hydrogenation of

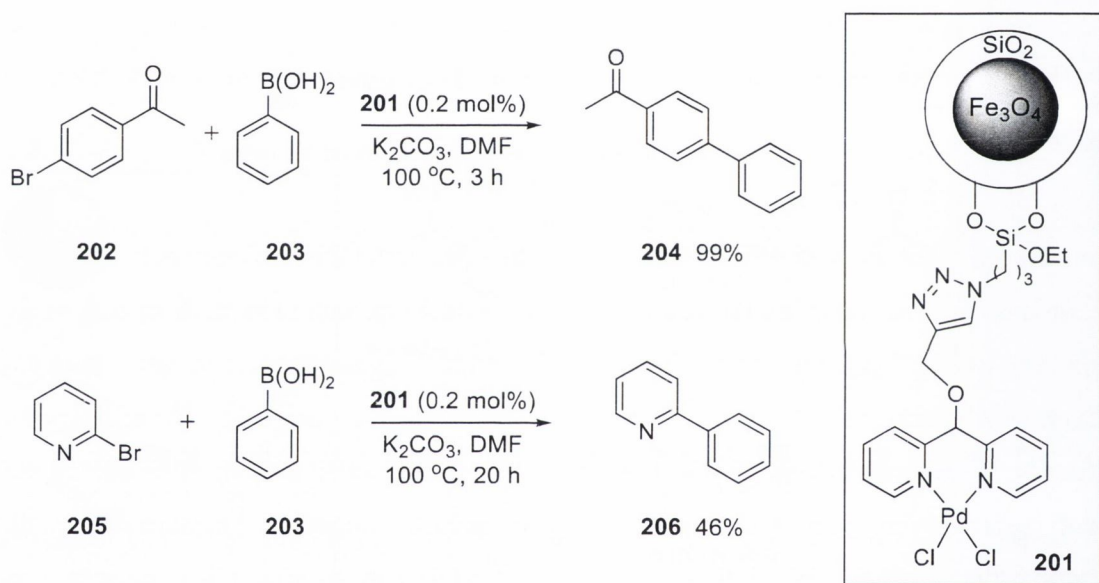
1-(naphthalen-1-yl)ethanone (**198**) with hydrogen gas under high pressure using 0.1 mol% catalyst loading in IPA in the presence of 1 mol% of potassium *tert*-butoxide. Catalyst **197** was capable of promoting the enantioselective reduction of **198** to the *sec*-alcohol product (*S*)-**20** in 98% *ee* and 99% conversion after 20 hours at room temperature (Scheme 1.50). In the asymmetric reduction of 1-(4-*tert*-butylphenyl)ethanone (**199**) under the same reaction conditions using catalyst **197** resulted in the corresponding *sec*-alcohol product (*S*)-**200** being present in 95% *ee* and 99% conversion (Scheme 1.50). In general the asymmetric hydrogenation of selected ketones promoted by magnetic nanoparticle supported catalyst **197** proved very effective with excellent activity observed. Catalyst **197** also exhibited excellent recyclability over 14 consecutive cycles without any appreciable loss in selectivity or conversion. However, on cycle 15 a dramatic loss in conversion was observed from 99% to 35% while enantioselectivity remained consistent with previous cycles.



Scheme 1.50 Asymmetric hydrogenation of ketones catalysed by MNP-supported catalyst **197**.¹⁸⁶

Palladium cross-coupling reactions are of great importance in organic synthesis. This was recognised in 2010 with the Nobel Prize in chemistry awarded to Richard F. Heck,¹⁸⁷ Ei-ichi Negishi¹⁸⁸ and Akira Suzuki¹⁸⁹ for palladium-catalysed cross coupling reactions in organic synthesis. In 2008 Gao *et al.* reported the immobilisation of di(2-pyridyl)methanol palladium complex on silica coated magnetic nanoparticles for the catalysis of Suzuki cross-coupling reactions.¹⁹⁰ Supported catalyst **201** proved very effective in the coupling of 4-substituted phenyl bromides with phenylboronic acid,

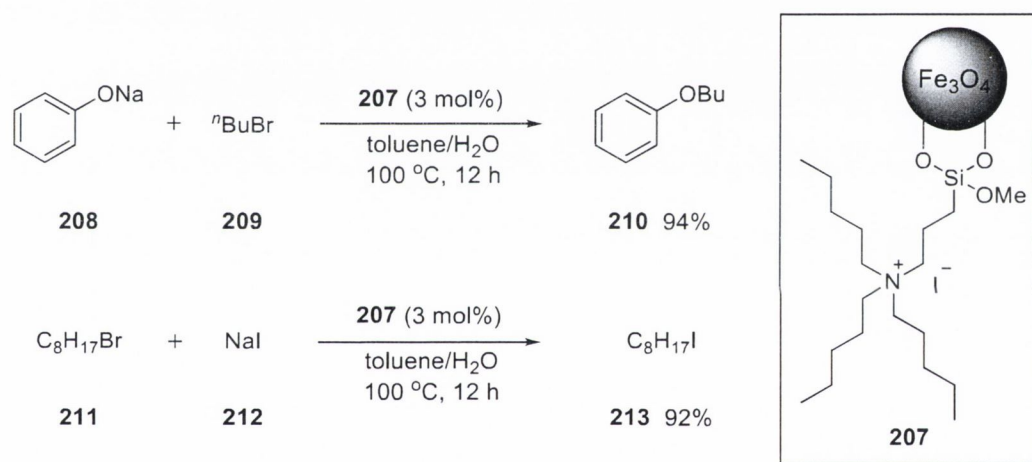
demonstrating short reaction times at low catalyst loading. 2-Substituted phenyl bromides and pyridines proved to be less reactive with longer reaction times required and lower yields observed. When the coupling of 1-(4-bromophenyl)ethanone (**202**) with phenylboronic acid in DMF at 100 °C using 0.2 mol% catalyst loading in the presence of potassium carbonate base, the diaryl product **204** was obtained in 99% yield after 3 hours reaction time (Scheme 1.51). In the coupling of 2-bromopyridine (**205**) with phenylboronic acid under the same reaction conditions only 46% yield was observed for the diaryl product **206** after 20 hours reaction time (Scheme 1.51). Despite the harsh reaction conditions, immobilised catalyst **201** was recovered and recycled for five consecutive cycles without any loss in catalytic activity.



Scheme 1.51 Suzuki-Miyaura coupling reaction using MNP-supported catalyst **201**.¹⁹⁰

The first example of a magnetic nanoparticle-supported organocatalyst was reported by Sato *et al.* in 2006.¹⁹¹ Sato and co-workers developed a range of supported quaternary phosphonium and ammonium salts derived from a tetra-*N*-butylammonium iodide phase-transfer catalyst, commonly used to promote reactions in a biphasic medium. The magnetic nanoparticle-supported ammonium iodide catalyst **207** proved the most effective and was employed at 3 mol% catalyst loading in the reaction of sodium phenolate (**208**) with 1-bromobutane (**20**) in a mixture of toluene and water at 100 °C (Scheme 1.52). The resulting phenol ether **210** was recovered in 94% yield after 12

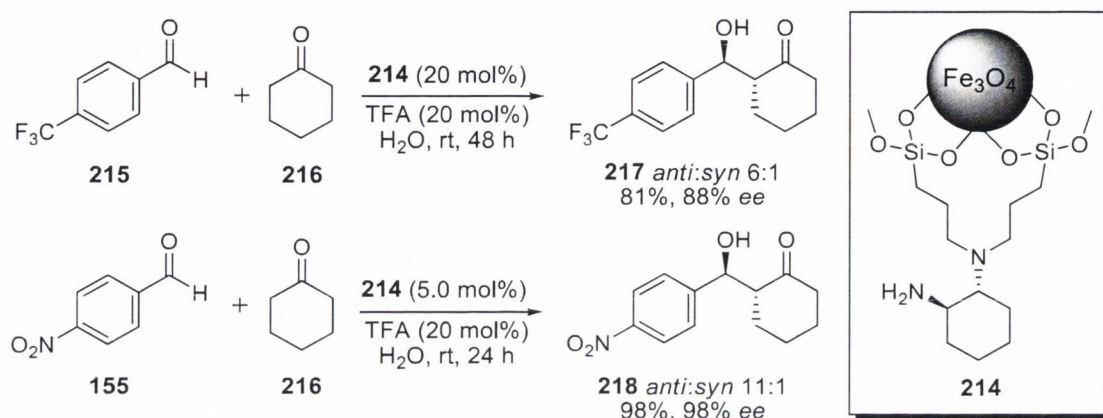
hours. Employing the homogeneous catalyst equivalent under otherwise identical reaction conditions afforded the ester product in 86% yield. Catalyst **207** was also employed at 3 mol% catalyst loading in the Finkelstein halogen exchange reaction of 1-bromooctane (**211**) with sodium iodide in toluene/water at 100 °C (Scheme 1.52). The resulting 1-iodooctane product (**213**) was recovered in 92% yield after 12 hours. Under similar reaction conditions using the homogeneous catalyst equivalent, the alkyl iodide product **213** was recovered in 92% yield after a 6 hour reaction time. This would suggest that the immobilised ammonium salt is slightly less active than the homogeneous catalyst in biphasic halogen exchange reactions. Catalyst **207** was recovered and recycled four times in the reaction of sodium phenolate (**208**) with 1-bromobutane (**209**) where a loss in activity of 5% was observed over the four cycles.



Scheme 1.52 MNP-supported ammonium iodide organocatalyst **207**.¹⁹¹

Lou and Cheng reported the immobilisation of an asymmetric amino organocatalyst on magnetic nanoparticles *via* a covalently attached alkoxy silane anchor.¹⁹² Immobilised asymmetric catalyst **214** was screened in the direct aldol reaction of cyclohexanone with various substituted aromatic aldehydes. In the direct aldol addition of cyclohexanone (**216**) to 4-(trifluoromethyl)benzaldehyde (**215**) using 20 mol% catalyst loading and 20 mol% TFA in water at room temperature, the aldol product **217** formed in a 6:1 *anti:syn* ratio in 81% yield after 48 hours reaction time. Chiral HPLC analysis determined the enantiopurity of the isolated *anti* isomer to be 88% *ee* (Scheme 1.53). Immobilised catalyst **214** proved to be more effective in the enantioselective aldol addition of

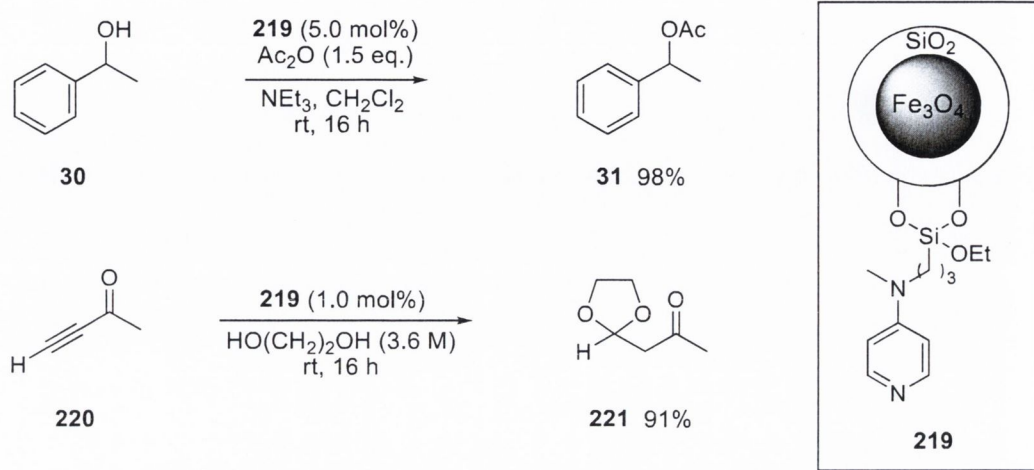
cyclohexanone to 4-nitrobenzaldehyde (**155**) under otherwise identical reaction conditions. The corresponding aldol product **218** was formed in an 11:1 *anti:syn* isomeric ratio in 98% yield after 24 hours reaction time, with the *anti*-isomer recovered in 98% *ee* (Scheme 1.53). Supported catalyst **214** was recovered and recycled over eleven consecutive cycles with small losses in enantioselectivity and yield observed of 9% and 8%, respectively. The diastereoselectivity of the reaction diminished dramatically over the eleven cycles from 11:1 on the first cycle to 4:1 on the final cycle.



Scheme 1.53 Direct aldol addition using MNP-supported asymmetric amino organocatalyst **214**.¹⁹²

In 2007 Connon *et al.* reported the immobilisation of a 4-*N,N*-dialkylaminopyridine organocatalyst on a silica coated magnetic nanoparticle *via* a covalently attached alkoxy silane anchor that displayed excellent recyclability across a wide range of substrates.¹⁹³ Catalyst **219** was initially evaluated in the acylation of 1-phenylethanol (**30**) with acetic anhydride at room temperature using 5 mol% catalyst loading, resulting in the ester product **31** at 98% conversion after 16 hours reaction time (Scheme 1.54). Catalyst **219** was recovered and recycled in the same reaction sequence 14 times without any appreciable loss in activity. Catalyst **219** exhibited remarkable activity at low catalytic loading of 1 mol% in the *bishydroxylation* of but-3-yn-2-one (**220**) with ethane-1,2-diol at room temperature giving the monoprotected 1,3-dicarbonyl product **221** in 91% yield (Scheme 1.54). In total catalyst **219** was recovered and recycled in 30 consecutive cycles with no apparent loss in activity. The recyclability of catalyst **219** achieved by Connon and co-workers has demonstrated the use of magnetic

nanoparticles as a practical and viability means of catalyst recovery at low catalytic loading.



Scheme 1.54 Nucleophilic transformations promoted by MNP-supported DMAP catalyst **219**.¹⁹³

1.3.5 Conclusion

The significance of organocatalysis as an attractive alternative to conventional metal based and enzymatic catalysis can largely be attributed to the economic and environmental advantages associated with their comparatively low cost and potentially low toxicity.¹⁰² The heterogenisation of organocatalysts to enable their recovery and recycling is seen as a major advantage in their further development as a practical and more sustainable means in the synthesis of target molecules.

The large number of immobilisation methodologies and processes to achieve this aim has resulted in large variations in results depending on the support strategy. The use of organic polymer supports such as polystyrene and polyethylene glycol has not been demonstrated to facilitate sufficient catalyst turnover to classify them as a durable catalyst immobilisation strategy.¹⁹⁴ This is evident from a low number of catalytic cycles per batch and the lack of reproducibility in most cases.

The use of inorganic supports such as clays and zeolites has demonstrated their durability to be superior to that of polymer supports, although it has also highlighted drawbacks to their viability as catalyst-supports. The ability of clays and zeolites to catalytically compete with the immobilised catalysts can often lead to unwanted side products and/or lower enantioselectivity values than those observed with the homogeneous counterparts. The immobilisation of catalysts *via* ionic interaction tends to suffer from catalyst leaching, resulting in lower catalytic activity as well as the potential of product contamination. The use of silica supports have proven more successful, although a true quantitative evaluation has not yet been demonstrated; Lectka and co-workers reported a silica-supported quinine-based catalyst capable of >100 cycles with no loss in yield or enantioselectivity but failed to disclose catalytic loading, which could suggest the use of a super-stoichiometric quantity of catalyst.¹⁷⁸

The use of magnetic nanoparticles-based solid-supports has been demonstrated as a durable and convenient means of catalyst recovery with the facile use of an external magnet followed by decantation to isolate the catalyst from the reaction components to excellent levels of recyclability.¹⁹³ Although the use of magnetic nanoparticle solid-supports is still in its infancy, they have already demonstrated the potential to surpass conventional polymeric and inorganic solid-supports as a highly desirable candidate in the field of heterogeneous catalysis.

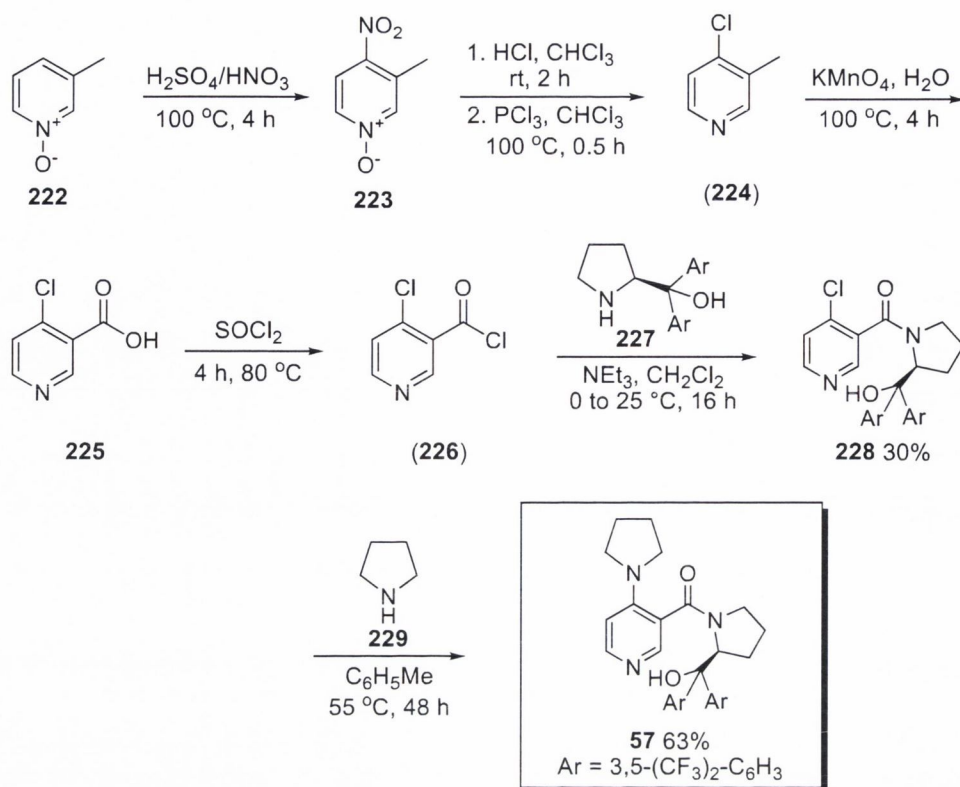
2.1 Synthetic strategy for the development of a magnetic-nanoparticle supported chiral 4-*N,N*-dialkylaminopyridine organocatalyst

At the commencement of this project there was a general absence of chiral, supported organocatalysts capable of achieving good yields and synthetically useful enantioselectivity levels over a number of cycles that would classify the catalyst as a truly viable recyclable heterogeneous system. This was better stated in a review by Benaglia:¹⁹⁵ “...in many more cases the supported catalysts performances fell short of the expectations. In addition, way too often the reasons of a failure have neither been understood nor tentatively explained. This has been particularly true in the case of chiral catalysts.”

The aim of this project was to develop a chiral organocatalyst anchored to a magnetic nanoparticle solid support, capable of achieving good enantioselectivity levels over a large number of cycles which would distinguish it as a truly active, selective and recyclable. Two questions arise:

- Which catalyst?
- And how to attach it?

We decided to use the highly versatile and selective chiral 4-*N,N*-dialkylaminopyridine organocatalyst previously developed by members of our group (Section 1.2.3.4). The primary reason for choosing this DMAP-derived stereoselective organocatalyst above others was its straightforward synthesis from readily available precursors (Scheme 2.1) and its inherent stability to air and moisture. Another very influential factor was the successful immobilisation of an achiral DMAP-derived catalyst on magnetic nanoparticles by a previous member our group that was capable of 30 consecutive cycles with any loss in activity.¹⁹³



Scheme 2.1 Synthesis of 4-*N,N*-dialkylaminopyridine chiral organocatalyst **57**.^{83,196,197}

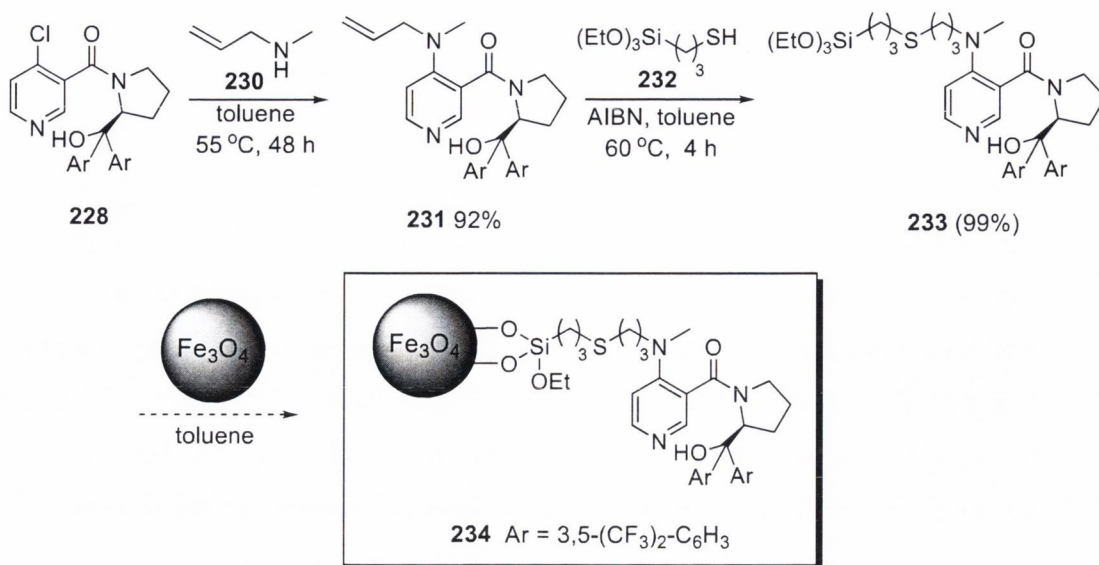
The synthesis of catalyst **57** started from the nitration of 3-methylpyridine-*N*-oxide (**222**) to give 3-methyl-4-nitropyridine-*N*-oxide (**223**, Scheme 2.1).¹⁹⁶ The next step involved the chlorination of **223** *via* a S_NAr reaction, followed by deoxygenation of the pyridine nitrogen using phosphorus trichloride in chloroform to give the intermediate 4-chloro-3-methylpyridine (**224**). The methyl group of **224** was subsequently oxidised to the corresponding carboxylic acid using potassium permanganate in water under reflux to give 4-chloro-nicotinic acid (**225**, Scheme 2.1).¹⁹⁷ 4-chloro-nicotinic acid was converted to the corresponding acyl acid chloride using thionyl chloride under reflux to give the intermediate **226** which was coupled the chiral amino alcohol **227** to give the chiral 4-chloro pyridine catalyst precursor **228**. Finally **228** was reacted with pyrrolidine (**229**) in toluene to give the chiral catalytic species **57**.⁸³ The chiral pendent substituent **227** was prepared from L-proline by first reacting with triphosgene, followed by the addition of triethylamine to give the corresponding cyclic anhydride. Subsequent

reaction of the anhydride with the appropriate Grignard gave the chiral amino alcohol **227**.¹⁹⁸

The chiral moiety that influences the asymmetric transformations carried out by **57** is substituted at the 3-position of the pyridine ring. In addition, the catalyst possesses the capacity to be alternatively substituted at the 4-position with an amine functionality which could facilitate its later attachment to the nanoparticle by serving as a linker. The link with the support in the 4-position would also allow a significant distance between the support and the chiral information, thereby minimising the potential risk of a negative impact of the latter on the stereochemical outcome of the reaction. Also, the amine substituent should preferably be achiral in order to avoid the introduction of any unnecessary stereocentres that could potentially influence enantioselectivity in an uncontrolled manner.

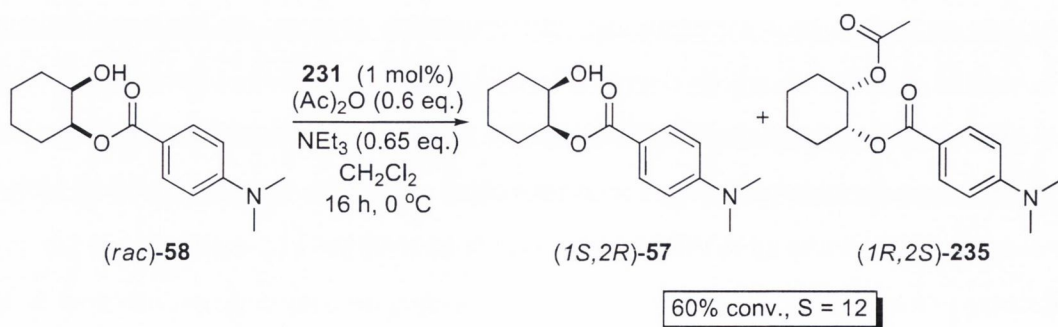
2.1.1 First generation system: design and synthesis of a 4-*N,N*-dialkylaminopyridine siloxane bound catalyst

The use of *N*-methylallylamine as the amino group substituent at the 4-position of the pyridine ring followed by a thiol-ene radical reaction using a (3-mercaptopropyl)-triethoxysilane anchor molecule was decided upon (Scheme 2.2). The triethoxysilane functionalised catalytic species can then be attached to the nanoparticle *via* siloxy group interchange with the hydroxy groups of both magnetic nanoparticles and silica coated magnetic nanoparticles. The use of alkoxy silane anchors to functionalise solid supports has proven to be a very popular immobilisation strategy, as the covalently attached anchor has shown a high degree of stability under a variety of reaction conditions.¹⁹⁹ The use of a triethoxysilane functionality to attach a catalyst directly to the surface of the magnetic nanoparticle (or to silica-coated magnetite nanoparticle) had already been accomplished using DMAP by Connon and co-workers.¹⁹³



Scheme 2.2 Synthetic route to potential MNP-supported chiral organocatalyst **234**

The synthesis and isolation of the 4-substituted allylamine catalyst **231** was straightforward; and utilised the same synthetic strategy as that shown in Scheme 2.1, to give the 4-chloronicotinic amide **228**. The pre-catalyst **228** was then reacted with the allylamine **230** in the S_NAr reaction to afford the product **231** in 92%. Subsequent evaluation of catalyst **231** showed it to be both active and selective in the acylative kinetic resolution of secondary alcohols. For example, the acylation of the *cis*-diol (*rac*)-**58** with catalyst **231** at 0 °C gave a selectivity factor of 12 at 60% conversion after 16 hours (Scheme 2.3).

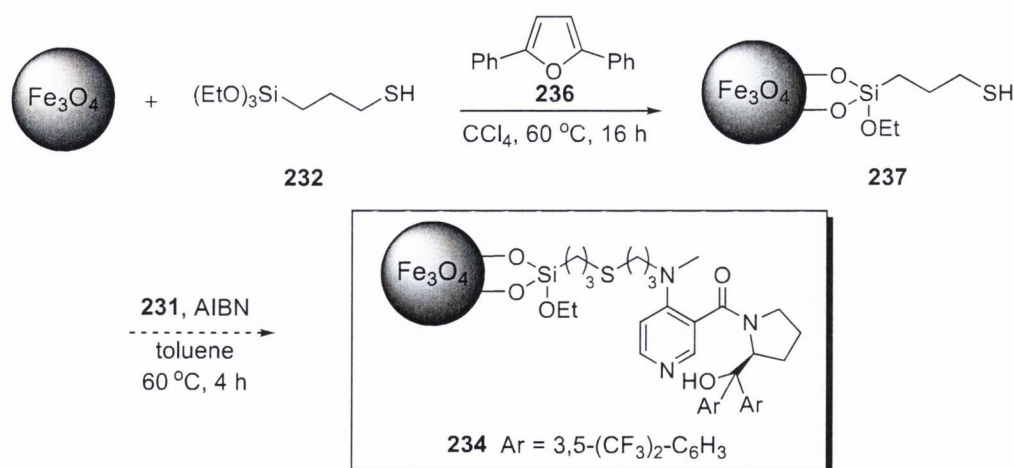


Scheme 2.3 Acylative KR of mono protected *cis*-diol (*rac*)-**58** with catalyst **231**

The final thiol-ene radical reaction of **231** with (3-mercaptopropyl)triethoxysilane (**232**) in toluene was observed to have gone to completion after 4 hours using $^1\text{H-NMR}$ spectroscopic analysis, affording product **233** in quantitative yield. However, major difficulties arose in the purification of **233**. Although many attempts were made to isolate a clean pure sample using column chromatography in various mobile phases, no pure sample was obtained. Attempts were also made to recrystallise and triturate the product from solution followed by filtration but these processes were also found to be unsuccessful.

2.1.2 Second generation system: attempted immobilisation of a catalyst precursor to a thiol-functionalised nanoparticle *via* a thiol-ene reaction

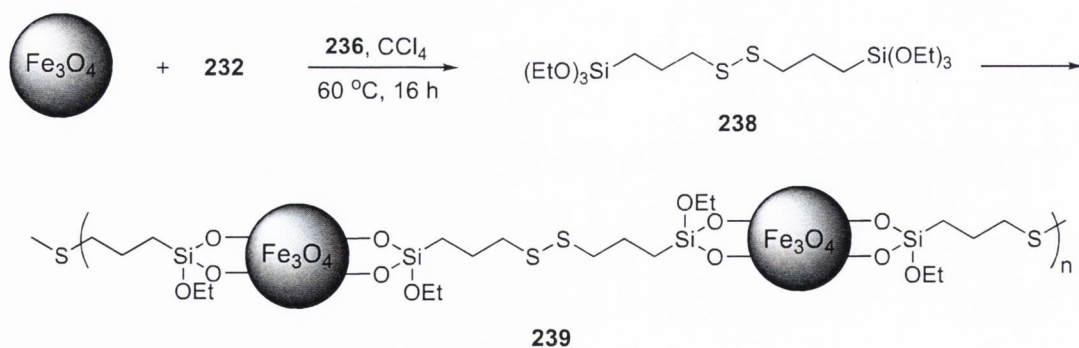
The problems encountered with the catalyst purification (Section 2.1.1) were presumably due to the presence of the hydrolytically unstable triethoxysilane group attached to the catalyst. The alternative approach of first attaching the triethoxysilane moiety **232** to the magnetic nanoparticle followed by coupling the allyl group of catalyst **231** to the magnetic nanoparticle functionalised 3-mercaptopropyl silane species **237** through a heterogeneous radical reaction was considered (Scheme 2.4). The initial addition of **232** to the magnetic nanoparticle was carried in carbon tetrachloride using 2,5-diphenylfuran (**236**) as an internal standard to determine the loading (Scheme 2.4).



Scheme 2.4 Synthetic route to MNP-supported organocatalyst **234**

The use of $^1\text{H-NMR}$ spectroscopic data allowed the loading of **232** onto the magnetic nanoparticle to be determined by comparing the integration of peaks associated with **232** to those of the 2,5-diphenylfuran internal standard. The $^1\text{H-NMR}$ spectra showed a decline in the peak integrals associated with substrate **232**, indicating its successful immobilisation onto the nanoparticle. The spectra also revealed the appearance of a triplet at a slightly lower chemical shift of approximately 0.11 ppm next to the quartet at 3.84 ppm (this signal was assigned to the protons of the carbon next to the thiol group), that could not be associated with the product formation. It was suspected that oxidation of the thiol was occurring to form the disulfide side product **238** (Scheme 2.5), in the presence of the magnetite nanoparticles, which would account for the observation of a new product in the crude reaction mixture.

The formation of **238** brings numerous problems regarding the accurate determination of substrate loading, where the direct substrate loading observations would be greatly complicated due to the simultaneous depletion of the thiol concentration *via* oxidation. Also of importance is the possible formation of **239**; the *bis*-triethoxysilane moiety **238** can potentially cross-link the magnetic nanoparticles together in a network of disulfide bonds, which could be very problematic for catalyst loading and nanoparticle dispersion in solution when attempting to agitate (Scheme 2.5).

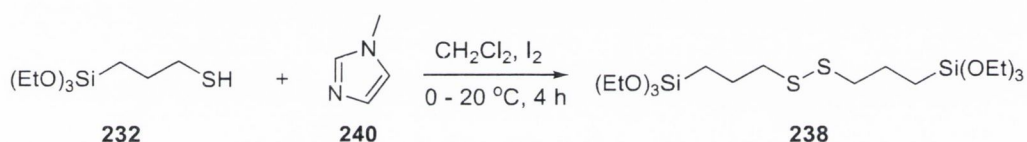


Scheme 2.5 Oxidation of thiol **232** to disulfide **238** in the presence of Fe_3O_4 MNP

The most probable reaction mechanism for the formation of the disulfide side product **238** in the presence of Fe_3O_4 is through a radical reaction pathway which was proposed by Murahashi *et al.* in their investigation into the Fe_2O_3 -catalyzed Baeyer-Villiger

oxidation of ketones.²⁰⁰ Carbon tetrachloride is also a popular organic solvent in radical reactions. The use of both alternative solvents and using silica coated nanoparticles were also attempted to avoid oxidation. However, while both of these strategies did reduce the extent of disulfide formation, they did not eliminate the problem completely.

The suspected oxidation of **232** was later independently confirmed by using molecular iodine in the presence of *N*-methylimidazole (**240**) to form the oxidised disulfide product **238** (Scheme 2.6), from **232**. Verification of the formation of **238** in the aforementioned loading experiment (Scheme 2.4) was then possible by comparing the ¹H-NMR spectra of the crude material from the reactions outlined in Schemes 2.4 and 2.6.



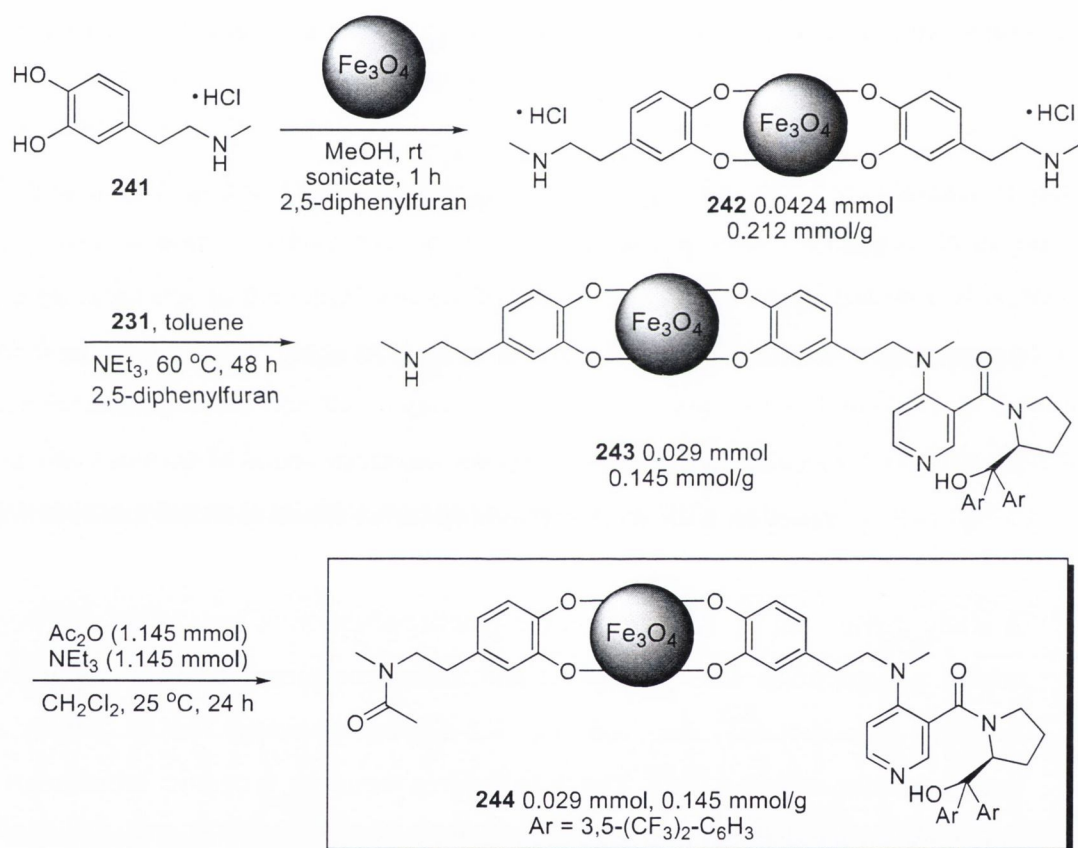
Scheme 2.6 Oxidation of thiol **232** to disulfide **238** using molecular iodine.³²

2.1.3 Third Generation system: catalyst immobilisation *via* a S_NAr reaction with an *N*-methyl dopamine functionalised nanoparticle

A study carried out by Xu *et al.* on the functionalisation of iron oxide and iron oxide coated nanoparticles with porphyrins and nickel complexes using dopamine derived anchors demonstrated the use of 1,2-dihydroxybenzene as a highly useful immobilisation strategy.^{201,202} The 1,2-dihydroxybenzene aromatic substituents of the dopamine are thought to covalently bond to the nanoparticle through metal oxide bonds. Studies by Xu and co-workers found the dopamine-based anchor to have exceptional thermal stability on the iron oxide surface.

The use of a 1,2-dihydroxybenzene-substituted anchor to immobilise a specific functional group on the surface of a magnetic nanoparticle would also seem like a promising approach to immobilise a catalytic species. The use of dopamine could potentially cause problems because the unhindered amine could catalyse the acyl transfer reaction, which is one of the main functions of the DMAP-based catalyst being

immobilised. This would lead to a non-stereoselective acylation being in competition with the desired asymmetric acylation reaction. A solution to this problem was envisaged by using the epinephrine derivative deoxyepinephrine hydrochloride (**241**) as the anchor, and coupling it to the 4-chloropyridine catalyst moiety **231** (Scheme 2.2) to give a tertiary amine at the 4-substituted position of the catalyst's pyridine ring (**243**, Scheme 2.7). The unreacted excess secondary amine of the deoxyepinephrine (**243**, Scheme 2.7) was then converted to the inactive amide using acetic anhydride under mild conditions leading to the MNP-supported heterogeneous catalytic species **244** (Scheme 2.7).

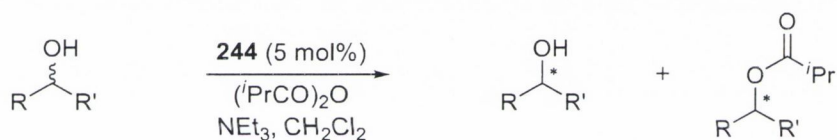


Scheme 2.7 Catalyst immobilisation strategy using deoxyepinephrine (**241**) anchor

2.1.3.1 Catalyst loading and preliminary evaluation

The catalyst loading strategy outlined in Scheme 2.7 proved successful. The initial step in the formation of the deoxyepinephrine-anchored magnetic nanoparticle **242** resulted

in a loading of 0.212 mmol/g. The heterogeneous nucleophilic aromatic substitution reaction, i.e. coupling the 4-chloropyridine moiety **231** to the deoxyepinephrine anchored nanoparticle **242** afforded the asymmetric DMAP derivative **243** at a loading of 0.145 mmol/g. Both the anchor and catalyst loadings were determined by $^1\text{H-NMR}$ spectroscopy using 2,5-diphenylfuran as the internal standard. The remaining unreacted deoxyepinephrine amounted to 0.067 mmol/g (i.e. the initial molar quantity of deoxyepinephrine loaded on to the nanoparticles minus the molar quantity of catalyst coupled to the immobilised deoxyepinephrine), was converted to the corresponding amide using acetic anhydride to give the heterogeneous magnetic nanoparticle supported chiral 4-*N,N*-dialkylaminopyridine catalyst **244** (Scheme 2.7). The magnetic nanoparticle supported chiral 4-*N,N*-dialkylaminopyridine catalyst **244** was subsequently evaluated in the acylative kinetic resolution of selected *sec*-alcohols to determine if the catalyst was reactive and if stereoselectivity could be achieved. Scheme 2.8 shows the generic acylation reaction scheme for various *sec*-alcohol substrates.



Scheme 2.8 Generic acylation reaction of *sec*-alcohols promoted by catalyst **244**

The evaluation of catalyst **244** in the acylative kinetic resolution of alcohols (*rac*)-**54**, (*rac*)-**58** and (*rac*)-**245**, (Figure 2.1) using 5 mol% catalyst loading was carried out in dichloromethane at various temperatures (Table 2.1). Alcohols **58** and **245** were prepared from the reaction of their respective cyclic *vic*-diols with the addition of 4-(dimethylamino)benzoyl chloride in dichloromethane at $-20\text{ }^\circ\text{C}$ (procedure 5.1.9.3 and 5.1.9.8). The acid chloride 4-(dimethylamino)benzoyl chloride was itself prepared by the addition of oxalyl chloride to the corresponding carboxylic acid in dichloromethane at $0\text{ }^\circ\text{C}$, then heating at reflux temperature for 2 hours and allowed to reach room temperature for a further 20 hours (procedure 5.1.9).

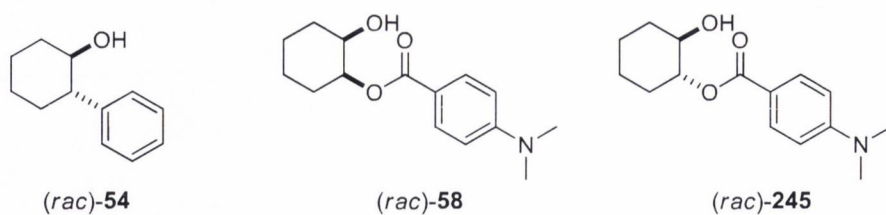


Figure 2.1 Alcohol substrates *(rac)*-54, *(rac)*-58 and *(rac)*-245

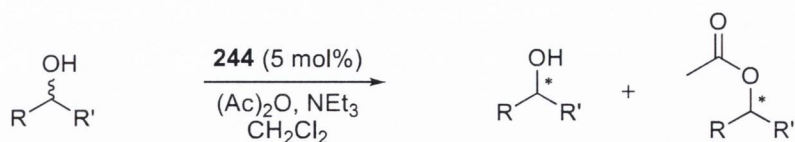
Table 2.1 Results for the evaluation of MNP-supported catalyst **244**

Entry	Alcohol	NEt ₃ (mol%)	(ⁱ PrCO) ₂ O (mol%)	Temp. (°C)	Time (h)	Conv. ^a (%)	Ester <i>ee</i> ^b (%)	Alcohol <i>ee</i> ^b (%)	Selectivity
1	54	85	80	20	16	28.1	49.2	19.2	3.53
2	54	85	80	20	16	37.3	45.7	27.2	3.46
3	57	85	80	20	16	32.9	56.6	27.8	4.70
4	245	85	80	0	8	5.2	5.1	0.3	1.11
5	245	85	80	20	16	15.0	44.0	7.8	2.78

^aDetermined using ¹H-NMR spectroscopy. ^bDetermined by CSP-HPLC using Daicel CHIRALCEL OD-H (4.6 mm x 25 cm) and CHIRALPAK AS (4.6 mm x 25 cm) columns.

Initial results revealed **244** to be capable of catalysing the enantioselective acylation of the racemic (*sec*)-alcohols tested. However, reactivity was greatly diminished relative to the homogeneous equivalent. Using 5 mol% catalyst loading, 0.80 equivalents of anhydride and 0.85 equivalents of base at 20 °C a conversion of 28.1% was achieved for the first cycle using substrate **54**, which gave a selectivity value of 3.53 (entry 1, Table 2.1). Repeating the experiment under identical reaction conditions resulted in a conversion of 37.3% and a selectivity of 3.46. (entry 2, Table 2.1). To further explore the ability of catalyst **244** to promote acylative kinetic resolution, substrate **51** was subsequently investigated which resulted in a conversion of 32.9% and a marginal increase in selectivity of 4.70 (entry 3, Table 2.1). To investigate the impact of temperature on **244**, substrate **245** was investigated in the acylative kinetic resolution at 0 °C. Unfortunately the results were not very promising with a conversion of 5.1% observed after 8 hours reaction and a selectivity of 1.11 (Entry 4, Table 2.1). Repeating the experiment at 20 °C and increasing the reaction time to 16 hours resulted in an increase in conversion and selectivity of 15.0% and 2.78 respectively (entry 5, Table 2.1). In order to bring about faster reactions capable of reaching *ca.* 50% conversion in

a convenient amount of time, we decided to change to the less hindered anhydride Ac₂O.



Scheme 2.9 Evaluation of catalyst **244** in the acylative KR of *sec*-alcohols

Table 2.2 Results from the evaluation of catalyst **244** using acetic anhydride

Entry	Alcohol	NEt ₃ (mol%)	Ac ₂ O (mol%)	Temp. (°C)	Time (h)	Conv. ^a (%)	Ester <i>ee</i> ^b (%)	Alcohol <i>ee</i> ^b (%)	Selectivity
1	54	85	80	0	5	9.9	51.7	5.7	3.32
2	58	85	150	20	16	66.2	43.2	84.4	6.24
3	245	85	150	20	16	60.6	26.7	41.1	2.49
4	58	85	150	0	16	41.2	58.0	40.6	5.54
5	58	85	80	20	16	45.6	59.1	49.5	6.25
6	58	85	150	0	16	34.8	60.6	32.3	5.54
7	58	85	150	30	6	14.2	60.3	10.0	4.45
8	58	85	100	20	16	36.0	61.3	34.5	5.80
9	58	85	200	20	16	62.5	47.0	78.2	6.22
10	58	85	250	20	16	68.3	40.5	87.2	6.15
11	58	80	200	20	18	58.4	45.7	64.0	4.98
12	58	80	200	20	20	74.0	33.3	95.0	6.38
13	58	80	200	20	20	61.5	47.4	75.8	6.07

^aDetermined using ¹H-NMR spectroscopy. ^bDetermined by CSP-HPLC using Daicel CHIRALCEL OD-H (4.6 mm x 25 cm) and CHIRALPAK AS (4.6 mm x 25 cm) columns..

Catalyst **244** proved to be capable of catalysing the enantioselective acylation of the selected racemic *sec*-alcohols **54**, **58** and **245**. Initial results revealed acetic anhydride to be more effective acylating agent than isobutyric anhydride in acylative kinetic resolution. Using 5% catalyst loading, substrate **54** reached a conversion of 9.9% at 0 °C in 5 hours, giving a selectivity value of 3.32 (entry 1, Table 2.2). Substrates **58** and **245** proved more reactive at 20 °C with conversions of 66.2% and 60.6% respectively after 16 hours. Selectivity values of 2.49 were observed for alcohol **245** and 6.24 for alcohol **58** (entries 2 and 3, Table 2.2). In an effort to increase the selectivity value of

substrate **58** the reaction at 0 °C was repeated under otherwise identical reaction conditions. However, this resulted in a reduction in conversion and selectivity of 41.2% and 5.54 respectively (entry 4, Table 2.2).

Repeated investigation into the selectivity and conversion of substrate **58** at 20 °C and 0 °C revealed the selectivity values to be consistent with previous experiments (entries 5 and 6, Table 2.2). The reduction in selectivity at 0 °C prompted a repeat of the previous experiment at 30 °C. However, this also led to a decrease in the selectivity to 4.45 (entry 7, Table 2.2). To investigate if catalyst **244** was performing equally well as initially observed, the acylative kinetic resolution of substrate **58** was repeated once again at 20 °C using 1, 2 and 2.5 molar equivalence of acetic anhydride (entries 8, 9 and 10, Table 2.2). Selectivity values remained consistent with previously observed values, although, conversion levels were slightly lower. To overcome the decrease in conversion and also in an effort to achieve the optimal conversion to deliver more desirable *ee* values, an increase in reaction time 18 hours was investigated (entry 11, Table 2.2). However, the optimal conversion was not achieved and it was also observed that the catalyst reactivity decreased over cycles.

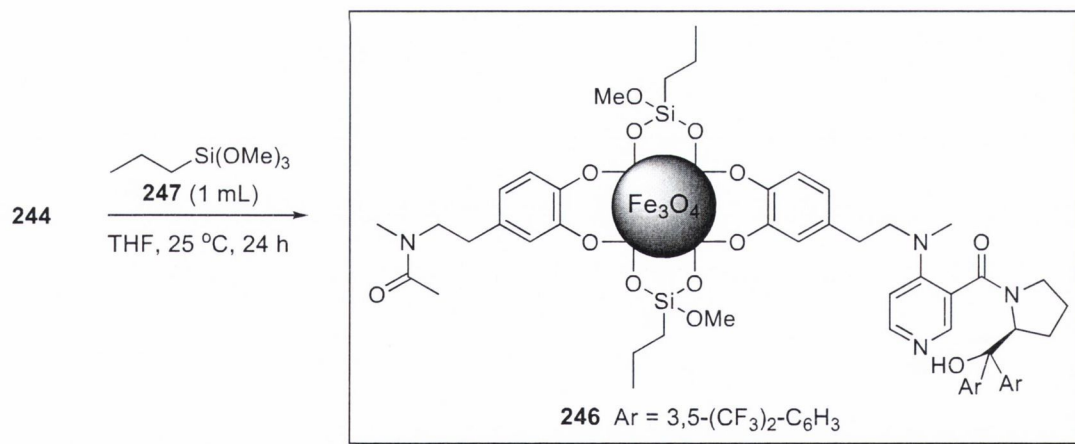
The decrease in selectivity and activity was associated with possible protonation of the catalyst pyridine ring, thus rendering it less active. Washing the catalyst with 10 equivalents of 1,8-diazobicyclo[5.4.0]undec-7-ene (DBU) and repeating the acylation of substrate **58** using 2.0 molar equivalence of acetic anhydride in a 20 hour reaction resulted restored activity and the accomplishment of more desirable *ee* values (entries 12 and 13, Table 2.2).

In order to improve on selectivity, reduced temperature acylations were carried out at 0 °C. Contrary to expectations from experiments carried out with the homogeneous catalyst **57**, (Section 1.2.3.4, Scheme 1.18) it was found that lower temperatures reduced selectivity, (Entries 1, 4 and 6, Table 2.2). In a bid to understand this, a catalytic acylation was also carried out at 30 °C. This was also found to reduce selectivity (Entry 7, Table 2.2). The reason for these contrasting results is not fully clear but it has been proposed that hydrogen bonding participates in the catalyst's mode of enantiodiscrimination,^{84,85} and elevated temperatures could potentially reduce the hydrogen bonding contribution of the catalyst's pendent hydroxy group. Reduced

selectivity at reduced temperature could be due to the magnetic nanoparticles aggregating in solution. (*i.e.* better magnetic affiliation for each other at lower temperatures, where the entropic penalty for such interactions is less significant).²⁰³ Surprisingly the use of the less hindered acetic anhydride led to increased reactivity and selectivity. Of the alcohol substrates tested, substrate **58** proved to be the most suitable with selectivity values > 6 being achieved under the optimised reaction conditions (Table 2.2).

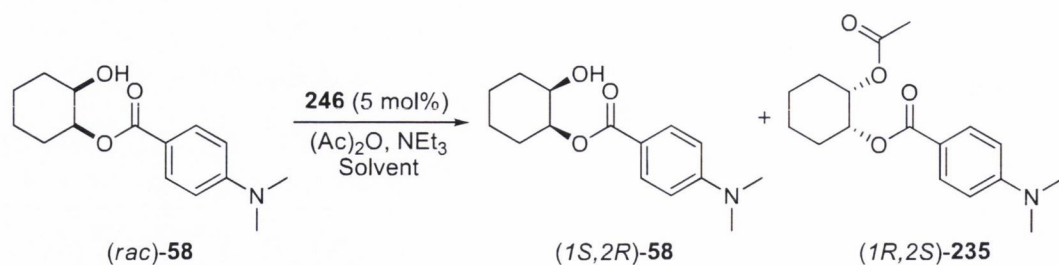
2.1.3.2 Optimisation of reaction parameters

Magnetic nanoparticles have a large surface-to volume ratio and therefore possess high surface energies. Consequently, they tend to aggregate so as to minimize the surface energies, which can be further minimised at reduced temperatures.²⁰⁴ In a bid to overcome the aggregation, the catalyst immobilised magnetic nanoparticles (**244**) was treated with *N*-propyltrimethoxysilane (4.34 mmol) to reduce exposure of the metal oxide surface, giving catalyst **246** (Scheme 2.10).



Scheme 2.10 Capping of the exposed nanoparticle surface with siloxane **247**

Catalyst **246** was subsequently tested in the acylative kinetic resolution using *sec*-alcohol (*rac*)-**58** with acetic anhydride to determine reactivity and selectivity under optimum reaction conditions (Scheme 2.11).



Scheme 2.11 Optimisation of reaction conditions using catalyst **246**

The use of *n*-propyltriethoxysilane to cap the magnetic nanoparticles proved very successful, with catalyst **246** demonstrating increased selectivity at reduced temperatures in the kinetic resolution of *sec*-alcohol (*rac*)-**58** (Table 2.3). In order to achieve *ee* values > 95% for the recovered alcohol at the optimal conversion rate as to deliver the highest possible yield, acetic anhydride and triethylamine loading was varied in each experiment. The initial objective of this experiment was to determine catalyst activity at both 20 °C and 0 °C. Using 1.0 and 0.85 molar equivalents of acetic anhydride and base, respectively, in the acylative kinetic resolution of (*rac*)-**58** promoted by **246** at 20 °C a selectivity value of 6.30 was achieved at 64.4% conversion, which resulted in 81.8% *ee* for the recovered alcohol (entry 1, Table 2.3). Repeating the experiment at 0 °C and increasing the anhydride loading to 2.0 molar equivalents gave an enhanced selectivity value of 7.07 at 86.9% conversion, giving the recovered alcohol in 99.9% *ee* (entry 2, Table 2.3).

Table 2.3 KR of (*rac*)-**58** promoted by catalyst **246** at variable temperatures

Entry	NEt ₃ (mol%)	Ac ₂ O (mol%)	Solvent	Temp. (°C)	Time (h)	Conv. ^a (%)	Ester <i>ee</i> ^b (%)	Alcohol <i>ee</i> ^b (%)	Selectivity
1	85	100	CH ₂ Cl ₂	20	20	64.4	45.3	81.8	6.30
2	85	200	CH ₂ Cl ₂	0	16	86.9	15.1	99.9	7.07
3	80	75	CH ₂ Cl ₂	20	20	43.4	57.9	44.4	5.72
4	60	200	CH ₂ Cl ₂	0	16	66.9	43.6	88.3	6.87
5	60	200	CH ₂ Cl ₂	0	16	79.4	25.6	98.6	6.52
6	80	75	CH ₂ Cl ₂	20	20	49.8	54.3	53.9	5.67
7	85	150	CH ₂ Cl ₂	0	16	61.8	48.4	78.1	6.46
8	85	150	CH ₂ Cl ₂	0	16	58.8	50.9	72.6	6.40

^aDetermined using ¹H-NMR spectroscopy. ^bDetermined by CSP-HPLC using Daicel CHIRALCEL OD-H (4.6 mm x 25 cm) and CHIRALPAK AS (4.6 mm x 25 cm) columns.

In order to determine the consistency of catalyst **246** between cycles in the acylative kinetic resolution of substrate **58** at 20 °C and 0 °C under different reagent loadings, we decided to repeat each experiment once. Catalyst **246** was employed in KR of **58** using 0.75 and 0.80 molar equivalents of acetic anhydride and base respectively at 20 °C. Selectivity values showed precise consistencies with results of 5.72 and 5.67. However, conversion proved less precise with 43.4% on the first attempt and 49.8% on the second (entries 3 and 6, Table 2.3) Repeating the experiment at 0 °C with 2.0 and 0.6 molar equivalents of acetic anhydride and triethylamine respectively, gave relatively consistent selectivity values once again of 6.87 and 6.52. However, conversion values did vary greatly in each cycle, with 66.9% on the first attempt and 79.4% on the second (entries 4 and 5, Table 2.3). Finally, repeating the experiment once again at 0 °C with 1.5 and 0.85 molar equivalents of anhydride and base respectively, resulted in more consistent results overall. Selectivity values of 6.46 and 6.40 were observed with conversions of 61.8 and 58.8 (entries 7 and 8, Table 2.3).

Although the ideal reaction conditions for achieving the optimal conversion and selectivity were not consistently attained to deliver high *ee* values, the experiments of table 2.3 did show great potential with each additional cycle. Entries 2 and 5 (Table 2.3) did give the desirable *ee* values > 95%, however, conversion varied greatly from one experiment to the other under identical reaction conditions. Entries 7 and 8 (Table 2.3) did show the consistency needed in kinetic resolution to deliver the desired high enantiomeric excess on each consecutive cycle. However, low conversion rates resulted in the preferably high *ee* being lower than anticipated.

In order to further improve the selectivity, the use of alternative solvents was then investigated in the reaction sequence using catalyst **246** (Scheme 2.11). The first solvent to be investigated was THF, a selectivity value of 5.02 was observed which was lower than that obtained for dichloromethane under the same reaction conditions (entry 1, Table 2.4). The slightly less polar MeTHF was also investigated, unfortunately a selectivity value of 5.02 was also observed for this solvent (entry 6, Table 2.4). The use of diisopropyl ether proved even less successful, with a selectivity value of 3.28 (entry 5, Table 2.4). The use of less polar solvents such as toluene and xylene were found to enhance selectivity at room temperature and repeated experiments using toluene also revealed the selectivity values to be consistent with previous cycles (Table 2.4, entries

2, 4 and 7). Although both solvents showed no significant difference in selectivity values, we decided to select toluene above xylene due to its cost and availability.

Table 2.4 Solvent screening in the acylative KR of alcohol **58** promoted by **246**

Entry	NEt ₃ (mol%)	Ac ₂ O (mol%)	Solvent	Temp. (°C)	Time (h)	Conv. ^a (%)	Ester <i>ee</i> ^b (%)	Alcohol <i>ee</i> ^b (%)	Selectivity
1	40	30	THF	20	6	25.5	60.9	20.8	5.02
2	85	80	toluene	20	6	28.3	67.5	26.6	6.66
3	85	80	xylene	20	6	17.2	69.9	14.5	6.51
4	85	80	toluene	20	6	30.7	66.0	29.3	6.46
5	85	80	DIPE	20	6	38.2	43.6	26.9	3.28
6	85	80	MeTHF	20	6	29.7	59.5	25.2	5.02
7	85	80	toluene	20	16	50.5	58.4	59.6	6.82

^aDetermined using ¹H-NMR spectroscopy. ^bDetermined by CSP-HPLC using Daicel CHIRALCEL OD-H (4.6 mm x 25 cm) and CHIRALPAK AS (4.6 mm x 25 cm) columns.

After further examination of the experimental procedures, in particular regarding the relative rate of agitation of the MNP in solution, it became evident that the increase in selectivity was not actually due to the reduction in temperature, but rather the manner in which the nanoparticles were agitated. The optimal rate of agitation was initially considered to be the rate at which the MNP were fully dispersed in the solution but at the same time not enough to cause them to get ejected from the solution onto the side of the reaction vessel. But it transpired that the small quantity of MNP that get ejected from the solution onto the side of the reaction vessel has less of an influence on the outcome of the reaction than the rate of agitation.

The major difference between the room temperature and reduced temperature experimental procedures consisted of the increased rate of agitation necessary to disperse the nanoparticles in the reaction vessel during the reduced temperature procedure. The experimental procedure was repeated to mimic the reduced temperature reaction conditions with the exclusion of the ice bath. This proved successful in delivering a higher selectivity in the kinetic resolution of *sec*-alcohol (*rac*)-**58** at 20 °C (Table 2.5). However a steady decline in conversion was still observed after each cycle (Table 2.5, entries 1, 2, 3 and 4). This was circumvented with a single wash with a solution of DBU in toluene, followed by three additional washes with dry toluene which

resulted in a dramatic increase in conversion from 49% to 70% (Table 2.5, entries 4 and 5). The continued use of catalyst **246** in the acylative KR of (*rac*)-**58** in the absence of a DBU solution wash between cycles revealed the conversion to be in decline with additional cycle (entries 7 and 8, Table 2.5).

Table 2.5 Optimisation of acylative KR reaction parameters using catalyst **246**

Entry	NEt ₃ (mol%)	Ac ₂ O (mol%)	solvent	Temp. (°C)	time (h)	Conv. ^a (%)	Ester <i>ee</i> ^b (%)	Alcohol <i>ee</i> ^b (%)	Selectivity
1	85	80	toluene	20	16	66	47.1	93.2	8.72
2	85	80	toluene	20	16	57	56.3	75.3	7.71
3	85	80	toluene	20	16	53	59.0	66.4	7.60
4	85	80	toluene	20	16	49	61.0	59.3	7.57
5	85	80	toluene	20	16	70	39.9	93.4	7.18
6	85	80	toluene	20	16	58	57.7	78.3	8.54
7	85	80	toluene	20	16	51	61.5	64.7	8.01

^aDetermined using ¹H-NMR spectroscopy. ^bDetermined by CSP-HPLC using Daicel CHIRALCEL OD-H (4.6 mm x 25 cm) and CHIRALPAK AS (4.6 mm x 25 cm) columns.

2.1.3.3 Kinetic resolution of *sec*-alcohols: substrate scope under optimised conditions

The next step was to investigate the substrate scope under the optimised conditions. The acylative kinetic resolution of the cyclic mono-protected diol (*rac*)-**58** with acetic anhydride in toluene promoted by immobilised catalyst **246** had delivered the highest selectivity factor. The screening of structurally similar substrates seemed a logical approach at this point. Substrates (*rac*)-**248**, (*rac*)-**249** and (*rac*)-**250** (Figure 2.2) were all evaluated in the acylative kinetic resolution promoted by catalyst **246** under optimised conditions. Substrate (*rac*)-**58** still gave the highest selectivity factor of 8.92, followed by the cyclic seven membered mono-protected diol (*rac*)-**249** with a selectivity factor of 6.37, then the eight and five membered cyclic substrates (*rac*)-**250** and (*rac*)-**248** gave selectivity values of 4.16 and 2.91, respectively (entries 1 - 4, Table 2.6).

Catalyst **246** was then evaluated in the acylative kinetic resolution of substrates that were previously resolved using the homogeneous catalyst counterpart with moderate to

good selectivity values.^{84,85} Substrates (*rac*)-**251**, (*rac*)-**252** and (*rac*)-**253** (Figure 2.2) proved the least successful with selectivity values from 1.63 to 2.12 (Entries 5, 6 and 7, Table 2.6). Alcohols (*rac*)-**54** and (*rac*)-**245** (Figure 2.1) proved to be more suitable substrates, achieving selectivity values of 4.27 and 3.88, respectively.

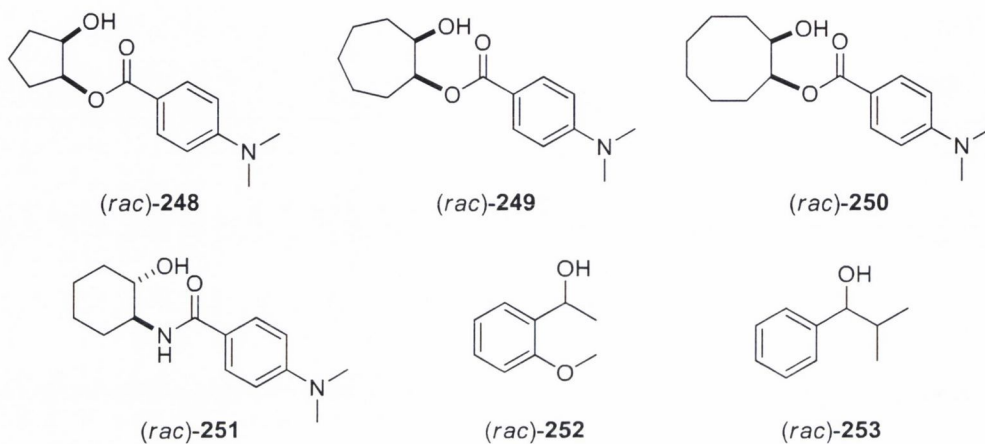


Figure 2.2 Alcohol substrates (*rac*)-**248**, (*rac*)-**249**, (*rac*)-**250**, (*rac*)-**251**, (*rac*)-**252** and (*rac*)-**253**

Alcohols **248**, **249**, **250** and **251** were prepared from the reaction of their respective cyclic *vic*-diols or cyclic amino alcohol with 4-(dimethylamino)benzoyl chloride in dichloromethane at $-20\text{ }^{\circ}\text{C}$, followed by the reaction mixture being allowed to reach room temperature for 16 hours (procedure 5.1.8.4, 5.1.8.5, 5.1.8.6 and 5.1.8.8). The α -aromatic alcohols **252** and **253** were prepared from reaction of their respective aromatic aldehydes with the appropriate Grignard reagent at $0\text{ }^{\circ}\text{C}$, followed by allowing the reaction mixture to reach room temperature for 14 hours (procedure 5.1.8.9 and 5.1.8.10).

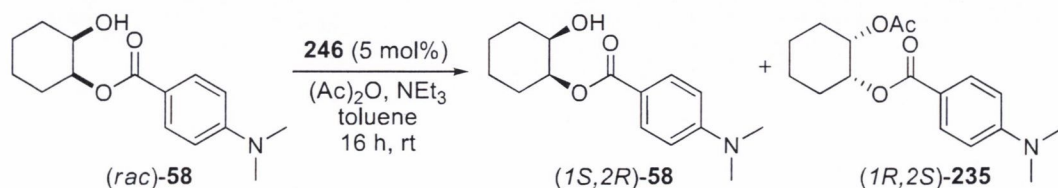
Table 2.6 Acylative KR of *sec*-alcohols under optimised conditions

Entry	Substrate	NEt ₃ (mol%)	Ac ₂ O (mol%)	Temp. (°C)	time (h)	Conv. ^a (%)	Ester <i>ee</i> ^b (%)	Alcohol <i>ee</i> ^b (%)	Selectivity
1	258	85	80	20	20	50.1	35.5	35.6	2.91
2	58	85	80	20	20	42.8	68.7	51.5	8.92
3	259	105	100	20	20	59.9	49.8	74.5	6.37
4	250	105	100	20	20	49.3	46.3	45.0	4.16
5	251	105	100	20	20	50.2	25.4	25.6	2.12
6	252	85	80	20	16	36.0	19.2	10.8	1.63
7	253	85	80	20	16	46.3	18.5	16.0	1.68
8	254	85	80	20	16	37.4	49.3	29.4	3.88
9	54	105	100	20	16	43.6	49.7	38.4	4.27

^aDetermined using ¹H-NMR spectroscopy. ^bDetermined by CSP-HPLC using Daicel CHIRALCEL OD-H (4.6 mm x 25 cm) and CHIRALPAK AS (4.6 mm x 25 cm) columns.

2.1.3.4 Recycling of the magnetic nanoparticle supported 4-*N,N*-dialkylaminopyridine catalyst

The fundamental idea of the heterogenisation of a homogeneous catalyst is to make the catalytic process more economical. In order to achieve this, the conservation of the catalyst over as many cycles as possible, while retaining activity and selectivity, are the main objectives, whereby the employment of the recyclable heterogeneous catalyst far outweighs the use of its homogeneous counterpart. To accurately analyse the recyclability of catalyst **246** a fresh batch of catalyst was prepared in the precise manner as outlined (*vide supra*, Section 2.1.3). The catalytic loading of the newly prepared specimen was determined to be 0.0805 mmol/g. The newly prepared catalyst **246** was then evaluated in the acylative kinetic resolution of substrate (*rac*)-**58** at 5 mol% catalyst loading with acetic anhydride using toluene solvent at room temperature (Scheme 2.12).

**Scheme 2.12** Recycling of catalyst **246** in the acylative KR of (*rac*)-**58**

Initial results revealed that catalyst **246** was very effective in kinetic resolution of *sec*-alcohol (*rac*)-**58** with a selectivity of 10.08 at 73% conversion achieved on the initial cycle, delivering the recovered alcohol in 99% *ee* (Table 2.7, entry 1). The same batch of catalyst was recycled a further 19 times using alcohol (*rac*)-**58** to great effect; selectivity values ranging from 10.55 to 9.02 and conversions ranging from 72% to 59%, giving the recovered alcohol in 99% to 82% *ee* (Table 2.7). A small decrease in catalyst activity was observed between cycles 11 to 16, however a small increase in anhydride loading resulted in a return to previous levels of performance (Table 2.7, entries 17 – 20).

Table 2.7 Recycling of catalyst **246** in the acylative KR of (*rac*)-**58**

Entry	Catalyst (mol%)	NEt ₃ (mol%)	Anhydride (mol%)	Conversion ^a (%)	Ester <i>ee</i> ^b (%)	Alcohol <i>ee</i> ^b (%)	Selectivity
1	5	125	120	73	39	99	10.08
2	5	125	120	69	44	98	10.01
3	5	125	120	72	39	99	10.42
4	5	125	120	69	44	97	9.87
5	5	125	120	71	41	98	9.78
6	5	125	120	67	48	97	10.55
7	5	125	120	67	46	96	9.52
8	5	125	120	68	45	97	9.54
9	5	125	120	66	49	94	9.47
10	5	125	120	67	47	95	9.57
11	5	125	120	65	50	92	9.02
12	5	125	120	62	53	87	8.84
13	5	125	120	61	55	86	8.95
14	5	125	120	64	51	91	9.17
15	5	125	120	61	55	86	9.03
16	5	125	120	59	57	82	9.03
17	5	145	140	65	50	93	9.37
18	5	145	140	63	53	89	9.07
19	5	145	140	66	49	94	9.27
20	5	145	140	65	49	93	9.17

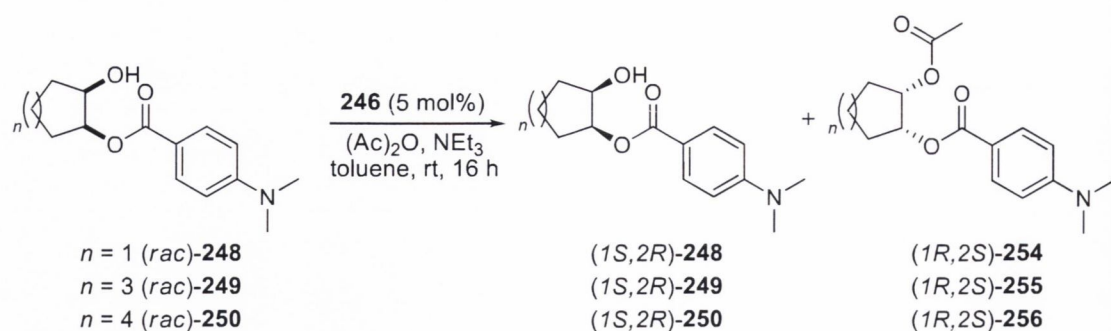
^aDetermined using ¹H-NMR spectroscopy. ^bDetermined by CSP-HPLC using Daicel CHIRALCEL OD-H (4.6 mm x 25 cm) and CHIRALPAK AS (4.6 mm x 25 cm) columns.

Catalyst **246** was demonstrated to be capable of practical acylative kinetic resolution of a *sec*-alcohol (*rac*)-**58** with acetic anhydride at ambient temperature over the 20 cycles. The rational next step was to investigate the useful lifespan of the catalyst and explore its use with other *sec*-alcohol substrates. The same batch of material used in the experiments outlined in Table 2.7 was then used to promote the kinetic resolution of a range of *sec*-alcohols, characterised by variable steric and electronic properties, with acetic anhydride at ambient temperature.

Employing the same catalyst recovery methodology used before we found that 5, 7 and 8-membered analogues of the mono-protected *cis*-diol (*rac*)-**58** (Scheme 2.13) could be resolved to afford the alcohols (1*S*,2*R*)-**248**, (1*S*,2*R*)-**249** and (1*S*,2*R*)-**250** in high enantiomeric excess (Scheme 2.13).

The kinetic resolution of alcohol (*rac*)-**248** promoted by catalyst **246** gave selectivity values of 3.30, 2.90 and 3.24, resulting in the recovered alcohol (1*S*,2*R*)-**248** being isolated in 93%, 86% and 89% *ee*, respectively (Table 2.8, entries 1-3). The kinetic resolution of the 8-membered cyclic mono-protected alcohol (*rac*)-**250** gave the recovered alcohol (1*S*,2*R*)-**250** in 70% to 73% *ee*, which corresponded to selectivity values 4.64, 4.71 and 4.37 (Table 2.8, entries 4-6). The kinetic resolution of the cyclic 7-membered mono-protected alcohol (*rac*)-**249** promoted by **246** proved the most successful of these cyclic alcohols. The alcohol (1*S*,2*R*)-**249** was recovered in 89%, 80% and 83% *ee*, giving selectivity values of 6.40, 6.71 and 6.09, respectively (Table 2.8, entries 7-9).

While *sec*-alcohols (*rac*)-**248**, (*rac*)-**249** and (*rac*)-**250** were resolved without difficulty, in line with findings from Fuji's group,⁹⁸ it was found that alternative ring sized diol derivatives proved considerably more challenging substrates than the 6-membered prototype.



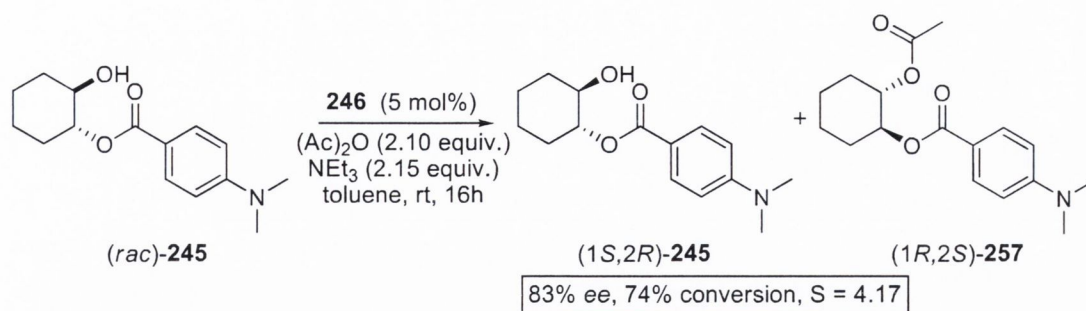
Scheme 2.13 Cycle 21 to 29: acylative KR of mono-protected diols (*rac*)-**248**, (*rac*)-**249** and (*rac*)-**250** promoted by catalyst **246**

Table 2.8 Recycling of catalyst **246** in the acylative KR of **248**, **249** and **250**

Entry	Substrate	<i>n</i>	Catalyst (mol%)	NEt ₃ (mol%)	Anhydride (mol%)	Conversion ^a (%)	Ester <i>ee</i> ^b (%)	Alcohol <i>ee</i> ^b (%)	Selectivity
1	227	1	5	185	180	87	14	93	3.30
2	227	1	5	185	180	86	14	86	2.90
3	227	1	5	185	180	84	16	89	3.24
4	229	4	5	210	200	63	41	70	4.64
5	229	4	5	210	200	63	41	70	4.71
6	229	4	5	210	200	66	37	73	4.37
7	228	3	5	185	180	69	40	89	6.40
8	228	3	5	185	180	62	43	80	6.71
9	228	3	5	185	180	66	43	83	6.09

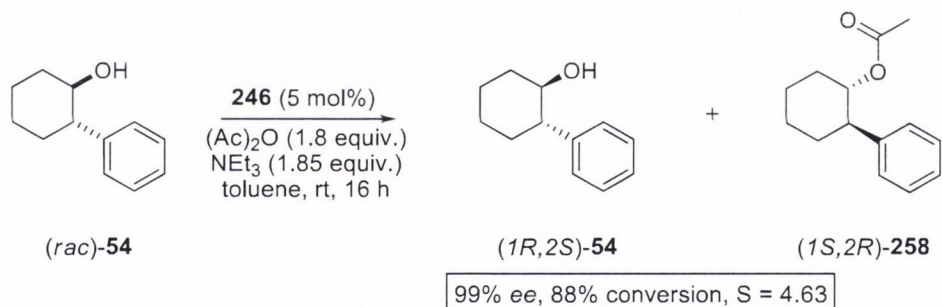
^aDetermined using ¹H-NMR spectroscopy. ^bDetermined by CSP-HPLC using Daicel CHIRALCEL OD-H (4.6 mm x 25 cm) and CHIRALPAK AS (4.6 mm x 25 cm) columns.

Continuing with the same supported catalyst used in the previous 29 experiments, the mono-substituted *sec*-alcohol (*rac*)-**245** with *trans* stereochemistry was also tolerated by catalyst **246**, allowing the alcohol product (*1S,2R*)-**245** to be recovered in 83% *ee* at 74% conversion, giving a selectivity factor of 4.17 (Scheme 2.14).



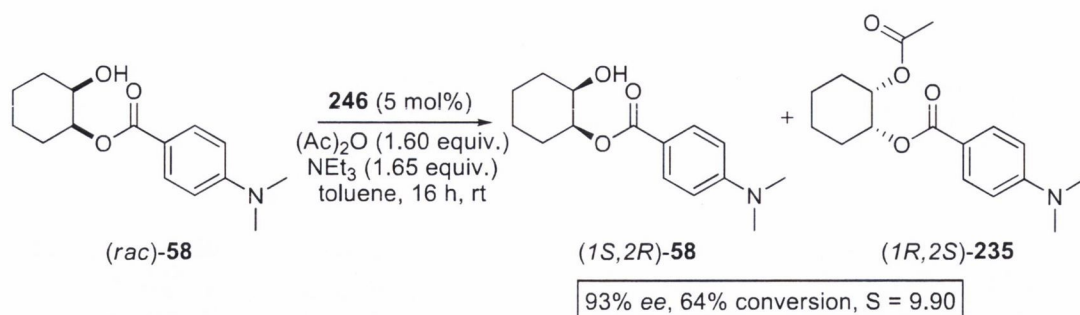
Scheme 2.14 Cycle 30: acylative KR of alcohol *(rac)*-**245** promoted by catalyst **246**

The phenyl substituted cyclic *sec*-alcohol *(rac)*-**54** also underwent acylative kinetic resolution by catalyst **246**, allowing the alcohol product *(1R,2S)*-**54** to be recovered in 99% *ee* at 88% conversion, giving a selectivity factor of 4.63 (Scheme 2.15). This amounted to a total of 31 consecutive cycles employing the same batch of magnetic nanoparticle-supported catalyst.



Scheme 2.15 Cycle 31: acylative KR of alcohol *(rac)*-**54** promoted by catalyst **246**

The interest was to ascertain the relative level of catalyst performance after being exposed to 31 iterative recycles. To determine this, the kinetic resolution of the initial *sec*-alcohol *(rac)*-**58** was undertaken once again under the same reaction conditions (Scheme 2.16). The now heavily recycled catalyst **246** performed exceptionally well, promoting the acylation with a selectivity factor of 9.9, giving the recovered *sec*-alcohol *(1S,2R)*-**58** in 93% *ee* at 64% conversion.



Scheme 2.16 Cycle 32: acylative KR of *(rac)*-**58** promoted by supported catalyst **246**

The analysis and characterisation of catalyst **246** was appreciatively carried out by Yurii K. Gun'ko and Renata Tekoriute of the CRANN Institute at the School of Chemistry, Trinity College Dublin using transmission electron microscopy (TEM), fourier transform infrared spectroscopy (FTIR) and thermogravimetric analysis (TGA) (Appendix 1). According to TEM analysis the average magnetite nanoparticle size was 8.1 ± 1.8 nm in diameter. After the magnetite nanoparticles were loaded with catalyst a decrease in aggregation of the magnetite nanoparticles without effect on the average particle size (7.9 ± 1.5 nm) was observed (Figure 2.3).

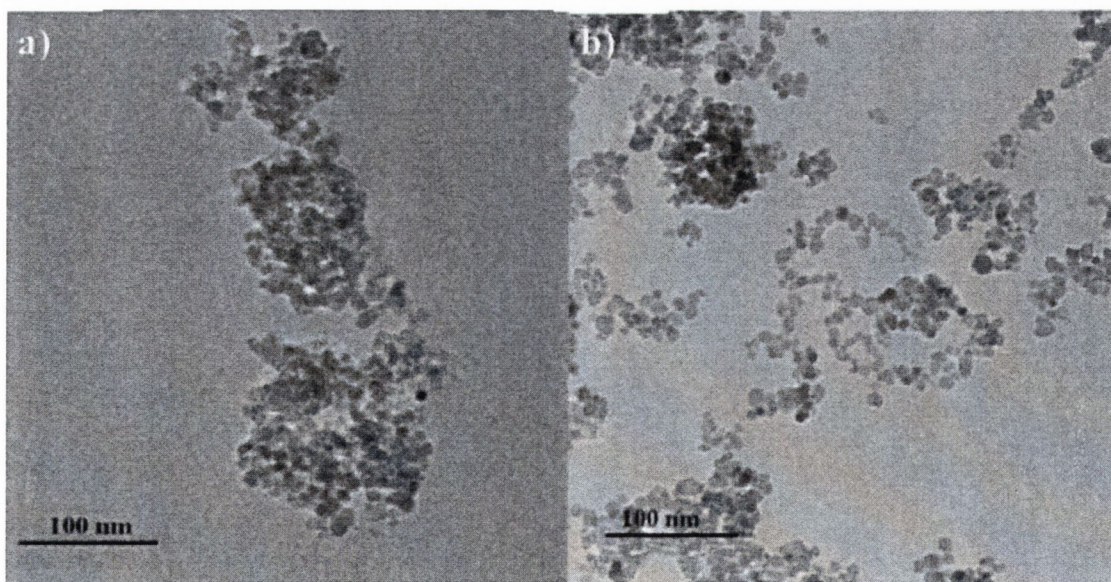


Figure 2.3 TEM images of a) magnetite nanoparticles, b) catalyst treated nanoparticles.

2.2 Conclusions

The initial synthetic strategy in the development of a chiral DMAP-based magnetic nanoparticle-supported catalyst proved unsuccessful. This was due to the inability to isolate a pure sample of the alkoxy silane DMAP derivative using column chromatography in various mobile phases. The recrystallisation and/or trituration of the derivative also proved unsuccessful. The reason for this still remains elusive considering an achiral DMAP alkoxy silane derivative catalyst was successfully isolated and purified by previous members of the Connon group.¹⁹³

The second synthetic strategy of first attaching a triethoxysilane moiety to the magnetic nanoparticle, followed by the heterogeneous coupling of the catalyst to the magnetic nanoparticle functionalised 3-mercaptopropyl silane species also failed (Section 2.1.2). This was associated with the oxidation of the thiol group of the 3-mercaptopropyl silane in the presence of the Fe₃O₄ magnetite nanoparticles and presumably air, which resulted in the formation of disulfide side products.

The third synthetic strategy, employing the use of a *N*-methyldopamine anchor proved successful. This was achieved by first immobilising the *N*-methyldopamine onto the magnetic nanoparticle, followed by the heterogeneous coupling of the 4-chloropyridine catalyst moiety to the *N*-methyldopamine-anchored magnetic nanoparticle (Section 2.1.3). Catalyst loading was determined by ¹H-NMR spectroscopy using 2,5-diphenylfuran as the internal standard. The final catalyst loading was determined to be 0.145 mmol/g. The unreacted *N*-methyldopamine anchored to the nanoparticle was converted to the corresponding amide using acetic anhydride to give the heterogeneous magnetic nanoparticle supported chiral 4-*N,N*-dialkylaminopyridine catalyst **244**. The final step involved the capping of the magnetic nanoparticle iron oxide exposed surface. This was accomplished by using *N*-propyltrimethoxysilane to give the catalyst **246** (Section 2.1.3.2).

This study has shown that a chiral organocatalyst which relies on a confluence of weak, easily perturbed van der Waals and hydrogen bonding interactions to promote enantioselective reactions, can be readily immobilised on magnetite nanoparticles. The resulting heterogeneous catalyst is highly active and is capable of promoting the kinetic

resolution of *sec*-alcohols with synthetically useful selectivity under process-scale friendly conditions (ambient temperature, low catalyst loading and acetic anhydride as the acylating agent) - which allows the isolation of resolved alcohols with good-excellent enantiomeric excess. The magnetic catalyst is simple to prepare, insensitive to air/moisture and easily recoverable by exposure of the reaction vessel to an external magnetic field.

Perhaps most importantly, the somewhat surprising lack of interaction between the nanoparticle core and the organocatalyst unit results in a chiral heterogeneous catalyst *which is recyclable to an unprecedented extent* – in this study it has been demonstrated to be reusable in a minimum of 32 consecutive cycles while retaining high activity and selectivity profiles.

As the sophistication of homogeneous catalysts emerging from the ever burgeoning organocatalysis field increases, the compatibility of this magnetite-nanoparticle immobilisation methodology with an organocatalyst known to be highly sensitive to its environment⁸³⁻⁸⁵ bodes well for the further general applicability of this emerging nanotechnology at the frontier of (asymmetric) catalysis.

3.1 Magnetic nanoparticle supported 9-*epi*-quinine urea based catalyst

Cinchona alkaloids are readily available and inexpensive naturally occurring catalysts that have *pseudo*-enantiomeric forms such as quinine, quinidine, cinchonine and cinchonidine. One of the key structural features associated with their synthetic utility is the presence of the tertiary quinuclidine nitrogen along with the polar hydroxyl functionality in close proximity. These features enable cinchona alkaloids to behave as bifunctional catalysts due to the presence of Lewis acidic (H-bonding hydroxy group) and Lewis basic (quinuclidine nitrogen) sites (Figure 3.1).

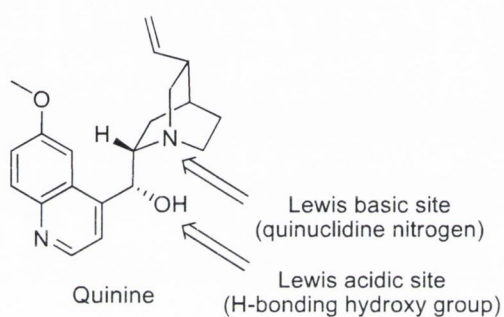


Figure 3.1 The Lewis acidic and Lewis basic sites of quinine

Pioneering work by Jacobsen and co-workers demonstrated the ability of urea and thiourea functional groups to act as powerful hydrogen-bond donors.^{205,206} Takemoto and co-workers also established the hydrogen-bond donating ability of thiourea, coupled with the basicity of tertiary amines to develop chiral bifunctional organocatalysts capable of enantioselective Michael and aza-Henry reactions.^{207,208} The ability of naturally occurring cinchona alkaloids to act as bifunctional organocatalysts coupled with the powerful hydrogen-bond donating ability of urea and thiourea derivatives led to the development of cinchona urea and thiourea bifunctional catalysts by Soós and co-workers.²⁰⁹ It has been shown by our group as well as others that these highly versatile catalysts can promote (*inter alia*) enantioselective Michael addition,^{210,211} Dynamic Kinetic Resolution (DKR),²¹² desymmetrisations,²¹³ Henry reactions²¹⁴ and transthioesterification processes,²¹⁵ while other groups have demonstrated their utility in a range of applications mostly in either addition or cycloadditions reactions.^{216,217} Due to the stability and reaction scope of the cinchona alkaloid derived 9-*epi*-quinine urea

259 (Figure 3.2), its candidacy as a magnetic nanoparticle supported catalyst would appear to be highly desirable.

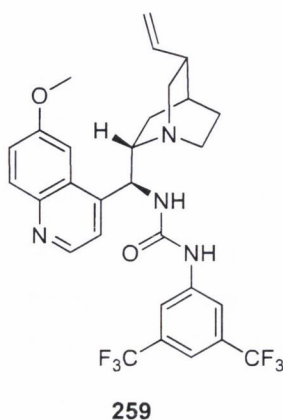


Figure 3.2 Potential heterogeneous catalyst 9-*epi*-quinine urea catalyst **259**

Two important factors when considering the heterogenisation of a chiral homogeneous catalyst is the catalyst anchoring site and the mode of attachment. It is a rational assumption that the anchoring site of the catalyst should be sufficiently remote from the ‘active catalytic site’ and any stereocentres so as not to interfere with catalytic activity or selectivity. The method used to immobilise the catalyst onto the magnetic nanoparticle support should proceed under relatively mild conditions so as not to cause unnecessary side reactions that could potentially result in catalyst decomposition.

The proposed catalyst for immobilisation **259** has potentially two positions which are sufficiently distant from the active catalytic site and stereocentres to merit their consideration as possible tether locations (Figure 3.2). Position **A** would appear to have potential for the insertion of a linking tether, due to its remoteness from the catalytic active sites. Synthetically this would involve the conversion of the methoxy group to a hydroxy group followed by the insertion of a linker *via* an ester or ether coupling to the appropriate tether.

Position **B** offers the best potential for a straight forward synthetic approach to a solid-support catalyst precursor involving a one-reaction strategy with the olefin side chain of catalyst **259** and an appropriate thiol linker *via* a thiol-ene radical reaction. A rational

choice of thiol linker is the relatively inexpensive and commercially available (3-mercaptopropyl)-triethoxysilane, due to the ability of the siloxane group to readily bind to the surface of magnetic nanoparticles.^{185,193,218}

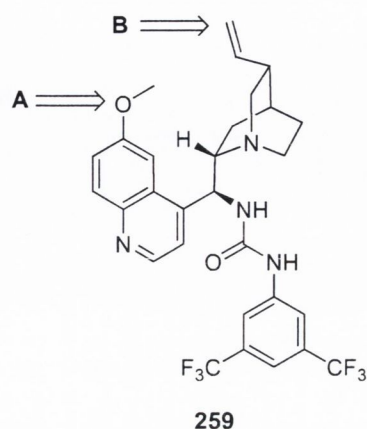
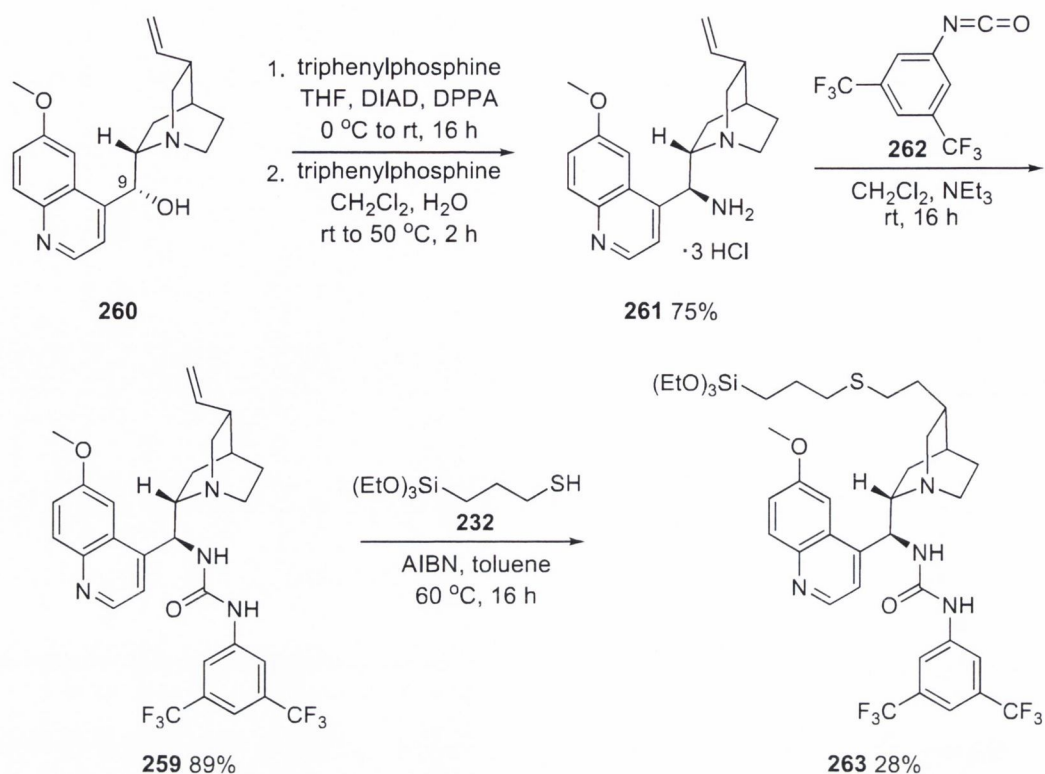


Figure 3.3 Proposed tethering positions for the immobilisation of catalyst **259**

3.1.1 Synthesis of catalyst precursor

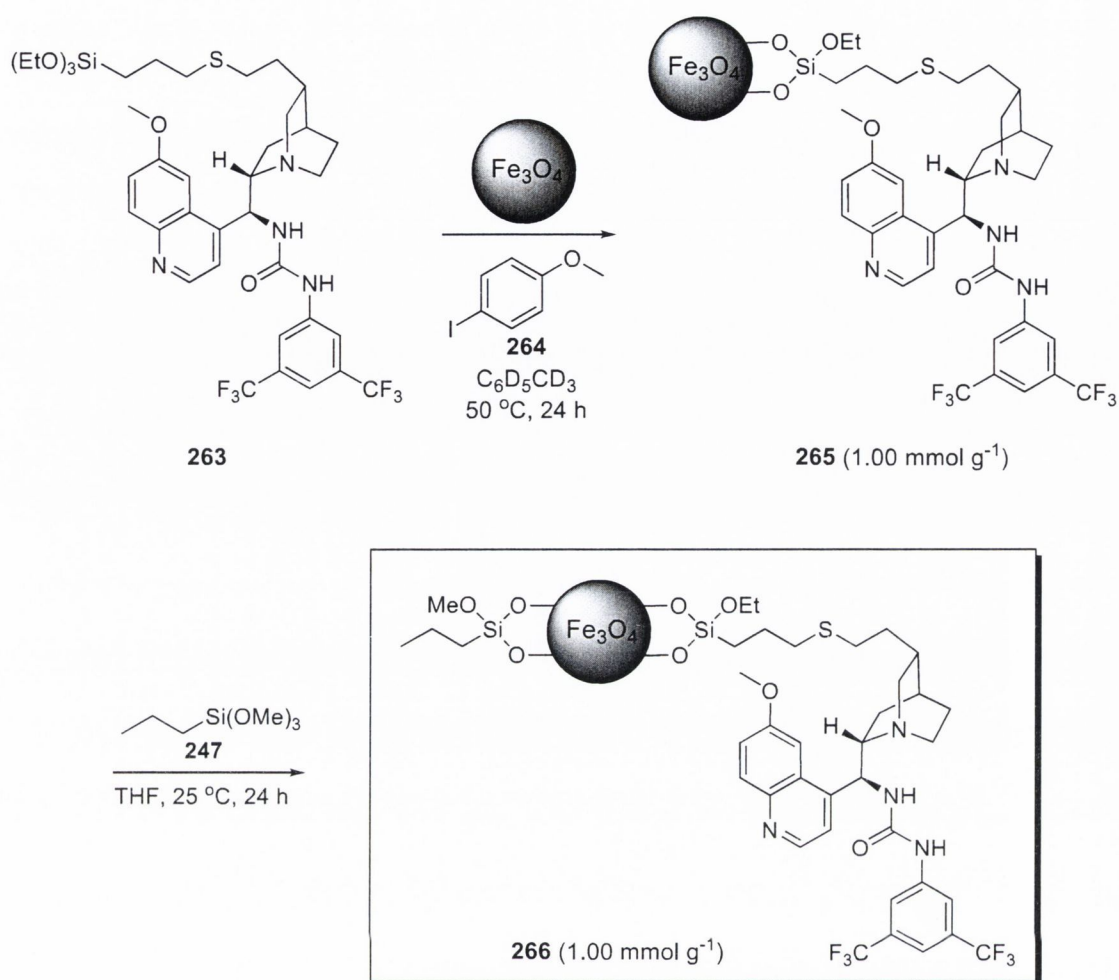
The synthesis of urea-based catalyst **259** was straight forward, the first step involved the amination of **260** at the C-9 position with a modified Mitsunobu reaction to give the 9-*epi*-quinine amine hydrochloride salt **261** (Scheme 3.1). This was followed by the coupling of isocyanate **262** to the amine salt in the presence of excess triethylamine base to give catalyst **259** (Scheme 3.1).²¹⁰ The final step in the preparation of the siloxane-modified catalyst precursor involved the radical thiol-ene reaction of (3-mercaptopropyl)-triethoxysilane with catalyst **259** using the radical initiator azobisisobutyronitrile (AIBN) in toluene at 60 °C for 16 hours to give **263**. Initial analysis of the reaction using ¹H-NMR spectroscopy demonstrated that the radical thiol-ene reaction reached 100% conversion in 16 hours. However, after purification using flash chromatography the actual product yield was found to be 28% (Scheme 3.1).



Scheme 3.1 Synthesis of siloxane catalyst precursor **263** from quinine

3.1.2 Catalyst loading

The synthesis of the magnetic nanoparticle supported catalyst **265** was performed at a moderate temperature (50 °C) in deuterated toluene over a 24 hour period in the presence of the internal standard 4-iodoanisole (**264**). Catalyst loading was determined to be 1.00 mmol g⁻¹ using ¹H-NMR spectroscopic analysis of the resulting solution which showed no traces of resonance corresponding to the catalyst loading precursor. The final step in the preparation of the magnetic nanoparticle-supported catalyst involved the capping of the nanoparticle's exposed surface using *N*-propyltrimethoxysilane (**247**) at 25 °C in THF to give catalyst **266** (Scheme 3.2).

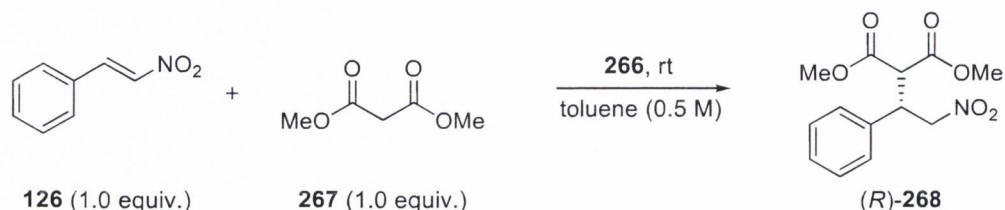


Scheme 3.2 Synthesis of MNP-supported bifunctional urea catalyst **266**

3.1.3 Catalyst evaluation: preliminary studies

Initial investigative studies involving the asymmetric Michael addition of dimethyl malonate (**267**) to (*E*)- β -nitrostyrene (**126**) promoted by the magnetic nanoparticle supported bifunctional organocatalyst **266** revealed it to be both active and capable of promoting enantioselective chemistry (Scheme 3.3). The first cycle was undertaken using 2 mol% catalyst loading in toluene at room temperature. This resulted in a 57% conversion after 40 hours, with 62% product *ee* (Table 3.1, entry 1). The low conversion rate prompted the need for higher catalytic loading, therefore, in the second cycle a catalyst loading of 5%, in an otherwise identical reaction, gave 79% conversion after 40 hours, resulting in 63% *ee* (Table 3.1, entry 2). To overcome the long reaction times in order to improve catalyst turnover, the reaction was repeated with the same

batch of catalyst in a 16 hour reaction using 5 mol% catalyst loading. Disappointingly, only 41% conversion was observed but *ee* did remain consistent with previous cycles at 60% (Table 3.1, entry 3). In order to verify the decline in catalyst performance, the reaction was repeated under identical conditions as the previous cycle with the same catalyst loading. Unfortunately this proved significantly worse with only 36% conversion and 56% *ee* observed (Table 3.3, entry 4).



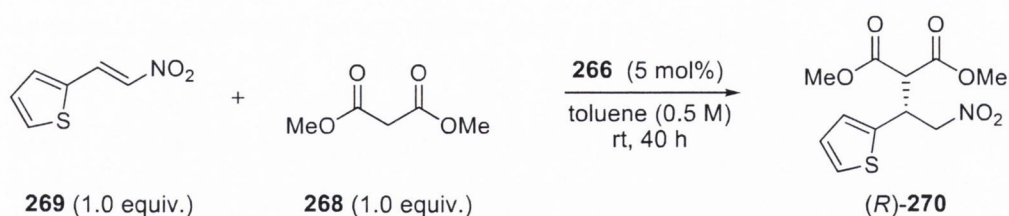
Scheme 3.3 Asymmetric Michael addition promoted by MNP-supported catalyst **266**

Table 3.1 Addition of dimethyl malonate to (*E*)- β -nitrostyrene catalysed by **266**

Entry	Catalyst loading (mol%)	Time (h)	Conversion (%) ^a	<i>ee</i> (%) ^b
1	2	40	57	62
2	5	40	79	63
3	5	16	41	60
4	5	16	36	56

^aDetermined using ¹H-NMR spectroscopy. ^bDetermined by CSP-HPLC using Daicel CHIRALCEL AD-H (4.6 mm x 25 cm) and CHIRALPAK AS (4.6 mm x 25 cm) columns.

The gradual decline in catalyst performance over the four cycles prompted the preparation of a fresh batch of MNP-supported catalyst using the same synthetic strategy as previously outlined (Section 3.1.2). The newly prepared batch of catalyst **266** was then employed in the asymmetric Michael addition of dimethyl malonate (**267**) to (*E*)-2-(2-nitrovinyl)thiophene (**269**, Scheme 3.4).



Scheme 3.4 Asymmetric Michael addition promoted by MNP-supported catalyst **266**

Our initial investigations into the asymmetric addition of dimethyl malonate to (*E*)-2-(2-nitrovinyl)thiophene (**269**) promoted by catalyst **266** appeared promising. Using 2.0 equivalents of dimethyl malonate and 5 mol% catalyst loading over a 40 hour reaction time gave the addition product **270** in 66% yield and 70% *ee* (Table 3.2, entry 1). The consistency of the catalyst performance was then investigated by repeating the process under the same reaction conditions as previously employed. Both yield and *ee* of the addition product were lower than those observed in the first cycle, with 52% yield and 65% *ee* obtained for product **270** (Table 3.2, entry 2). To further evaluate the full potential of catalyst **266**, the process was repeated for a third consecutive cycle under identical reaction conditions. Conversion in the third cycle proved quite disappointing (35%) while *ee* remained consistent with the previous cycles at 64% (Table 3.2, entry 3).

Table 3.2 Addition of dimethyl malonate to (*E*)-2-(2-nitrovinyl)thiophene

Entry	Conversion (%) ^a	<i>ee</i> (%) ^b
1	66	70
2	52	65
3	35	64

^aDetermined using ¹H-NMR spectroscopy. ^bDetermined by CSP-HPLC using Daicel CHIRALCEL AD-H (4.6 mm x 25 cm) and CHIRALPAK AS (4.6 mm x 25 cm) columns.

The employment of catalyst **266** in the asymmetric addition of dimethyl malonate to (*E*)-2-(2-nitrovinyl)thiophene proved less successful than anticipated, with a sharp decline in conversion observed in the third cycle. This led to the reinvestigation of the asymmetric addition of dimethyl malonate to (*E*)-β-nitrostyrene where the reduced

reaction times of 20 hours and a catalytic loading of 5 mol% could potentially prolong the catalyst life expectancy.

The synthesis of a new batch of MNP-supported catalyst **266** was undertaken *via* the same process as previously outlined where catalyst loading was determined to be 1.00 mmol g⁻¹ using ¹H-NMR spectroscopic analysis. In the first reaction, 79% conversion and 58% *ee* were observed (Table 3.3, entry 1). The second cycle was consistent with the first one, where the addition product was recovered in 76% conversion and 62% *ee* (Table 3.3, entry 2). Repeating the catalytic cycle under identical conditions for a third consecutive cycle gave 70% conversion and 60% *ee* for the addition product (Table 3.3, entry 3). Continuing with the same batch of catalyst a fourth cycle was undertaken, however, conversion had greatly diminished to 45% while *ee* remained consistent with previous cycles at 64% (Table 3.3, entry 4).

Table 3.3 Asymmetric Michael addition of dimethyl malonate to (*E*)- β -nitrostyrene

Entry	Conversion ^a (%)	<i>ee</i> ^b (%)
1	79	58
2	76	62
3	70	60
4	45	64

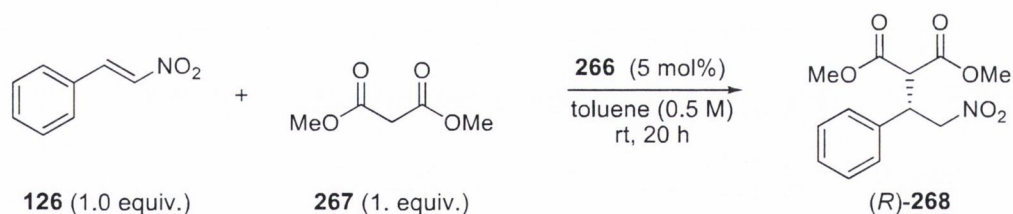
^aDetermined using ¹H-NMR spectroscopy. ^bDetermined by CSP-HPLC using Daicel CHIRALCEL AD-H (4.6 mm x 25 cm) and CHIRALPAK AS (4.6 mm x 25 cm) columns.

3.1.4 Asymmetric Michael additions to nitroolefins catalysed by magnetic nanoparticle supported catalyst **266**

Following our preliminary studies into the asymmetric Michael addition of dimethyl malonate to nitroolefins we determined that shorter reaction times favoured catalyst longevity. The use of (*E*)- β -nitrostyrene as opposed to (*E*)-2-(2-nitrovinyl)thiophene helped to facilitate this necessity by requiring shorter reaction times to achieve a desirable conversion to the addition product. To fully investigate the ability of catalyst **266** in the asymmetric Michael addition, the preparation of a new batch of MNP-

catalyst was undertaken using the same procedure as outlined in Section 3.1.2. The catalyst loading was determined to be 1.00 mmol g⁻¹ using ¹H-NMR spectroscopic analysis.

The newly prepared MNP-catalyst **266** was investigated in the asymmetric addition of dimethyl malonate to (*E*)- β -nitrostyrene at 20 °C using 5 mol% catalyst loading in a 0.5M solution in toluene over a 20 hour reaction time (Scheme 3.5). Preliminary results revealed that the newly prepared catalyst could perform better than in previous studies, with 70% conversion and 71% *ee* observed in the first cycle (Table 2.4, entry 1). Repeating the reaction process under identical reaction conditions gave results consistent with the first cycle where conversion and *ee* were 70% and 72% respectively. Repeating the process for a third consecutive cycle under the same reaction conditions gave a conversion consistent with the first two cycles at 71% with the *ee* marginally higher at 77% (Table 3.4, entry 3). To continue our evaluation of catalyst **266** the reaction was repeated a fourth time under the same reaction conditions as previously mentioned. However, a sharp decline in conversion was observed with the addition product only reaching 46% conversion (Table 3.4, entry 4). Due to the swift decline in catalyst performance the *ee* for the fourth cycle was not determined.



Scheme 3.5 Asymmetric Michael addition promoted by MNP-supported catalyst **266**

Table 3.4 Asymmetric Michael addition of dimethyl malonate to (*E*)- β -nitrostyrene

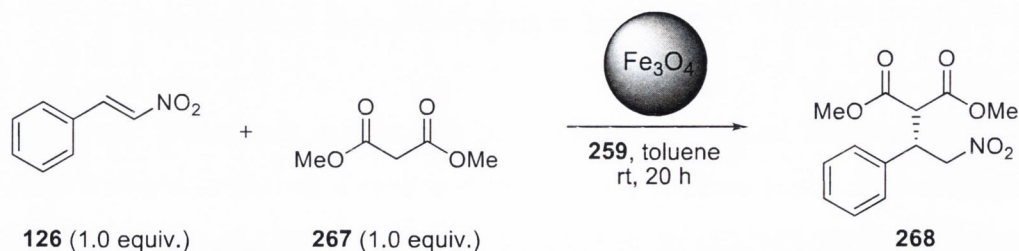
Entry	Conversion (%) ^a	<i>ee</i> (%) ^b
1	70	71
2	70	72
3	71	77
4	46	n.d.

^aDetermined using ¹H-NMR spectroscopy.

^bDetermined by CSP-HPLC using Daicel CHIRALCEL AD-H (4.6 mm x 25 cm) and CHIRALPAK AS (4.6 mm x 25 cm) columns.

Interestingly the decline in catalyst activity was observed whether or not the catalyst was employed in a reaction. A newly prepared batch of catalyst **266** was stored under an inert atmosphere for two days after the initial investigation to determine its ability. The repeat experiment showed the catalyst to be less active in the asymmetric Michael addition, delivering only 50% conversion as opposed to 68% in the first cycle, although *ee* was consistent with the first cycle. This would suggest that the decrease in catalyst activity was not solely dependent on activity but rather a function of time.

Our next subject of interest was to investigate the potential role of the magnetite nanoparticle in reducing the catalyst efficiency from a stereoselectivity perspective. This was accomplished using the homogeneous urea catalyst **259** (Scheme 3.1) to promote the asymmetric Michael addition of dimethyl malonate to (*E*)- β -nitrostyrene in the presence of the equivalent quantity of capped magnetite nanoparticles as that used in the heterogeneous catalyst system (Scheme 3.6).

**Scheme 3.6** Investigation of magnetic nanoparticle potential influence on *ee*

Our first experiment demonstrated that no uncatalysed background reaction between **126** and **267** occurred in the absence of both catalyst **259** and magnetic nanoparticles (Table 3.5, entry 1). Our next objective was to determine the efficiency of catalyst **259** to promote the asymmetric Michael addition of dimethyl malonate to (*E*)- β -nitrostyrene. Under otherwise identical reaction conditions to that used in the heterogeneous catalyst system, the addition product was obtained with 90% conversion and 94% *ee* (Table, entry 2). Under the same reaction conditions with the exclusion of catalyst **259** and using the equivalent quantity of unfunctionalised capped magnetic nanoparticles (200 mg) as that present in the heterogeneous catalyst system, a 6% conversion and 0% *ee* was observed (Table 3.5, entry 3). The final experiment involved the inclusion of both catalyst and capped magnetic nanoparticles in the asymmetric Michael addition under the same reaction conditions. The addition product was observed in 100% conversion and 84% *ee* (Table 3.5, entry 4). The ability of the magnetic nanoparticles to catalyse the symmetric Michael addition in parallel to the asymmetric Michael Addition promoted by catalyst **259** precludes their use as a suitable heterogeneous solid support.

Table 3.5 Results from MNP potential influence on *ee*

Entry	Catalyst loading (mol%)	Nanoparticle (mg/mg of 126)	Conversion (%) ^a	<i>ee</i> (%) ^b
1	0	0	0	-
2	5	0	90	94
3	0	3.36	6	0
4	5	3.36	100	84

^aDetermined using ¹H-NMR spectroscopy. ^bDetermined by CSP-HPLC using Daicel CHIRALCEL AD-H (4.6 mm x 25 cm) and CHIRALPAK AS (4.6 mm x 25 cm) columns.

In an attempt to better understand the fate of catalyst **266** after multiple cycles, the characterisation of three batches of nanoparticles was undertaken: one batch which had not been loaded with catalyst, one batch which was functionalised with catalyst and used in the asymmetric Michael addition and one which had also been loaded with catalyst but not used in any catalytic processes using transmission electron microscopy (TEM), fourier transform infrared spectroscopy (FTIR), thermogravimetric analysis (TGA) and X-ray diffraction (XRD) (Appendix 1). The analysis and characterisation of

catalyst **266** was appreciatively undertaken by Yurii K. Gun'ko and Dr Gemma-Louise Davies of the CRANN Institute at the School of Chemistry, Trinity College Dublin.

According to TEM analysis the average nanoparticle diameter was determined to be 10 ± 2 nm. The batch of catalyst loaded nanoparticles that underwent several cycles showed no change in either morphology or nanoparticle size relative to the unused catalyst immobilised nanoparticles using TEM analysis. FTIR analysis showed the successful functionalisation of the magnetic nanoparticles and also demonstrated that no degradation or damage appeared to occur after several cycles. TGA analysis showed an increase in organic material on the catalyst loaded nanoparticles after several cycles, indicating an alteration in composition from repeated use. This change in composition could potentially be responsible for the decrease in catalyst activity over time. The nature of the change is not obvious, as FTIR and XRD analysis displayed no change in the composition of the core nanoparticle or the nature of the organic functionalities.

3.2 Conclusion

This study demonstrated the successful immobilisation of a quinine derived urea organocatalyst that relies on weak van der Waals and hydrogen bonding interactions onto magnetic nanoparticles. Despite promising initial results the decline in catalyst performance was apparent after three to four cycles. The preparation of immobilised catalyst precursor **263** via a thiol-ene radical reaction proved to be a straight forward synthetic strategy, although the final yield after purification was relatively low at 28%. The immobilisation of **263** demonstrated to be more economical with 100% loading observed in 24 hours to give the magnetic nanoparticle supported catalyst **264** in 1.00 mmol g^{-1} . The final step involved the capping of any potentially exposed iron oxide surface using *N*-propyltrimethoxysilane to give the MNP-supported catalyst **266**.

Initial evaluation of catalyst **266** demonstrated its ability to be both active and capable of promoting enantioselective in the asymmetric Michael-type additions of dimethyl malonate to nitroolefins. However, it also demonstrated that catalyst **266** was less effective than its homogeneous counterpart even at higher catalytic loadings. Gradual improvements in the procedure with repeated analysis did result in a small improvement in conversion and enantioselectivity, although not to the same level as that obtained in

the homogeneous catalyst. Investigation into the role the magnetite nanoparticles exerted on the homogeneous system did lend insight into the lower levels of enantioselectivity observed. However, it did not account for poor catalyst activity.

Determining the reason for the rapid loss in catalyst activity after three to four cycles proved more elusive. One factor did emerge from the repeated preparation and employment of catalyst **266** in asymmetric Michael additions. The loss in catalyst activity was consistent with each batch of newly prepared catalyst and the degradation of each batch was, to the same degree, a time dependent process regardless of workload. This is evident when comparing the results of the addition of dimethyl malonate to (*E*)-2-(2-nitrovinyl)thiophene (**269**) as opposed to (*E*)- β -nitrostyrene (**126**). The reaction times for the addition of dimethyl malonate to **269** took 40 hours to reach a *circa* 70% conversion, which is almost double that for the addition to **126**. However, a decline in conversion was only observed after 80 hours of catalytic activity when using (*E*)-2-(2-nitrovinyl)thiophene as opposed to a consistent decline was observed after 60 hours using (*E*)- β -nitrostyrene.

Comparatively examining the results of catalyst **266** with that of the DMAP-based heterogeneous catalyst **246** (Section 2.1.3.4) suggests that the successful heterogenisation of a catalyst hinges on the structure of the catalyst being immobilised. This is evident from the DMAP-based catalyst being able to successfully promote the acylative kinetic resolution of a range of *sec*-alcohols over 30 cycles without any appreciative loss in activity, whereas the quinine derived urea catalyst **266** showed a sharp loss in activity after only 4 cycles. In relation to the utilisation of magnetite nanoparticles as a solid support, another aspect of considerable importance is the reaction sequence and whether or not the nanoparticles are capable of competitive promotion the reaction. The magnetite nanoparticles were capable of promoting the Michael addition of dimethyl malonate to nitroolefins whereas they were found to be inert in the acylative kinetic resolution of *sec*-alcohols.

4.1 Proline-derived catalysts for the kinetic resolution of alcohols

Enantioenriched secondary alcohols are perhaps one of the most important classes of building blocks available to the chemist interested in asymmetric synthesis. Among the most straightforward methodologies for accessing these compounds is the acylative KR of the corresponding racemic materials. While enzyme-based catalysis protocols have been available for some time,^{219,220} the development of artificial small-molecule catalysts for these reactions has emerged as a powerful alternative tool over the past two decades.^{16,88,89,120} A variety of catalytic systems for the acylative kinetic resolution of secondary alcohols has been developed. These were recently categorised by Schreiner and Müller¹⁹ as belonging to distinct groups: phosphines and phosphinites (Section 1.2.4.5), 4-*N,N*-dialkylaminopyridines (Section 1.2.3), *N*-alkylimidazoles (Section 1.2.4.1), amidines (Section 1.2.4.4), vicinal diamines (Section 1.2.4.3) and *N*-heterocyclic carbenes (Section 1.2.4.2).

The development of a series of chiral proline-derived 4-*N,N*-dialkylaminopyridine catalysts by our group for the kinetic resolution of *sec*-alcohols revealed some very interesting structure-activity relationship characteristics.⁸⁵ Catalysts **53** and **56** (Figure 4.1) were readily prepared from the same amino acid (L-proline). However, when employed in the acylative kinetic resolution of *sec*-alcohols they were found to preferentially acylate opposite antipodes (Section 1.2.3.4).

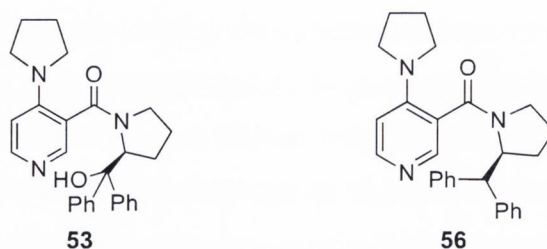


Figure 4.1 Chiral proline-derived 4-*N,N*-dialkylaminopyridine catalysts **53** and **56**

We were interested in investigating what role the hydroxy functionality on the pendent chiral moiety played in the catalytic process: *i.e.* whether it influences the stereochemical outcome acting as an acid or a base (general acid or general base catalysis respectively). To investigate the general acid/base hypothesis, the substitution

of the hydroxy group for alternative functional groups which can only function as an acid, a base or a neutral moiety could lend insight into this conundrum.

Our strategy was a qualified success: the optimum catalysts **53**⁸⁴ and **56**⁸⁵ are readily prepared from L-proline and were capable of synthetically useful enantioselective acylation ($s > 10$, maximum of 30)²¹ of a variety of *sec*-alcohols (including challenging sp^2 - sp^2 carbinol substrates).⁸³ Leigh *et al.* have subsequently utilised **53** as a tool in the operation of a molecular ratchet.²²¹ However – with the exception of their ability to sp^2 - sp^2 carbinols – these catalysts are easily out-performed by the benchmark literature systems in the KR of all other classes of *sec*-alcohols. In addition, the factors which are responsible for enantiodiscrimination are numerous and subtle. For instance, a combination of catalyst screening, ¹H-NMR spectroscopic, X-ray crystallographic and computational studies⁸⁵ provided evidence that four characteristics of the acylated catalyst (Figure 4.2) are crucial:

- A. more enantioselective acylation occurs using substrates bearing electron-rich aromatic rings, indicating possible π -stacking with the pyridinium unit.
- B. the presence of the hydroxyl group. When this is replaced with a hydrogen atom (*e.g.* catalyst **53**), both activity and selectivity diminish. In addition the opposite substrate enantiomer is preferred (albeit with very low selectivity).
- C. the larger alkyl group of the acyl unit resides in the more hindered catalyst hemisphere.
- D. a rigidifying C-H- π interaction between the pyridine H-2 and one of the pendent aromatic rings which strengthens considerably upon acylation of the catalyst.

While the impact of A, C and D were investigated by altering the substrate, acylating agent and catalyst aromatic substituents, the clearly dominant influence of B (*i.e.* the hydroxyl group) was only investigated in a superficial fashion. Since this group

influences both catalyst activity and the magnitude/sense of enantiodiscrimination, we were interested in determining how this moiety affects the stereochemical outcome of the acylation and ascertaining if this key functionality could be used as an enantiodiscrimination switch – *i.e.* that a pair of catalysts – both derived from the considerably less inexpensive L-proline enantiomer - could be designed to be capable of participating in acylative KR processes while selecting for opposite enantiomers with approximately equal facility. We therefore synthesised a small library of novel catalysts in which the key hydroxy group has been exchanged for alternative functional groups.

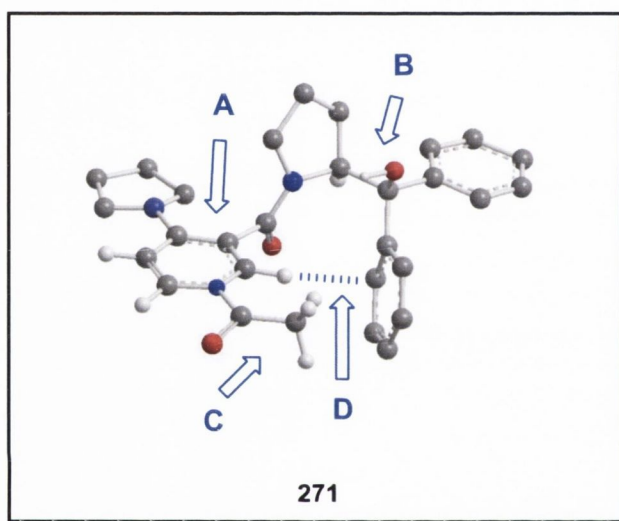
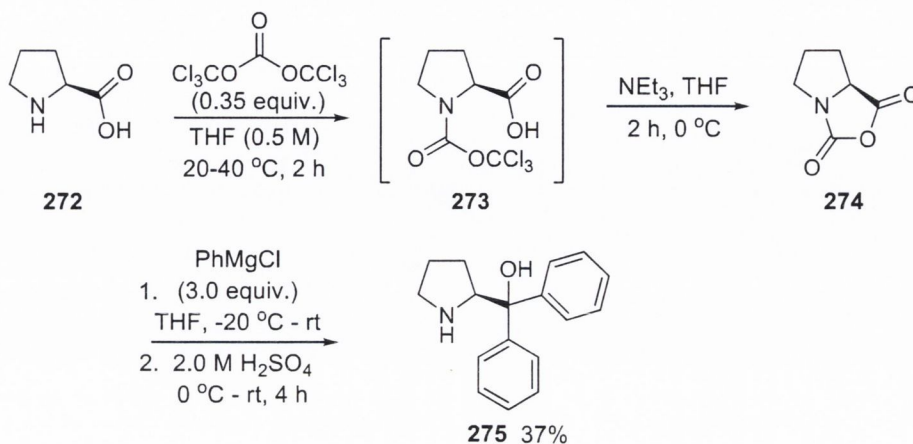


Figure 4.2 Influential factors governing previously developed DMAP analogues.⁸⁵

4.1.1 Synthesis of the hydroxy chiral pendent moiety 275

The most rational approach to the synthesis of various chiral substituted DMAP-based catalysts is to first synthesise the chiral substituent, followed by the necessary transformations to afford the desired catalyst structure. The synthesis of the chiral pendant moiety, (*S*)-(-)- α,α -diphenyl-2-pyrrolidinemethanol (**275**), from L-proline (**272**) is outlined in Scheme 4.1. This involved the formation of the carbamate intermediate from L-proline using triphosgene in THF at 20 °C and heating to 40 °C for 2 hours before allowing the reaction mixture to reach room temperature. This was followed by the addition of triethylamine in THF to form the anhydride **274**. The cyclic anhydride was treated with 3 equivalents of phenylmagnesium chloride in THF at -20 °C, and then

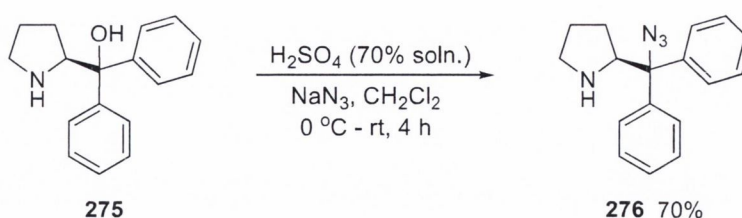
allowed to reach room temperature over 16 hours.¹⁹⁸ The reaction was quenched with the addition of 2.0 molar sulfuric acid at 0 °C to give **275** in a 37% yield (Scheme 4.1).



Scheme 4.1 Synthesis of chiral amino alcohol **275** from L-proline.¹⁹⁸

4.1.2 Synthesis of a chiral azide analogue of **276**

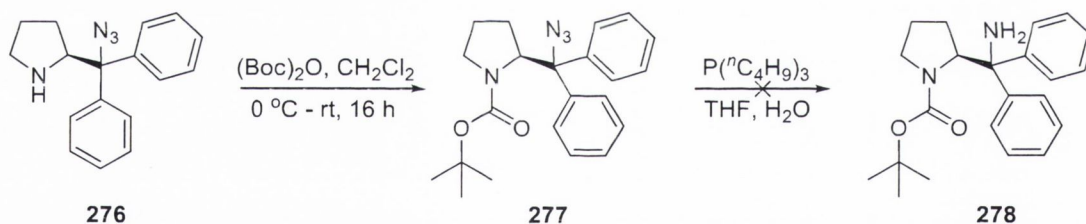
The synthesis of an azide substituted analogue of the chiral moiety **275** involved the acid catalysed $\text{S}_{\text{N}}1$ reaction by first forming the carbocation intermediate which is then attacked by the hydrazoic acid to give the azide product (Scheme 4.2). This was carried out with the slow addition of sodium azide to a biphasic solution of CH_2Cl_2 and 70% solution of H_2SO_4 containing **275** at 0 °C.²²² After the addition was completed, the reaction was then allowed to reach room temperature for 4 hours to give the azide **276** in 70% yield.



Scheme 4.2 Synthesis of chiral amino azide **276** from the amino alcohol **275**.²²²

4.1.2.1 Synthesis of chiral moiety of basic characteristic from azide **276**

The protection of amine **276** using BOC anhydride followed by the reduction of the azide functionality of compound **277** using the Staudinger reaction proved unsuccessful. Despite the use of the less hindered phosphine derivative tributylphosphine as opposed the standard triphenylphosphine no reduction was observed (Scheme 4.3). The protection of the secondary amine using BOC anhydride was straightforward; the amino azide **276** was dissolved in dry CH_2Cl_2 and cooled to $0\text{ }^\circ\text{C}$. BOC anhydride was added in small portions over a 10 minute period and subsequently the reaction was allowed to reach room temperature for 16 hours to give the azide carbamate **277**. The reduction of **277** was initially attempted using triphenylphosphine in THF over 24 hours followed by the addition of water. No product was observed under these conditions so the decision to the more reactive and less hindered tributylphosphine was undertaken. No evidence to support the formation of either a phosphazide or the iminophosphorane intermediates after 72 hours using $^1\text{H-NMR}$ spectroscopy led to the assumption that substrate **277** was too sterically hindered to undergo the initial phosphazide formation (Scheme 4.3).

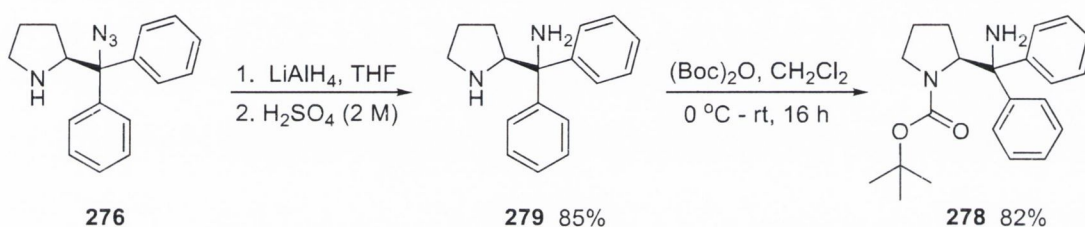


Scheme 4.3 Attempted reduction of azide using the Staudinger reaction.

The alternative approach of first reducing the azide using lithium aluminium hydride (LiAlH_4) followed by the selective protection of the secondary amine using BOC anhydride proved more successful (Scheme 4.4). The initial reductive step was carried out in THF at $0\text{ }^\circ\text{C}$ with the slow addition of small portions of LiAlH_4 over a 10 minute period while maintaining the temperature below $10\text{ }^\circ\text{C}$. After the addition was complete, the reaction was allowed to reach room temperature for 16 hours. The reaction vessel was cooled to $0\text{ }^\circ\text{C}$ before the excess LiAlH_4 was quenched with the slow addition of water. This was followed with the addition of a 2M solution of H_2SO_4 to ensure the

complete degradation of any remaining LiAlH_4 , Li_3AlH_6 and LiH to give the diamine product **279** in 85% yield (Scheme 4.4).

The selective protection of the secondary amine proceeded without any difficulties due to the more hindered environment of the primary amine (Scheme 4.4). The diamine **279** was first dissolved in CH_2Cl_2 and cooled to $-40\text{ }^\circ\text{C}$. This was followed by the slow addition of BOC anhydride previously dissolved in a small quantity CH_2Cl_2 over a 10 minute period. The temperature was maintained at $-40\text{ }^\circ\text{C}$ for a further 2 hours before being allowed to reach room temperature for 4 hours to give the mono-protected amine **278** in 82% yield (Scheme 4.4).



Scheme 4.4 Synthesis of *vic*-diamine **279** and BOC protected amine **278**

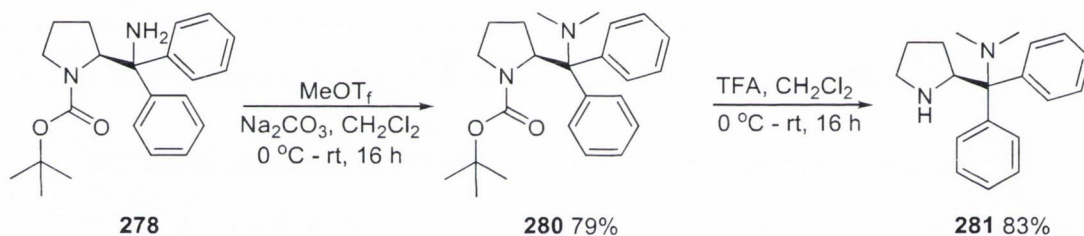
4.1.2.2 Synthesis of chiral substrate of basic characteristic

Our next aim in the preparation of a functionalised chiral pendant was to transform the primary amine functional group of **278** to a tertiary amine in order to avoid it undergoing acylation when employed in the acylative KR of alcohols. The obvious approach in the preparation of tertiary amines from primary amines is to employ a reductive amination procedure using formaldehyde in a formic acid solution known as the Eschweiler–Clarke reaction.^{223,224} This method proved problematic due to the formation of both the mono-methyl and the dimethyl products, despite the use of elevated temperatures and long reaction times ($90\text{ }^\circ\text{C}$, 72 h).

To overcome this problem the use of a more reactive alkylating agent was envisaged to be necessary. The use of methyl iodide is well documented to excessively alkylate amines to generate the quaternary ammonium salt.²²⁵ The use of methyl triflate as the methylating agent proved very effective in generating the tertiary amine **280** (Scheme

4.5). The BOC protected amine **278** was dissolved in dry CH_2Cl_2 under an argon atmosphere. Dry sodium carbonate was added and the mixture was cooled to $0\text{ }^\circ\text{C}$. Two equivalents of methyl triflate were slowly added *via* syringe over 5 minutes and the mixture was allowed to stir for further 30 minutes at $0\text{ }^\circ\text{C}$. The reaction was then allowed to reach room temperature for 16 hours to give the dimethyl amine product **280** in 79% yield.

The deprotection of **280** proved straightforward using trifluoroacetic acid in CH_2Cl_2 (Scheme 4.5). Compound **280** was dissolved in CH_2Cl_2 and cooled to $0\text{ }^\circ\text{C}$ under an argon atmosphere. Four equivalents of trifluoroacetic acid were added *via* syringe over 10 minutes and the temperature was maintained at $0\text{ }^\circ\text{C}$ for a further 30 minutes. The reaction was then allowed to reach room temperature for 16 hours before the isolation and purification of the target molecule **281** in 83% yield (Scheme 4.5).

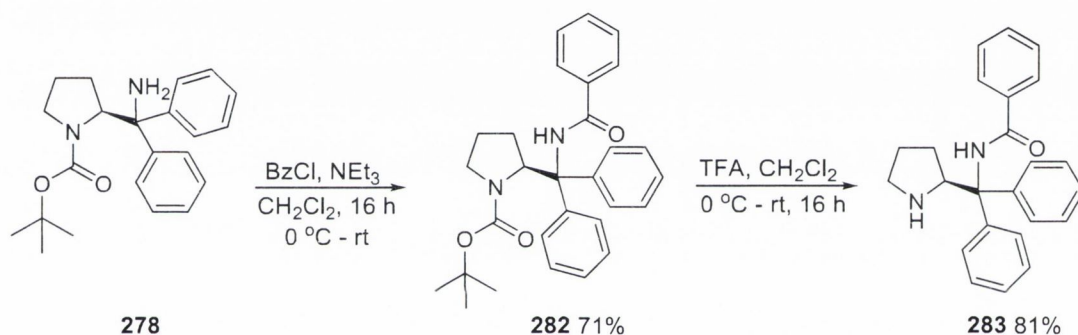


Scheme 4.5 Synthesis of dimethyl amine **281** using methyl triflate

4.1.2.3 Synthesis of chiral substituent with acidic characteristic

Our next aim was to synthesise an alternative chiral moiety that would potentially be hydrogen-bond donating in nature, in order to determine whether the hydroxy group of the chiral moiety influences the stereochemical outcome acting as a general acid in the acylative kinetic resolution of *sec*-alcohols. If this were the case, the introduction of an acidic functional group could potentially lead to the same sense of chemical induction. However, an important factor is to ensure that the $\text{p}K_{\text{a}}$ of the acid is greater than that of the protonated catalyst in order to avoid catalyst inactivation by protonation. We decided on an amide, where the acidic proton has a $\text{p}K_{\text{a}} > 20$, whereas the $\text{p}K_{\text{a}}$ of protonated DMAP is approximately 9.2.²²⁶

The synthesis of the BOC-protected benzoyl amide **282** proceeded without any difficulty starting from the BOC-protected primary amine **278** and coupling with benzoyl chloride at reduced temperature in CH_2Cl_2 solvent. This was followed by the deprotection of the amine using TFA (Scheme 4.6). Substrate **278** was dissolved in CH_2Cl_2 followed by the addition 5.0 equivalents of distilled triethylamine and cooled to $0\text{ }^\circ\text{C}$ using an ice bath. 1.2 Equivalents of freshly distilled benzoyl chloride were slowly added over 5 minutes. After the addition was complete the reaction was kept at $0\text{ }^\circ\text{C}$ for a further 30 minutes before being allowed to reach room temperature for 16 hours to give **282** in 71% yield after purification. The BOC deprotection of **282** was carried out in CH_2Cl_2 at $0\text{ }^\circ\text{C}$ using TFA to give the chiral amide salt which was subsequently free based and purified to give the product **283** in 81% yield (Scheme 4.6).

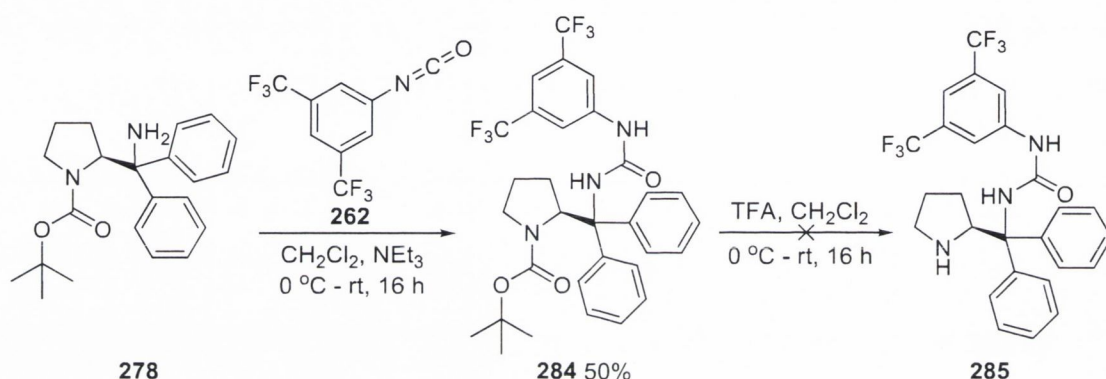


Scheme 4.6 Synthesis of chiral amide pendant moiety **283**

4.1.2.4 Attempted synthesis of a urea substituted chiral pendant

We were also interested in investigating the potential role a chiral urea moiety could play in influencing the enantioselective outcome in acylative KR. This investigation was largely influenced by work done Seidel *et al.* who used a chiral urea promoter in combination with DMAP in the acylative KR of amines with great success.²²⁷ Our approach to the synthesis of a chiral urea pendant proceeded from the mono-protected *vic*-diamine **278** being coupled to the isocyanate **262** to give the urea **284**. This was followed with the attempted BOC deprotection of **284** using TFA to give the amino urea product **285** (Scheme 4.7). The BOC-protected *vic*-diamine **278** was dissolved in CH_2Cl_2 under an argon atmosphere. Triethylamine was added and the reaction vessel was cooled to $0\text{ }^\circ\text{C}$, followed by the slow addition of the *bis*-trifluoro isocyanate **262**.

After the addition was complete the reaction vessel was allowed to reach room temperature for 16 hours to give the BOC protected urea compound **284** in 50% yield (Scheme 1.7). The attempted deprotection of the amine was carried out in the same manner as the other chiral analogues using TFA in CH_2Cl_2 . However, this approach proved unsuccessful in delivering the desired urea product **285** despite numerous attempts under alternative reaction conditions. This prompted us to develop an alternative synthetic strategy of first coupling the diamine **279** to the DMAP catalyst, followed by its reaction with the isocyanate **262** to give the desired product.

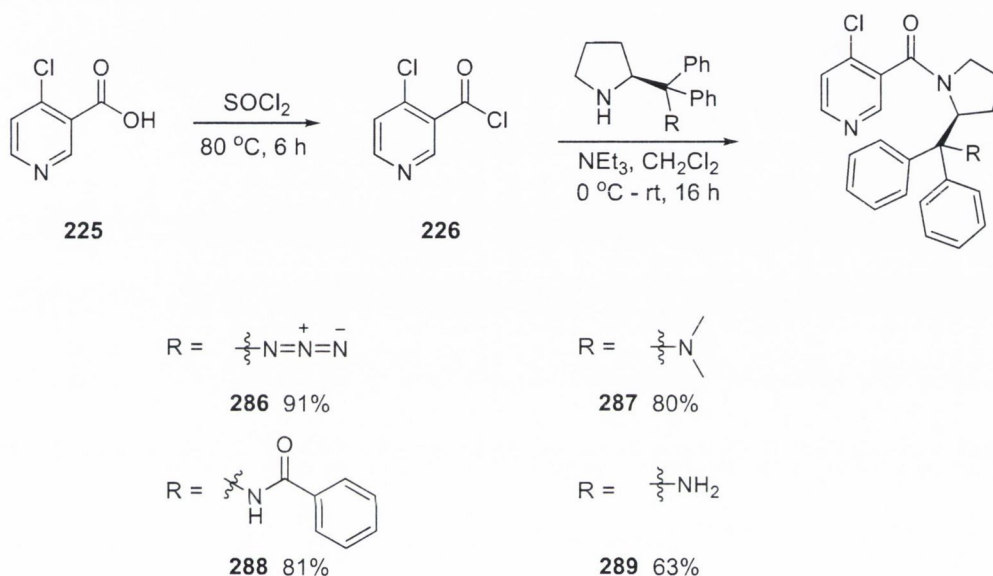


Scheme 4.7 Attempted synthesis of chiral amino urea substrates **285**

4.1.3 Synthesis of chiral substituted 4-chloro pyridine derivatives

The synthesis of 4-chloro-nicotinic acid (**225**) catalyst precursor was first undertaken. This was prepared from the commercially available 3-methylpyridine-*N*-oxide by first nitrating the pyridine ring at the 4-position *via* an electrophilic aromatic substitution reaction using a ten-fold excess of an equimolar quantity of nitric acid and sulphuric acid to give 3-methyl-4-nitropyridine-*N*-oxide (**223**, 69%, procedure 5.1.1).¹⁹⁶ **223** was then converted to 4-chloro-nicotinic acid by first deoxygenating the pyridine nitrogen using PCl_3 , followed by the chlorination of the pyridine ring *via* a $\text{S}_{\text{N}}\text{Ar}$ reaction using dry HCl in chloroform. Finally the methyl substituent was oxidised to the corresponding carboxylic acid using KMnO_4 in water to give the catalyst precursor **225** in 36% yield (procedure 5.1.2).¹⁹⁷

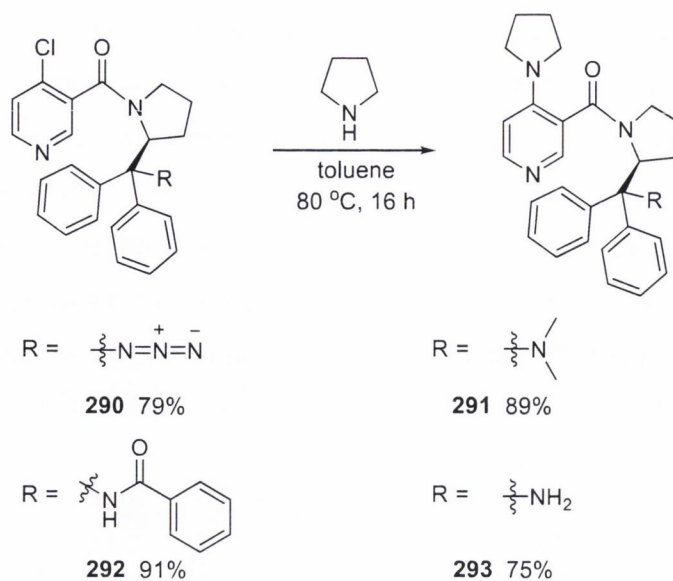
Our next aim was to couple the proline derived chiral groups containing the dimethyl amine **281**, amide **283**, amine **279** and azide **276** functional groups to the 4-chloropyridine carboxylic acid species **225** (Scheme 4.8). 4-Chloro-nicotinic acid (**225**) was first converted to the corresponding acyl chloride using thionyl chloride under a moisture-free atmosphere by heating to 80 °C for 6 hours. The resulting acyl chloride was coupled to the appropriate amine in the presence of triethylamine base to give the 4-chloropyridine amides **286-289** (Scheme 4.8).



Scheme 4.8 Synthesis of substituted 4-chloro pyridines **286**, **287**, **288** and **289**

4.1.3.1 Synthesis of final catalysts bearing alternative functional groups

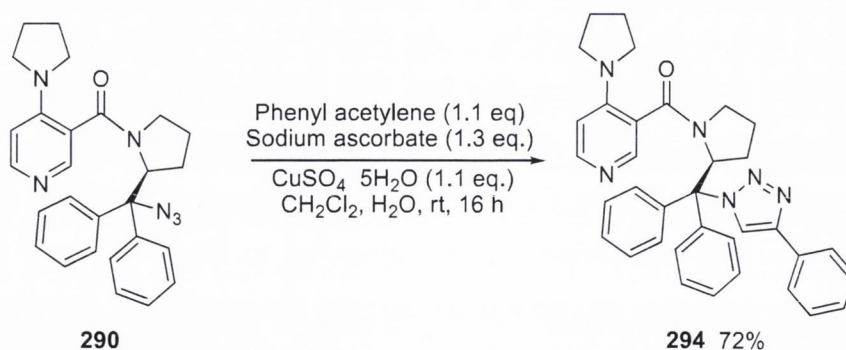
The final step in the preparation of the chiral DMAP catalyst analogues involved the S_NAr of the 4-chloronicotinamides **286**, **287**, **288** and **289** with pyrrolidine to give 4-amino substituted chiral catalysts **290**, **291**, **292** and **293** (Scheme 4.9). The synthesis of each was carried out using the same procedure: a reaction vessel was charged with the appropriate 4-chloronicotinamide and dissolved in toluene. Excess pyrrolidine (5.0 equiv.) was added *via* syringe and the reaction heated to 80 °C of 16 hours to give the final chiral DMAP analogues.



Scheme 4.9 Synthesis of chiral DMAP analogues **290**, **291**, **292** and **293**

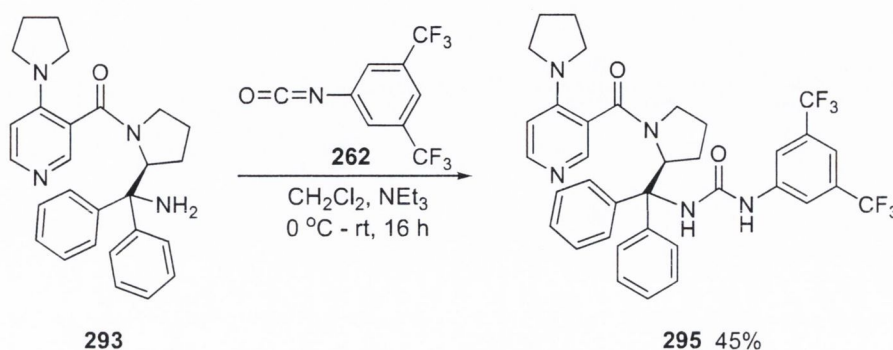
4.1.3.2 Synthesis of triazole and urea functionalised DMAP-based catalyst

The synthesis of a 1,2,3-triazole-substituted DMAP-based catalyst **294** was conveniently accomplished from the azide substituted DMAP-based catalyst **290** via the azide-alkyne Huisgen cycloaddition reaction with phenyl acetylene (Scheme 4.10).²²⁸ The previously prepared azide **290** and phenyl acetylene were dissolved in CH_2Cl_2 at room temperature. $\text{CuSO}_4 \cdot 5\text{H}_2\text{O}$ (1.1 equiv.), sodium ascorbate (1.3 equiv.) and distilled H_2O were added and the flask was left stirring at room temperature for 16 hours to give the triazole **294** in a 72% yield after purification (Scheme 4.10).



Scheme 4.10 Synthesis of a chiral triazole functionalised DMAP analogue **294**

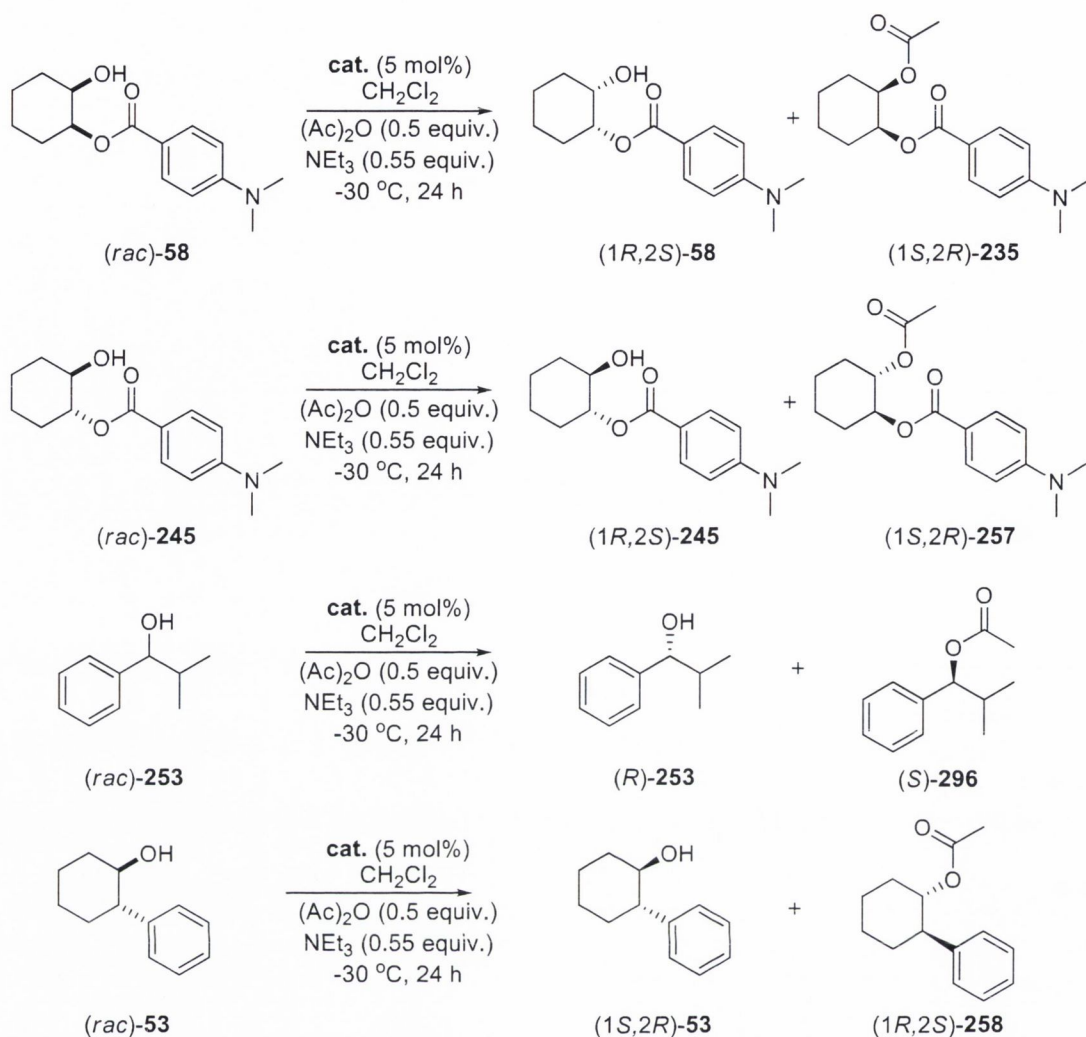
The synthesis of the urea substituted catalyst proceeded from the the amine **293** with the addition of isocyanate **262** in CH_2Cl_2 at 0°C . The reaction was then allowed to reach room temperature for 16 hours to give the urea substituted catalyst **295** in 45% yield after purification.



Scheme 4.10 Synthesis of chiral urea functionalised DMAP analogues **295**

4.2 Investigations into the acylative KR of *sec*-alcohols using novel chiral catalysts

Our next aim was to investigate the small library of novel chiral catalysts in which the key hydroxy group of the parent catalyst **53** had been exchanged with either another H-bond donating moiety (*i.e.* amide and urea **292** and **295**, respectively), a small group which would not be expected to readily participate in H-bonding interactions (*i.e.* azide **290**), a weak H-bond acceptor (*i.e.* triazole **294**) or a relatively strong H-bond acceptor (*i.e.* tertiary amine **291**), in the acylative KR of a range of racemic *sec*-alcohols (Scheme 4.11).



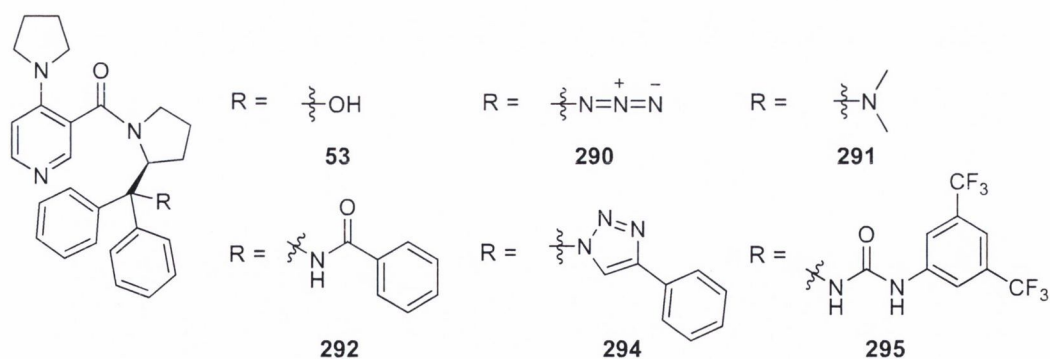
Scheme 4.11 AKR of *sec*-alcohols catalysed by **53**, **290**, **291**, **292**, **294** and **295**

Beginning with the mono-protected *cis*-diol (*rac*)-**58**, it was found that the hydrogen bond donating catalysts **292** and **295** preferentially catalysed the acetylation of the same enantiomer of (*rac*)-**58** as the parent catalyst **53**, however the selectivity factor was considerably lower. While the amide-substituted catalyst **292** promoted the reaction with higher selectivity than **53**, use of **295** led to almost racemic products (Table 4.1, entries 1-3). Most interestingly, catalysts **290** and **294**, which are considered devoid of hydrogen-bond donating functionality, selected for the opposite enantiomer in the acylation process with marginally improved selectivity compared to reactions by catalyst **53** (Table 4.1, entries 4-5). The use of the dimethylamine-substituted catalyst **291** resulted in considerably more selective resolution than is possible using either **53** or any of the novel catalysts utilised in this study (Table 4.1, entries 6).

Table 4.1 AKR of *sec*-alcohols catalysed by **53**, **290**, **291**, **292**, **294** and **295**

Entry	Alcohol	Catalyst	Conv. ^a (%)	Ester <i>ee</i> ^b (%)	Alcohol <i>ee</i> ^b (%)	Selectivity
1	(<i>rac</i>)- 58	53	48	33	31	2.6
2	(<i>rac</i>)- 58	292	5	58	3	3.9
3	(<i>rac</i>)- 58	295	18	4	1	1.1
4	(<i>rac</i>)- 58	290	37	-49	-29	-3.9
5	(<i>rac</i>)- 58	294	13	-47	-7	-2.9
6	(<i>rac</i>)- 58	291	37	-65	-38	-6.9
7	(<i>rac</i>)- 245	53	50	25	25	2.1
8	(<i>rac</i>)- 245	292	7	18	1	1.5
9	(<i>rac</i>)- 245	295	36	19	11	1.6
10	(<i>rac</i>)- 245	291	22	-24	-7	-1.7
11	(<i>rac</i>)- 253	53	50	26	26	2.1
12	(<i>rac</i>)- 253	295	38	20	12	1.7
13	(<i>rac</i>)- 253	291	55	-21	-26	-2.0
14	(<i>rac</i>)- 54	292	16	8	2	1.2
15	(<i>rac</i>)- 54	295	27	23	9	1.7
16	(<i>rac</i>)- 54	290	8	28	2	1.8
17	(<i>rac</i>)- 54	291	38	-13	-8	-1.4

^aDetermined using ¹H-NMR spectroscopy. ^bDetermined by CSP-HPLC using Daicel CHIRALCEL OD-H (4.6 mm x 25 cm) and CHIRALPAK AS (4.6 mm x 25 cm) columns

**Figure 4.3** Structure of catalysts **53**, **290**, **291**, **292**, **294** and **295** under investigation

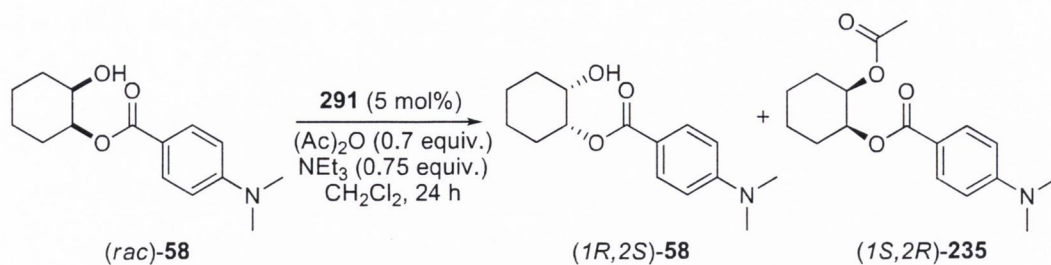
This trend was repeated when the corresponding mono-protected *trans*-diol (*rac*)-**245** was employed in the acylation process: reactions involving catalysts equipped with hydrogen bond donors (i.e. catalysts **292** and **295**), led to the preferential acylation of

the same enantiomer as that observed in resolutions promoted by **53** (Table 4.1, entries 7-9). Employment of the basic catalyst **291** in the acylative KR of (*rac*)-**245** furnished antipodean products, however, at a lower selectivity than that observed for the *cis*-diol counterpart (Table 4.1 entry 10). This trend had been observed in previous studies,^{84,85} where the *trans*-diol on the whole is a less suitable substrate from an enantioselectivity perspective than the *cis*-diastereomer.

Similar observations were also evident for the acylative KR of the benzyl alcohol derivative (*rac*)-**253**: the urea substituted catalyst **293** preferentially acylated the same enantiomer as catalyst **53**, whereas the tertiary amine substituted catalyst **291** favoured the acylation of the opposite antipode (Table 4.1, entries 11-13). The acylative KR of the more sterically hindered substrate *trans*-2-phenylcyclohexanol (*rac*)-**54** broke the previously observed trends: catalysts **292**, **293** and **290** all preferentially acylated the same enantiomer whereas the dimethyl amine substituted catalyst **291** gave the antipodean products (Table 4.1, entries 14-17). The overall results demonstrated that catalyst **291** – which possesses the same configuration at the molecule's only chiral centre as **53** – promotes the kinetic resolution of *sec*-alcohols with the opposite sense of enantiodiscrimination.

4.2.1 Investigation of the influence of reaction temperature on selectivity

We were also interested in ascertaining the influence of reaction temperature on the catalytic process. Accordingly, the acylative KR of substrate (*rac*)-**58** catalysed by **291** was carried out at 20 degree intervals from 0 °C to -60 °C using 5 mol% catalyst loading in CH₂Cl₂ with 0.7 and 0.75 equivalents of acetic anhydride and triethylamine respectively (Scheme 4.12). As anticipated, the enantioselectivity of the process gradually increased with decreasing temperature until -60 °C (Table 4.2, entries 1-4). Intriguingly, lowering the temperature by a further 10 °C to -70 °C had little effect and a further reduction in temperature to -80 °C brought about a considerable loss of selectivity (Table 4.2, entry 5 and 6). Considerable experimentation confirmed that this curious temperature dependence was entirely reproducible.



Scheme 4.12 Acylative KR of *(rac)*-**58** promoted by catalyst **291** at variable temperatures

Table 4.2 Acylative KR of *(rac)*-**58** catalysed by **291** at various temperatures

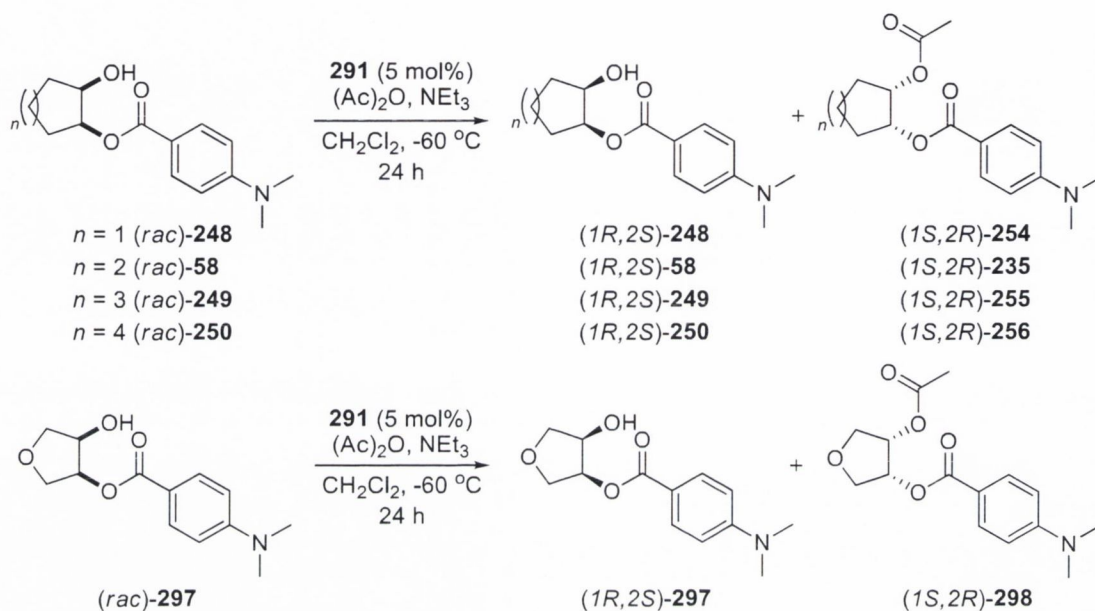
Entry	Temp. (°C)	Conv. ^a (%)	Ester <i>ee</i> ^b (%)	Alcohol <i>ee</i> ^b (%)	Selectivity
1	0	66	41	80	5.4
2	-20	60	50	77	6.4
3	-40	57	55	74	7.3
4	-60	49	63	61	8.0
5	-70	42	67	48	7.9
6	-80	31	65	30	6.4

^aDetermined using ¹H-NMR spectroscopy. ^bDetermined by CSP-HPLC using Daicel CHIRALCEL OD-H (4.6 mm x 25 cm) and CHIRALPAK AS (4.6 mm x 25 cm) columns

4.2.2 KR of mono-protected diols under optimised conditions

We found that catalyst **291** could also be used to promote the enantioselective acylation of other alcohols (Scheme 4.13). Under optimised conditions the substituted cyclopentanol substrate *(rac)*-**248** could be resolved with high enantioselectivity (*i.e.* $s = 10$) allowing the isolation of the recovered unreacted *(1R,2S)*-alcohol in 99% *ee* at 73% conversion (Table 4.3, entry 1). Similarly, *(rac)*-**58** could be enantioselectively acylated to give the alcohol recovered in 91% *ee* at 65% conversion, equating to a selectivity value of 8.3 (Table 4.3, entry 2). Consistent with the results of studies earlier carried out independently by Fuji *et al.*⁹⁸ larger ring systems proved more challenging: the 7- and 8-membered cyclic alcohols *(rac)*-**249** and *(rac)*-**250** underwent less selective acylation, however the enantioselectivity of the process was sufficient to allow the isolation of the alcohols in high-excellent *ee* at *ca.* 70% conversion, corresponding to

selectivity values of 4.7 and 5.1 respectively (Table 4.3, entries 3-4). The heterocyclic alcohol (*rac*)-**297** proved a more challenging substrate in the acylative KR processes and underwent acylation with low levels of enantiodiscrimination, resulting in a selectivity of 2.8 (Table 4.3, entry 5).



Scheme 4.13 Acylative KR of mono-promoted diols promoted by catalyst **291**

Table 4.3 Acylative KR of **58**, **248**, **249**, **250** and **297** catalysed by **291**

Entry	Alcohol	Anhydride (equiv.)	Base (equiv.)	Conv. ^a (%)	Alcohol <i>ee</i> ^b (%)	Selectivity
1	248	1.0	1.05	73	99	10.0
2	58	2.5	2.55	65	91	8.3
3	249	2.5	2.55	70	81	4.7
4	250	2.5	2.55	74	90	5.1
5	297	0.7	0.75	52	37	2.8

^aDetermined using $^1\text{H-NMR}$ spectroscopy. ^bDetermined by CSP-HPLC using Daicel CHIRALCEL OD-H (4.6 mm x 25 cm) and CHIRALPAK AS (4.6 mm x 25 cm) columns

4.2.3 $^1\text{H-NMR}$ spectroscopic analysis of catalysts mode of action

In an attempt to clarify the origin of the ability of **53** and **291** to preferentially acylate opposing enantiomers of *sec*-alcohols, we undertook a comparative $^1\text{H-NMR}$ spectroscopic analysis of both systems – a technique which had proven useful in elucidating the mode of action of **53** in a study that was previously undertaken by our group (Figure 4.2).⁸⁵ An analysis of this data is intriguing: the $\pi\text{-H}$ interaction which is clearly a feature of both **53** and its methylated and acylated counterparts **53a** and **53b** respectively (as can be seen from the sign and magnitude of $\Delta\delta\text{H-2}$) is not observed in the case of the dimethylamino catalyst **291** (Table 4.4, entries 1-4). However, on methylation of **291** to give **291a** (Table 4.4, entry 5), an upfield shift at H-2 occurs which is characteristic of a conformational change driven by the $\pi\text{-H}$ interaction. It is significant that this interaction appears to be weaker in this system (*i.e.* $\Delta\delta\text{H-2} = -0.53$; as opposed to -0.81 in the case of **53** \rightarrow **53a**, Table 4.4, entries 1, 2, 4 and 5).

The same interaction can be observed upon acetylation of **291** to yield **291b** (Table 2.4, entry 6). These conformational changes can perhaps be best appreciated by comparing the data associated with **53** and **291** (and their methylated/alkylated derivatives) with the $^1\text{H-NMR}$ chemical shifts associated with the corresponding achiral pyrrolidinamide-based materials **299**, **299a** and **299b** (Table 2.4, entries 7-9). Here one can see that in the case of catalyst **291**, $\delta\text{H-2}$, $\delta\text{H-5}$ and $\delta\text{H-6}$ are almost identical to the corresponding resonances associated with **299** (implying that no $\pi\text{-H}$ interactions are taking place), however upon both alkylation and acylation of **291**, the change in chemical shift at H-2 is clearly consistent with the development of such an interaction. More difficult to definitively explain at this juncture is the $\Delta\delta$ at H-6 when **291** is acetylated (*i.e.* **299b**, Table 2.4, entry 9): an unexpectedly high chemical shift of 8.06 was observed (compare with entries 3 and 6). In addition, we could not detect an NOE with either H-2 or H-6 when the methyl group of the acetyl moiety was irradiated.

What does seem clear is that the conformation/rotameric preferences of **299b** are similar but not exactly analogous to those of **53b**. Therefore, the different selectivity profiles exhibited by the two catalysts may be due to both conformational factors and hydrogen-bond donation/acceptance by the pendent OH/NMe₂ functionality.

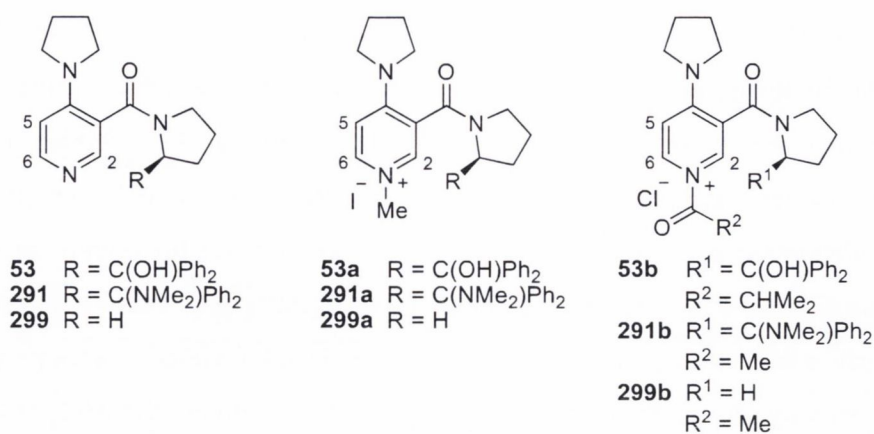


Figure 4.4 Catalysts **53**,⁸⁵ **291** and **299** and analogues investigated in ¹H-NMR studies

Table 4.4 Selected ¹H-NMR of **53**, **291** and **299** and methylated/acetylated analogues

Entry	Cat.	$\delta\text{H-2}^{\text{a,b,c}}$	$\delta\text{H-5}^{\text{a,b,c}}$	$\delta\text{H-6}^{\text{a,b,c}}$	$\delta\text{CH}_3/\text{HCR}_2^{\text{a,b,c}}$
1	53	7.33	6.45	8.09	-
2	53a	6.52	6.80	8.04	3.88
		(-0.81)	(0.45)	(-0.05)	
3	53b	8.06	7.15	9.10	4.14
		(0.73)	(0.70)	(1.01)	
4	291	8.26	6.48	8.15	-
5	291a	7.71	6.97	8.43	4.17
		(-0.53)	(0.49)	(0.28)	
6	291b	8.24	6.68	8.06	2.25
		(-0.02)	(0.20)	(-0.09)	
7	299	8.19	6.47	8.16	-
8	299a	8.17	6.90	8.21	4.21
		(-0.02)	(0.43)	(0.05)	
9	299b	8.72	7.32	9.32	4.11
		(0.53)	(0.85)	(1.16)	

^a δ Is quoted in ppm in CDCl₃ as solvent. ^bValue in parenthesis represents $\Delta\delta$: the change in chemical shift of the proton indicated on methylation or acylation (in ppm), a negative value for $\Delta\delta$ indicates an upfield shift. ^cAll pyridine ring proton resonances were unambiguously assigned by NMR spectroscopy (¹H-¹H COSY, ¹H-¹³C COSY, NOE and 1-D TOCSY experiments).

4.3 Conclusion

The synthesis of a unique suite of readily prepared, L-proline-derived catalysts which differ only by the characteristics of a remote substituent has been accomplished. When this substituent is capable of donating hydrogen bonds the catalyst promotes the preferential acylation of the opposite enantiomer of a racemic *sec*-alcohol to that acylated when the substituent is a basic amine capable of accepting hydrogen bonds, despite both catalysts possessing the same configuration at their only stereogenic centre.

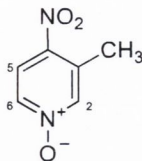
The dimethylamino catalyst **291** exhibited a similar activity and selectivity profile to that associated with the hydroxy catalyst **53**; thus it is now possible to access both enantiomers of a given racemic *sec*-alcohol from catalysts derived from one antipode of proline. The precise mode of action which facilitates catalysts **53** and **291** to preferentially acylate opposite antipodes proved somewhat elusive. However, ¹H-NMR spectroscopic analysis indicates that **291** undergoes a similar, yet not exactly analogous conformational change to **53** upon methylation/acylation which brings the remote stereochemical information to bear on the acylation event *via* an ‘induced-fit’ type mechanism.

5.1 Experimental

General

Proton Nuclear Magnetic Resonance spectra were recorded on a 400 MHz spectrometer in CDCl₃ and DMSO-d₆ referenced relative to residual CHCl₃ and DMSO-d₆ ($\delta = 7.26$ and $\delta = 2.50$ ppm respectively). Chemical shifts are reported in ppm and coupling constants in Hertz. Carbon NMR spectra were recorded on the same instrument (100 MHz) with total proton decoupling. All melting points are uncorrected. Infrared spectra were obtained on a Perkin Elmer Spectrum One Spectrometer. Flash chromatography was carried out using silica gel, particle size 0.04-0.063 mm. TLC analysis was performed on precoated 60F₂₅₄ slides, and visualised by either UV irradiation or KMnO₄ staining. Specific rotation measurements were made on a Rudolph research analytical Autopol IV instrument, and are quoted in units of 10⁻¹ deg cm² g⁻¹. THF was distilled over sodium-benzophenone ketyl radical before use. Methylene chloride, toluene and triethylamine were distilled over calcium hydride. Analytical CSP-HPLC was performed using Daicel CHIRALCEL OD-H (4.6 mm x 25 cm), CHIRALCEL AD-H (4.6 mm x 25 cm) and CHIRALPAK AS (4.6 mm x 25 cm) columns. Unless otherwise stated, all chemicals were obtained from commercial sources and used as received. All reactions were carried out in oven-dried glassware under an atmosphere of nitrogen or argon unless otherwise stated.

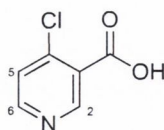
5.1.1 3-Methyl-4-nitropyridine-*N*-oxide (**223**)¹⁹⁶



A 250 mL round bottom flask containing a stirring bar and 66.00 mL of nitric acid (92.38 g, 1.466 mol) was fitted with a 100 mL pressure equalising dropping funnel and cooled to 0 °C in ice bath. 78.00 mL of sulfuric acid (143.80 g, 1.466 mol) was added dropwise *via* dropping funnel with vigorous stirring and the solution was left to equilibrate (ca. 30 min). 3-Methylpyridine-*N*-oxide (20.00 g, 0.1833 mol) was added slowly over a half hour period and the reaction was then allowed to reach room temperature. The round bottom flask was then fitted with a reflux condenser and slowly heated to reflux temperature for four hours. After the flask reached room temperature, the reaction mixture was poured onto crushed ice (ca. 100 mL) and then basified to pH 3.4 with sodium carbonate. The resulting yellow precipitate was filtered through a medium frit, sintered-glass funnel and the filtrate extracted with CH₂Cl₂ (3 x 20 mL). The extracts were combined with the precipitate obtained from filtration and solvent removed *in vacuo*. The product was recrystallised from acetone to give **223** (19.46 g, 69%). M.p. 139-142 °C, (lit.,¹⁹⁶ 137-139 °C).

δ_{H} (400 MHz, CDCl₃): 2.64 (s, 3H, CH₃), 8.04 (d, 1H, J 7.5, H-5), 8.13 (dd, 1H, J 7.5, J 1.5, H-6), 8.15 (app.s, 1H, H-2).

5.1.2 4-Chloro-nicotinic acid (**225**)¹⁹⁷

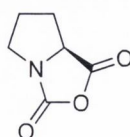


A 2 L three-necked round bottom flask containing a stirring bar was charged with 3-methyl-4-nitropyridine-*N*-oxide (**223**, 18.40 g, 0.1194 mol) and dissolved in CHCl₃ (400 mL). The solution was saturated with dry HCl giving the yellow precipitate 4-

chloro-3-methylpyridine-*N*-oxide. The flask was cooled to 0 °C in an ice bath and allowed to equilibrate (*ca.* 30 min). PCl₃ (31.20 mL, 0.358 mol) was added drop-wise *via* dropping funnel while maintaining a temperature below 5 °C. After addition was complete the reaction mixture was allowed to reach room temperature and then gently heated to initiate the exothermic reaction with occasional cooling when the reaction became too vigorous. After the reaction subsided the flask was heated to reflux temperature for 30 min. to ensure completion. The CHCl₃ was removed *in vacuo* and the resulting residue was dissolved in 300 mL of ice water. The solution was basified to pH 8 with the addition of sodium carbonate and then steam distilled to give 4-chloro-3-methylpyridine and water. In a 500 ml round bottom flask containing a stirring bar the 4-chloro-3-methylpyridine/water solution was dispersed and 200 mL of water and KMnO₄ (46.13 g) was added. The flask was fitted with a reflux condenser and heated under reflux for 4 hours. The solution was steam distilled to remove any unreacted 4-chloro-3-methylpyridine. After cooling the precipitated MnO₂ was removed by filtration through celite. The resulting liquid was reduced in volume from *circa* 200 to 50 mL *in vacuo* and acidified to pH 3 with conc. HCl to give a precipitate. The precipitate was isolated by filtration through a medium frit, sintered-glass funnel. The resulting solid was washed with acetone (25.0 mL) and air dried to give a pale yellow powder, (6.70 g, 36%), M.p. 118 °C, (*dec.*), (*lit.*,¹⁹⁷ 120 °C).

δ_{H} (400 MHz, DMSO): 7.68 (d, 1H, J 5.5, H-5), 8.66 (d, 1H, J 5.5, H-6), 8.94 (s, 1H, H-2).

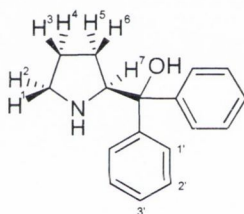
5.1.3 Tetrahydro-pyrrol[1,2-*c*]oxazole-1,3-dione (274)¹⁹⁸



A 100 mL three-necked round bottom flask fitted with an argon inlet tube, 50 mL addition funnel and a Teflon-coated thermocouple probe, containing dry THF (15.0 mL) was charged with L-proline (**272**, 1.15 g, 10.0 mmol) under an atmosphere of argon. To the well-stirred, cooled (15-20 °C) suspension was added a solution of triphosgene (1.04 g, 3.50 mmol) in THF (10.0 mL) over a 30 min. period while maintaining the internal

temperature at 15-20 °C. The mixture was warmed to 30-40 °C and aged for 30 min. Once homogeneous, the reaction mixture was aged an additional 30 min. at 30-35 °C and then cooled to 15-20 °C. While maintaining the internal temperature at 15-20 °C, the reaction mixture was concentrated *in vacuo* to 10% of the original volume. The residue was dissolved in dry THF (22.5 mL) and the solution was cooled to 0-5 °C. With good agitation, dry NEt₃ (1.53 mL, 11.0 mmol) was added over 15 min. while maintaining the internal temperature at 0-5 °C. After the addition was complete, the mixture was aged for 30 min. at 0-5 °C and then filtered through an enclosed, medium frit, sintered-glass funnel. The resultant cake of NEt₃·HCl was washed with THF (10.0 mL). The filtrate and THF washes were combined to afford a solution containing **274** (*ca.* 9.5-10.0 mmol) that was used immediately without further purification.

5.1.3.1 (S)-Diphenyl(pyrrolidin-2-yl)methanol (**275**)¹⁹⁸



A 1 L three-necked flask fitted equipped with a temperature probe, 250 mL addition funnel containing the THF solution **274** (260.1 mmol in 250 mL THF) and stirring bar was charged with a solution of phenylmagnesium chloride in THF (781.0 mmol) and cooled to -20 °C. The THF solution of **274** was added over a 1 hour period while maintaining the internal temperature below -10 °C. After the addition was complete, the mixture was aged for 2 h at 0 °C then allowed to reach room temperature with continuous stirring for 16 h. The reaction was quenched with the addition of 2M aqueous H₂SO₄ (39 mL, 781 mmol), over a 0.5-1.0 h period, while maintaining the internal temperature below 20 °C. During the quench a thick white precipitate of MgSO₄ formed. The mixture was agitated for 1 h at 0 °C and then filtered through a medium-frit, sintered-glass funnel. The MgSO₄ cake was washed free of residual product with THF (3 x 50 mL). The filtrate and THF washes were combined and concentrated *in vacuo* to *ca.* 10% of the original volume. The crude mixture was basified with 2M NaOH (6 mL, 12 mmol) and diluted with CH₂Cl₂ (50 mL). The

organic layer was washed with H₂O (2 x 40 mL), dried (MgSO₄) and concentrated *in vacuo*. Purification by column chromatography (EtOAc, R_f = 0.12) gave **275** (25.0 g, 37 %) as a white solid. M.p. 77-78 °C, (lit.,¹⁹⁸ 79-79.5 °C). $[\alpha]_D^{20} = -55.4$ (c 1.000, CHCl₃) (lit.,¹⁹⁸ $[\alpha]_D^{22} -48.5$ (c = 0.323, MeOH).

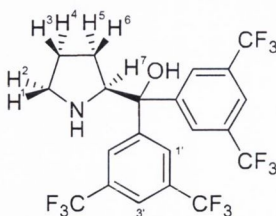
δ_H (400 MHz, CDCl₃): 1.62-1.81 (m, 4H, H-3, H-4, H-5, H-6), 2.44 (s, 1H, NH), 2.96-3.02 (m, 1H, H-1), 3.05-3.09 (m, 1H, H-2), 4.31 (dd, 1H, J 7.5, 7.5, H-7), 7.24 (d, J 7.5, 2H, H-3'), 7.32-7.38 (m, 4H, H-2'), 7.58 (d, 2H, J 8.0, H-1'), 7.65 (d, 2H, J 8.0, H-1').

5.1.3.2 3,5-[bis(Trifluoromethyl)phenyl]magnesium bromide (**300**)²²⁹



A 50 mL round bottom flask charged with 1-bromo-3,5-bis-trifluoromethyl-benzene (6.90 mL, 40.0 mmol), THF (20.0 mL) and a stirring bar was placed under an atmosphere of argon, then cooled to -15 °C. A solution of *iso*-propyl magnesium bromide (20 mL, 2.0 M in THF) was slowly added *via* syringe. The resulting solution was allowed to stir at -10 °C for 2 h and used immediately.

5.1.3.3 bis-(3,5-bis-Trifluoromethyl-phenyl)-pyrrolidin-2-yl-methanol (**227**)²²⁹

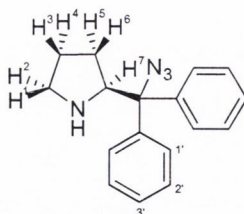


A 100 mL three-necked flask fitted with a 50 mL addition funnel containing the THF solution of **274** (10.0 mmol in 50 mL THF) and stirring bar was charged with a solution

of 3,5-[bis(trifluoromethyl)phenyl]magnesium bromide (**300**, 40 mmol) and cooled to -15 °C. The THF solution of **274** was added over a 1 h period while maintaining the internal temperature between -10 and -15 °C. After the addition was complete, the mixture was allowed to warm to room temperature with continuous stirring for 16 h. The reaction was quenched with the addition of 2.0 M aqueous H₂SO₄ (40 mmol), over a 0.5-1.0 h period, while maintaining the internal temperature below 20 °C. During the quench a thick white precipitate of MgSO₄ formed. The mixture was agitated for 1 h at 0 °C and filtered through a medium-frit, sintered-glass funnel. The MgSO₄ cake was washed free of residual product with THF (3 x 10 mL). The filtrate and THF washes were combined and concentrated *in vacuo* to *ca.* 10% of the original volume. The crude mixture was basified with 2M NaOH (6 mL, 12.0 mmol) and diluted with CH₂Cl₂ (50 mL). The organic layer was washed with H₂O (2 x 40 mL), dried (MgSO₄) and concentrated *in vacuo*. Purification by column chromatography (98:2 CH₂Cl₂-NEt₃, R_f = 0.15) gave **227** (1.87 g, 36 %) as a white solid. M.p. 110-114 °C, (lit.,²²⁹ 110-112 °C). [α]_D²⁰ = -34.4 (c 1.00, CHCl₃). Spectral data for this compound is consistent with that in the literature.⁸³

δ_{H} (400 MHz, CDCl₃): 1.54-1.64 (m, 2H, H-5, H-6), 1.73 (s, 1H, N-H), 1.78-1.83 (m, 2H, H-3, H-4), 3.06-3.11 (m, 2H, H-1, H-2), 4.37 (dd, 1H, J 7.5, 7.5, H-7), 5.09 (s, 1H, OH), 7.79 (s, 2H, H-3'), 7.98 (s, 2H, H-1'), 8.07 (s, 2H, H-1').

5.1.3.4 (*S*)-2-(Azidodiphenylmethyl)pyrrolidine (**276**)²³⁰



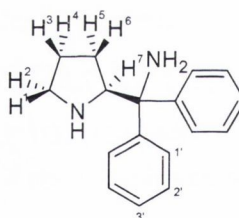
A 50 mL round bottom flask containing a stirring bar was charged with amino alcohol (*S*)-(-)- α,α -diphenyl-2-pyrrolidinemethanol (**275**, 1.00 g, 3.95 mmol), H₂SO₄ (5 mL, 70% (aq.)) and CHCl₃ (5 mL) were added cautiously and the solution was cooled to 0 °C. Sodium azide (531 mg, 7.89 mmol) was added in small portions over 20 min with

continuous stirring. After addition, the reaction was allowed to reach room temperature for 4 h. The reaction was quenched with the addition of a saturated solution of NaHCO_3 (25 mL) and the azide product extracted with CHCl_3 (3 x 30 mL). The organic extracts were combined, dried (MgSO_4) and the solvent was removed *in vacuo*. Purification by column chromatography (EtOAc, $R_f = 0.42$), gave **276** (767 mg, 70%) as a beige viscous liquid that crystallised upon standing. M.p. 69-70 °C. $[\alpha]_D^{20} = -113.0$ (c 1.10, CHCl_3). The spectral and physical data for this compound are consistent with that in the literature.²³⁰

δ_{H} (400 MHz, CDCl_3): 1.58-1.79 (m, 4H, H-3, H-4, H-5, H-6), 2.94-3.04 (m, 2H, H-1, H-2), 4.29 (dd, 1H, J 9.0, J 7.5, H-7), 7.18-7.21 (m, 2H, H-3'), 7.22-7.34 (m, 4H, H-2'), 7.53 (d, 2H, J 8.0, H-1'), 7.60 (d, 2H, J 8.0, H-1').

HRMS (m/z -ES): $[\text{M}+\text{H}]^+$ calcd. for $\text{C}_{17}\text{H}_{19}\text{N}_4$ 279.1610; found, 279.1612.

5.1.3.5 (S)-Diphenyl(pyrrolidin-2-yl)methanamine (**279**)²³¹



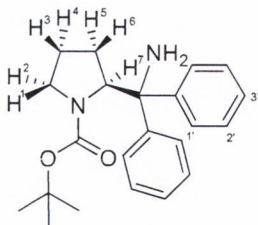
A 100 mL three-necked flask with stirring bar was fitted with a temperature probe and charged with (*S*)-2-(azidodiphenylmethyl)pyrrolidine (**253**, 700 mg, 2.52 mmol) and dry THF (40 mL) then cooled to 0 °C. LiAlH_4 (190 mg, 5.03 mmol) was added in small portions with continuous stirring while maintaining the temperature below 10 °C. Following the addition the reaction was allowed to reach room temperature for 16 h. The flask was cooled to 0 °C and water (2.0 mL) was added *via* a syringe over a 20 min. followed by the addition of H_2SO_4 (2.0 mL, 2.0 M (aq.)). The solvent was removed *in vacuo* and the resulting solid was dispersed in a saturated solution of NaHCO_3 (25 mL) and the crude product extracted in CH_2Cl_2 (3 x 25 mL). The organic extracts were combined, dried (MgSO_4) and the solvent removed *in vacuo*. (Note: care must be taken

when removing the solvent as the product is volatile under reduced pressure). Alternatively the diamine can be converted to the salt with the addition of TFA prior to removing the solvent. Liberation of the free base for purification by column chromatography can be accomplished with the addition of Na_2CO_3 (2.0 equiv.) in CH_2Cl_2 (5 mL), followed by filtration. Purification by column chromatography (4:1 EtOAc-MeOH, $R_f = 0.12$), gave **279** (540 mg, 85%) as a translucent liquid. $[\alpha]_{\text{D}}^{20} = +52.6$ (c 1.00, CHCl_3). The spectral and physical data for this compound are consistent with that in the literature.²³¹

δ_{H} (400 MHz, CDCl_3): 1.56-1.80 (m, 4H, H-3, H-4, H-5, H-6), 2.04 (s, 1H, N-H), 2.90-3.02 (m, 2H, H-1, H-2), 4.26 (dd, 1H, J 9.0, J 4.0, H-7), 7.16-7.22 (m, 2H, H-3'), 7.28-7.31 (m, 4H, H-2'), 7.46-7.51 (m, 4H, H-1').

HRMS (m/z -ES): $[\text{M}+\text{H}]^+$ calcd. for $\text{C}_{17}\text{H}_{21}\text{N}_2$ 253.1705; found, 253.1698.

5.1.3.6 (*S*)-*tert*-Butyl-2-(aminodiphenylmethyl)pyrrolidine-1-carboxylate (278)



A 50 mL three-necked flask with stirring bar was charged with **279** (250 mg, 0.99 mmol), NEt_3 (137 μL , 0.57 mmol), dry CH_2Cl_2 (15 mL) and cooled to $-40\text{ }^\circ\text{C}$. A solution of di-*tert*-butyl dicarbonate (205 mg, 0.94 mmol) in dry CH_2Cl_2 (5 mL) was added with continuous stirring over a 10 min. period and the temperature was maintained at $-40\text{ }^\circ\text{C}$ for 2 h, then allowed to reach room temperature and left for a further 4 h. The solvent was removed *in vacuo* and the resulting solid was dissolved in CH_2Cl_2 (25 mL) and extracted from a saturated solution of NaHCO_3 (25 mL) using CH_2Cl_2 (3 x 25 mL). The organic extracts were combined, dried (MgSO_4) and the solvent removed *in vacuo*. Purification by column chromatography (4:1 CH_2Cl_2 -EtOAc,

$R_f = 0.30$) gave **278** (286 mg, 82%) as a white fluffy solid. M.p. 84-87 °C. $[\alpha]_D^{20} = -38.2$ (c 0.33, CHCl_3).

δ_H (400 MHz, CDCl_3): 0.85-0.97 (m, 1H, H-6), 1.39 (s, 9H, $(\text{CH}_3)_3$) 1.49-1.58 (m, 1H, H-4), 1.86-1.92 (m, 1H, H-5), 2.11-2.19 (m, 1H, H-3), 2.83-3.02 (m, 1H, H-2), 3.36-3.42 (m, 1H, H-1), 4.96-5.05 (m, 1H, H-7), 7.25-7.36 (m, 10H, Ar-H).

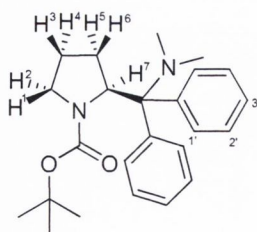
(Note: the phenyl rings are diastereotopic).

δ_C (100 MHz, CDCl_3): 23.6, 27.9, 28.5, 47.6, 64.4 (q), 65.4 (q), 79.2, 126.2, 126.3, 127.2, 127.4, 127.5, 128.0, 144.9 (q), 147.2 (q), 155.9 (q).

ν_{max} (neat)/ cm^{-1} : 3376, 3311, 2972, 2929, 1668, 1405, 1164, 1111, 967, 844, 755, 700.

HRMS (m/z -ES): $[\text{M}+\text{H}]^+$ calcd. for $\text{C}_{22}\text{H}_{29}\text{N}_2\text{O}_2$ 353.2229; found, 353.2242.

5.1.3.7 (*S*)-*tert*-Butyl-2-((dimethylamino)diphenylmethyl)pyrrolidine-1-carboxylate (**280**)



A 50 mL round bottom flask with stirring bar was charged with **278** (280 mg, 0.80 mmol), Na_2CO_3 (550 mg, 4.00 mmol) and dry CH_2Cl_2 (30 mL). The flask was fitted with a septum and placed under an argon atmosphere and cooled to 0 °C. Methyl triflate (175 μL , 1.60 mmol) was added *via* syringe over 5 min. with continuous stirring. After maintaining the temperature at 0 °C for 30 min. the reaction vessel was allowed to reach

room temperature for a further 16 h. The reaction was quenched with the addition of water (20 mL) and the product was extracted with CH₂Cl₂ (3 x 25 mL). The organic extracts were combined, dried (MgSO₄) and the solvent was removed *in vacuo*. Purification by column chromatography (19:1 CH₂Cl₂-EtOAc, R_f = 0.18) gave **280** (210 mg, 79% yield) as a white solid. M.p. 60-64 °C. $[\alpha]_D^{20} = -97.0$ (c 0.50, CHCl₃).

δ_H (400 MHz, CDCl₃): 0.53-0.68 (m, 1H, H-6), 0.83-0.90 (m, 1H, H-4), 1.24-1.31 (m, 1H, H-5), 1.48 (s, 9H, (CH₃)₃), 1.61-1.66 (m, 1H, H-3), 1.92-2.10 (m, 6H, N(CH₃)₂), 2.88-2.96 (m, 1H, H-2), 3.41-3.48 (m, 1H, H-1), 5.35-5.44 (m, 1H, H-7), 7.25-7.38 (m, 8H, H-1', H-2'), 7.56 (s, 2H, H-3').

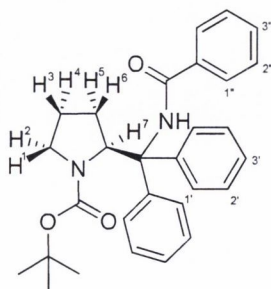
(Note: the phenyl rings are diastereotopic)

δ_C (100 MHz, CDCl₃): 22.2, 28.1, 28.3, 29.2, 49.2, 60.0 (q), 76.7 (q), 79.7, 127.9, 128.7, 129.6, 129.8, 131.5, 132.0, 137.2 (q), 142.2 (q), 157.9 (q).

ν_{\max} (neat)/cm⁻¹: 2929, 1691, 1385, 1362, 1158, 1148, 952, 756, 696.

HRMS (*m/z* -ES): $[M+H]^+$ calcd. for C₂₄H₃₃N₂O₂ 381.2542; found, 381.2551.

5.1.3.8 (*S*)-*tert*-Butyl-2-(benzamidodiphenylmethyl)pyrrolidine-1-carboxylate (**282**)



A 250 mL round bottom flask with stirring bar was charged with **278** (1.50 g, 4.25 mmol), NEt₃ (650 μL, 4.68 mmol) and dry THF (100 mL). The flask was fitted with a septum, put under an argon atmosphere and cooled to 0 °C. Benzoyl chloride (598 mg, 4.25 mmol) was added *via* syringe over 5 min. with continuous stirring, after which it was allowed to reach room temperature and left stirring for 16 h. The crude reaction mixture was transferred to a separating funnel charged with a saturated solution of NaHCO₃ (50 mL) and the crude product was extracted with CH₂Cl₂ (3 x 50 mL). The organic extracts were combined, dried (MgSO₄) and the solvent was removed *in vacuo*. Purification by column chromatography (9:1 CH₂Cl₂-hexane, R_f = 0.15) gave **282** (1.38 g, 71% yield) as a white fluffy solid. M.p. 139-143 °C. $[\alpha]_D^{20} = +56.4$ (c 1.00, CHCl₃).

δ_H (400 MHz, CDCl₃): 0.66-0.73 (m, 1H, H-6), 1.38-1.45 (m, 1H, H-4), 1.53 (s, 9H, (CH₃)₃), 1.83-1.89 (m, 1H, H-5), 2.08-2.16 (m, 2H, H-2, H-3), 3.30-3.35 (m, 1H, H-1), 5.42 (dd, 1H, J 9.0, J 3.5, H-7), 7.28-7.46 (m, 11H, H-1' x 2, H-2', H-3', H-2'', H-3''), 7.91 (d, 2H, J 7.5, H-1'), 8.01 (d, 2H, J 8.0, H-1''), 9.78 (s, 1H, N-H).

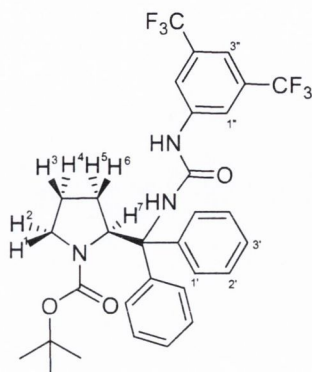
(Note: the phenyl rings are diastereotopic)

δ_C (100 MHz, CDCl₃): 23.0, 27.5, 28.4, 47.8, 64.5, 69.6 (q), 80.9 (q), 127.0, 127.1, 127.3, 127.4, 127.5, 128.0, 129.0, 129.7, 130.8, 134.9 (q), 137.4 (q), 141.5 (q), 158.3 (q), 164.8 (q).

ν_{max} (neat)/cm⁻¹: 3298, 3059, 2977, 1662, 1537, 1490, 1391, 1363, 1157, 696.

HRMS (*m/z* -ES): [M+H]⁺ calcd. for C₂₉H₃₃N₂O₃ 479.2311; found, 479.2311.

5.1.3.9 (S)-tert-Butyl-2-((3-(3,5-bis(trifluoromethyl)phenyl)ureido)diphenylmethyl)pyrrolidine-1-carboxylate (284)



A 250 mL round bottom flask with stirring bar was charged with **278** (1.00 g, 2.83 mmol), NEt_3 (800 μL , 5.67 mmol) and dry toluene (100 mL). The flask was fitted with a septum, placed under an argon atmosphere and cooled to 0 °C. 3,5-bis(trifluoromethyl)phenyl isocyanate (588 μL , 3.40 mmol) was added *via* syringe over 5 min. with continuous stirring, after which it was allowed to reach room temperature and left stirring for 16 h. The solvent and volatiles were removed under *vacuo* and the remaining mixture was transferred to a separating funnel charged with a saturated solution of NaHCO_3 (50 mL) and the crude product was extracted with CH_2Cl_2 (3 x 50 mL). The organic extracts were combined, dried (MgSO_4) and the solvent was removed *in vacuo*. Purification by column chromatography (7:3 CH_2Cl_2 -hexane, $R_f = 0.30$) gave **284** (860 mg, 50% yield) as a white fluffy solid. M.p. 111-115 °C. $[\alpha]_{\text{D}}^{20} = +75.0$ (c 0.10, CHCl_3).

δ_{H} (400 MHz, CDCl_3): 0.64-0.73 (m, 1H, H-6), 1.35-1.45 (m, 1H, H-4), 1.57 (s, 9H, $(\text{CH}_3)_3$), 1.76-1.86 (m, 1H, H-5), 2.09-2.18 (m, 2H, H-2, H-3), 3.29-3.36 (m, 1H, H-1), 5.16-5.23 (m, 1H, H-7), 6.60 (s, 1H, NH), 7.30-7.42 (m, 9H, Ar-H x 8, H-3''), 7.71 (s, 2H, H-1'' x 2), 7.79 (d, 2H, J 7.5, H-1' x 2), 8.97 (s, 1H, NH).

(Note: the phenyl rings are diastereotopic and q* denotes a quartet multiplicity signal)

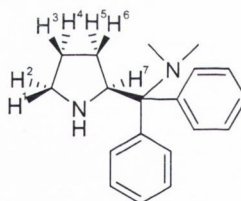
δ_C (100 MHz, $CDCl_3$): 22.3, 27.4, 28.0, 47.6, 64.8, 68.9 (q), 80.9 (q), 114.8, 117.9, 122.7 (q*, 1J 272.1) (q), 127.1, 127.4, 128.4, 128.7, 131.4 (q*, 2J 34.2) (q), 136.9, 139.6 (q), 140.4 (q), 141.3, 151.1 (q), 151.9 (q), 158.1 (q).

δ_F (376 MHz, $CDCl_3$): -63.4.

ν_{max} (neat)/ cm^{-1} : 3177, 2931, 2714, 3665, 1668, 1534, 1473, 1381, 1275, 1170, 1125, 877, 739, 700, 681.

HRMS (m/z -ES): $[M+Na]^+$ calcd. for $C_{31}H_{31}F_6N_3O_3Na$ 630.2167; found, 630.2164.

5.1.3.10 (S)-N,N-Dimethyl-1,1-diphenyl-1-(pyrrolidin-2-yl)methanamine (281)



A 250 mL three-necked flask with stirring bar, fitted with a temperature probe was charged with **280** (2.00 g, 5.26 mmol) and dry CH_2Cl_2 (65 mL). The flask was fitted with a septum and put under an argon atmosphere and cooled to 0 °C. Trifluoroacetic acid (1.60 mL, 21.02 mmol) was added *via* syringe over 10 min. with continuous stirring. After maintaining the temperature at 0 °C for 30 min. the reaction vessel was allowed to reach room temperature and left stirring for a further 16 h. The solvent and volatiles were removed *in vacuo* and the resulting material was dissolved in a mixture of CH_2Cl_2 (25 mL) and NaOH (25 mL, 2.0 M). The product was extracted with CH_2Cl_2 (3 x 25 mL), the organic extracts were combined, dried ($MgSO_4$) and the solvent was

removed *in vacuo*. Purification by column chromatography (9:1 EtOAc-MeOH, $R_f = 0.12$) gave **281** (1.23 g, 83% yield) as a viscous oil. $[\alpha]_D^{20} = -31.7$ (c 0.30, CHCl_3).

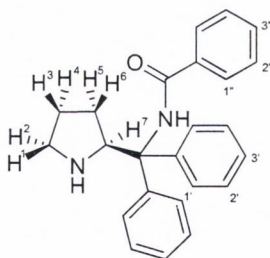
δ_H (400 MHz, CDCl_3): 0.71 (dd, 1H, J 9.5, J 5.5, H-6), 1.44-1.51 (m, 2H, H-3, H-4), 1.84-1.87 (m, 1H, H-5), 2.06 (s, 3H, NCH_3), 2.07 (s, 3H, NCH_3), 2.08-2.28 (m, 1H, H-2), 2.63-2.67 (m, 1H, H-1), 4.42-4.48 (m, 1H, H-7), 7.29-7.46 (m, 10H, Ar-H).

δ_C (100 MHz, CDCl_3): 23.9, 26.6, 45.8, 59.2, 72.3, 76.8 (q), 127.1, 127.3, 127.7, 142.1 (q).

ν_{max} (neat)/ cm^{-1} : 2930, 2787, 1672, 1444, 1198, 1174, 1126, 1022, 1001, 754, 718, 703.

HRMS (m/z -ES): $[\text{M}+\text{H}]^+$ calcd. for $\text{C}_{19}\text{H}_{25}\text{N}_2$ 281.2018; found, 281.2005.

5.1.3.11 (S)-N-(Diphenyl(pyrrolidin-2-yl)methyl)benzamide (283)



Prepared in a similar manor as compound **281** using a 100 mL round bottom flask charged with **282** (1.00 g, 2.19 mmol), dry CH_2Cl_2 (25.0 mL) and trifluoroacetic acid (1.00 mL, 8.76 mmol). Purification by column chromatography (9:1 EtOAc-MeOH, $R_f = 0.18$) gave **283** (630 mg, 81% yield) as a white solid. M.p. 161-164 °C. $[\alpha]_D^{20} = -14.2$ (c 0.50, CHCl_3).

δ_H (400 MHz, CDCl_3): 1.62-1.89 (m, 4H, H-3, H-4, H-5, H-6), 3.02-3.15 (m, 2H, H-1, H-2), 4.20-4.49, (m, 1H, H-7), 7.27-7.40 (m, 8H, H-1' x 4, H-2' x 4), 7.47-7.51 (m, 2H, H-3' x 2), 7.55 (d,

	1H, J 7.0, H-3''), 7.64 (d, 2H, J 7.0, H-2''), 7.91 (d, 2H, J 7.0, H-1''), 8.00 (s, 1H, HN).
δ_C (100 MHz, CDCl ₃):	25.0, 28.0, 46.4, 65.8 (q), 77.2, 127.1, 127.4, 127.6, 127.8, 128.7, 134.9, 137.1 (q), 141.7 (q), 167.5 (q).
ν_{\max} (neat)/cm ⁻¹ :	2961, 1662, 1578, 1476, 1445, 1286, 1186, 1073, 1032, 800, 755, 697.
HRMS (<i>m/z</i> -ES):	[M+H] ⁺ calcd. for C ₂₄ H ₂₅ N ₂ O 357.1961; found, 357.1968.

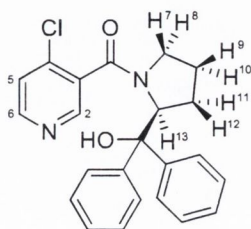
5.1.4 Procedure A: general procedure for the preparation of 4-chloronicotinamide analogues *via* acyl chloride – amine coupling

An oven dried round bottom flask with stirring bar was charged with 4-chloro-nicotinic acid (1.0 eq.) and SOCl₂ (20.0 eq.). The flask was fitted with a reflux condenser equipped with a calcium chloride guard tube and heated at reflux temperature for 6 h. After which time the flask was allowed to reach room temperature and placed under an argon atmosphere, then cooled to 0 °C in an ice bath. The resulting acyl chloride product was triturated out of solution with the addition of diethyl ether (50-100 mL) *via* syringe over 30 min. The precipitate was filtered through a medium-frit, sintered-glass funnel, washed with diethyl ether (3 x 5 mL) and suction dried in an argon atmosphere to give 4-chloronicotinoyl chloride as a yellow solid. The acyl chloride was immediately transferred to a round bottom flask equipped with stirring bar and charged with dry CH₂Cl₂ (10-20 mL) under an argon atmosphere. The flask was cooled to 0 °C in an ice bath and allowed to equilibrate for 10 min.

A separate round bottom flask equipped with a stirring bar was charged with the appropriate amine (1.0 eq.), NEt₃ (5.0 eq.) and CH₂Cl₂ (10-20 mL) under an argon atmosphere and cooled to 0 °C in an ice bath. The latter solution was added to the former solution over a 10 min. period with continuous stirring, and then allowed to reach room temperature for 16 h. After which CH₂Cl₂ (20-40 mL) was added to the reaction mixture, the resulting solution was then washed with a saturated solution

NaHCO₃ (2 x 30 mL) and brine (2 x 30 mL), dried (MgSO₄) and the solvent removed *in vacuo*. The resulting 4-chloronicotinamides were purified by column chromatography.

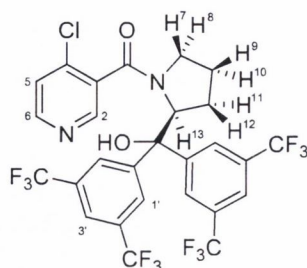
5.1.4.1 (S)-(4-Chloropyridin-3-yl)(2-(hydroxydiphenylmethyl)pyrrolidin-1-yl)methanone (301)⁸⁴



General procedure A was followed using 4-chloro-nicotinic acid (**225**, 392 mg, 2.49 mmol) and SOCl₂ (3.63 mL, 49.80 mmol). The crude acyl chloride intermediate was triturated from solution with diethyl ether (100 mL) and the resulting 4-chloronicotinoyl chloride was dispersed in dry CH₂Cl₂ (20 mL). (*S*)-diphenyl(pyrrolidin-2-yl)methanol (510 mg, 2.49 mmol), NEt₃ (1.70 mL, 12.45 mmol) in CH₂Cl₂ (20 mL) was used in the second step to afford the desired product. Purification by column chromatography (1:1 EtOAc-CH₂Cl₂, R_f = 0.12) gave **301** (484 mg, 38% yield) as a white solid. M.p. 62-64 °C. (lit.,⁸⁴ 64-66 °C). [α]_D²⁰ = -90.5 (c 0.20, CHCl₃).

δ_H (400 MHz, CDCl₃): 1.74-1.79 (m, 2H, H-9, H-10), 2.04-2.10 (m, 1H, H-11), 2.23-2.28 (m, 1H, H-12), 2.90-2.96 (m, 1H, H-7), 3.10-3.15 (m, 1H, H-8), 5.33 (app. t, 1H, J 5.5, H-13), 6.51 (s, 1H, OH), 7.20-7.61 (m, 11H, Ar-H, H-5), 8.15 (s, 1H, H-2), 8.55 (d, 1H, J 7.0, H-6).

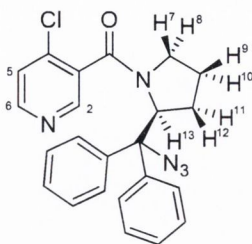
5.1.4.2 *(S)*-(2-(bis(3,5-bis(Trifluoromethyl)phenyl)(hydroxy)methyl)pyrrolidin-1-yl)(4-chloropyridin-3-yl)methanone (**228**)⁸³



General procedure A was followed using 4-chloro-nicotinic acid (**225**, 457 mg, 2.90 mmol) and SOCl_2 (2.20 mL, 58.00 mmol). The crude acyl chloride intermediate was triturated from solution with diethyl ether (100 mL) and the resulting 4-chloronicotinoyl chloride was dispersed in dry CH_2Cl_2 (20 mL). (*S*)-diphenyl(pyrrolidin-2-yl)methanol (**227**, 1.523 g, 2.90 mmol), NEt_3 (2.02 mL, 14.50 mmol) and CH_2Cl_2 (20 mL) were used in the second step to give the crude product. Purification by column chromatography (CH_2Cl_2 , $R_f = 0.15$) gave **228** (557 mg, 30%) as a white solid. M.p. 79-81 °C, (lit.,⁸³ 78-80 °C). $[\alpha]_D^{20} = -66.4$ (c 0.400, CHCl_3).

δ_{H} (400 MHz, CDCl_3): 1.52-1.56 (m, 1H, H-9), 1.73-1.77 (m, 1H, H-10), 1.88-1.93 (m, 1H, H-11), 2.17-2.23 (m, 1H, H-12), 3.08-3.13 (m, 1H, H-7), 3.30-3.35 (m, 1H, H-8), 5.34 (dd, 1H, J 8.0, 8.2, H-13), 7.20 (s, 1H, OH), 7.40 (d, 1H, J 5.5, H-5), 7.92 (s, 3H, H-1', H-3'), 7.96 (s, 1H, H-3'), 8.10 (s, 2H, H-1'), 8.32 (s, 1H, H-2), 8.55 (d, 1H, J 5.5, H-6).

5.1.4.3 (S)-2-(Azidodiphenylmethyl)pyrrolidin-1-yl(4-chloropyridin-3-yl) methanone (286)



General procedure A was followed using 4-chloro-nicotinic acid (**225**, 200 mg, 1.27 mmol) and SOCl_2 (1.85 mL, 25.40 mmol). The crude acyl chloride intermediate was triturated from solution with diethyl ether (60 mL) and the resulting 4-chloronicotinoyl chloride was dispersed in dry CH_2Cl_2 (15 mL). (S)-2-(Azidodiphenylmethyl)pyrrolidine (**276**, 354 mg, 1.27 mmol), NEt_3 (0.90 mL, 6.35 mmol) and CH_2Cl_2 (15 mL) were used in the second step to afford the crude product. Purification by column chromatography (CH_2Cl_2 , $R_f = 0.20$) gave **286** (485 mg, 91%) as a viscous oil. $[\alpha]_{\text{D}}^{20} = -56.0$ (c 0.05, CHCl_3).

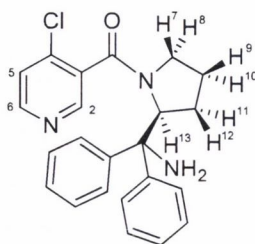
δ_{H} (400 MHz, CDCl_3): 1.39-1.48 (m, 1H, H-9), 1.71-1.80 (m, 1H, H-10), 2.15-2.25 (m, 1H, H-11), 2.23-2.45 (m, 1H, H-12), 2.91-2.99 (m, 1H, H-7), 3.06-3.13 (m, 1H, H-8), 5.81-5.85 (m, 1H, H-13), 7.31-7.51 (m, 11H, Ar-H, H-5), 8.44 (s, 1H, H-2), 8.52 (d, 1H, J 8.0, H-6).

δ_{C} (100 MHz, CDCl_3): 23.5, 31.9, 48.1, 61.5, 77.3 (q), 124.8, 128.3, 128.5, 128.8, 133.5, 135.3, 140.1, 140.8 (q), 150.8 (q), 168.6 (q).

ν_{max} (neat)/ cm^{-1} : 3057, 2929, 2103, 1734, 1649, 1446, 1412, 1389, 1252, 759, 699, 656.

HRMS (m/z -ES): $[\text{M}+\text{Na}]^+$ calcd. for $\text{C}_{23}\text{H}_{20}\text{ClN}_5\text{NaO}$ 440.1254; found, 440.1245.

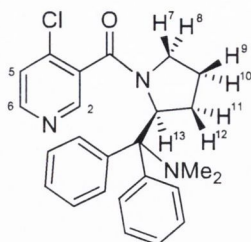
5.1.4.4 (S)-2-(2-(Aminodiphenylmethyl)pyrrolidin-1-yl)(4-chloropyridin-3-yl)methanone (289)



General procedure A was followed using 4-chloro-nicotinic acid (**225**, 1.000 g, 6.35 mmol) and SOCl_2 (9.20 mL, 126.92 mmol). The crude acyl chloride intermediate was triturated from solution with diethyl ether (100 mL) and the resulting 4-chloronicotinoyl chloride was dispersed in dry CH_2Cl_2 (20 mL). (S)-Diphenyl(pyrrolidin-2-yl)methanamine (**279**, 1.601 g, 6.34 mmol), NEt_3 (4.50 mL, 31.82 mmol) and CH_2Cl_2 (20 mL) were used in the second step to afford the crude product. Purification by column chromatography (99:1 EtOAc- NEt_3 , $R_f = 0.25$) followed by recrystallisation from CH_2Cl_2 gave **289** (980 mg, 63%) as a white solid. M.p. 141-144 °C. $[\alpha]_D^{20} = -52.1$ (c 0.05, CHCl_3).

δ_{H} (400 MHz, CDCl_3):	1.54-1.74 (m, 4H, H-9, H-10, NH_2), 2.04-2.10 (m, 1H, H-11), 2.27-2.39 (m, 1H, H-12), 2.82-2.90 (m, 1H, H-8), 3.01-3.08 (m, 1H, H-7), 4.37 (m, 1H, H-13), 7.31-7.57 (m, 11H, Ar-H, H-5), 8.51-8.54 (m, 2H, H-2, H-6).
δ_{C} (100 MHz, CDCl_3):	22.3, 28.9, 45.3, 72.6 (q), 76.8, 126.1, 127.1, 128.1, 128.4, 128.8, 132.0, 133.1 (q), 150.6 (q), 158.2 (q), 161.8 (q).
ν_{max} (neat)/ cm^{-1} :	2987, 2774, 1671, 1498, 1448, 1188, 1132, 1034, 838, 799, 762, 721, 701.
HRMS (m/z):	$[\text{M}+\text{H}]^+$ calcd. For $\text{C}_{23}\text{H}_{23}\text{ClN}_3\text{O}$ 392.1524; found, 392.1540.

5.1.4.5 (S)-(4-Chloropyridin-3-yl)(2-((dimethylamino)diphenylmethyl)pyrrolidin-1-yl)methanone (287)



General procedure A was followed using 4-chloro-nicotinic acid (**225**, 559 mg, 3.55 mmol) and SOCl_2 (5.14 mL, 71.00 mmol). The crude acyl chloride intermediate was triturated from solution with diethyl ether (100 mL) and the resulting 4-chloronicotinoyl chloride was dispersed in dry CH_2Cl_2 (20 mL). (*S*)-*N,N*-Dimethyl-1,1-diphenyl-1-(pyrrolidin-2-yl) methanamine (**281**, 1.000 g, 3.55 mmol), NEt_3 (2.50 mL, 17.75 mmol) and CH_2Cl_2 (20 mL) were added in the second step to afford the crude product. Purification by column chromatography (9:1 CH_2Cl_2 -EtOAc, $R_f = 0.25$) gave **287** (1.20 g, 80%) as a white solid. M.p. 79-84 °C. $[\alpha]_{\text{D}}^{20} = -137.0$ (c 0.40, CHCl_3).

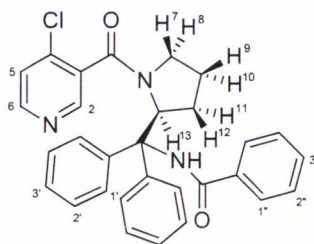
δ_{H} (400 MHz, CDCl_3): 1.24-1.42 (m, 2H, H-9, H-10), 1.87-1.94 (m, 2H, H-11, H-12), 2.07 (s, 6H, NMe_2), 2.19-2.25 (m, 1H, H-7), 2.71-2.76 (m, 1H, H-8), 5.93 (dd, 1H, J 9.0, 7.5, H-13), 7.29-7.41 (m, 11H, H-5, Ar-H) 8.48 (d, 1H, J 8.0, H-6), 8.58 (s, 1H, H-2).

δ_{C} (100 MHz, CDCl_3): 24.2, 31.0, 40.3, 50.5, 58.5 (q), 77.2, 124.9, 126.8, 127.2, 130.6, 131.5, 133.6, 141.0 (q), 148.9 (q), 150.5 (q), 166.4 (q).

ν_{max} (neat)/ cm^{-1} : 2953, 2868, 2830, 2786, 1649, 1573, 1551, 1411, 1388, 1150, 1084, 756, 706, 679.

HRMS (m/z -ES): $[\text{M}+\text{H}]^+$ calcd. for $\text{C}_{25}\text{H}_{27}\text{ClN}_3\text{O}$ 420.1837; found, 420.1842.

5.1.4.6 (S)-N-((1-(4-Chloronicotinoyl)pyrrolidin-2-yl)diphenylmethyl)benzamide (288)



General procedure A was followed using 4-chloro-nicotinic acid (**225**, 177 mg, 1.12 mmol) and SOCl_2 (1.62 mL, 22.40 mmol). The crude acyl chloride intermediate was triturated from solution with diethyl ether (50 mL) and the resulting 4-chloronicotinoyl chloride was dispersed in dry CH_2Cl_2 (10 mL). (*S*)-*N*-(diphenyl(pyrrolidin-2-yl)methyl)benzamide (**283**, 400 mg, 1.12 mmol), NEt_3 (0.94 mL, 6.72 mmol) and CH_2Cl_2 (10 mL) were used in the second step to afford the crude product. Purification by column chromatography (9:1 CH_2Cl_2 -EtOAc, $R_f = 0.20$) gave **288** (450 mg, 81%) as a white solid. M.p. 249-253 °C. $[\alpha]_{\text{D}}^{20} = -47.5$ (c 0.40, CHCl_3).

δ_{H} (400 MHz, CDCl_3): 1.20-1.28 (m, 1H, H-9), 1.40-1.47 (m, 1H, H-10), 1.61-1.78 (m, 1H, H-11), 2.01-2.11 (m, 1H, H-12), 2.25-2.34 (m, 1H, H-7), 2.86-2.94 (m, 1H, H-8), 5.82-5.90 (m, 1H, H-13), 7.27-7.46 (m, 10H, Ar-H x 8, H-5, H-3''), 7.60 (d, 2H, J 7.5, H-1'), 7.88 (d, 2H, J 8.0, H-2''), 8.00 (d, 2H, J 8.0, H-1''), 8.38 (s, 1H, H-2), 8.56 (s, 1H, H-6), 9.92 (s, 1H, HN).

δ_{C} (100 MHz, CDCl_3): 23.4, 27.2, 49.8, 69.4 (q), 76.8, 124.8, 126.9, 127.0, 127.3, 127.9, 128.5, 129.2, 130.8, 134.0, 135.9, 140.2 (q), 146.9 (q), 150.0 (q), 164.5 (q), 172.3 (q).

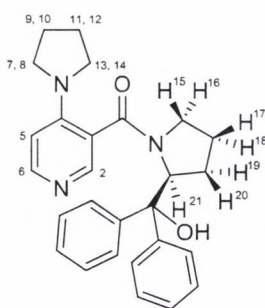
ν_{max} (neat)/ cm^{-1} : 3257, 1665, 1621, 1573, 1541, 1490, 1329, 1146, 1081, 841, 698, 676.

HRMS (m/z -ES): $[M+Na]^+$ calcd. for $C_{30}H_{26}ClN_3O_2Na$ 518.1611; found, 518.1619.

5.1.5 Procedure B: general procedure for the preparation of 4-aminonicotinamide analogues *via* S_NAr reaction

A three-necked flask with stirring bar, equipped with a reflux condenser and temperature probe was put under an argon atmosphere was charged with the appropriate 4-chloronicotinamide (1.0 eq.), NEt_3 (5.0 eq.) and toluene (0.5 M). Pyrrolidine (5.0 eq.) was added *via* syringe with continuous stirring and the reaction was heated to 80 °C of 16 h. The volatiles were removed *in vacuo* and the resulting solid was dissolved in CH_2Cl_2 (30 mL) and washed with a concentrated solution of $NaHCO_3$ (2 x 30 mL). The organic layer was isolated, dried ($MgSO_4$) and the solvent removed *in vacuo* to give the crude 4-aminonicotinamide product.

5.1.5.1 (*S*)-(2-(Hydroxydiphenylmethyl)pyrrolidin-1-yl)(4-(pyrrolidin-1-yl)pyridin-3-yl)methanone (**53**)⁸⁴

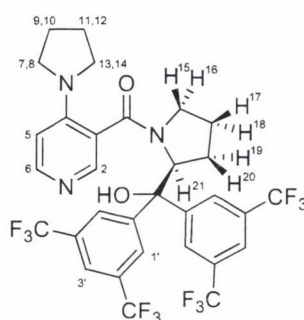


General procedure B was followed using the 4-chloronicotinamide (**301**) (100 mg, 0.25 mmol), NEt_3 (177 μ L, 1.27 mmol), toluene (500 μ L) and pyrrolidine (160 μ L, 1.27 mmol). Purification by column chromatography (49:1 EtOAc- NEt_3 , R_f = 0.12) gave **53** (67 mg, 62%) as a white solid. M.p. 144-145. (lit.,⁸⁴ 144-146 °C). $[\alpha]_D^{20}$ = -92.0 (c 1.0, $CHCl_3$).

δ_H (400 MHz, $CDCl_3$): 0.95-1.18 (m, 2H, H-17, H-19), 1.80-2.20 (m, 6H, H-9, H-10, H-11, H-12, H-18, H-20), 2.90-3.15 (m, 3H, H-7, H-8,

H-13), 3.40-3.55 (m, 3H, H-14, H-15, H-16), 5.20 (dd, 1H, J 9.0, 8.5, H-21), 6.45 (d, 1H, J 6.0, H-5), 7.25-7.38 (m, 5H, Ar-H), 7.41-7.60 (m, 6H, Ar-H, H-2), 8.09 (d, 1H, J 6.0, H-6).

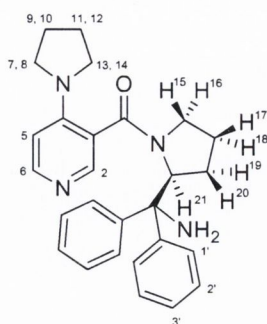
5.1.5.2 **(S)-2-(bis(3,5-bis(Trifluoromethyl)phenyl)(hydroxy)methyl)pyrrolidin-1-yl(4-(pyrrolidin-1-yl)pyridin-3-yl)methanone (57)**⁸³



General procedure B was followed using the 4-chloronicotinamide **228** (150 mg, 0.22 mmol), NEt₃ (157 μL, 1.13 mmol), toluene (440 μL) and pyrrolidine (94 μL, 1.13 mmol). Purification by column chromatography (EtOAc, R_f = 0.13) gave **57** (101 mg, 63%) as a white solid. M.p. 120-121, (lit.,¹⁹³ 120-122 °C). [α]_D²⁰ = -58.2 (c 0.200, CHCl₃).

δ_H (400 MHz, CDCl₃): 1.60-2.32 (m, 8H, H-9, H-10, H-11, H-12, H-17, H-18, H-19, H-20), 2.86-3.30 (m, 3H, H-7, H-8, H-15), 3.42-4.50 (m, 2H, H-13, H-14), 3.68-3.74 (m, 1H, H-16), 5.01-5.27 (m, 1H, H-21), 6.51 (d, 1H, J 5.5, H-5), 7.45 (s, 1H, H-2), 7.82-8.26 (m, 7H, H-6, Ar-H).

5.1.5.3 (S)-2-(2-(Aminodiphenylmethyl)pyrrolidin-1-yl)(4-(pyrrolidin-1-yl)pyridin-3-yl)methanone (293)



General procedure B was followed using the 4-chloronicotinamide **289** (118 mg, 0.23 mmol), NEt_3 (160 μL , 1.15 mmol), toluene (460 μL) and pyrrolidine (124 μL , 1.15 mmol). Purification by column chromatography (9:1 EtOAc-MeOH, $R_f = 0.15$) gave **293** (94 mg, 74%) as a white solid. M.p. 135-137 $^\circ\text{C}$. $[\alpha]_D^{20} = -90.0$ (c 0.05, CHCl_3).

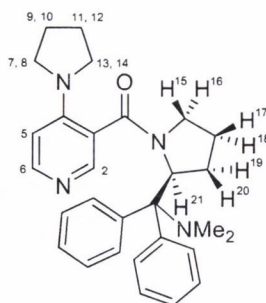
δ_{H} (400 MHz, CDCl_3): 1.20-1.29 (m, 1H, H-17), 1.55-1.63 (m, 1H, H-18), 1.86-1.93 (m, 2H, H-9, H-10), 2.02-2.10 (m, 3H, H-11, H-12, H-19), 2.22-2.23 (m, 1H, H-20), 2.93-3.10 (m, 3H, H-13, H-14, H-16), 3.27-3.32 (m, 1H, H-15), 3.42-3.51 (m, 2H, H-7, H-8), 5.58-5.62 (m, 1H, H-21), 6.45 (d, 1H, J 7.5, H-5), 7.17-7.48 (m, 8H, Ar-H x 8), 7.59 (d, 2H, J 8.0, H-1' x 2), 8.10 (s, 1H, H-2), 8.15 (d, 1H, J 7.5, H-6).

δ_{C} (100 MHz, CDCl_3): 23.1, 25.1, 28.1, 34.7, 49.0, 51.1, 63.0, 66.2 (q), 76.8, 108.2, 126.5, 126.8, 127.1, 127.8, 144.8, 146.5 (q), 149.3 (q), 154.7 (q), 169.2 (q).

ν_{max} (neat)/ cm^{-1} : 2924, 2872, 1623, 1587, 1536, 1506, 1482, 1459, 1445, 1420, 1375, 1304, 1238, 1198, 1173, 1065, 1032, 975, 920, 866, 807, 745, 700, 661.

HRMS (m/z -ES): $[\text{M}+\text{H}]^+$ calcd. for $\text{C}_{27}\text{H}_{31}\text{N}_4\text{O}$ 427.2498; found, 427.2512.

5.1.5.4 (S)-2-((Dimethylamino)diphenylmethyl)pyrrolidin-1-yl)(4-(pyrrolidine-1-yl)pyridin-3-yl)methanone (291)



General procedure B was followed using the 4-chloronicotinamide **287** (1.140 g, 2.72 mmol), NEt_3 (1.90 mL, 13.60 mmol), toluene (5.44 mL) and pyrrolidine (1.14 mL, 13.60 mmol). Purification by column chromatography (9:1 EtOAc-MeOH, $R_f = 0.20$) to give **291** (1.10 g, 89%) as a pale yellow solid. M.p. 79-81 °C. $[\alpha]_D^{20} = -191.5$ (c 0.850, CHCl_3).

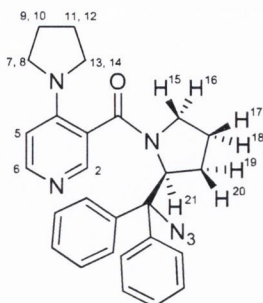
δ_{H} (400 MHz, CDCl_3): 1.02-1.10 (m, 1H, H-17), 1.27-1.37 (m, 1H, H-18), 1.44-1.53 (m, 1H, H-9), 1.84-2.23 (m, 12H, NMe_2 , H-10, H-11, H-12, H-15, H-16, H-19), 2.97-3.05 (m, 2H, H-7, H-8), 3.20-3.26 (m, 1H, H-20), 3.44-3.52 (m, 2H, H-13, H-14), 5.94 (dd, 1H, J 7.0, J 7.0, H-21), 6.48 (d, 1H, J 8.5, H-5), 7.30-7.48 (m, 10H, Ar-H), 8.14 (d, 1H, J 8.5, H-6), 8.25 (s, 1H, H-2).

δ_{C} (100 MHz, CDCl_3): 23.4, 25.6, 27.4, 40.3, 49.1, 49.7, 51.6, 57.9, 75.9 (q), 108.5, 117.7, 126.7, 126.8, 127.1, 130.5, 131.4, 148.9 (q), 149.6 (q), 150.0 (q), 170.3 (q).

ν_{max} (neat)/ cm^{-1} : 2950, 2870, 2831, 2786, 1631, 1584, 1396, 1136, 976, 723, 706, 682.

HRMS (m/z -ES): $[\text{M}+\text{H}]^+$ calcd. for $\text{C}_{29}\text{H}_{35}\text{N}_4\text{O}$ 455.2811; found, 455.2818.

5.1.5.5 (S)-(2-(Azidodiphenylmethyl)pyrrolidin-1-yl)(4-(pyrrolidin-1-yl)pyridin-3-yl)methanone (290)



General procedure B was followed using the 4-chloronicotinamide **286** (500 mg, 1.20 mmol), NEt_3 (836 μL , 6.00 mmol), toluene (2.40 mL) and pyrrolidine (501 μL , 836 mmol). Purification by column chromatography (EtOAc, $R_f = 0.12$) gave **290** (430 mg, 79%) as a white solid. M.p. 80-86 $^\circ\text{C}$. $[\alpha]_D^{20} = -67.1$ (c 0.170, CHCl_3).

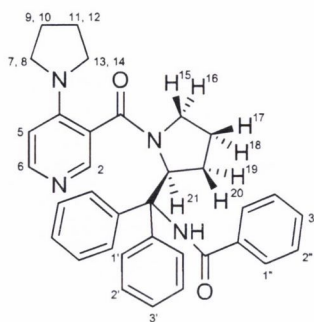
δ_{H} (400 MHz, CDCl_3): 1.42-1.52 (m, 1H, H-18), 1.65-1.45 (m, 1H, H-17), 1.84-1.92 (m, 3H, H-9, H-10, H-11), 1.94-1.99 (m, 1H, H-12), 2.11-2.19 (m, 1H, H-20), 2.25-2.36 (m, 1H, H-19), 2.99-3.08 (m, 2H, H-15, H-7), 3.42-3.51 (m, 4H, H-8, H-13, H-14, H-16), 5.81-5.83 (m, 1H, H-21), 6.46 (d, 1H, J 7.5, H-5), 7.29-7.47 (m, 10H, Ar-H), 8.10 (s, 1H, H-2), 7.15 (d, 1H, J 7.5, H-6).

δ_{C} (100 MHz, CDCl_3): 23.4, 25.6, 30.9, 34.6, 42.3, 47.5, 49.4, 60.9, 75.6 (q), 108.6, 116.9 (q), 128.1, 128.3, 128.7, 140.3 (q), 140.9, 148.5 (q), 149.9, 169.8 (q).

ν_{max} (neat)/ cm^{-1} : 2970, 2873, 2103, 1629, 1585, 1395, 1373, 1302, 1246, 1198, 722, 700.

HRMS (m/z -ES): $[\text{M}+\text{H}]^+$ calcd. for $\text{C}_{27}\text{H}_{29}\text{N}_6\text{O}$ 453.2403; found, 453.2397.

5.1.5.6 (S)-N-(Diphenyl(1-(4-(pyrrolidin-1-yl)nicotinoyl)pyrrolidin-2-yl)methyl)benzamide (292)



General procedure B was followed using the 4-chloronicotinamide **288** (310 mg, 0.62 mmol), NEt_3 (432 μL , 3.10 mmol), toluene (1.24 mL) and pyrrolidine (259 μL , 3.10 mmol). Purification by column chromatography (1:1 EtOAc- CH_2Cl_2 , $R_f = 0.10$) gave **292** (300 mg, 91%) as a white solid. M.p. 141-146 $^\circ\text{C}$. $[\alpha]_D^{20} = -105.3$ (c 0.20, CHCl_3).

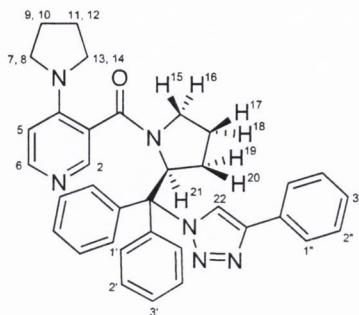
δ_{H} (400 MHz, CDCl_3): 1.27-1.52 (m, 3H, H-9, H-17, H-18), 1.67-2.29 (m, 5H, H-10, H-11, H-12, H-19, H-20), 3.08-3.21 (m, 2H, H-7, H-8), 3.26-3.36 (m, 2H, H-15, H-16), 3.51-3.60 (m, 2H, H-13, H-14), 5.71-5.80 (m, 1H, H-21), 6.51 (d, 1H, J 7.5, H-5), 7.29-7.64 (m, 11H, Ar-H x 8, H-2'' x 2, H-3''), 7.81-7.95 (m, 5H, H-1' x 2, H-1'' x 2, H-2), 8.15 (d, 1H, J 7.5, H-6), 9.94 (s, 1H, HN).

δ_{C} (100 MHz, CDCl_3): 22.7, 25.1, 27.5, 48.7, 51.0, 64.2, 69.7 (q), 76.8, 108.2, 116.2, 126.8, 127.1, 127.4, 127.9, 128.4, 129.4, 130.6, 134.1 (q), 136.1 (q), 140.4 (q), 147.7 (q), 148.5, 164.7 (q), 171.2 (q).

ν_{max} (neat)/ cm^{-1} : 3271, 2962, 2871, 1670, 1607, 1504, 1483, 1460, 1411, 1374, 1300, 1139, 973, 804, 771, 697.

HRMS (m/z -ES): $[\text{M}+\text{H}]^+$ calcd. for $\text{C}_{34}\text{H}_{35}\text{N}_4\text{O}_2$ 531.2760; found, 531.2763.

5.1.5.7 (S)-2-(2-(Diphenyl(4-phenyl-1H-1,2,3-triazol-1-yl)methyl)pyrrolidin-1-yl)(4-(pyrrolidin-1-yl)pyridin-3-yl)methanone (294)



A 10 mL round bottom flask with stirring bar was charged with azide **290** (200 mg, 0.44 mmol) and phenyl acetylene (55 μ L, 0.49 mmol) dissolved in CH_2Cl_2 (880 μ L) at room temperature. $\text{CuSO}_4 \cdot 5\text{H}_2\text{O}$ (122 mg, 0.49 mmol), sodium ascorbate (114 mg, 0.57 mmol) and distilled H_2O (88 μ L) were added, and the flask was allowed to stir at room temperature for 16 hours. The contents were then transferred to a separating funnel and CH_2Cl_2 (20 mL) was added. The solution was washed with a saturated solution of NaHCO_3 (2 x 25 mL) and brine (2 x 25 mL). The organic layer was separated, dried (MgSO_4) and the solvent was removed *in vacuo*. Purification by column chromatography (9:1 EtOAc-MeOH, $R_f = 0.15$) afforded the triazole product **294** (182 mg, 74%) as a beige solid. M.p. 69-72 $^\circ\text{C}$. $[\alpha]_{\text{D}}^{20} = -149.0$ (c 0.10, CHCl_3).

δ_{H} (400 MHz, CDCl_3): 1.08-1.15 (m, 1H, H-18), 1.26-1.36 (m, 1H, H-19), 1.57-1.66 (m, 1H, H-17), 1.73-1.84 (m, 2H, H-9, H-10), 2.08-2.16 (m, 2H, H-11, H-12), 2.22-2.30 (m, 1H, H-20), 2.42-2.51 (m, 1H, H-16), 3.01-3.10 (m, 2H, H-7, H-8), 3.25-3.31 (m, 1H, H-15), 3.44-3.51 (m, 2H, H-13, H-14), 6.42-6.54 (m, 2H, H-5, H-21), 7.30-7.59 (m, 14H, Ar-H x 10, H-2'' x 2, H-3'', H-22), 7.80 (m, 3H, H-1'' x 2, H-6), 8.11 (s, 1H, H-2).

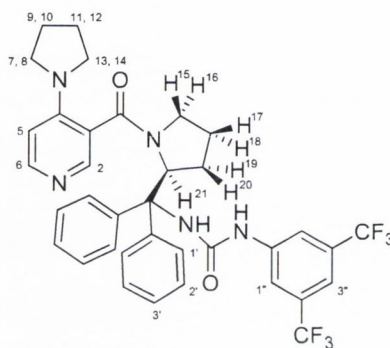
δ_{C} (100 MHz, CDCl_3): 28.9, 49.41, 49.43, 52.2, 61.5, 76.8 (q), 77.7, 108.3, 122.1, 125.2, 127.5, 127.7, 127.8, 128.0, 128.2, 128.3, 128.6,

129.1, 129.9 (q), 139.5 (q), 140.2 (q), 145.9 (q), 149.5, 164.2 (q), 170.5 (q).

ν_{\max} (neat)/ cm^{-1} : 2924, 2854, 2103, 1740, 1647, 1574, 1551, 1493, 1446, 1411, 1388, 1251, 699, 654.

HRMS (m/z -ES): $[\text{M}+\text{H}]^+$ calcd. for $\text{C}_{35}\text{H}_{35}\text{N}_6\text{O}$ 555.2872; found, 555.2868.

5.1.5.8 (S)-1-(3,5-bis(trifluoromethyl)phenyl)-3-(diphenyl(1-(4-(pyrrolidin-1-yl)nicotinoyl)pyrrolidin-2-yl)methyl)urea (295)



A 5 mL round bottom flask with stirring bar, under an argon atmosphere was charged with amine **293** (100 mg, 0.23 mmol) and dry CH_2Cl_2 (2.0 mL). 3,5-bis(trifluoromethyl)phenyl isocyanate (45 μL , 0.25 mmol) was added and the reaction was left at room temperature for 16 hours. The contents were then transferred to a separating funnel and CH_2Cl_2 (20 mL) was added and the solution was washed with a saturated solution of NaHCO_3 (2 x 25 mL). The organic layer was separated, dried (MgSO_4) and the solvent was removed *in vacuo*. Purification by column chromatography (9:1 EtOAc-MeOH, $R_f = 0.28$) gave the urea **295** (71 mg, 45%) as a beige solid. M.p. 144-146 $^\circ\text{C}$. $[\alpha]_{\text{D}}^{20} = -43.3$ (c 0.03, CHCl_3).

δ_{H} (400 MHz, DMSO): 1.16-1.24 (m, 2H, H-17, H-18), 1.36-1.44 (m, 1H, H-19), 1.78-1.83 (m, 4H, H-9, H-10, H-11, H-12), 1.91-2.00 (m, 2H, H-13, H-14), 2.12-2.21 (m, 1H, H-20), 3.00-3.11 (m, 2H, H-7, H-8), 3.25-3.32 (m, 2H, H-15, H-16), 5.51-5.56 (m, 1H, H-21), 6.60 (d, 1H, J 5.5, H-5), 7.24-7.46 (m, 9H,

Ar-H x 8, H-2), 7.58 (s, 1H, H-3''), 7.59 (d, 2H, J 7.5, H-1' x 2), 7.99 (s, 2H, H-1'' x 2), 8.07 (d, 1H, J 5.5, H-6), 8.86 (s, 1H, N-H), 9.70 (s, 1H, NH).

(Note: the use of q* denotes a quartet multiplicity signal)

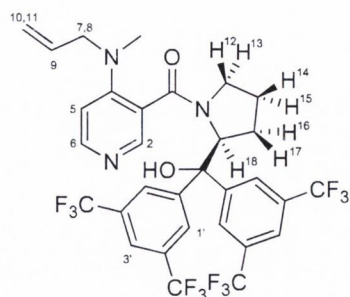
δ_C (100 MHz, CDCl₃): 22.9, 24.2, 25.2, 29.4, 39.7, 42.6, 45.7, 61.8 (q), 76.8, 115.1, 117.7, 118.8, 125.6 (q*, J¹ 272) (q), 127.5, 127.8, 128.4, 128.9, 131.6 (q*, J² 33) (q), 139.0, 140.4 (q), 146.9 (q), 147.9 (q), 152.0 (q), 158.6 (q), 168.4 (q).

δ_F (376MHz, DMSO): -62.21.

ν_{\max} (neat)/cm⁻¹: 2926, 2257, 1718, 1619, 1571, 1471, 1447, 1377, 1274, 1168, 1122, 999, 976, 947, 928, 882, 843, 809, 752, 726, 700, 681.

HRMS (*m/z* -ES): [M+H]⁺ calcd. for C₃₆H₃₄F₆N₅O₂ 682.2617; found, 682.2607.

5.1.5.9 (S)-4-(Allyl(methyl)amino)pyridin-3-yl(2-(hydroxydiphenylmethyl)pyrrolidin-1-yl)methanone (231)



A 10 mL round bottom flask equipped with stirring bar was charged with **228** (557 mg, 0.838 mmol) and toluene (2.5 mL) and put under an argon atmosphere. To this was added *N*-methylallylamine (0.20 mL, 2.094 mmol) with stirring and the resulting solution was heated 55 °C for 48 hours. CH₂Cl₂ (20 mL) was then added and the

solution was washed with a saturated solution of NaHCO₃ (2 x 30 mL) and brine (2 x 30 mL). The organic layer was separated, dried (MgSO₄) and the solvent was removed *in vacuo*. Purification by column chromatography (1:1 EtOAc-CH₂Cl₂, R_f = 0.25), gave **231** (387 mg, 66%) as a white solid. M.p. 94-97 °C. $[\alpha]_D^{20} = -38.4$ (c 0.100, CHCl₃).

Note: **231** exists in two rotameric forms in the ¹H-NMR and ¹³C-NMR time-frame.

Major and minor rotamer

δ_H (400 MHz, CDCl₃): 1.72-2.08 (m, 4H, H-14, H-15, H-16, H-17), 2.70-3.15 (m, 4H, N-Me₂, H-12), 3.63-3.94 (m, 3H, H-7, H-8, H-13), 5.05-5.29 (m, 3H, H-10, H-11, H-18), 5.75-5.88 (m, 1H, H-9), 6.63 (d, 1H, J 6.0, H-5), 7.38 (s, 1H, H-2), 7.87-8.23 (m, 7H, H-6, Ar-H).

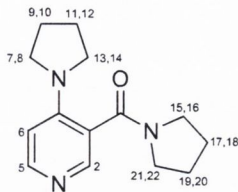
(Note: the use of q* denotes a quartet multiplicity signal)

δ_C (100 MHz, CDCl₃): 23.7, 31.5, 38.3, 52.6, 56.1, 69.2, 76.4 (q), 110.1, 118.0 (q), 117.9, 118.5, 121.9 (q*, ¹J 180.5) (q), 122.2 (q*, ¹J 180.5) (q), 127.5, 127.7, 131.7 (q*, ²J 32.5) (q), 131.6 (q*, ²J 32.5) (q), 144.5 (q), 146.5 (q), 148.2, 148.8 (q), 150.6, 172.5 (q).

δ_F (376MHz, DMSO): -63.12.

ν_{\max} (neat)/cm⁻¹: 3245, 2924, 2288, 1644, 1372, 1132, 682.

HRMS (*m/z* -ES): [M+H]⁺ calcd. for C₃₁H₂₆F₁₂N₃O₂ 699.1755; found; 699.1751.

5.1.5.10 Pyrrolidine-1-yl-(4-pyrrolidin-1-yl-pyridin-3-yl)-methanone (**299**)

A 10 mL round bottom flask charged with **225** (90 mg, 0.57 mmol) and SOCl_2 (500 μL , 5.7 mmol) was fitted with a reflux condenser and heated under reflux conditions for 4 hour. Removal of SOCl_2 by distillation gave 4-chloronicotinic acid chloride hydrochloride salt as a yellow solid. This was placed under an atmosphere of argon, cooled to 0 °C and THF (4 mL) was added *via* syringe. Pyrrolidine (238 μL , 2.85 mmol) was added *via* syringe and the yellow solution was left to stir for 4 h. Subsequently, another aliquot of pyrrolidine (95 μL , 1.14 mmol) was added, and the resulting solution was left to heat at reflux temperature overnight. CH_2Cl_2 (25 mL) was then added and the resulting solution washed with NaHCO_3 (25 mL x 2) and brine (25 mL x 2). The organic extracts were separated, dried (MgSO_4) and the solvent was removed *in vacuo*. Purification by column chromatography gave **299** (95 mg, 68%) as a white solid. M.p. 126-128 °C. $[\alpha]_{\text{D}}^{20} = -34.8$ (c 0.12, CHCl_3).

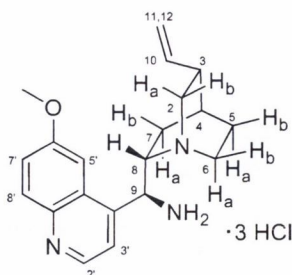
δ_{H} (400 MHz, CDCl_3): 1.92-1.99 (m, 8H, H-9, H-10, H-11, H-12, H-17, H-18, H-19, H-20), 3.17-3.68 (m, 8H, H-7, H-8, H-13, H-14, H-15, H-16, H-21, H-22), 6.47 (d, 1H, J 6.0, H-5), 8.14-8.19 (m, 2H, H-2, H-6).

δ_{C} (100 MHz, CDCl_3): 24.2, 25.1, 25.3, 45.3, 48.2, 48.3, 107.9, 117.7, 148.2, 148.5 (q), 149.2 (q), 168.4 (q).

ν_{max} (neat)/ cm^{-1} : 3356, 2289, 1590, 1261, 792.

HRMS (m/z -ES): $[\text{M}+\text{H}]^+$ calcd. For $\text{C}_{14}\text{H}_{20}\text{N}_3\text{O}$ 246.1606; found, 246.1605.

5.1.6 (S)-(6-Methoxyquinolin-4-yl)((2S,4S,5R)-5-vinylquinuclidin-2-yl) methanamine (3·HCl salt) (261)²⁰⁹

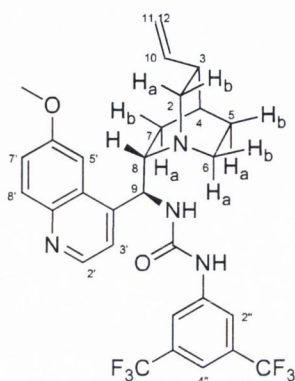


A 250 mL three-necked flask with temperature probe, equipped with a stirring bar, under an argon atmosphere was charged with quinine (4.20 g, 12.95 mmol), triphenylphosphine (4.07 g, 15.53 mmol) and dry THF (80 mL). The solution was cooled to 0 °C with continuous stirring and diisopropyl azodicarboxylate (DIAD) (3.01 mL, 15.53 mmol) was added *via* syringe, followed by diphenylphosphoryl azide (DPPA) (3.20 mL, 15.53 mmol) and the reaction allowed to reach room temperature for 16 hours. The flask was fitted with a reflux condenser and heated to 50 °C for 2 hours, then allowed to reach room temperature. Triphenylphosphine (4.07 g, 15.53 mmol) was added in one portion and the reaction was reheated to 50 °C of a further 2 hours. After cooling to ambient temperature, H₂O (5 mL) was added and the reaction flask was left stirring for 4 hours. The solvent was removed *in vacuo* and the resulting residue dissolved in CH₂Cl₂ (100 mL), acidified with HCl (100 mL, 2.0 M) and the aqueous layer was washed with CH₂Cl₂ (3 x 50 mL). The aqueous solution was concentrated *in vacuo* to afford the crude product. Dissolving the crude product in hot MeOH and triturating with EtOAc afforded the pure product **261** (3.10 g, 75%) as a fluffy yellow solid. M.p. 220-222 °C (dec.), (lit.,²⁰⁹ 220 - 222 °C). $[\alpha]_D^{20} = +15.2$ (*c* 1.00, CH₃OH).

δ_H (400 MHz, D₂O): 1.11 (dd, 1H, J 13.9, 7.3, H-7a), 1.84 (app. t, 1H, H-7b), 1.96-2.14 (m, 3H, H-4, H-5a, H-5b), 2.83-2.99 (m, 1H, H-3), 3.42-3.60 (m, 2H, H-6b, H-2a), 3.82 (dd, 1H, J 13.2, 11.0, H-2b), 3.92-4.04 (m, 1H, H-6a), 4.14 (s, 3H, OCH₃), 4.38 (app. dd, 1H, H-8), 5.20 (app. d, 1H, H-11), 5.22 (app. d, 1H, H-12), 5.71 (d, 1H, J 9.5, H-9), 5.84 (ddd, 1H, J 17.6, 11.0, 6.6, H-10), 7.70 (app. s, 1H, H-5'), 7.78

(dd, 1H, J 9.5, 2.2, H-7'), 7.96 (d, 1H, J 5.9, H-3'), 8.15 (d, 1H, J 9.5, H-8'), 8.87 (d, 1H, J 5.9, H-2').

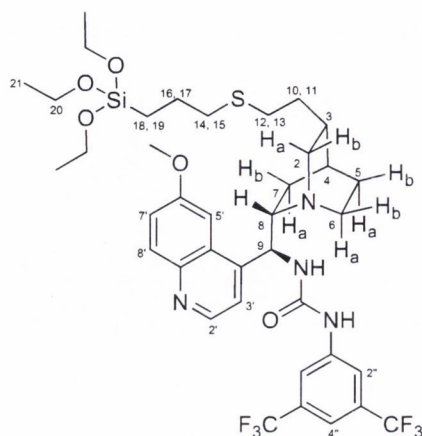
5.1.6.1 1-(3,5-bis(Trifluoromethyl)phenyl)-3-((S)-(6-methoxyquinolin-4-yl)((2S,4S,5R)-5-vinylquinuclidin-2-yl)methyl)urea (259**)²⁰⁹**



A 250 mL round bottom flask under an argon atmosphere was charged with **261** (2.00 g, 6.18 mmol) and dry CH₂Cl₂ (60 mL). NEt₃ (3.45 mL, 24.70 mmol) was added *via* syringe with continuous stirring, followed by 3,5-bis-(trifluoromethyl)phenyl isocyanate (1.26 mL, 7.42 mmol) and the reaction was left at room temperature for 16 hours. The solvent was removed *in vacuo* and the crude product was purified by column chromatography (9:1 EtOAc-MeOH, R_f = 0.28) to afford the urea product **259** (1.83 g, 89%) as a pale yellow solid. M.p. 152-155 °C, (lit.,²⁰⁹ 152-155 °C). [α]_D²⁰ = +24.4 (c 1.0, CHCl₃).

δ_H (600 MHz, CD₃OD): 0.88-1.02 (m, 1H, H-7a), 1.60-1.82 (m, 4H, H-4, H-7b, H-5a, H-5b), 2.42-2.50 (m, 1H, H-3), 2.82-2.99 (m, 2H, H-2a, H-6b), 3.29 (dd, 1H, J 13.6, 9.9, H-2b), 3.40-3.57 (m, 2H, H-8, H-6a), 4.04 (s, 3H, OCH₃), 5.05 (app. d, 1H, H-11), 5.11 (app. d, 1H, H-12), 5.63 (app. s, 1H, H-9), 5.95 (ddd, 1H, J 17.0, 10.2, 7.2, H-10), 7.44-7.52 (m, 2H, H-7', H-4''), 7.59 (d, 1H, J 4.6, H-3'), 7.86 (d, 1H, J 2.0, H-5'), 7.97 (s, 2H, H-2'' x 2), 7.99 (d, 1H, J 9.0, H-8'), 8.72 (d, 1H, J 4.6, H-2').

5.1.6.2 **1-(3,5-bis(Trifluoromethyl)phenyl)-3-((S)-(6-methoxyquinolin-4-yl) ((2S,4S,5R)-5-(2-(3-(triethoxysilyl)propylthio)ethyl)quinuclidin-2-yl)methyl)urea (263)**



A 5 mL round bottom flask, equipped with a stirring bar, was charged with urea **259** (300 mg, 0.52 mmol) and azobisisobutyronitrile (AIBN, 51 mg, 0.31 mmol). The flask was fitted with a septum and flushed with argon. Dry toluene (2.0 mL) was added *via* syringe followed by (3-mercaptopropyl)-triethoxysilane (313 mL, 1.30 mmol) and the resulting mixture was heated to 60 °C and stirred for 16 h. The solvent was removed *in vacuo* and the residue purified by column chromatography (9:1 EtOAc-NEt₃, R_f = 0.45) gave **263** in a 28% yield (40 mg) as an amorphous beige solid. M.p. 77-81 °C. $[\alpha]_D^{20} = +9.2$ (*c* 1.0, CHCl₃).

δ_H (400 MHz, CDCl₃): 0.72-0.76 (m, 2H, H-18, H-19), 0.97-1.02 (m, 1H, H-7a), 1.22 (t, 9H, J 11.0, H-21), 1.47-1.76 (m, 9H, H-3, H-4, H-5a, H-5b, H-7b, H-10, H-11, H-16, H-17), 2.10-2.19 (m, 1H, H-6a), 2.33-2.39 (m, 2H, H-14, H-15), 2.49-2.53 (m, 2H, H-12, H-13), 2.70-2.77 (m, 1H, H-2a), 3.06-3.17 (m, 1H, H-2b), 3.32-3.40 (m, 1H, H-6b), 3.55 (s, 1H, H-8), 3.80 (q, 6H, J 11.0, H-20), 4.03 (s, 3H, OCH₃), 5.51 (s, 1H, H-9), 6.69 (s, 1H, NH), 7.39-7.41 (m, 2H, H-4'', H-5'), 7.45 (dd, J 2.4, 6.8, 1H, H-7'), 7.72-7.74 (m, 3H, H-2'', H-3'), 8.10 (d, J 9.2, 1H, H-8'), 8.24 (s, 1H, NH), 8.85 (d, J 4.4, 1H, H-2').

(Note: the sue of q* denotes a quartet multiplicity signal)

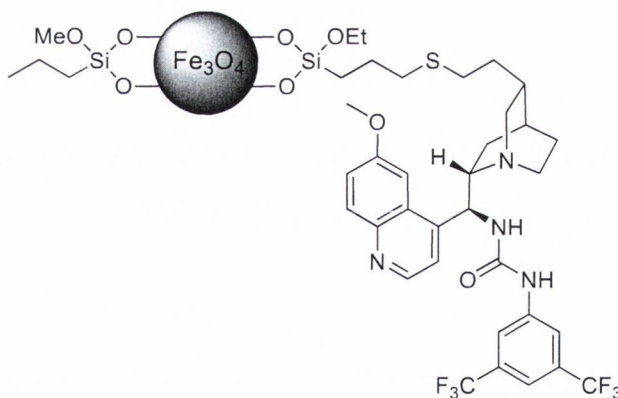
δ_C (100 MHz,CDCl₃): 9.9, 18.3, 23.2, 25.1, 26.9, 27.9, 29.7, 33.7, 34.4, 35.3, 41.5, 50.7, 55.8, 57.0, 58.4, 59.7, 101.9, 115.4, 188.0, 118.2 (q*, ³J 4.0), 122.5, 123.0 (q*, ¹J 273.0) (q), 128.5, 132.0, 132.0 (q*, ²J 30.5) (q), 140 (q), 144.3 (q), 145.1 (q), 147.2 (q), 154.6 (q), 158.5 (q).

δ_F (376MHz, CDCl₃): -63.67.

ν_{\max} (neat)/cm⁻¹: 2974, 2928, 1703, 1622, 1566, 1509, 1387, 1276, 1241, 1226, 1169, 1101, 944, 780, 681.

HRMS (*m/z* -ES): [M+H]⁺ calcd. for C₃₈H₅₁N₄F₆SSi 817.3248; found; 817.3267.

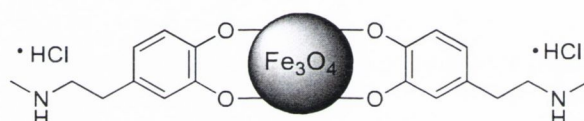
5.1.6.3 Synthesis of magnetic nanoparticle-supported urea catalyst **266**



A 50 mL reaction vessel was charged with siloxane **263** (0.020 mmol, 16.30 mg) and 4-iodoanisole (internal standard, 0.020 mmol, 4.70 mg). The reaction vessel was placed under an argon atmosphere and fitted with a septum and dry C₆D₅CD₃ (4.0 mL) was added *via* syringe. At this point ¹H-NMR spectroscopic analysis (*t* = 0 min) was carried out. Magnetite nanoparticles (Fe₃O₄, 200.0 mg) were then added in one portion and the resulting suspension was sonicated for 5 min. at room temperature. The resulting mixture was heated to 50 °C for 24 h under mechanical agitation. The vessel was then

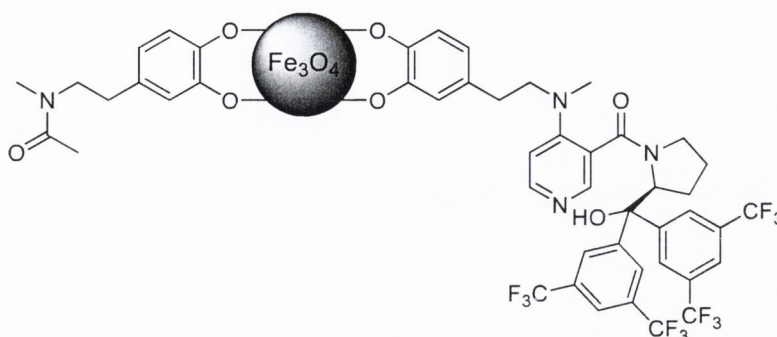
placed in proximity to an external magnet and the solution was separated from the nanoparticles *via* a pasteur pipette. Catalyst loading (1.00 mmol g^{-1}) was determined by $^1\text{H-NMR}$ spectroscopic analysis of the resulting solution which showed no traces of the peaks corresponding to the catalyst loading precursor. The remaining particles were subjected to five consecutive washing cycles with dry toluene (4.0 mL) which was decanted in the presence of an external magnet. In order to cap the remaining oxide surface of the nanoparticles, 5.0 mL of dry toluene was added to the nanoparticles under an argon atmosphere, *n*-propyltriethoxysilane (1.0 mL) *via* syringe and the suspension shaken under mechanical agitation at $50 \text{ }^\circ\text{C}$ for 16 h. The reaction solution was decanted in the presence of an external magnet and the nanoparticles were washed five times with dry toluene (5.0 mL) before being evaluated as a recyclable catalyst.

5.1.7 Synthesis of *N*-methyl dopamine anchored support (242)



A 50 mL reaction vessel was charged with *N*-methyl dopamine (20.37 mg, 0.100 mmol) and 2,5-diphenylfuran (internal standard, 22.03 mg 0.100 mmol). CD_3OD (6.0 mL) was added and the vessel placed on a mechanical shaker for 30 min. to equilibrate. $^1\text{H-NMR}$ spectrum was recorded ($T = 0$) and the sample returned to the to the reaction vessel. The reaction vessel was then charged with magnetite (Fe_3O_4 , 200.00 mg) and sonicated for 40 minutes at room temperature. The vessel was then placed over an external permanent magnet (1.4 tesla) for 2 hours and a second $^1\text{H-NMR}$ spectrum recorded ($T = 40 \text{ min}$). $^1\text{H-NMR}$ spectrum showed 0.039 mmol of *N*-methyl dopamine immobilised onto the 200.00 mg of magnetite relative to the internal standard, which is equivalent to $0.195 \text{ mmol g}^{-1}$.

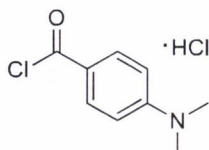
5.1.7.1 Magnetic nanoparticle-supported substituted 4-aminopyridine catalyst **246**



A 50 mL reaction vessel containing the nanoparticles **242** was charged with chloropyridine **231** (95.7 mg, 0.144 mmol) and 2,5-diphenylfuran (31.7 mg, 0.144 mmol). The vessel was fitted with a septum and flushed with argon. Dry toluene (6 mL) was added *via* syringe and the resulting mixture shaken on a mechanical shaker for 30 min. to fully dissolve the reaction components, after which time $^1\text{H-NMR}$ spectroscopic analysis ($t = 0$ min) was carried out to confirm the initial charge of chloropyridine **231**. Triethylamine (43 μL , 0.312 mmol) was added *via* syringe and the resulting suspension was heated under mechanical agitation at 60 $^\circ\text{C}$ for 48 h. At this point $^1\text{H-NMR}$ spectroscopic analysis indicated that 0.0161 mmol of **231** had undergone the $\text{S}_{\text{N}}\text{Ar}$ reaction; resulting in a catalyst loading of 0.0805 mmol g^{-1} . The reaction solution was decanted in the presence of an external magnet and the nanoparticles washed twice with dry THF and once with dry toluene. To protect free amine functionality which had not reacted with **242**, dry CH_2Cl_2 (6 mL) was added to the vessel under an argon atmosphere. Acetic anhydride (108 μL , 1.145 mmol) and triethylamine (160 μL , 1.145 mmol) was added sequentially *via* syringe and the resulting suspension shaken under mechanical agitation for 24 h at room temperature. The reaction solution was decanted in the presence of an external magnet and the nanoparticles washed twice with dry THF. In order to cap the remaining oxide surface of the nanoparticles dry THF (6 mL) was added to the nanoparticles under an argon atmosphere, *n*-propyltriethoxysilane (1 mL) was added *via* syringe and the suspension shaken under mechanical agitation at 40 $^\circ\text{C}$ for 16 h. The reaction solution was decanted in the presence of an external magnet and the nanoparticles were washed twice with dry THF (6 mL) and once with toluene (6

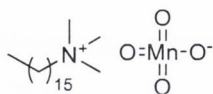
mL). If the particles were not required for immediate use they were subsequently dried under high vacuum.

5.1.8 4-(Chlorocarbonyl)-*N,N*-dimethylbenzenaminium chloride (**302**)²³²



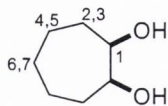
A 500 mL three-necked round bottom flask with stirring bar was fitted with a reflux condenser containing a calcium chloride guard tube and charged with 4-(dimethylamino)benzoic acid (2.00 g, 12.11 mmol) and dry CH₂Cl₂ (200 mL). Oxalyl chloride (1.24 mL, 14.53 mmol) was added and the flask was stirred at reflux temperature for 2 hours, then allowed to reach room temperature and stirred for a further 20 hours. The solvent and excess oxalyl chloride were removed *in vacuo* gave **280** as a pale yellow solid in a proportional yield, which was used without any further purification.

5.1.8.1 Cetyltrimethylammonium permanganate (CTAP) (**303**)²³³



To a 500 mL round bottom flask containing a stirred solution of potassium permanganate (3.17 g, 20 mmol) in water (100 mL) at 20 °C, a solution of cetyltrimethylammonium bromide (8.02 g, 22 mmol) in water (100 mL) was added dropwise over 20 minutes. A fine violet precipitate formed immediately. Stirring was continued for 30 min., the product isolated by filtration under suction, washed thoroughly with water, and dried in a desiccator over phosphorus pentoxide *in vacuo* for 3 hours at room temperature gave **303** as a fluffy violet solid, (6.50 g, 80%). The reagent was stored in a brown bottle in a refrigerator and used within three months.

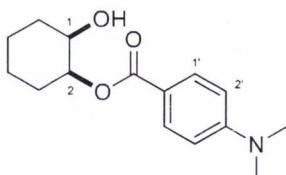
5.1.8.2 (meso)-Cycloheptane-1,2-diol (**304**)²³⁴



A solution of CTAP (**303**) (2.02 g, 5 mmol) in *t*-butyl alcohol (20 ml) and water (5 ml) was added dropwise to a stirred solution of the cycloheptene (651 mg, 5 mmol) in *t*-butyl alcohol (4 ml) was continuously stirred for 2 hours. CHCl_3 (50 ml) and a 5% solution of aqueous sodium hydroxide solution (15 ml) were added and the mixture was stirred for 30 min. The organic layer was separated and aqueous phase was extracted with chloroform (3 x 50 mL). The combined organic extracts were dried (MgSO_4) and the solvent was removed *in vacuo*. The product was purified by column chromatography (1:1 EtOAc- CH_2Cl_2 , $R_f = 0.25$), which gave **304** (740 mg, 27%) as a transparent oil. B.p. 250 °C, (lit.,²³⁴ 248.8 °C).

δ_{H} (400 MHz, CDCl_3): 1.81-1.39 (m, 10H, H-2, H-3, H-4, H-5, H-6, H-7), 2.08 (d, 2H, J 4.0, H-1), 3.85-3.90 (m, 2H, OH).

5.1.8.3 (rac)-(cis)-4-Dimethylamino-benzoic acid 2-hydroxy-cyclohexyl ester (**58**)⁹⁸

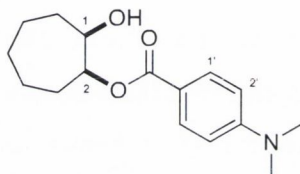


A 1L three-necked round bottom flask fitted with a 250 mL addition funnel charged with 4-dimethylamino-benzoyl chloride HCl salt (3.00 g, 13.6 mmol) in dry CH_2Cl_2 (250 mL). The round bottom flask was charged with (*cis*)-cyclohexane-1,2-diol (1.58 g, 13.6 mmol), DMAP (16 mg, 0.13 mmol), NEt_3 (2.8 mL, 20.4 mmol) in dry CH_2Cl_2 (150 mL) and a stirring bar was placed under an atmosphere of Ar then cooled to 0 °C. The acid chloride solution was added slowly over a 45 min. period and the resulting solution was allowed to warm to room temperature and stirred for 16 h. The majority of the CH_2Cl_2 was removed *in vacuo* until approximately 30 mL remained. The resulting

solution was washed with a saturated solution of NaHCO_3 (3 x 20 mL) and organic extracts were separated and combined, dried (MgSO_4) and the solvent removed *in vacuo*. Purification by column chromatography (CH_2Cl_2 , $R_f = 0.2$), gave **58** (1.84 g, 41%) as a white/pale yellow solid. M.p. 119-121 °C, (lit.,⁹⁸ 120-122 °C).

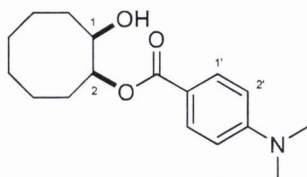
δ_{H} (400 MHz, CDCl_3): 1.40-1.49 (m, 2H, H-5, H-7), 1.67-2.17 (m, 6H, H-3, H-4, H-6, H-8, H-9, H-10), 3.07 (s, 6H, NMe_2), 3.96 (m, 1H, H-1), 5.15-5.21 (m, 1H, H-2), 6.68 (d, 2H, J 9.0, H-2'), 7.94 (d, 2H, J 9.0, H-1').

5.1.8.4 (rac)-(cis)-2-Hydroxycycloheptyl 4-(dimethylamino)benzoate (**249**)⁹⁸



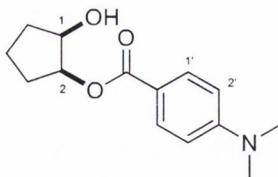
A 500 mL three-necked round bottom flask fitted with a 100 mL addition funnel charged with 4-dimethylamino-benzoyl chloride hydrochloride salt (1.50 g, 6.8 mmol) in dry CH_2Cl_2 (100 mL). The round bottom flask was charged with (*cis*)-cycloheptane-1,2-diol (885 mg, 6.8 mmol), DMAP (8 mg, 0.07 mmol), NEt_3 (2.8 mL, 20.4 mmol) in dry CH_2Cl_2 (100 mL) and a stirring bar was placed under an atmosphere of Ar then cooled to 0 °C. The acid chloride solution was added slowly over a 45 min. period and the resulting solution was allowed to warm to room temperature and stirred for 16 h. The CH_2Cl_2 was reduced *in vacuo* to about 25 mL and washed with a saturated solution of NaHCO_3 (3 x 20 mL). The organic extracts were separated, dried (MgSO_4) and the solvent was removed *in vacuo*. Purification by column chromatography (CH_2Cl_2 , $R_f = 0.2$), gave **249** (705 mg, 37%) as a white solid. M.p. 67-68 °C, (lit.,⁹⁸ 66-67 °C).

δ_{H} (400 MHz, CDCl_3): 1.51-1.88 (m, 9H, H-4, H-5, H-6, H-7, H-8, H-9, H-10, H-11, H-12), 2.01-2.17 (m, 1H, H-3), 2.60 (s, 1H, OH), 3.08 (s, 6H, NMe_2), 4.04-4.09 (m, 1H, H-1), 5.23 (m, 1H, H-2), 6.71 (d, 2H, J 9.0, H-2'), 7.95 (d, 2H, J 9.0, H-1').

5.1.8.5 (rac)-(cis)-2-Hydroxycyclooctyl 4-(dimethylamino)benzoate (250)⁹⁸


Prepared in the same manner as **249** using 4-dimethylamino-benzoyl chloride hydrochloride salt (1.53 g, 6.93 mmol) in dry CH₂Cl₂ (100 mL). The round bottom flask was charged with (*cis*)-cyclooctane-1,2-diol (1.00 mg, 6.93 mmol), DMAP (8 mg, 0.07 mmol) and NEt₃ (3.8 mL, 27.72 mmol) in dry CH₂Cl₂ (100 mL). Purification by column chromatography (CH₂Cl₂, R_f = 0.18), gave **250** (705 mg, 37%) as a white solid. M.p. 65-66 °C, (lit.,⁹⁸ 66-68 °C).

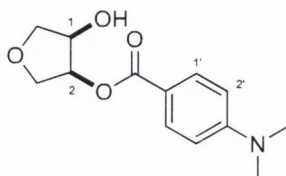
δ_{H} (400 MHz, CDCl₃): 0.86-0.93 (m, 2H, H-9, H-10), 1.25-1.35 (m, 2H, H-7, H-8), (m, 7H, H-4, H-5, H-6, H-11, H-12, H-13, H-14), 2.14-2.23 (m, 1H, H-3), 3.08 (s, 6H, NMe₂), 4.07-4.14 (m, 1H, H-1), 5.27-5.33 (m, 1H, H-2), 6.75 (d, 2H, J 9.0, H-2'), 7.95 (d, 2H, J 9.0, H-1').

5.1.8.6 (rac)-(cis)-2-Hydroxycyclopentyl 4-(dimethylamino)benzoate (248)⁹⁸


Prepared in the same manner as **249** using 4-dimethylamino-benzoyl chloride hydrochloride salt (1.50 g, 6.8 mmol) in dry CH₂Cl₂ (100 mL). The round bottom flask was charged with (*cis*)-cyclopentane-1,2-diol (695 mg, 6.8 mmol), DMAP (8 mg, 0.07 mmol) and NEt₃ (2.8 mL, 20.4 mmol) in dry CH₂Cl₂ (100 mL). Purification by column chromatography (CH₂Cl₂, R_f = 0.2), gave **248** (1.12 g, 66%) as a white solid. M.p. 92-94 °C, (lit.,⁹⁸ 92-93 °C).

δ_{H} (400 MHz, CDCl_3): 1.77-1.86 (m, 1H, H-6), 1.90-2.01 (m, 4H, H-4 H-5, H-7, H-8), 2.06-2.17 (m, 1H, H-3), 3.07 (s, 6H, NMe_2), 4.30-4.31 (m, 1H, H-1), 5.18-5.23 (m, 1H, H-2), 6.67 (d, 2H, J 9.0, H-1'), 7.93 (d, 2H, J 9.0, H-1').

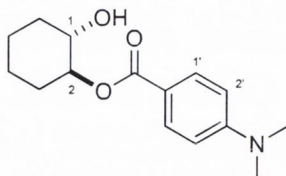
5.1.8.7 **(rac)-(cis)-4-Hydroxytetrahydrofuran-3-yl-4-(dimethylamino)benzoate (297)**⁹⁷



Prepared in the same manner as **249** using 4-dimethylamino-benzoyl chloride hydrochloride salt (1.50 g, 6.8 mmol) in dry CH_2Cl_2 (100 mL). The round bottom flask was charged with (*cis*)-tetrahydrofuran-3,4-diol (885 mg, 6.8 mmol), DMAP (8 mg, 0.07 mmol) and NEt_3 (2.8 mL, 20.4 mmol) in dry CH_2Cl_2 (100 mL). Purification by column chromatography (CH_2Cl_2 , $R_f = 0.2$), gave **297** (705 mg, 37%) as a white solid. M.p 120-121 °C, (lit.,⁹⁷ 120-121 °C).

δ_{H} (400 MHz, CDCl_3): 3.04 (s, 6H, NMe_2), 3.82-3.85 (m, 1H, H-6), 3.98-4.00 (m, 1H, H-5), 4.01-4.06 (m, 1H, H-4), 4.07-4.21 (m, 1H, H-3), 4.54-4.59 (m, 1H, H-1), 5.35-5.39 (m, 1H, H-2), 6.67 (d, 2H, J 9.0, H-2'), 7.94 (d, 2H, J 9.0, H-1').

5.1.8.8 **(rac)-(trans)-2-Acetyloxycyclohexyl 4-(dimethylamino)benzoate (245)**⁹⁷

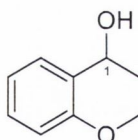


A 250 mL three-necked round bottom flask fitted with a 50 mL addition funnel charged with 4-dimethylamino-benzoyl chloride (2.50 g, 13.6 mmol) in dry THF (50 mL). The

round bottom flask was charged with (*trans*)-cyclohexane-1,2-diol (1.58 g, 13.6 mmol), DMAP (16 mg, 0.13 mmol), NEt₃ (2.8 mL, 20.4 mmol) in dry THF (50 mL) and a stirring bar was placed under an atmosphere of argon then cooled to 0 °C. The acid chloride solution was added slowly over a 45 min. period and the resulting solution was allowed to warm to room temperature and stirred for 16 h. The THF was removed *in vacuo* and the resulting solid was dissolved in CH₂Cl₂ (30 mL) and washed with a saturated solution of NaHCO₃ (3 x 40 mL). The organic extracts were separated, dried (MgSO₄) and the solvent was removed *in vacuo*. Purification by column chromatography (CH₂Cl₂, R_f = 0.2), gave **245** (1.84 g, 41%) as a white solid. M.p 120-121 °C, (lit.,⁹⁷ 120-121 °C).

δ_{H} (400 MHz, CDCl₃): 1.31-1.49 (m, 4H, H-5, H-6, H-7, H-8), 1.74-1.79 (m, 2H, H-9, H-10), 2.11-2.18 (m, 2H, H-3, H-4), 2.55 (s, 1H, OH), 3.07 (s, 6H, NMe₂), 3.70-3.77 (m, 1H, H-1), 4.78-4.84 (m, 1H, H-2), 6.67 (d, 2H, J 9.0, H-2'), 7.94 (d, 2H, J 9.0, H-1').

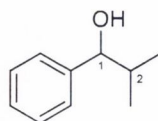
5.1.8.9 (*rac*)-1-(2-Methoxyphenyl)ethanol (**252**)²⁰¹



A 25 mL round bottom flask charged with 2-methoxybenzaldehyde (3.50 g, 25.71 mmol), THF (250 mL) and a stir bar was placed under an atmosphere of argon, cooled to 0 °C and left to stir for 10 min. Methyl magnesium bromide (14.13 ml, 28.27 mmol, 2.0 M) was added *via* syringe over a 10 min. period after which the resulting solution was allowed to reach room temperature and stirred for 14 h. The reaction was quenched with the addition of H₂O (10 mL) and extracted with CH₂Cl₂ (3 x 25 mL). The resulting organic extracts were combined and washed with a concentrated solution of NaHCO₃ (2 x 25 mL) and brine (2 x 25 mL). The organic phase were separated, dried (MgSO₄) and the solvent removed *in vacuo*. Purification by column chromatography (CH₂Cl₂, R_f = 0.35) gave **252** (2.43 g, 62%) as a colourless oil. The physical and spectroscopic data were compatible with those in the literature.^{65,201}

δ_{H} (400 MHz, CDCl_3): 1.53 (d, 3H, J 6.5, CH_3), 3.80 (s, 3H, OCH_3), 4.95 (q, 1H, J 6.5, H-1), 7.01-7.16 (m, 4H, Ar-H).

5.1.8.10 (*rac*)-2-Methyl-1-phenylpropan-1-ol (**253**)²⁰⁶



A 25 mL round bottom flask charged with benzoic acid (5.00 g, 47.12 mmol), THF (500 mL) and a stirrer was placed under an atmosphere of argon, cooled to 0 °C and left to stir for 10 mins. Methyl magnesium bromide (25.92 ml, 51.83 mmol, 2.0 M) was added *via* syringe over a 10 min. period after which the resulting solution was allowed to reach room temperature and stirred for 16 h. The reaction was quenched with the slow addition of H_2O (10 mL) and extracted with CH_2Cl_2 (3 x 25 mL). The resulting organic extracts were combined and washed with a concentrated solution of NaHCO_3 (2 x 25 mL) and brine (2 x 25 mL). The organic extracts were separated, dried (MgSO_4) and the solvent removed *in vacuo*. Purification by column chromatography (4:6 Hexane- CH_2Cl_2 , $R_f = 0.25$) gave **253** (4.6 g, 65%) as a colourless oil. The physical and spectroscopic data were compatible with those in the literature.^{84,235}

δ_{H} (400 MHz, CDCl_3): 0.82 (d, 3H, J 7.0, CH_3), 1.03 (d, 3H, J 7.0, CH_3), 2.01 (m, 1H, H-2), 4.39 (d, 1H, J 7.0, H-1), 7.30-7.39 (m, 5H, Ar-H).

5.1.9 General procedure C: acylative kinetic resolution of alcohols (**58**, **248**, **249**, **250**, **251**, **252** and **233**) promoted by magnetic nanoparticle supported catalyst **246**

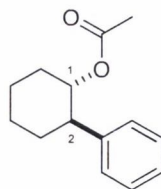
A 50 mL reaction vessel containing catalyst **246** (200 mg, 0.0161 mmol) was charged with the appropriate alcohol (0.322 mmol) and placed under an atmosphere of argon (balloon). Dry toluene (6 mL) and triethylamine (56 mL, 0.403 mmol) were added by syringe and the resulting suspension shaken under mechanical agitation for *circa* 30

min. Acetic anhydride (37 mL, 0.386 mmol) was then added by syringe and the suspension shaken for a further 16 h at room temperature. The reaction was then quenched by the addition of methanol (40 mL) followed by further shaking for 1 h. The reaction vessel was then placed over an external magnet until the reaction suspension became transparent and the liquid was then decanted. The reaction solution was concentrated *in vacuo*, the residue was then dissolved in a minimum of a 1:1 CH₂Cl₂/EtOAc solution and passed through a plug of silica gel. The resulting solution containing the recovered alcohol and its acylated analogue was concentrated *in vacuo* and used for CSP HPLC analysis.

Work up: the magnetic nanoparticles were then washed with dry THF (6 mL) and the solution decanted off in the presence of the external magnet. This was followed by the addition of another 6 mL of dry THF and 120 μ L (mmol) of DBU. The reaction vessel was shaken for 15 minutes at room temperature. The reaction vessel was then placed over the external magnet for 1 hour, after which the solution decanted off in the presence of the external magnet. This was followed by two additional washes in dry toluene (6 mL), with the solutions decanted off in the presence of the external magnet and the magnetic nanoparticles were kept under an argon atmosphere.

5.1.9.1 General procedure D: acylative kinetic resolution of (*rac*)-(*sec*)-alcohols promoted by homogeneous catalysts 53, 290, 291, 292, 294, and 295

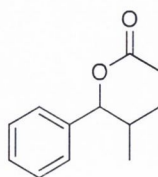
A 1 mL reaction vessel charged with catalyst (1.0 – 5.0 mol%) and a small magnetic stirring bar was placed under an atmosphere of argon (balloon). To this was added the appropriate *sec*-alcohol followed by the addition of CH₂Cl₂ (0.20 M). After allowing the reaction mixture to equilibrate for 5 to 10 min. NEt₃ was added. The resulting solution was left to stir for *circa*. 30 min. at the selected temperature the reaction was to be performed at. Acetic anhydride was subsequently added *via* syringe. After the reaction time was complete, the reaction was quenched by the addition of MeOH (4.0 molar equiv.). Solvents were removed *in vacuo*. The alcohol and its ester were separated from the catalyst by passing a concentrated solution of the crude in CH₂Cl₂ through a pad of silica gel.

5.1.9.2 (*trans*)-2-Phenylcyclohexyl acetate (**258**)²³⁶

General procedure C was followed using (*rac*)-**54** (58 mg, 0.322 mmol), NEt₃ (83 μL, 0.596 mmol) and acetic anhydride (54 μL, 0.580 mmol). Both the ester and its alcohol were passed through a pad of silica gel in a concentrated solution of CH₂Cl₂ prior to ¹H-NMR and HPLC analysis, giving **258** in 99% *ee*. The physical and spectroscopic data were compatible with those in the literature.²³⁶

δ_{H} (400 MHz, CDCl₃): 1.32-1.57 (m, 4H, H-5, H-6, H-7, H-8), 1.77-1.98 (m, 6H, H-3, H-4, H-9, CH₃), 2.06-2.18 (m, 1H, H-10), 2.62-2.72 (m, 1H, H-2), 4.97-5.09 (m, 1H, H-1), 7.14-7.38 (m, 5H, Ar-H).

HPLC data: Chiralcel OD-H (4.6 mm x 25 cm), hexanes/*i*PrOH, 99.9/0.1, 1.0 mL min⁻¹, RT, UV detection at 220 nm. Retention times: 13.3 min. (major) and 14.6 min. (minor).

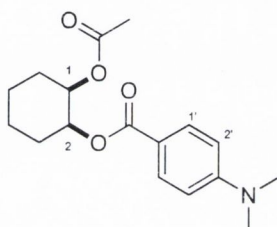
5.1.9.3 2-Methyl-1-phenylpropyl acetate (**305**)⁸⁴

General procedure C was followed using (*rac*)-**253** (48 mg, 0.322 mmol), NEt₃ (38 μL, 0.274 mmol) and acetic anhydride (24 μL, 0.258 mmol). Both the ester and its alcohol were passed through a pad of silica gel in a concentrated solution of CH₂Cl₂ prior to ¹H-NMR and HPLC analysis. **305** (18.5% *ee*). Physical and spectroscopic data were compatible with that in the literature.⁸⁴

δ_{H} (400 MHz, CDCl_3): 0.82 (d, 3H, J 6.5, CH_3), 0.99 (d, 3H, J 6.5, CH_3), 2.07-2.16 (m, 4H, H-2, Ac- CH_3), 5.49 (d, 1H, J 7.5, H-1), 7.29-7.38 (m, 5H, Ar-H).

HPLC Data: Chiralcel OD-H (4.6 x 250 mm), hexane/*i*PrOH, 90/10, 1.0 mL min^{-1} , RT, UV detection at 220 nm, retention times: 17.4 min. and 34.6 min.

5.1.9.4 **(*cis*)-4-Dimethylamino-benzoic acid 2-acetoxy-cyclohexyl ester (235)**⁹⁸

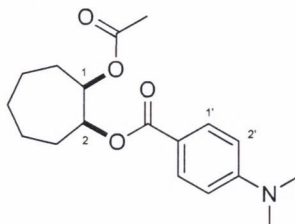


General procedure C was followed using **58** (85 mg, 0.322 mmol), NEt_3 (56 μL , 0.403 mmol) and acetic anhydride (36 μL , 0.386 mmol). Both the ester and its alcohol were passed through a pad of silica gel in a concentrated solution of CH_2Cl_2 prior to $^1\text{H-NMR}$ and HPLC analysis. The physical and spectroscopic data were compatible with that in the literature.⁹⁸

δ_{H} (400 MHz, CDCl_3): 1.42-1.52 (m, 4H, H-5, H-6, H-7, H-8), 1.77 (m, 2H, H-9, H-10), 1.96 (s, 3H, CH_3), 2.08 (m, 1H, H-3), 2.20 (m, 1H, H-4), 3.06 (s, 6H, NMe_2), 4.94-5.32 (m, 2H, H-1, H-2), 6.66 (d, 2H, J 9.0, H-2'), 7.90 (d, 2H, J 9.0, H-1').

HPLC Data: Chiralcel OD-H (4.6 x 250 mm), hexane/*i*PrOH, 90/10, 1.0 mL min^{-1} , RT, UV detection at 220 nm, retention times: 9.8 min. (minor) and 11.9 min. (major).

5.1.9.5 (cis)-2-Acetoxyoctyl 4-(dimethylamino)benzoate (255)⁹⁸

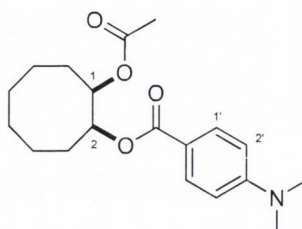


General procedure C was followed using **249** (89 mg, 0.322 mmol), NEt₃ (83 μL, 0.596 mmol) and acetic anhydride (54 μL, 0.580 mmol). Both the ester and its alcohol were passed through a pad of silica gel in a concentrated solution of CH₂Cl₂ prior to ¹H-NMR and HPLC analysis. The physical and spectroscopic data were compatible with that in the literature.⁹⁸

δ_H (400 MHz, CDCl₃): 1.58-1.85 (m, 9H, H-3, H-4, H-5, H-6, H-7, H-8, H-9, H-10, H-11), 2.02-2.12 (m, 4H, CH₃, H-12), 3.07 (s, 6H, NMe₂), 5.13-5.14 (m, 1H, H-2), 5.33-5.37 (m, 1H, H-1), 6.70 (d, 2H, J 9.0, H-2'), 7.94 (d, 2H, J 9.0, H-1').

HPLC Data: Chiralcel OD-H (4.6 x 250 mm), hexane/*i*PrOH, 90/10, 1.0 mL min⁻¹, RT, UV detection at 220 nm, retention times: 9.1 min. (minor) and 11.3 min. (major).

5.1.9.6 (cis)-2-Acetoxyoctyl 4-(dimethylamino)benzoate (256)⁹⁸



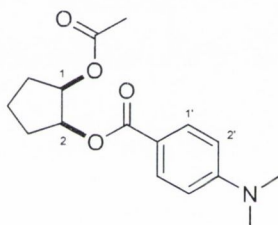
General procedure C was followed using **250** (103 mg, 0.322 mmol), NEt₃ (94 μL, 0.274 mmol) and acetic anhydride (60 μL, 0.644 mmol). Both the ester and its alcohol were passed through a pad of silica gel in a concentrated solution of CH₂Cl₂ prior to ¹H-

NMR and HPLC analysis. The physical and spectroscopic data were compatible with those in the literature.⁹⁸

δ_{H} (400 MHz, CDCl_3): 1.59-1.91 (m, 11H, H-3, H-4, H-5, H-6, H-7, H-8, H-9, H-10, H-11, H-12, H-13, H-14), 2.04-2.21 (m, 4H, H-3, CH_3), 3.06 (s, 6H, NMe_2), 5.23-5.38 (m, 2H, H-1, H-2), 6.67 (d, 2H, J 9.0, H-2'), 7.91 (d, 2H, J 9.0, H-1').

HPLC Data: Chiralcel OD-H (4.6 x 250 mm), hexane/*i*PrOH, 90/10, 1.0 mL min^{-1} , RT, UV detection at 220 nm, retention times: 8.6 min. (minor) and 12.3 min. (major).

5.1.9.7 (*cis*)-2-Acetoxy-cyclopentyl 4-(dimethylamino)benzoate (**254**)⁹⁸

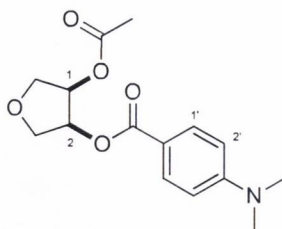


General procedure C was followed using **248** (80 mg, 0.322 mmol), NEt_3 (83 μL , 0.596 mmol) and acetic anhydride (54 μL , 0.580 mmol). Both the ester and its alcohol were passed through a pad of silica gel in a concentrated solution of CH_2Cl_2 prior to ^1H -NMR and HPLC analysis. The physical and spectroscopic data were compatible with those in the literature.⁹⁸

δ_{H} (400 MHz, CDCl_3): 1.64-1.74 (m, 1H, H-5), 1.86-1.94 (m, 3H, H-3, H-4, H-6), 2.01-2.14 (m, 5H, H-7, H-8, CH_3), 3.06 (s, 6H, NMe_2), 5.23-5.27 (m, 1H, H-2), 5.34-5.38 (m, 1H, H-1), 6.66 (d, 2H, J 7.5, H-2'), 7.91 (d, 2H, J 7.5, H-1').

HPLC Data: Chiralcel OD-H (4.6 x 250 mm), hexane/*i*PrOH, 90/10, 1.0 mL min^{-1} , RT, UV detection at 220 nm, retention times: 14.7 min. (minor) and 25.0 min. (major).

5.1.9.8 (cis)-4-acetoxytetrahydrofuran-3-yl-4-(dimethylamino)benzoate (298)⁹⁸

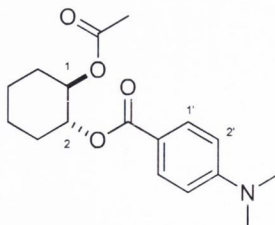


General procedure D was followed using **297** (81 mg, 0.322 mmol), NEt₃ (83 μL, 0.596 mmol) and acetic anhydride (54 μL, 0.580 mmol). Both the ester and its alcohol were separated from the catalyst by passing the crude through a pad of silica gel in a concentrated solution of CH₂Cl₂ prior to ¹H-NMR and HPLC analysis. The physical and spectroscopic data were compatible with those in the literature.⁹⁸

δ_H (400 MHz, CDCl₃): 2.06 (s, 3H, CH₃), 3.08 (s, 6H, NMe₂), 3.91-3.98 (m, 2H, H-3, H-5), 4.12-4.16 (m, 1H, H-3), 4.20-4.24 (m, 1H, H-6), 5.44-5.47 (m, 1H, H-2), 5.51-5.55 (m, 1H, H-1), 6.69 (d, 2H, J 9.0, H-2'), 7.91 (d, 2H, J 9.0, H-1').

HPLC Data: Chiralcel OD-H (4.6 x 250 mm), hexane/*i*PrOH, 90/10, 1.0 mL min⁻¹, RT, UV detection at 220 nm, retention times: 8.1 min. (minor) and 11.5 min. (major).

5.1.9.9 (1R,2S)-(trans)-4-Dimethylamino-benzoic acid 2-acetoxy-cyclohexyl ester (257)⁹⁸



General procedure C was followed using (*rac*)-**245** (85 mg, 0.322 mmol), NEt₃ (96 μL, 0.692 mmol) and acetic anhydride (63 μL, 0.676 mmol). Both the ester and its alcohol

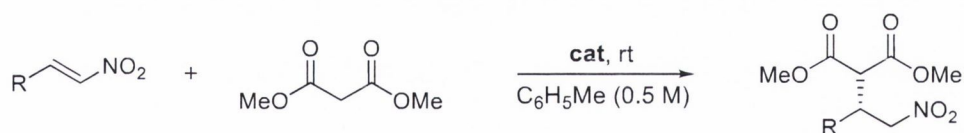
were passed through a pad of silica gel in a concentrated solution of CH_2Cl_2 prior to ^1H -NMR and HPLC analysis. M.p. 124-127 °C. The physical and spectroscopic data were compatible with that in the literature.⁹⁸

δ_{H} (400 MHz, CDCl_3): 1.42-1.52 (m, 4H, H-5, H-6, H-7, H-8), 1.76-1.80 (m, 2H, H-3, H-4), 1.96 (s, 3H, CH_3), 2.06-2.10 (m, 1H, H-9), 2.18-2.22 (m, 1H, H-10), 3.06 (s, 6H, NMe_2), 4.94-5.06 (m, 2H, H-1, H-2), 6.66 (d, 2H, J 9.0, H-2'), 7.90 (d, 2H, J 9.0, H-1').

δ_{C} (100 MHz, CDCl_3): 20.7, 23.1, 23.2, 29.8, 29.9, 39.7, 73.2, 73.3, 110.3, 116.6 (q), 130.9, 152.8 (q), 160.3 (q), 165.9 (q).

HPLC Data: Chiralcel AD-H (4.6 x 250 mm), hexane/*i*PrOH, 90/10, 1.0 mL min^{-1} , RT, UV detection at 220 nm, retention times: 11.9 min. (major) and 22.4 min. (minor).

5.1.10 General procedure E: the addition of dimethyl malonate to nitrostyrenes promoted by magnetic nanoparticle-supported catalyst **266** (Table 3.1 to Table 3.5)

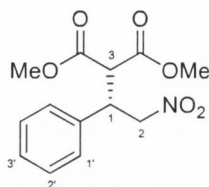


A 50 mL reaction vessel containing catalyst **266** (200 mg, 0.020 mmol) was charged with nitroolefin (0.400 mmol) and placed under an atmosphere of Ar (balloon). Dry toluene (1 mL) was added *via* syringe and the resulting suspension shaken under mechanical agitation for *ca.* 30 min. Dimethylmalonate (91 μL , 0.800 mmol) was then added *via* syringe and the suspension shaken at room temperature. The reaction was stopped by placing the reaction vessel over an external magnet. The reaction vessel was kept over the external magnet until the reaction suspension became transparent (approximately 2 h) and the liquid was then decanted and the nanoparticles washed with

dry toluene (3 mL). The combined toluene washings were concentrated *in vacuo* and the conversion determined by $^1\text{H-NMR}$ spectroscopy.

Work up: the magnetic nanoparticles were washed with dry toluene (3 mL) and the reaction vessel was put shaking for 15 minutes at room temperature. The vessel was then placed over the external magnet for 1 hour, after which the solution decanted off in the presence of the external magnet. This was followed by two additional washes in dry toluene (3 mL), with the solutions decanted off in the presence of the external magnet and the magnetic nanoparticles were kept under an argon atmosphere.

5.1.10.1 (S)-Dimethyl 2-(2-nitro-1-phenylethyl)malonate (**268**)²³⁷



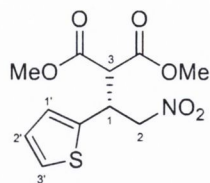
Procedure E was followed using (*E*)- β -nitrostyrene (59.7 mg, 0.400 mmol) and dimethyl malonate (91 μL , 0.800 mmol) in 1.0 mL (0.5 M) of dry toluene. The residue was purified by column chromatography (1:1, Hexane- CH_2Cl_2) gave **268** as a white solid. M.p 62–64 $^\circ\text{C}$, (lit.,²³⁷ 62-64 $^\circ\text{C}$). $[\alpha]_{\text{D}}^{20} = +18.4$ (*c* 0.87, CHCl_3 , 72% *ee*).

δ_{H} (400 MHz, CDCl_3): 3.59 (s, 3H, OCH_3), 3.79 (s, 3H, OCH_3), 3.88 (d, 1H, *J* 9.0, H-3), 4.26 (app. t, 1H, H-1), 4.87-4.98 (m, 2H, H-2), 7.24-7.26 (m, 2H, H-1'), 7.31-7.37 (m, 3H, H-2', H-3').

HPLC Data: Chiralcel AD-H (4.6 x 250 mm), hexane/*i*PrOH, 90/10, 1.0 mL min^{-1} , RT, UV detection at 220 nm, retention times: 17 min. (minor) and 29 min. (major).

The physical and spectroscopic data associated with this compound are consistent with those in the literature.²¹⁰

5.1.10.2 (R)-Dimethyl 2-(2-nitro-1-(thiophen-2-yl)ethyl)malonate (**270**)²¹⁰



Procedure E was followed using (*E*)-2-(2-nitrovinyl)thiophene (62.1 mg, 0.400 mmol) and dimethyl malonate (91 μ L, 0.800 mmol) in 1 mL (0.5 M) of dry toluene. The residue was purified by column chromatography (1:1, Hexane-CH₂Cl₂) gave **270** as a translucent oil. $[\alpha]_{\text{D}}^{20} = -7.6$ (*c* 0.50, CHCl₃, 70% *ee*).

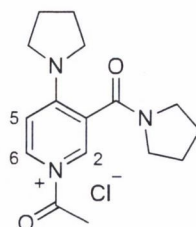
δ_{H} (400 MHz, CDCl₃): 3.68 (s, 3H, OCH₃), 3.77 (s, 3H, OCH₃), 3.92 (d, 1H, J 7.2, H-3), 4.57 (app. t, 1H, J 5.2, 8.0, H-1), 4.89-4.99 (m, 2H, H-2), 6.93-6.96 (m, 2H, H-1', H-2'), 7.24 (d, 1H, J 5.2, H-3').

HPLC Data: Chiralcel AD-H (4.6 x 250 mm), hexane/*i*PrOH, 80/20, 1.0 mL min⁻¹, RT, UV detection at 220 nm, retention times: 9.3 min. (minor) and 11.6 min. (major).

The physical and spectroscopic data associated with this compound are consistent with those in the literature.²¹⁰

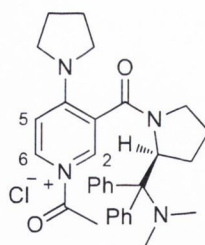
5.1.11 General procedure F: general procedure for the acylation of catalysts **291** and **299**

To a 5 mL round bottom flask charged with the appropriate catalyst (0.07 mmol) in CH₂Cl₂ (500 μ L) was added freshly distilled acyl chloride (0.70 mmol) via syringe and the resulting solution stirred at room temperature. After TLC analysis indicated complete conversion of the starting material, the resulting solution was concentrated *in vacuo*, taken up in CDCl₃ (400 μ L) and analysed by ¹H-NMR spectroscopy.

5.1.11.1 Acylation of catalyst **299** for $^1\text{H-NMR}$ analysis (**299b**)

Procedure F was followed using catalyst **299** (17.2 mg, 0.07 mmol) in CH_2Cl_2 (500 μL), with the addition of acyl chloride (44 μL , 0.70 mmol), followed by concentration of the resultant solution and analysis of the product (**299b**) in CDCl_3 by $^1\text{H-NMR}$ spectroscopy.

δ_{H} (400 MHz, CDCl_3): 1.95-1.19 (m, 8H, H-9, H-10, H-11, H-12, H-17, H-18, H-19, H-20), 3.25-3.57 (m, 8H, H-7, H-8, H-13, H-14, H-15, H-16, H-21, H-22), 4.11 (s, 3H, CH_3), 7.32 (d, 1H, J 6.0, H-5), 8.72 (s, 1H, H-2), 9.32 (d, 1H, J 6.0, H-6)

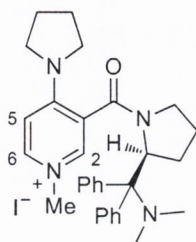
5.1.11.2 Acylation of catalyst **291** for $^1\text{H-NMR}$ analysis (**291b**)

Procedure F was followed using catalyst **291** (25.6 mg, 0.07 mmol) in CH_2Cl_2 (500 μL), with the addition of acyl chloride (44 μL , 0.70 mmol), followed by concentration of the resultant solution and analysis of the product (**291b**) in CDCl_3 by $^1\text{H-NMR}$ spectroscopy.

δ_{H} (400 MHz, CDCl_3): 1.13-1.22 (m, 1H, H-17), 1.32-1.44 (m, 2H, H-18, H-9), 1.92-2.27 (m, 15H, NMe_2 , CH_3 , H-10, H-11, H-12, H-15, H-16, H-19), 3.01-3.19 (m, 3H, H-7, H-8, H-20), 3.58-

3.65 (m, 2H, H-13, H-14), 5.91 (dd, 1H, J 7.0, J 7.0, H-21), 6.68 (d, 1H, J 8.5, H-5), 7.33-7.54 (m, 10H, Ar-H), 8.06 (d, 1H, J 8.5, H-6), 8.24 (s, 1H, H-2).

5.1.11.3 Methylation of catalyst **291** for $^1\text{H-NMR}$ analysis (**291a**)



To a 5 mL round bottom flask charged with catalyst **291** (32 mg, 0.07 mmol) in CH_2Cl_2 (500 μL) was added iodomethane (4.5 μL , 0.70 mmol) *via* syringe and the resulting solution stirred at room temperature. After TLC analysis indicated complete conversion of the starting material, the resulting solution was concentrated *in vacuo* to give the crude product **291a**, which was taken up in CDCl_3 (400 μL) and analysed by $^1\text{H-NMR}$ spectroscopy.

δ_{H} (400 MHz, CDCl_3): 1.22-1.36 (m, 2H, H-17, 18), 1.40-1.49 (m, 1H, H-9), 1.77-2.24 (m, 12H, NMe_2 , H-10, H-11, H-12, H-15, H-16, H-19), 2.88-3.96 (m, 2H, H-7, H-8), 3.45-3.53 (m, 1H, H-20), 3.57-3.68 (m, 2H, H-13, H-14), 4.17 (s, 3H, CH_3), 5.81 (m, 1H, H-21), 6.97 (d, 1H, J 8.5, H-5), 7.23-7.45 (m, 10H, Ar-H), 7.71 (s, 1H, H-2), 8.43 (d, 1H, J 8.5, H-6).

5.2 Appendix

5.2.1 Analysis and characterisation of catalyst 246

The analysis and characterisation of catalyst **246** was appreciatively carried out by Yurii K. Gun'ko and Renata Tekoriute of the CRANN Institute at the School of Chemistry, Trinity College Dublin using transmission electron microscopy (TEM), fourier transform infrared spectroscopy (FTIR) and thermogravimetric analysis (TGA).

According TEM average magnetite nanoparticles size in diameter 8.1 ± 1.8 nm. After the magnetite nanoparticles were loaded with catalyst TEM analysis indicated a decrease in aggregation of the magnetite nanoparticles without effect on the average particle size (7.9 ± 1.5 nm) (Figure 2.1).

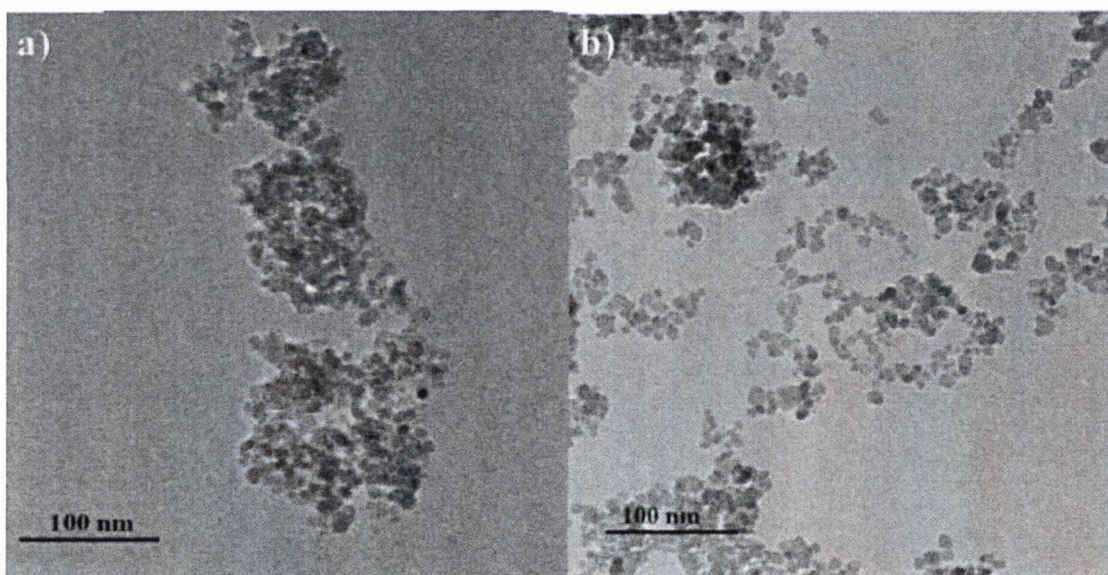


Figure 2.3 TEM images of a) magnetite nanoparticles, b) catalyst treated nanoparticles. Scale bar 100 nm.

FTIR spectra of the magnetite nanoparticles were recorded (Figure 2.2). The sample reveal stretches at 3430 , 1647 , and 580 cm^{-1} . These represent OH-groups on the surface of the particles, associated water molecules with the surface and the Fe-O stretch respectively.

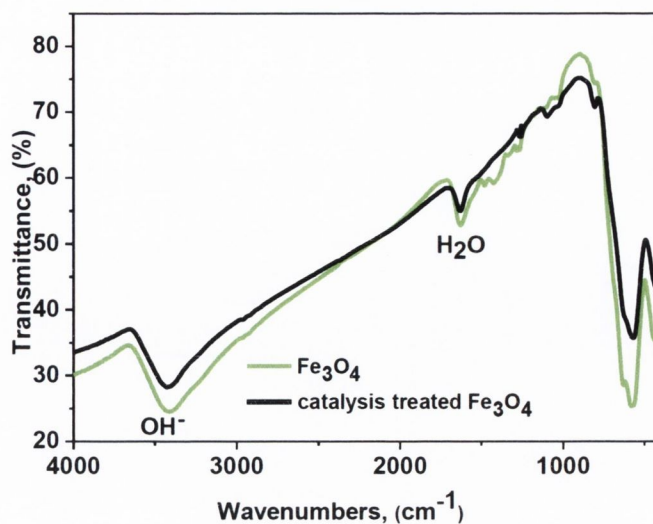


Figure 2.4 FTIR spectra of magnetite nanoparticles (black) magnetite nanoparticles, (green) catalyst treated magnetite nanoparticles.

TGA of the pure magnetite nanoparticles and catalyst-treated magnetite nanoparticles were carried out. Figure 2.3 shows the TGA curve for pure magnetite nanoparticles (black) and catalyst-treated nanoparticles (green). Small weight lost (~2%) was observed around 100 °C due to degradation and the loss of adsorbed H₂O on the surface of the magnetite nanoparticles and other residual organic solvent (EtOH) remaining from washing procedure. The insert D-TGA curve shows 8% weight lost at *ca.* 288 °C for the catalyst-treated magnetite nanoparticles. This weight loss corresponds to the decomposition of organic groups from the surface of the nanoparticles.

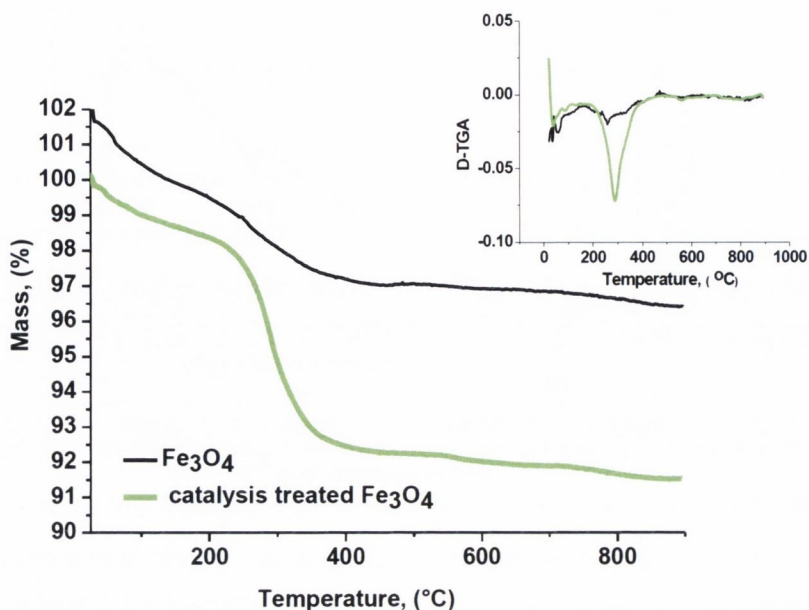


Figure 2.5 TGA spectra of magnetite (black) magnetite nanoparticles, (green) catalyst treated magnetite nanoparticles.

An XRD pattern was recorded for catalyst loaded magnetite nanoparticles before it was employed in catalysis (Figure 2.4). The reflection peaks obtained were readily indexed to (531), (440), (400), (311), and (220) planes of inverse spinel magnetite. The patterns were found to coincide with the JCPDS database for magnetite. The average particle size has been calculated from the peak width at half height maximum, which occurs at 35.5 degrees 2θ for magnetite, using the Debye-Scherrer equation.²³⁸ The average size was determined to be 5.2 nm.

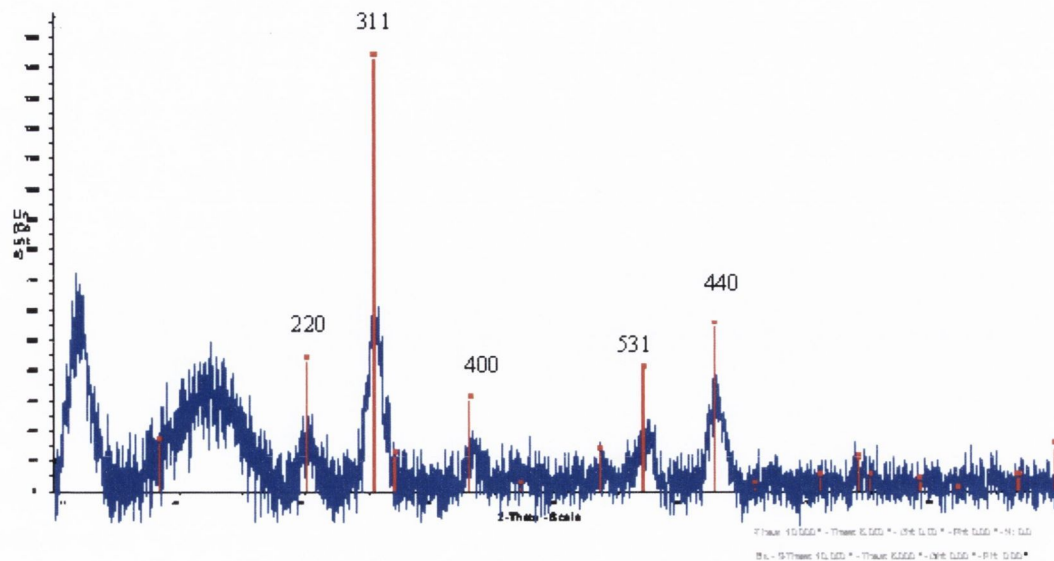


Figure 2.6 X-ray diffraction pattern of magnetite nanoparticles. Key: 9, (blue) magnetite nanoparticles, (red) pattern magnetite from JCPDS database.

5.2.2 Analysis and characterisation of catalyst 266

The analysis and characterisation of catalyst **266** was appreciatively undertaken by Yurii K. Gun'ko and Gemma-Louise Davies of the CRANN Institute at the School of Chemistry, Trinity College Dublin using transmission electron microscopy (TEM), fourier transform infrared spectroscopy (FTIR), thermogravimetric analysis (TGA) and X-ray diffraction (XRD).

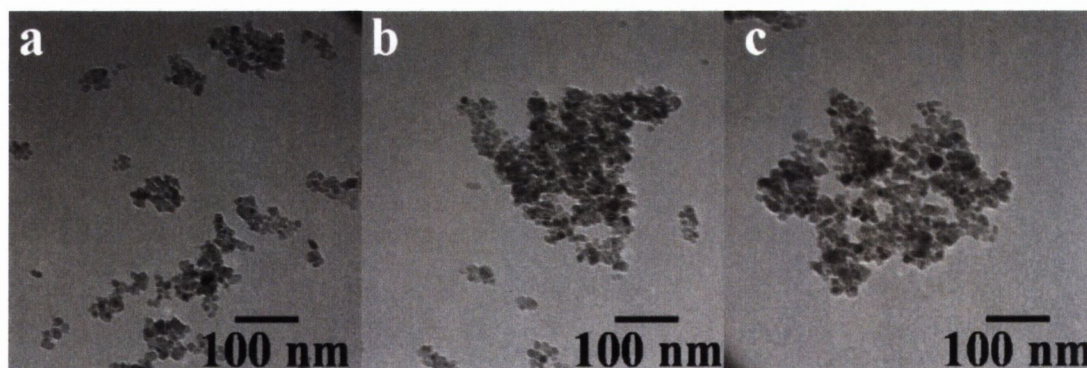


Figure 3.3 TEM images of (a) magnetite nanoparticles, (b) urea catalyst-loaded nanoparticles (**266**) and (c) urea catalyst-loaded nanoparticles (**266**) after recycling several times. Scale bar 100 nm.

The FTIR spectra for the magnetite nanoparticles before and after loading with the bifunctional urea catalyst are shown in Figure 3.4. The spectrum for magnetite nanoparticles alone (black line) shows a stretching vibration at 3440 cm^{-1} which incorporates the contributions from both symmetrical (ν_1) and asymmetrical (ν_3) modes of the O-H bonds which are attached to the surface iron atoms. The presence of an adsorbed water layer is confirmed by a stretch for the vibrational mode of water found at 1635 cm^{-1} . In the spectra for the catalyst-loaded nanoparticles, additional stretches between 1740 and 860 cm^{-1} representing the various functionalities of the urea catalyst are noted. There appear to be very few differences between the spectra of the catalyst treated nanoparticles before and after recycling, indicating no changes or degradation of the catalyst treated magnetite nanoparticles after recycling several times.

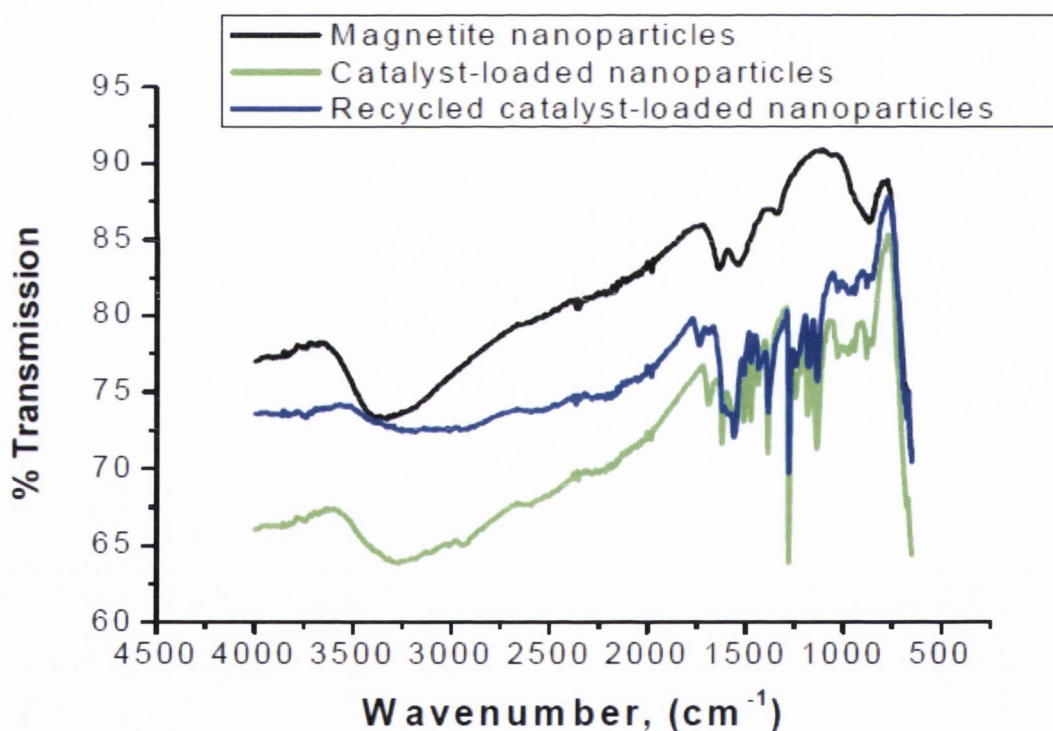


Figure 3.4 FTIR Spectra of magnetic nanoparticles, catalyst-loaded nanoparticles and recycled catalyst loaded nanoparticles

TGA was carried out on the magnetite nanoparticles before and after treatment with the bifunctional urea catalyst (Figure 3.5). TGA can show bond formation between the

magnetite nanoparticles and the catalyst. The total weight loss from the magnetite nanoparticles alone is ~2%. Much of this small weight percentage loss is due to the loss of strongly adsorbed water and surface hydroxyl groups from the particles which takes place between 30 and 250 °C. Slight changes in the curve after 500 °C are due to a phase change of the material from magnetite to maghemite. The curve representing the catalyst-loaded magnetite nanoparticles before recycling shows a total weight loss of 9.5%. The curve representing the catalyst-loaded magnetite nanoparticles after recycling shows a total weight loss of 10.8%. Above 120 °C, organic groups representative of the functionalised catalyst are desorbed from the nanoparticles. This confirms the 3 functionalisation of the nanoparticles with the catalyst, as expected. The difference in mass lost between the two catalyst-loaded magnetite nanoparticle samples shows that there is a slight change in the surface functionality of the nanoparticles after they are recycled. The increased mass lost from the recycled sample suggests the presence of a higher mass percentage of the organic functionality, perhaps implying a hydrolysis or adsorption process of the surface functionalities occurring over the course of multiple recycling. Examination of the D-TGA curves for the two samples (inset, Figure 3.5) indicates a slight shift in the temperature at which the final organic species is lost, again perhaps indicating a partial degradation of this group due to recycling.

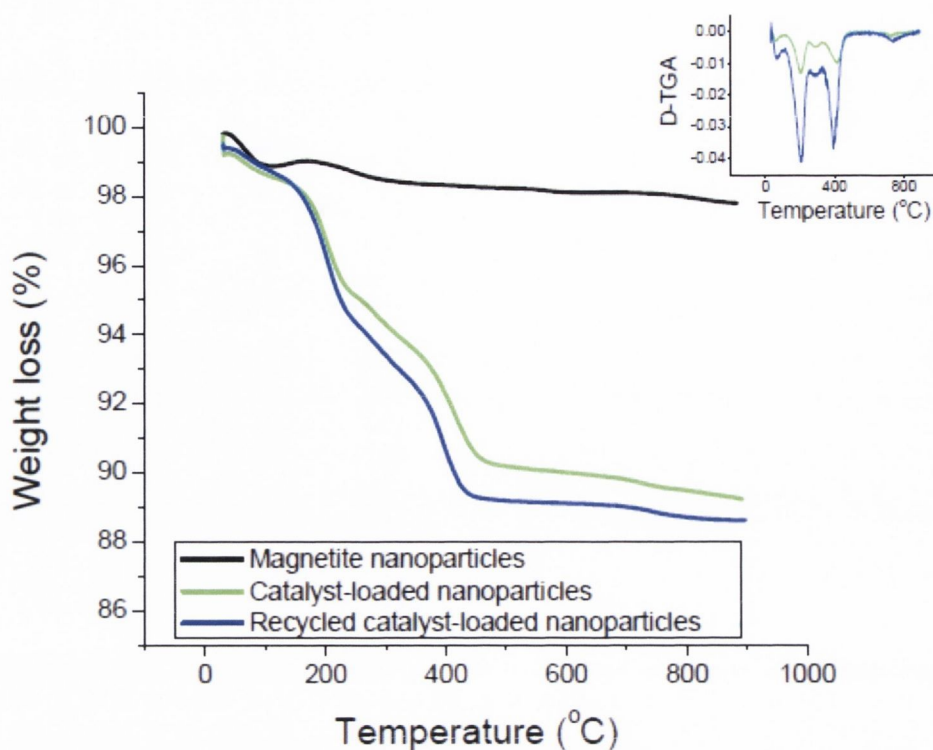


Figure 3.5 TGA curves of percentage mass lost on heating from 30-900 °C of magnetite nanoparticles (black), urea catalyst-loaded magnetite nanoparticles before recycling (green) and after recycling several times (blue).

A dry solid powder sample was used to collect XRD patterns of the sample of magnetite nanoparticles and the bifunctional urea catalyst-loaded nanoparticles before and after recycling (Figure 3.6). The observed patterns both correspond well to the JCPDS database for magnetite. The average particle size has been calculated from the peak width at half maximum of the peak at 35.5 degrees 2θ , using the Debye-Scherrer equation. The average particle size was found to be 10.99 nm, which is in close agreement with the particle size as calculated from TEM. The calculated size was the same for the magnetite before and after loading with catalyst and subsequent recycling. The interlayer spacings (d_{hkl}), calculated using the Bragg equation, agree well with the data for standard magnetite (Table 3.6). The lattice parameter a has been calculated from the inter planar spacing of the most intense peak, which for magnetite is the (311) hkl line. The a lattice parameter was calculated as 0.840 nm, which coincides closely with the value for magnetite (0.839 nm). The peaks at 12.2 and 74 degrees 2θ appear

due to the lamp present in the XRD machine. The peak at 23 degrees 2θ is due to the silica gel used to adhere the sample to the glass holder.

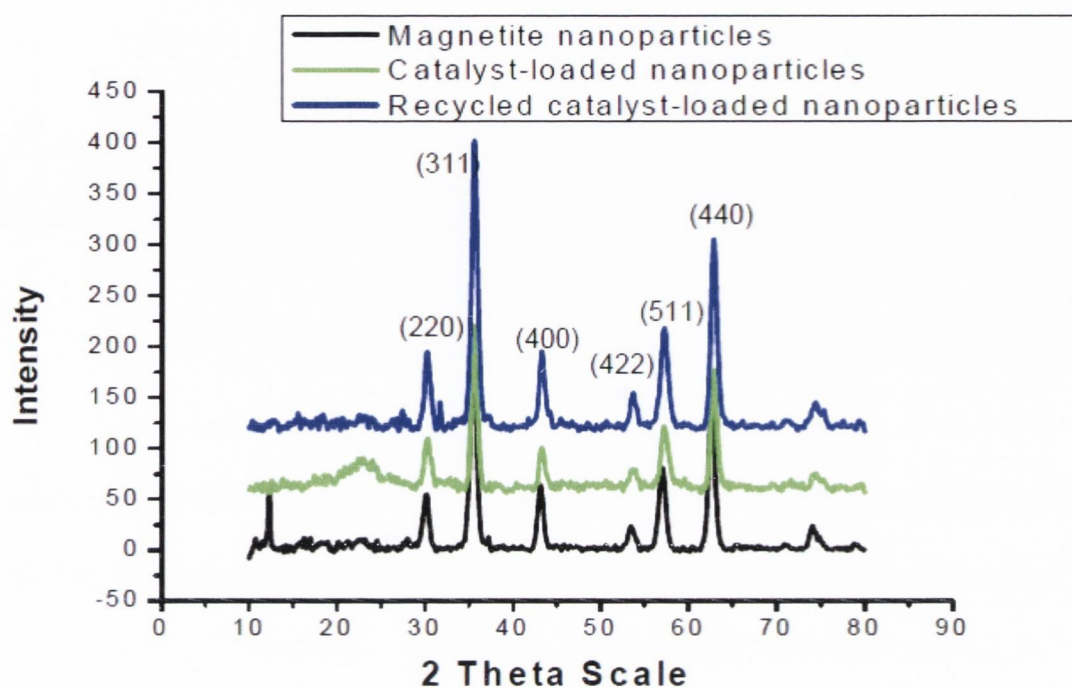


Figure 3.6 XRD patterns of magnetite nanoparticles (black), urea catalyst-loaded nanoparticles before recycling (green) and after recycling several times (blue).

Table 3.6 Lattice parameters and interlayer spacing for magnetite nanoparticles

Sample	(hkl)					
	1	2	3	4	5	6
Prepared Fe_3O_4	0.296	0.253	0.210	0.171	0.161	0.148
Standard Fe_3O_4	0.296	0.253	0.209	0.171	0.161	0.148

References

1. A. D. McNaught and A. Wilkinson, *IUPAC Compendium of Chemical Terminology*, 2 edn., Wiley-Blackwell, London, 1997.
2. P. Cintas, *Angew. Chem. Int. Ed.*, 2007, **46**, 4016.
3. R. A. Hegstrom and D. K. Kondepudi, *Sci. Am.*, 1990, **262**, 108.
4. W. W. Westerfeld and D. A. Richert, *J. Biol. Chem.*, 1950, **184**, 163.
5. I. Ali, V. K. Gupta, H. Y. Aboul-Enein, P. Singh and B. Sharma, *Chirality Rev.*, 2007, **19**, 453.
6. R. Noyori, *Asymmetric Catalysis in Organic Synthesis*, John Wiley & Sons, Inc., Chichester, 1994.
7. W. S. Knowles, *Angew. Chem. Int. Ed.*, 2002, **41**, 1998.
8. R. Noyori, *Angew. Chem. Int. Ed.*, 2002, **41**, 2008.
9. K. B. Sharpless, *Angew. Chem. Int. Ed.*, 2002, **41**, 2024.
10. M. Benaglia, *New J. Chem.*, 2006, **30**, 1525.
11. N. E. Leadbeater and M. Marco, *Chem. Rev.*, 2002, **102**, 3217.
12. C. E. Song and S.-G. Lee, *Chem. Rev.*, 2002, **102**, 3495.
13. C. H. Bartholomew and R. J. Farrauto, *Fundamentals of Industrial Catalytic Processes*, 2 edn., John Wiley & Sons Inc., Hoboken, 2006.
14. S. France, D. J. Guerin, S. J. Miller and T. Lectka, *Chem. Rev.*, 2003, **103**, 2985.
15. P. R. Schreiner, *Chem. Soc. Rev.*, 2003, **32**, 289.
16. E. Vedejs and M. Jure, *Angew. Chem. Int. Ed.*, 2005, **44**, 3974.
17. R. Silverman, *Organic Chemistry of Enzyme-Catalyzed Reactions*, 2 edn., Academic Press, London, 2002.
18. M. T. Reetz, B. List, S. Jaroch and H. Weinmann, *Organocatalysis (Ernst Schering Foundation Symposium Proceedings)*, Springer-Verlag, Berlin Heidelberg, 2008.
19. C. E. Müller and P. R. Schreiner, *Angew. Chem. Int. Ed.*, 2011, **50**, 6012.
20. *IUPAC Compendium of Chemical Technology*, 1996, **68**, 2211.
21. H. B. Kagan and J. C. Fiaud, *Top. Stereochem.*, 1988, **18**, 249.
22. C. S. Chen, Y. Fujimoto, G. Girdaukas and C. J. Sih, *J. Am. Chem. Soc.*, 1982, **104**, 7294.
23. P. I. Dalko, *Enantioselective Organocatalysis: Reactions and Experimental Procedures*, Wiley-VCH, Weinheim, 2007.
24. Y. Miyake, T. Iwata, K.-G. Chung, Y. Nishibayashi and S. Uemura, *Chem. Commun.*, 2001, 2584.
25. F. Iwasaki, T. Maki, O. Onomura, W. Nakashima and Y. Matsumura, *J. Org. Chem.*, 2000, **65**, 996.
26. M.-H. Lin and T. V. RajanBabu, *Org. Lett.*, 2002, **4**, 1607.
27. J. M. Berg, J. L. Tymoczko and L. Stryer, *Biochemistry*, W. H. Freeman and Co., New York, 2002.
28. C. J. Sih and S.-H. Wu, *Top. Stereochem.*, 2007, **19**, 63.
29. H. D. Dakin, *J. Physiol.*, 1903, **30**, 253.
30. A. Ghanem, *Tetrahedron*, 2007, **63**, 1721.
31. D. Rotticci, *Understanding and Engineering the Enantioselectivity of Candida Antarctica Lipase B towards sec-Alcohols*, Kungliga Tekniska Högskolan, Stockholm, 2000.

32. M. T. Rubino, M. Agamennone, C. Campestre, P. Campiglia, V. Cremasco, R. Faccio, A. Laghezza, F. Loiodice, D. Maggi, E. Panza, A. Rossello and P. Tortorella, *Chem. Med. Chem.*, 2011, **6**, 1258.
33. J. i. Uenishi, T. Hiraoka, S. Hata, K. Nishiwaki, O. Yonemitsu, K. Nakamura and H. Tsukube, *J. Org. Chem.*, 1998, **63**, 2481.
34. G. Bringmann, M. Breuning and S. Tasler, *Synthesis*, 1999, 525.
35. L. Pu, *Chem. Rev.*, 1998, **98**, 2405.
36. C. Orrenius, N. Öhrner, D. Rotticci, A. Mattson, K. Hult and T. Norin, *Tetrahedron: Asymm.*, 1995, **6**, 1217.
37. S. Bertelsen and K. A. Jørgensen, *Chem. Soc. Rev.*, 2009, **38**, 2178.
38. E. Vedejs, O. Daugulis and S. T. Diver, *J. Org. Chem.*, 1996, **61**, 430.
39. I. Held, S. Xu and H. Zipse, *Synthesis*, 2007, 1185.
40. V. P. Krasnov, D. A. Gruzdev and G. L. Levit, *Eur. J. Org. Chem.*, 2012, **2012**, 1471.
41. S. K. Chaudhary and O. Hernandez, *Tetrahedron Lett.*, 1979, **20**, 99.
42. C. I. Sheppard, J. L. Taylor and S. L. Wiskur, *Org. Lett.*, 2011, **13**, 3794.
43. H. D. Dakin and R. West, *J. Biol. Chem.*, 1928, **78**, 91.
44. H. D. Dakin and R. West, *J. Biol. Chem.*, 1928, **78**, 745.
45. H. D. Dakin and R. West, *J. Biol. Chem.*, 1928, **78**, 757.
46. F. Rezgui and M. M. El Gaied, *Tetrahedron Lett.*, 1998, **39**, 5965.
47. Y. Wei and M. Shi, *Acc. Chem. Res.*, 2010, **43**, 1005.
48. L. M. Litvinenko and A. I. Kirichenko, *Dokl. Akad. Nauk SSSR*, 1967, **176**, 197.
49. S. Xu, I. Held, B. Kempf, H. Mayr, W. Steglich and H. Zipse, *Chem. Eur. J.*, 2005, **11**, 4751.
50. L. I. Bondarenko, A. I. Kirichenko, L. M. Litvinenko, I. N. Dmitrenko and V. D. Kobets, *J. Org. Chem. USSR*, 1981, 2310.
51. E. Vedejs and X. Chen, *J. Am. Chem. Soc.*, 1996, **118**, 1809.
52. J. C. Ruble and G. C. Fu, *J. Org. Chem.*, 1996, **61**, 7230.
53. G. C. Fu, *Acc. Chem. Res.*, 2000, **33**, 412.
54. B. Tao, J. C. Ruble, D. A. Hoic and G. C. Fu, *J. Am. Chem. Soc.*, 1999, **121**, 5091.
55. J. E. Wilson and G. C. Fu, *Angew. Chem. Int. Ed.*, 2004, **43**, 6358.
56. S. Arai, S. Bellemin-Laponnaz and G. C. Fu, *Angew. Chem. Int. Ed.*, 2001, **40**, 234.
57. G. Höfle, W. Steglich and H. Vorbrüggen, *Angew. Chem. Int. Ed.*, 1978, **17**, 569.
58. W. Steglich and G. Höfle, *Tetrahedron Lett.*, 1970, **11**, 4727.
59. A. H. Mermerian and G. C. Fu, *J. Am. Chem. Soc.*, 2003, **125**, 4050.
60. A. H. Mermerian and G. C. Fu, *J. Am. Chem. Soc.*, 2005, **127**, 5604.
61. S. Bellemin-Laponnaz, J. Tweddell, J. C. Ruble, F. M. Breitling and G. C. Fu, *Chem. Commun.*, 2000, 1009.
62. J. C. Ruble, J. Tweddell and G. C. Fu, *J. Org. Chem.*, 1998, **63**, 2794.
63. S. Y. Lee, J. M. Murphy, A. Ukai and G. C. Fu, *J. Am. Chem. Soc.*, 2012, **134**, 15149.
64. J. Liang, J. C. Ruble and G. C. Fu, *J. Org. Chem.*, 1998, **63**, 3154.
65. B. L. Hodous, J. C. Ruble and G. C. Fu, *J. Am. Chem. Soc.*, 1999, **121**, 2637.
66. S. L. Wiskur and G. C. Fu, *J. Am. Chem. Soc.*, 2005, **127**, 6176.
67. A. C. Spivey, T. Fekner and H. Adams, *Tetrahedron Lett.*, 1998, **39**, 8919.
68. A. C. Spivey, T. Fekner, S. E. Spey and H. Adams, *J. Org. Chem.*, 1999, **64**, 9430.

69. A. C. Spivey, T. Fekner and S. E. Spey, *J. Org. Chem.*, 2000, **65**, 3154.
70. Y. Shen and C.-F. Chen, *Chem. Rev.*, 2011, **112**, 1463.
71. M. S. Newman and D. Lednicer, *J. Am. Chem. Soc.*, 1956, **78**, 4765.
72. M. S. Newman, W. B. Lutz and D. Lednicer, *J. Am. Chem. Soc.*, 1955, **77**, 3420.
73. M. S. Newman and R. M. Wise, *J. Am. Chem. Soc.*, 1956, **78**, 450.
74. C. Schmuck, *Angew. Chem. Int. Ed.*, 2003, **42**, 2448.
75. T. J. Katz, *Angew. Chem. Int. Ed.*, 2000, **39**, 1921.
76. K. Shinohara, Y. Sannohe, S. Kaieda, K. Tanaka, H. Osuga, H. Tahara, Y. Xu, T. Kawase, T. Bando and H. Sugiyama, *J. Am. Chem. Soc.*, 2010, **132**, 3778.
77. M. T. Reetz, E. W. Beuttenmüller and R. Goddard, *Tetrahedron Lett.*, 1997, **38**, 3211.
78. M. R. Crittall, H. S. Rzepa and D. R. Carbery, *Org. Lett.*, 2011, **13**, 1250.
79. N. Mittal, D. X. Sun and D. Seidel, *Org. Lett.*, 2012, **14**, 3084.
80. Y. Sohtome, A. Tanatani, Y. Hashimoto and K. Nagasawa, *Tetrahedron Lett.*, 2004, **45**, 5589.
81. C. K. De, E. G. Klauber and D. Seidel, *J. Am. Chem. Soc.*, 2009, **131**, 17060.
82. E. G. Klauber, C. K. De, T. K. Shah and D. Seidel, *J. Am. Chem. Soc.*, 2010, **132**, 13624.
83. C. Ó Dálaigh and S. J. Connon, *J. Org. Chem.*, 2007, **72**, 7067.
84. C. Ó Dálaigh, S. J. Hynes, D. J. Maher and S. J. Connon, *Org. Biomol. Chem.*, 2005, **3**, 981.
85. C. Ó Dálaigh, S. J. Hynes, J. E. O'Brien, T. McCabe, D. J. Maher, G. W. Watson and S. J. Connon, *Org. Biomol. Chem.*, 2006, **4**, 2785.
86. T. W. Bentley, H. C. Harris, Z. H. Ryu, G. T. Lim, D. D. Sung and S. R. Szajda, *J. Org. Chem.*, 2005, **70**, 8963.
87. T. W. Bentley, R. O. Jones and I. S. Koo, *J. Chem. Soc., Perkin Trans. 2*, 1994, 753.
88. R. P. Wurz, *Chem. Rev.*, 2007, **107**, 5570.
89. S. J. Connon, *Lett. Org. Chem.*, 2006, **3**, 333.
90. T. Poisson, M. Penhoat, C. Papamicaël, G. Dupas, V. Dalla, F. Marsais and V. Levacher, *Synlett*, 2005, 2285.
91. S. A. Shaw, P. Aleman and E. Vedejs, *J. Am. Chem. Soc.*, 2003, **125**, 13368.
92. S. Yamada, T. Misono and Y. Iwai, *Tetrahedron Lett.*, 2005, **46**, 2239.
93. G. Naraku, N. Shimomoto, T. Hanamoto and J. Inanaga, *Enantiomer*, 2000, **5**, 135.
94. D. Díez, M. J. Gil, R. F. Moro, N. M. Garrido, I. S. Marcos, P. Basabe, F. Sanz, H. B. Broughton and J. G. Urones, *Tetrahedron: Asymm.*, 2005, **16**, 2980.
95. J. G. Seitzberg, C. Dissing, I. Søjtofte, P.-O. Norrby and M. Johannsen, *J. Org. Chem.*, 2005, **70**, 8332.
96. T. Kawabata, R. Stragies, T. Fukaya and K. Fuji, *Chirality*, 2003, **15**, 71.
97. G. Priem, B. Pelotier, S. J. F. Macdonald, M. S. Anso and I. B. Campbell, *J. Org. Chem.*, 2003, **68**, 3844.
98. T. Kawabata, M. Nagato, K. Takasu and K. Fuji, *J. Am. Chem. Soc.*, 1997, **119**, 3169.
99. T. Kawabata, K. Yamamoto, Y. Momose, H. Yoshida, Y. Nagaoka and K. Fuji, *Chem. Commun.*, 2001, 2700.
100. S. Yamada and M. Ichikawa, *Tetrahedron Lett.*, 1999, **40**, 4231.
101. S. Yamada, T. Misono, M. Ichikawa and C. Morita, *Tetrahedron*, 2001, **57**, 8939.
102. P. I. Dalko and L. Moisan, *Angew. Chem. Int. Ed.*, 2004, **43**, 5138.

103. S. J. Miller, G. T. Copeland, N. Papaioannou, T. E. Horstmann and E. M. Ruel, *J. Am. Chem. Soc.*, 1998, **120**, 1629.
104. G. T. Copeland, E. R. Jarvo and S. J. Miller, *J. Org. Chem.*, 1998, **63**, 6784.
105. E. R. Jarvo, G. T. Copeland, N. Papaioannou, P. J. Bonitatebus and S. J. Miller, *J. Am. Chem. Soc.*, 1999, **121**, 11638.
106. C. Bakhtiar and E. H. Smith, *J. Chem. Soc., Perkin Trans. 1*, 1994, 239.
107. T. Kano, K. Sasaki and K. Maruoka, *Org. Lett.*, 2005, **7**, 1347.
108. T. Sano, K. Imai, K. Ohashi and T. Oriyama, *Chem. Lett.*, 1999, 265.
109. T. Sano, K. Ohashi and T. Oriyama, *Synthesis*, 1999, 1141.
110. T. Oriyama, K. Imai, T. Sano and T. Hosoya, *Tetrahedron Lett.*, 1998, **39**, 3529.
111. V. B. Birman, E. W. Uffman, H. Jiang, X. Li and C. J. Kilbane, *J. Am. Chem. Soc.*, 2004, **126**, 12226.
112. V. B. Birman and H. Jiang, *Org. Lett.*, 2005, **7**, 3445.
113. V. B. Birman and X. Li, *Org. Lett.*, 2006, **8**, 1351.
114. V. B. Birman and L. Guo, *Org. Lett.*, 2006, **8**, 4859.
115. A. Pesciulli, B. Procuranti, C. J. O' Connor and S. J. Connon, *Nat Chem*, 2010, **2**, 380.
116. H. Pellissier, *Adv. Synth. Catal.*, 2011, **353**, 1613.
117. C.-H. Wong and G. M. Whitesides, *Enzymes in Synthetic Organic Chemistry*, Elsevier Science, Oxford, 1994.
118. N. Öhrner, C. Orrenius, A. Mattson, T. Norin and K. Hult, *Enzym. Microb. Technol.*, 1996, **19**, 328.
119. V. D. Bumbu, X. Yang and V. B. Birman, *Org. Lett.*, 2013, **15**, 2790.
120. G. C. Fu, *Acc. Chem. Res.*, 2004, **37**, 542.
121. G. C. Fu, *Acc. Chem. Res.*, 2006, **39**, 853.
122. V. B. Birman, H. Jiang, X. Li, L. Guo and E. W. Uffman, *J. Am. Chem. Soc.*, 2006, **128**, 6536.
123. X. Li, P. Liu, K. N. Houk and V. B. Birman, *J. Am. Chem. Soc.*, 2008, **130**, 13836.
124. B. Hu, M. Meng, Z. Wang, W. Du, J. S. Fossey, X. Hu and W. P. Deng, *J. Am. Chem. Soc.*, 2010, **132**, 17041.
125. E. Vedejs and S. T. Diver, *J. Am. Chem. Soc.*, 1993, **115**, 3358.
126. E. Vedejs and O. Daugulis, *J. Am. Chem. Soc.*, 1999, **121**, 5813.
127. S. M. George, *Chem. Rev.*, 1995, **95**, 475.
128. J. A. Gladysz, *Chem. Rev.*, 2002, **102**, 3215.
129. M. Benaglia, A. Puglisi and F. Cozzi, *Chem. Rev.*, 2003, **103**, 3401.
130. E. J. Delaney, L. E. Wood and I. M. Koltz, *J. Am. Chem. Soc.*, 1982, **104**, 799.
131. G. Priem, I. B. Campbell, S. J. F. Macdonald and M. S. Anson, *Synlett*, 2003, 679.
132. R. B. Merrifield, *J. Am. Chem. Soc.*, 1963, **85**, 2149.
133. J. Priestley, *Experiments and observations relating to the various branches of natural philosophy with a continuation of the observations on air*, Printed [sic] for J. Johnson, no. 72, St. Paul's Church-Yard, London, 1779.
134. H. Davy, *Phil. Trans. Roy. Soc.*, 1817, **107**, 77.
135. L. Stephen, *Dictionary of National Biography*, Smith, Elder & Co., London, 1888.
136. E. Davy, *Phil. Trans. Roy. Soc.*, 1820, **110**, 108.
137. J. W. Döbereiner, *Ann. Chim. Phys.*, 1823, **24**, 91.
138. D. McDonald, *Platinum Metals Rev.*, 1965, **9**, 136.

139. G. Ertl, H. Knözinger, F. Schüth and J. Weitkamp, *Handbook of Heterogeneous Catalysis*, 2 edn., Wiley-VCH, Weinheim, 2008.
140. A. F. Trindade, P. M. P. Gois and C. A. M. Afonso, *Chem. Rev.*, 2009, **109**, 418.
141. Q.-H. Fan, Y.-M. Li and A. S. C. Chan, *Chem. Rev.*, 2002, **102**, 3385.
142. J. Lu and P. H. Toy, *Chem. Rev.*, 2009, **109**, 815.
143. M. A. Hierl, E. P. Gamson and I. M. Klotz, *J. Am. Chem. Soc.*, 1979, **101**, 6020.
144. F. Guendouz, R. Jacquier and J. Verducci, *Tetrahedron*, 1988, **44**, 7095.
145. S. Arseniyadis, P. V. Subhash, A. Valleix, A. Wagner and C. Mioskowski, *Chem. Commun.*, 2005, 3310.
146. P. Hodge, E. Khoshdel, J. Waterhouse and J. M. J. Fréchet, *J. Chem. Soc., Perkin Trans. 1*, 1985, 2327.
147. B. Clapham, C.-W. Cho and K. D. Janda, *J. Org. Chem.*, 2001, **66**, 868.
148. T. Oriyama, K. Imai, T. Hosoya and T. Sano, *Tetrahedron Lett.*, 1998, **39**, 397.
149. T. J. Dickerson, N. N. Reed and K. D. Janda, *Chem. Rev.*, 2002, **102**, 3325.
150. R. Annunziata, M. Benaglia, M. Cinquini, F. Cozzi and G. Tocco, *Org. Lett.*, 2000, **2**, 1737.
151. A. Puglisi, M. Benaglia, M. Cinquini, F. Cozzi and G. Celentano, *Eur. J. Org. Chem.*, 2004, **2004**, 567.
152. K. A. Ahrendt, C. J. Borths and D. W. C. MacMillan, *J. Am. Chem. Soc.*, 2000, **122**, 4243.
153. N. A. Paras and D. W. C. MacMillan, *J. Am. Chem. Soc.*, 2002, **124**, 7894.
154. W. S. Jen, J. J. M. Wiener and D. W. C. MacMillan, *J. Am. Chem. Soc.*, 2000, **122**, 9874.
155. M. Benaglia, G. Celentano and F. Cozzi, *Adv. Synth. Catal.*, 2001, **343**, 171.
156. H. Miyabe, S. Tuchida, M. Yamauchi and Y. Takemoto, *Synthesis*, 2006, 3295.
157. M. Heitbaum, F. Glorius and I. Escher, *Angew. Chem. Int. Ed.*, 2006, **45**, 4732.
158. P. McMorn and G. J. Hutchings, *Chem. Soc. Rev.*, 2004, **33**, 108.
159. C. Baerlocher, W. H. Meier and D. H. Olson, *Atlas of Zeolite Framework Types*, 6 edn., Elsevier Science, Amsterdam, 2007.
160. F. R. Ribeiro, A. E. Rodrigues, L. D. Rollmann and C. Naccache, *Zeolites: Science and Technology*, Martinus Nijhoff Publishers, The Hague, 1984.
161. K. Smith, *Solid Supports and Catalysts in Organic Synthesis*, Ellis Horwood and PTR Prentice Hall, New York, 1992.
162. R. J. Davis, *J. Catal.*, 2003, **216**, 396.
163. X. Gao and J. Xu, *Appl. Clay Sci.*, 2006, **33**, 1.
164. S. Lopez-Orozco, A. Inayat, A. Schwab, T. Selvam and W. Schwieger, *Adv. Mater.*, 2011, **23**, 2602.
165. A. Corma, M. Iglesias, M. V. Martín, J. Rubio and F. Sánchez, *Tetrahedron: Asymm.*, 1992, **3**, 845.
166. A. Corma, S. Iborra, I. Rodríguez, M. Iglesias and F. Sánchez, *Catal. Lett.*, 2002, **82**, 237.
167. L. E. Martinez, J. L. Leighton, D. H. Carsten and E. N. Jacobsen, *J. Am. Chem. Soc.*, 1995, **117**, 5897.
168. J. M. Fraile, J. I. García, J. Massam and J. A. Mayoral, *J. Mol. Catal. A: Chem.*, 1998, **136**, 47.
169. D. A. Annis and E. N. Jacobsen, *J. Am. Chem. Soc.*, 1999, **121**, 4147.
170. A. M. Segarra, R. Guerrero, C. Claver and E. Fernández, *Chem. Eur. J.*, 2003, **9**, 191.
171. C. A. McNamara, M. J. Dixon and M. Bradley, *Chem. Rev.*, 2002, **102**, 3275.

172. F. Bigi, S. Carloni, R. Maggi, A. Mazzacani, G. Sartori and G. Tanzi, *J. Mol. Catal. A: Chem.*, 2002, **182–183**, 533.
173. D. G. I. Petra, P. C. J. Kamer, P. W. N. M. van Leeuwen, K. Goubitz, A. M. Van Loon, J. G. de Vries and H. E. Schoemaker, *Eur. J. Inorg. Chem.*, 1999, 2335.
174. A. J. Sandee, D. G. I. Petra, J. N. H. Reek, P. C. J. Kamer and P. W. N. M. van Leeuwen, *Chem. Eur. J.*, 2001, **7**, 1202.
175. W. Zhuang, N. Gathergood, R. G. Hazell and K. A. Jørgensen, *J. Org. Chem.*, 2001, **66**, 1009.
176. A. Corma, H. Garcia, A. Moussaif, M. J. Sabater, R. Zniber and A. Redouane, *Chem. Commun.*, 2002, 1058.
177. R. A. Shiels, K. Venkatasubbaiah and C. W. Jones, *Adv. Synth. Catal.*, 2008, **350**, 2823.
178. D. Bernstein, S. France, J. Wolfer and T. Lectka, *Tetrahedron: Asymm.*, 2005, **16**, 3481.
179. J. Gao, H. Gu and B. Xu, *Acc. Chem. Res.*, 2009, **42**, 1097.
180. Z. Li, L. Wei, M. Y. Gao and H. Lei, *Adv. Mater.*, 2005, **17**, 1001.
181. S. Chikazumi, S. Taketomi, M. Ukita, M. Mizukami, H. Miyajima, M. Setogawa and Y. Kurihara, *J. Magn. Magn. Mater.*, 1987, **65**, 245.
182. T. Hyeon, *Chem. Commun.*, 2003, 927.
183. D. W. Elliott and W.-X. Zhang, *Environ. Sci. Technol.*, 2001, **35**, 4922.
184. V. Polshettiwar, R. Luque, A. Fihri, H. Zhu, M. Bouhrara and J. M. Basset, *Chem. Rev.*, 2011, **111**, 3036.
185. A.-H. Lu, E. L. Salabas and F. Schüth, *Angew. Chem. Int. Ed.*, 2007, **46**, 1222.
186. A. Hu, G. T. Yee and W. Lin, *J. Am. Chem. Soc.*, 2005, **127**, 12486.
187. R. F. Heck and J. P. Nolley, *J. Org. Chem.*, 1972, **37**, 2320.
188. E. Negishi, A. O. King and N. Okukado, *J. Org. Chem.*, 1977, **42**, 1821.
189. N. Miyaura, K. Yamada and A. Suzuki, *Tetrahedron Lett.*, 1979, **20**, 3437.
190. G. Lv, W. Mai, R. Jin and L. Gao, *Synlett*, 2008, 1418.
191. M. Kawamura and K. Sato, *Chem. Commun.*, 2006, 4718.
192. S. Luo, X. Zheng and J.-P. Cheng, *Chem. Commun.*, 2008, 5719.
193. C. Ó Dálaigh, S. A. Corr, Y. Gun'ko and S. J. Connon, *Angew. Chem. Int. Ed.*, 2007, **46**, 4329.
194. F. Cozzi, *Adv. Synth. Catal.*, 2006, **348**, 1367.
195. M. Benaglia, A. Puglisi and F. Cozzi, *Chem. Rev.*, 2003, **103**, 3401.
196. W. Herz and L. Tsai, *J. Am. Chem. Soc.*, 1954, **76**, 4184.
197. E. V. Brown, *J. Am. Chem. Soc.*, 1954, **76**, 3167.
198. D. J. Mathre, T. K. Jones, L. C. Xavier, T. J. Blacklock, R. A. Reamer, J. J. Mohan, E. T. T. Jones, K. Hoogsteen, M. W. Baum and E. J. J. Grabowski, *J. Org. Chem.*, 1991, **56**, 751.
199. M. Benaglia, *New J. Chem.*, 2006, **30**, 1525.
200. S.-I. Murahashi, Y. Oda and T. Naota, *Tetrahedron Lett.*, 1992, **33**, 7557.
201. H. Gu, K. Xu, Z. Yang, C. K. Chang and B. Xu, *Chem. Commun.*, 2005, 4270.
202. C. Xu, K. Xu, H. Gu, R. Zheng, H. Liu, X. Zhang, Z. Guo and B. Xu, *J. Am. Chem. Soc.*, 2004, **126**, 9938.
203. C. M. Sorensen, *Magnetism in Nanoscale Materials in Chemistry*, Wiley-Interscience Publication, New York, 2001.
204. W. Wu, Q. He and C. Jiang, *Nanoscale Res. Lett.*, 2008, **3**, 397.
205. M. S. Sigman and E. N. Jacobsen, *J. Am. Chem. Soc.*, 1998, **120**, 4901.
206. M. S. Taylor and E. N. Jacobsen, *J. Am. Chem. Soc.*, 2004, **126**, 10558.

207. T. Okino, Y. Hoashi, T. Furukawa, X. Xu and Y. Takemoto, *J. Am. Chem. Soc.*, 2005, **127**, 119.
208. T. Okino, Y. Hoashi and Y. Takemoto, *J. Am. Chem. Soc.*, 2003, **125**, 12672.
209. B. Vakulya, S. Varga, A. Csámpai and T. Soós, *Org. Lett.*, 2005, **7**, 1967.
210. S. H. McCooney and S. J. Connon, *Angew. Chem. Int. Ed.*, 2005, **44**, 6367.
211. S. H. McCooney, T. McCabe and S. J. Connon, *J. Org. Chem.*, 2006, **71**, 7494.
212. A. Peschiulli, C. Quigley, S. Tallon, Y. K. Gun'ko and S. J. Connon, *J. Org. Chem.*, 2008, **73**, 6409.
213. A. Peschiulli, Y. Gun'ko and S. J. Connon, *J. Org. Chem.*, 2008, **73**, 2454.
214. C. Palacio and S. J. Connon, *Org. Lett.*, 2011, **13**, 1298.
215. S. Tallon, A. C. Lawlor and S. J. Connon, *Arkivoc*, 2011, **iv**, 115.
216. Y. Wang, R.-G. Han, Y.-L. Zhao, S. Yang, P.-F. Xu and D. J. Dixon, *Angew. Chem. Int. Ed.*, 2009, **48**, 9834.
217. Y. Wang, H. Li, Y.-Q. Wang, Y. Liu, B. M. Foxman and L. Deng, *J. Am. Chem. Soc.*, 2007, **129**, 6364.
218. C. Bianchini and P. Barbaro, *Top. Catal.*, 2002, **19**, 17.
219. C.-S. Chen and C. J. Sih, *Angew. Chem. Int. Ed.*, 1989, **28**, 695.
220. F. Theil, *Chem. Rev.*, 1995, **95**, 2203.
221. M. Alvarez-Pérez, S. M. Goldup, D. A. Leigh and A. M. Z. Slawin, *J. Am. Chem. Soc.*, 2008, **130**, 1836.
222. C. L. Arcus and R. J. Mesley, *J. Chem. Soc.*, 1953, 178.
223. W. Eschweiler, *Ber. Dtsch. Chem. Ges.*, 1905, **38**, 880.
224. H. T. Clarke, H. B. Gillespie and S. Z. Weisshaus, *J. Am. Chem. Soc.*, 1933, **55**, 4571.
225. J. Clayden, N. Greeves, S. Warren and P. Wothers, *Organic Chemistry*, Oxford University Press, Oxford, 2000.
226. F. G. Bordwell, *Acc. Chem. Res.*, 1988, **21**, 456.
227. C. Kantra De, E. G. Klauber and D. Seidel, *J. Am. Chem. Soc.*, 2009, **131**, 17060.
228. R. Huisgen, *Angew. Chem. Int. Ed.*, 1963, **2**, 633.
229. M. Marigo, T. C. Wabnitz, D. Fielenbach and K. A. Jørgensen, *Angew. Chem. Int. Ed.*, 2005, **44**, 794.
230. Z. Shi, B. Tan, W. W. Y. Leong, X. Zeng, M. Lu and G. Zhong, *Org. Lett.*, 2010, **12**, 5402.
231. J. Luis Olivares-Romero and E. Juaristi, *Tetrahedron*, 2008, **64**, 9992.
232. D. E. Lynch, R. Hayer, S. Beddows, J. Howdle and C. D. Thake, *J. Heterocyclic Chem.*, 2006, **43**, 191.
233. B. S. Furniss, A. J. Hannaford, P. W. G. Smith and A. R. Tatchell, *Vogel's Textbook of Practical Organic Chemistry*, 5th edn., Pearson Prentice Hall, Harrow, 1989.
234. S. H. Chanteau and J. M. Tour, *J. Org. Chem.*, 2003, **68**, 8750.
235. Y. Kobayashi, K. Kodama and K. Saigo, *Org. Lett.*, 2004, **6**, 2941.
236. A.-H. A. Youssef, S. M. Sharaf and F. M. El Hegazy, *J. Prakt. Chem.*, 1982, **324**, 725.
237. M. Terada, H. Ube and Y. Yaguchi, *J. Am. Chem. Soc.*, 2006, **128**, 1454.
238. A. L. Patterson, *Phys. Rev.*, 1939, **56**, 978.